1993

Seasonal hydrology and geochemistry of two small high Arctic catchments, Axel Heiberg Island, Northwest Territories

Julia Boike
Wilfrid Laurier University

SEASONAL HYDROLOGY AND GEOCHEMISTRY OF TWO SMALL HIGH ARCTIC CATCHMENTS, AXEL HEIBERG ISLAND, N.W.T

By

Julia Boike
H.B.Sc., University of Freiburg, Germany, 1990

THESIS
Submitted to the Department of Geography
in partial fulfilment of the requirements
for the Masters of Arts degree
Wilfrid Laurier University
1993

ISBN 0-315-81533-7

ABSTRACT

This study examines hydrological and geochemical processes in a continuous permafrost setting in the Canadian High Arctic on Axel Heiberg Island (79°25'N; 90°45'W) with the following objective: to identify spatial and seasonal variation in hydrology and geochemistry of the East Inflow (EIF) and West Inflow (WIF) sub basins draining into Colour Lake and relate them to processes operating in the basins.

Field work in the catchment was carried out between 20 May to 16 August 1991 and 23 July to 20 August 1992. Surface flow and suprapermafrost groundwater in the active layer were monitored to assess seasonal changes in flowpaths of water. Water samples were taken from streams, suprapermafrost groundwaters and precipitation and analyzed for total dissolved solids (TDS), pH and major cations and anions.

Hydrological and chemical processes are examined in three periods 1. snowmelt (1-12 June) 2. period of active layer development (12 June to 2 August) and 3. the rainstorm (2 August to 10 August). Results show that several processes are responsible for the observed spatial and temporal changes in the hydrology and chemistry of the streams. In the WIF/W, a large proportion of snowmelt water refreezes on boulders of the felsenmeer forming ground ice. Three results identify the melting of ground ice as an important stream flow generating factor in the WIF/W during the period of active layer development: 1. diurnal cycles in discharge 2. a positive significant correlation between air temperature and discharge 3. TDS are inversely correlated with discharge. The hydrological regime of the WIF/W, which shows the characteristics of a proglacial regime is therefore best described as "melting ground ice regime". In the EIF, geomorphological characteristics of the basin result in a higher proportion of water travelling through the active layer, thus the response of discharge to high air temperatures is significantly lagged for 2 days ("modified melting ground ice" regime).

Chemical differences of the two streams are related to geological sources. Seasonal changes of ions in the EIF are related to two hydrological and chemical different source areas within the EIF basin. The seasonally increasing concentrations of ions during the third period of active layer development in both streams are explained by two processes: 1. increasing contribution of suprapermafrost groundwater to the stream runoff as a result of higher storage capacities of the active layer towards the end of the summer and 2. seasonally increasing ion concentrations of suprapermafrost groundwater with a longer residence time of water in the soil. Sulphate is the ion with the highest export rate for all streams. In the EIF, the sum of Ca^{2+} and SO_4^{2-} is more than 90% of the total TDS exported. In the WIF/W, the percentage of Ca^{2+} and SO_4^{2-} exported is seasonally increasing from 83 to 90%. Overall, the rainstorm is the dominating event in both streams in terms of total export of TDS.

ACKNOWLEDGEMENTS

This thesis was accomplished with the help of many people and organizations. First, I wish to thank my supervisor Dr.Mike English for the helpful guidance during various stages of my thesis and the unique possibility to work in the Arctic. Special thanks are also given to my committee members Dr.Sherry Schiff (Department of Earth Sciences, University of Waterloo), Dr.Mike Stone and Dr.Houston Saunderson from Wilfrid Laurier University for their helpful comments. Field work would not have been possible without financial support of the following organizations: a Natural Science and Engineering Council of Canada operating grant awarded to Drs. Mike English and Sherry Schiff; a Northern Scientific Training Grant (Department of Indian Affairs and Northern Development, Canada); the Polar Continental Shelf Project (Energy Mines and Resources, Canada); the Cold Regions Research Centre of Wilfrid Laurier University. The following people contributed valuable field assistance in the arctic: Alex Lamb, Sebastian Rau, Mike English and Alex MacLean. Special thanks go to: Dr.Dean Jeffries for using the Ion Chromatograph at Canada's Centre for Inland Waters, Burlington; Sebastian Rau from the Department of Geology, University of Freiburg for preparing the thin sections of rock samples and comments throughout my thesis; Martin Cassel for introducing me to the statistics package SPSS/PC; Richard Elgood and Pier Paul Overduin for proof reading parts of the first manuscript and battling with my often mysterious use of English.

Gratitude is expressed to the Canadian Government for their financial assistance in form of a Government of Canada Award for the last year of the M.A. program.

Finally, I would like to thank my family and friends in Germany and Canada for their continuous encouragement and support during my unforgettable stay in Canada.

TABLE OF CONTENTS

Abstract i
Acknowledgements ii
List of Figures vi
List of Tables x
List of Colour Prints xiii

CHAPTER 1- INTRODUCTION AND LITERATURE REVIEW

1.1. The role of polar regions in the global cycle 1
1.2.1. Hydrological properties of permafrost 3
1.2.2. Permafrost hydrology 6
1.2.3. Isotopes and permafrost 8
1.2.4. Impact of global warming on the permafrost environment 10
1.3. Previous research in the Colour Lake Basin 13
1.4. Purpose and scope 14
1.5. Study location 15
1.6. Climate 15
1.7. Geological setting 21
1.8. Glacial history and origin of Colour Lake 22

CHAPTER 2- METHODS

2. Site Investigations
2.1. Introduction 25
2.1.2. Basin Characteristics and Topography 26
2.1.3. Surficial geology, permafrost, soils 31
2.1.4. Vegetation 32
2.1.5. General hydrology 33
2.2. Field Methods
2.2.1. Surface runoff 34
2.2.2. Subsurface flow 36
2.2.3. Hydraulic head readings and hydraulic conductivity testing 42
2.2.4. Permafrost depth probing 43
2.2.5. Soil sampling 43
2.2.6. Weather observations 44
2.2.7. Snow Survey 45
2.2.8. Sampling strategy 45
2.3. Analytical and Laboratory Methods
2.3.1. Water sampling methods 47
2.3.2. Soil preparation and analysis 48
2.3.3. Cation and anion analysis 49
2.3.4. Tritium analysis 49

2.3.5. Thin sections and description of rock samples 50
2.4. Statistical data treatment 50

CHAPTER 3- THE SNOWMELT
3.1. Introduction: Climate and division into hydrological periods 51
3.2. The snowmelt period
3.2.1. Snow distribution and onset of snowmelt 54
3.2.2. Snowmelt hydrology 56
3.3. Chemistry
3.3.1. Snow chemistry 62
3.3.2. Snowmelt chemistry 67
3.4. Discussion 73

CHAPTER 4- THE PERIOD OF ACTIVE LAYER DEVELOPMENT
4.1. Introduction 82
4.2. Period of active layer development: subperiod 1
(12 June to 5 July, 1991)
4.2.1. Hydrology 82
4.2.2. Chemistry 88
4.3. Period of active layer development: subperiod 2
(6 July to 17 July, 1991)
4.3.1. Hydrology 92
4.3.2. Chemistry 97
4.4. Period of active layer development: subperiod 3
(18 to 1 August, 1991)
4.4.1. Hydrology 98
4.4.2. Chemistry 107
4.5. Discussion 112

CHAPTER 5- THE RAINSTORM
5.1. Introduction 122
5.2.1. Hydrology 123
5.2.2. Chemistry 133
5.2.3. Discussion 136

CHAPTER 6- SUMMARY AND DISCUSSION:
SEASONAL HYDROLOGY AND CHEMISTRY
6.1. Introduction 141
6.1.1. Classification of arctic streamflow regimes and
application for the streams in the Colour Lake catchment 141
6.1.2. Seasonal changes in stream chemistry 144
6.1.3. Suprapermafrost groundwater flow in the active layer ... 152
6.1.4. Discussion of charge imbalances 159

6.1.5. Geological sources for the chemistry of waters
in the EIF and WIF basin 160
6.2. Total export of ions from the watersheds 169
6.3. Conclusions 174

CHAPTER 7- CONCLUSIONS
. . . . 176

References 181
Appendix A 191
Appendix B 192
Appendic C 208

LIST OF FIGURES

Figure 1.1.	Colour Lake location map	16
Figure 1.2.	Air photo showing the Colour Lake watershed and its environment	17
Figure 1.3.	Geological map of the Base Camp area	23
Figure 2.1.	The Colour Lake catchment	27
Figure 2.2.	Air photo showing the sub basins of the Colour Lake catchment and geomorphological characteristics	29
Figure 2.3.	Photograph showing the deep valleys in the WIF basin	30
Figure 2.4.	Instrumentation of the Colour Lake catchment	35
Figure 2.5.	Snow survey sites in the EIF and WIF basins	46
Figure 3.1.	Precipitation, air temperatures and hydrographs for the EIF, WIF/W and WIF/2 for May to August, 1991	52
Figure 3.2.	Discharge, pH and TDS concentrations in the EIF stream during snowmelt, 1-11 June, 1991	63
Figure 3.3.	Discharge, pH and TDS concentrations in the WIF/W stream during snowmelt, 1-11 June, 1991	64
Figure 3.4.	Discharge, pH and TDS concentrations in the WIF/2 stream during snowmelt, 1-11 June, 1991	65
Figure 3.5.	Daily variation in net-radiation during snowmelt, 1-11 June, 1991	66
Figure 3.6.	Air temperatures at 30 and 50 cm depth and in surface mosses recorded at a felsenmeer site, upper WIF basin, during snowmelt, 1-11 June, 1991	66
Figure 3.7.	Discharge against TDS concentrations and linear correlation coefficent for the three streams during snowmelt, 1991	72

Figure 4.1. Air temperature, precipitation and hydrographs of the EIF and WIF/W streams during the period of active layer development, 12 July to 2 August, 1991 83

Figure 4.2. Discharge, pH and TDS concentrations of the WIF/W stream and active layer development in the EIF and WIF basins during the period of active layer development, 12 July to 2 August, 1991 86

Figure 4.3. Discharge, pH and TDS concentrations of the EIF stream and active layer development in the EIF and WIF basins during the period of active layer development, 12 July to 2 August, 1991 87

Figure 4.4. Discharge against TDS concentrations and linear correlation coefficient for the WIF/W stream during the period of active layer development, subperiod 1 to 3, 1991 90

Figure 4.5. Discharge against TDS concentrations and linear correlation coefficient for the EIF stream during the period of active layer development, subperiod 1 to 3, 1991 91

Figure 4.6. Diurnal variations in net-radiation, discharge, water temperature, pH and TDS concentrations in the WIF/W stream, 12 to 13 July, 1991 94

Figure 4.7. Diurnal variations in net-radiation, discharge, pH and TDS concentrations in the EIF stream, 12 to 13 July, 1991 95

Figure 4.8. Water temperatures of the EIF (30 June to 5 July) and WIF/W streams (5 July to 1 August), 1991 96

Figure 4.9. Linear regression analysis for mean daily temperature and total daily discharge for the EIF and WIF/W streams during the period of active layer development, subperiod 1 to subperiod 3, 1991 100

Figure 4.10. Linear regression analysis for mean daily temperature and 24 and 48 hours delay in discharge of the EIF stream during the third period of active layer development, 1991 101

Figure 4.11. Spatial sampling to investigate the source of the SW seep, 19 July, 1991 103

Figure 4.12. Water flowpaths identified in the EIF and WIF basins and division of the WIF basin into the WIF/W and WIF/2 sub watersheds 104

Figure 4.13. Spatial stream sampling in EIF basin, 19 July 1991 110

Figure 4.14. Areas with high potential for ground ice in EIF and WIF basins 115

Figure 4.15. Spatial stream sampling of waters in the WIF and EIF basins, 12 August, 1992 117

Figure 5.1. Precipitation record and discharge, pH and TDS concentrations for the EIF stream during the rainstorm, 2 to 10 August, 1991 129

Figure 5.2. Precipitation record and discharge, pH and TDS concentrations for the WIF/W stream during the rainstorm, 2 to 10 August, 1991 130

Figure 5.3. Precipitation record and discharge, pH and TDS concentrations for the WIF/2 stream during the rainstorm, 2 to 10 August, 1991 131

Figure 5.4. Runoff coefficients (precipitation volume/runoff volume) for the three basins from 2 to 3 August, 1991 133

Figure 5.5. Discharge against TDS concentrations and linear correlation coefficient for the three streams during the rainstorm, 2 to 10 August, 1991 135

Figure 6.1. Discharge, pH and TDS of the EIF stream from May to August, 1991 145

Figure 6.2. Discharge, pH and TDS of the WIF/W stream from May to August, 1991 146

Figure 6.3. Discharge, pH and TDS of the WIF/2 stream from May to August, 1991 147

Figure 6.4. Ion concentrations of the EIF stream from May to August, 1991 148

Figure 6.5. Ion concentrations of the WIF/W stream from

May to August, 1991 149

Figure 6.6. Ion concentrations of the WIF/2 stream from May to August, 1991 150

Figure 6.7. Shallow groundwater piezometric head and the development of the active layer from May to August, 1991 153

Figure 6.8. Cation ratios of suprapermafrost groundwaters of the EIF and WIF basin, 1991 162

Figure 6.9. Cation ratios of the EIF, WIF/W and WIF/2 streams, 1991 . . . 162

Figure 6.10. Cation and anion ratios of EIF, WIF/W and WIF/2 streams, 1991 163

Figure 6.11. Load of TDS (mg/s) for the EIF, WIF/W and WIF/2 streams from May to August, 1991 170

LIST OF TABLES

Table 1.1. Mean monthly temperature and mean monthly maximum and minimum temperature for the years 1969, 1970 and 1972 at Base Camp, Axel Heiberg Island, N.W.T. 19

Table 1.2. Formations identified in the Colour Lake Catchment 22

Table 2.1. Size of the Colour Lake catchment and sub basins 28

Table 2.2. Depth of soil mini-piezometers in the WIF and EIF basins 39

Table 2.3. Installed deep and shallow piezometers in Colour Lake 41

Table 3.1. Precipitation at Colour Lake and Eureka, May to August 1991 .. 51

Table 3.2. Summary of climatic characteristics for the hydrological periods, May to August, 1991 53

Table 3.3. Snow cover depletion during snowmelt in the WIF and EIF basin, 1991 56

Table 3.4. Hydrograph characteristics of the WIF/W and EIF streams during snowmelt, 1991 59

Table 3.5. Premelt snow chemistry in the Colour Lake catchment 62

Table 3.6. Mean, maximum and minimum values of chemical characteristics of the EIF, WIF/W and WIF/2 streams during snowmelt, 1 to 11 June, 1991 69

Table 3.7. Linear correlation coefficients for discharge and TDS and discharge and acidity for the three streams during snowmelt, 1-11 June, 1991 71

Table 3.8. Development of the active layer in the EIF and WIF basins, 28 May to 12 June, 1991 77

Table 3.9. Tritium concentrations (T.U.) in the three streams during snowmelt, 7 June, 1991 79

Table 4.1. Mean, maximum and minimum values of chemical characteristics of the EIF and WIF/W stream during the

first period of active layer development, 1991 84

Table 4.2. Summary of bivariate and multivariate regression analysis among discharge, mean daily temperature and daily precipitation during the period of active layer layer development, 1991 88

Table 4.3. Linear correlation coefficients for discharge and TDS and discharge and pH for the EIF and WIF streams during the first period of active layer development, 1991 92

Table 4.4. Mean, maximum and minimum values of chemical characteristics of the EIF and WIF/W streams during the second part of active layer development, 1991 93

Table 4.5. Linear correlation coefficients for discharge and TDS and discharge and pH for the EIF and WIF streams during the the third period of active layer development, 1991 97

Table 4.6. Tritium concentrations from selected sites during the active layer period, 1991 102

Table 4.7. Mean, maximum and minimum values of chemical characteristics of the EIF and WIF/W stream during the third period of active layer development, 1991 106

Table 4.8. Linear correlation coefficients for discharge, TDS and pH for the EIF and WIF streams during the third period of active layer development, 1991 108

Table 4.9. Summary of precipitation chemistry, 1991 111

Table 5.1. Examples of exceptional precipitation events recorded from stations in the high arctic 122

Table 5.2. Mean, maximum and minimum values of chemical characteristics of the EIF, WIF/W and WIF/2 streams during the rainstorm, 2 to 13 August, 1991 127

Tables 5.3. Active layer thickness in the EIF and WIF basins during the rainstorm, 6 August 1991 128

Table 5.4. Rain intensity, net basin precipitation input during rainstorm, 1 to 3 August, 1991 132

Tables 5.5. Linear correlation coefficients for discharge and TDS and discharge and acidity for the three streams during the rainstorm, 2 to 13 August, 1991 134

Table 5.6. Tritium concentrations in the three streams during the rainstorm, 13 of August, 1991 139

Table 6.1. Summary of seasonal hydrological and chemical characteristics of the three streams, 1991 143

Table 6.2. Alkalinity concentrations of the EIF, WIF/W and and WIF/2 streams, 1991 151

Table 6.3. Water depth, depth in sediment and hydraulic conductivity of shallow, mini-piezometers, 1991 154

Table 6.4. Seasonal chemistry of suprapermafrost groundwaters extracted at two sites in the EIF and WIF basin, 1991 156

Table 6.5. Tritium concentrations from selected sites during the period of active layer development, 1991 158

Table 6.6. Total export and daily normalized rates of TDS and discharge for the three streams during the hydrological periods, 1991 . . . 172

Table 6.7. Percentage of ions of total export exported from the three streams during the hydrological periods, 1991 173

Table 6.8. Ratio of total load of TDS (kg) and total discharge (m^3) during the hydrological periods for the three streams, 1991 . . . 173

LIST OF COLOUR PRINTS

Colour Print 1. EIF stream weir, 8 June, 1991 37

Colour Print 2. WIF/W stream weir, 19 July, 1991. 38

Colour Print 3. Salt crusts on east slope of EIF basin, 9 June, 1991 74

Colour Print 4. Close-up of east slope salt crusts, 9 June, 1991 75

Colour Print 5. EIF basin on 3 August, 1991 105

Colour Print 6. Ground ice under boulders EIF basin, June 1991 114

Colour Print 7. Overland flow at WIF/W during the rainstorm, 7 August 1991 124

Colour Print 8. Sediment delta at Gordon Greek during rainstorm, 3 August 1991 125

Colour Print 9. Discharge of suprapermafrost groundwater into Colour Lake at mini-piezometer MP5 during rainstorm, 3 August 1991 126

Colour Print 10. Thin section of quartz-sandstone of the Heiberg Formation in polarized light 166

Colour Print 11. Thin section of quartz-sandstone of Heiberg Formation 167

Colour Print 12. Thin section of quartz-sandstone of Heiberg Formation 168

CHAPTER 1 INTRODUCTION AND LITERATURE REVIEW

1.1. The role of polar regions in the global cycle

Polar regions are under increasing pressure because of expanding development, environmental pollution problems ("arctic haze", "ozone hole"; Kondrat'yev *et al.*, 1991) and the potential for global climate warming. Climate warming has become one of the most important issues facing us today, yet the extent and consequences are still unknown. Three dimensional, computer simulated General Circulation Models (GCM's) predict the greatest temperature increase in high latitudes which will change the natural landscape and landscape forming processes. Polar regions, zones of complex interactions between geosphere, cryosphere, atmosphere, hydrosphere and biosphere, have a major influence on the global climate, ocean circulation and the biochemical cycles. Therefore it is important to understand the interacting role of polar regions in the global cycle. Examples of global consequences of climate change effects in high latitudes are given below. Estimations have shown that permafrost destruction along the Lena and Yenisey rivers in Siberia would reduce discharge by 50% (Kondrat'yev *et al.*, 1991). Decreased river runoff would change the salinity and ice coverage of the arctic ocean, therefore affecting the arctic sea circulation and the transport of global water masses. Another global implication is the production and release of the greenhouse gases methane and carbon dioxide from the permafrost. Climate warming would increase the methane flux into the atmosphere by (1) releasing trapped methane in the permafrost and (2) decomposition of organic matter and methane hydrates frozen in the permafrost (IGCCP, 1990). Also, the production of carbon dioxide by the decomposition of organic matter will be an important factor in the global carbon cycle. The fact, that large quantities of organic material are frozen within the permafrost and the uncertainty of the effects of climate change (for example the depth to which the permafrost thaws and therefore exposes the organic material to the atmosphere) makes prediction about the production of greenhouse gases very difficult. Another large uncertainty factor is the response of the ice covers (sea ice and glacier ice) to climate change and their interaction with water vapour in the atmosphere. Climate warming could result in reduction of the annual extent of the sea ice and land snow cover, which would decrease the albedo. However, the reduction of the albedo, which could enforce the climate warming process ("albedo-feedback mechanism") may also be compensated by an increase of cloud cover (due to a larger extent of open water and intensification of evaporation) and reflection of short wave radiation (Kondrat'yev *et al.*, 1991). On the other hand, a higher cloud coverage would prevent long wave radiation from departing and being lost to the atmosphere, thus making the "albedo-feedback-mechanism" even more complex.

More understanding about the past climates and climate driving forces is needed for the prediction of future climate. In this sense, the contributions of research in polar regions is very important. Two main sources of information can be distinguished:

1. Paleoclimatic information stored in ice cores, marine and lacustrine sediments and permafrost can be used for the reconstruction of paleoclimates. Further, natural and anthropogenic induced climate changes factors can be distinguished (Stuiver *et al.*, 1976).

2. Permafrost, a product of climatic conditions, is very sensitive to temperature changes. Therefore, changes in the characteristics of permafrost and permafrost related processes can be used as indicators of global ecological changes (Smith, 1986; Washburn, 1979/1980; Lachenbruch and Marshall, 1986).

1.2.1. Hydrological properties of permafrost

Studies on hydrological properties of permafrost have mainly focused on the migration of moisture during freezing and thawing processes (Harris, 1988; Cheng and Chamberlain, 1988; Woo and Marsh, 1990). Frozen ground has traditionally been considered to be a hydrologically inactive and impermeable medium (Williams and Smith, 1989). The following paragraph will therefore discuss some thermodynamical and hydrological properties of frozen material, which permit water and ion movement in permafrost.

Permafrost is defined as "ground continuously below 0°C for two years or more" (National Research Council Canada, 1988). In continuous permafrost areas permafrost occurs everywhere (with the exception of small taliks) and is separated from the discontinuous permafrost zone, where some areas are free of permafrost (National Research Council Canada, 1988). The seasonally freezing and thawing top layer of the ground in areas underlain by permafrost is called the active layer (National Research Council Canada, 1988). Depth of the active layer, which can range from a few centimetres in the high Arctic to several metres farther south, depends on factors such as vegetation and snow cover, slope and aspect, thermal properties, texture and bulk density of soil and rock material, mean annual ground temperature and drainage (Williams and Smith, 1989).

The definition of permafrost is solely based on the temperature of the medium, consequently permafrost can contain no water at all or water at temperatures below 0°C. In a frozen soil system a film of unfrozen water surrounds the soil particles. Two factors determine the thickness of the water film: temperature and grain size of the soil. Temperature and water film are related, with increasing temperature the water film increases. This film is also thicker in fine-grained soils, because small soil particles have a larger surface area with more effective adhesion and cohesion forces. Another possibility for the existence of liquid in permafrost is the freezing point depression of highly concentrated waters. Water forming a continuous film around soil particles enables ion migration by diffusion. Because of the factors mentioned above, ion migration will decrease with decreasing temperature and increasing grain size (Kane and Stein, 1983). Injection of labelled sodium and chloride ions into a dry (0.5 to 2%) and cold (-3 to -14 °C) frozen ground was part of an experiment undertaken by Ugolini and Anderson (1973). Their results show that ionic movement took place through the interconnected films of liquid and that chloride is more mobile than sodium. The direction of ion migration is dependent on temperature, concentration, moisture and pressure gradients. During the experimental freezing of moist sand, ions migrated towards the unfrozen zone. In silt and clay, however, migration was observed towards the freezing front (Qiu *et al.*, 1988). Other mechanisms during freezing, such as the formation of an ice lens, may further influence the direction of ion movement.

Permafrost is not an impermeable barrier to water movement and should rather be described with the term aquitard than aquiclude (van Everdingen, 1990). Infiltration of meltwater into frozen soil is possible because of pore-pressure and gravitational gradients (Kane and Stein, 1983) and is highest at sites with high hydraulic conductivities. The hydraulic conductivity increases with decreasing ice content (probably due to open pore space) and decreasing grain size (Woo and Marsh, 1990; Kane and Stein, 1983; Kane *et al.*, 1978; Cheng and Chamberlain, 1988). Other evidence for water infiltration into frozen ground is given by Munter (1986) who observed groundwater recharge through frozen soils during winter following a precipitation event. He concluded that the governing factor for groundwater recharge in permafrost regions is the availability of precipitation, not the reduced permeability of the soil. Clearly, more field and laboratory studies on physical and chemical properties of permafrost should be carried out to improve understanding of engineering and permafrost hydrology related problems.

1.2.2. Permafrost hydrology

Permafrost plays an important role in the hydrological cycle, because it controls water movement and quality. In the High Arctic most of the hydrological processes cease during the winter and take place during the short summer season from May to August. The high arctic streamflow regime is characterized by high discharge rates during snowmelt and rainstorms and represents a typical arctic-nival regime (Woo, 1990). The main factors governing snowmelt runoff are the distribution and snow water equivalent of the winter snow cover. Deep snow filled valleys, perennial snowbanks and basal ice layers can be the source of streamflow for the entire thaw year (Lewkowicz and French, 1982a; Lewkowicz and Young, 1991; Woo *et al.*, 1982).

The rapid response (overland flow) of a watershed underlain by continuous permafrost during snowmelt and rainstorms occurs due to the limited infiltration and storage capacity of the ground (Cogley and McCann, 1976), which is strongly dependent on antecedent moisture conditions and the hydraulic conductivity of the soil. With the deepening of the active layer the infiltration and storage capacity are increased and hydrological processes become more concentrated in the zone of the active layer. Factors determining the water content of the active layer are the hydraulic conductivity of the soil, hydrological inputs such as snowmelt, rainfall, evaporation and the thermal and hydrological processes within the active layer (Woo and Marsh, 1990). The phreatic zone that develops above the frost table and within the active layer, is called the suprapermafrost groundwater. During the development of the active layer this saturated zone moves downwards with the frost table. The thickness and extent of the suprapermafrost groundwater system are highly variable depending on the source of water. With the seasonal thickening of the active layer the storage potential for incoming precipitation increases, which is an important factor in sustaining base flow in some watersheds (Woo *et al.*, 1983). Marsh and Woo (1977) calculated that the suprapermafrost groundwater accounts for 89% of the total water input to a small pond in the high arctic. The water from the melting of the frozen ground itself seems insignificant for stream runoff in the Imnavait watershed in Alaska, because it is directly lost by evaporation or plant uptake and does therefore not provide runoff during the summer (Kane *et al.*, 1989; Kane and Hintzmann, 1988). Melting of the frozen ground was not a source of soil moisture at three different study sites (polar desert, gravel, fen) near Resolute (Woo and Marsh, 1990). However, sites with a very high massive ice content can supply water for abundant subsurface moisture and suprapermafrost groundwater, as it was observed during the summer of 1988 on Hot Weather Creek/Ellesmere Island (Edlund *et al.,* 1990).

The local configuration of permafrost is important in determining local recharge or discharge rates. Taliks, unfrozen zones beneath large river or lakes within the permafrost (National Research Council Canada, 1988), exist due to the heat conducted from the water to the sediments (Gold and Lachenbruch, 1973). A so called "open talik system" may therefore connect the supra- and subpermafrost groundwater (groundwater below the permafrost). Attempts have been made to quantify the importance of subpermafrost groundwater for lake water balances. A study of the hydrogeology of a small lake in central Alaska showed that the lake was recharged from a subpermafrost aquifer through the talik system (Kane and Slaughter, 1973). Water balance calculations for a Mackenzie Delta lake suggest that the lake is connected to the subpermafrost groundwater system through a talik, but because of the low hydraulic conductivities of the lake sediments the amount seems to be insignificant (Marsh, 1986).

1.2.3. Isotopes and permafrost

The isotopical compositions of permafrost yield information about the climate during formation, and the origin and genesis of waters. Isotope analysis ($\delta^{18}O$) of ground ice and ice wedges in East-Siberia has been successfully applied to identify the transition zone between the Pleistocene and Holocene epoch (Vaikmäe, 1991). The radioactive isotope Tritium (^{3}H) in natural waters originates in part from nuclear bomb testing started in 1953. The half-life of ^{3}H is 12.5 years, therefore it can be used to date and study the movement of younger permafrost waters (Freeze and Cherry, 1979).

Isotopic signatures of waters from permafrost cores in the Mackenzie River Delta identified three different zones of groundwater activity by the analysis of ^{3}H and $\delta^{18}O$: The upper permafrost zone with high ^{3}H values representing the zone of modern meteoric recharge water, a lower zone of old water without ^3H and an intermediate zone of mixing (Michel and Fritz, 1982). Studies carried out in Siberia (Chizhov *et al.*, 1983) and in the Yukon Territory (Burn and Michel, 1988) also show high concentrations of ^3H 0.3-0.5 m below the permafrost table indicating the infiltration and movement of meteoric waters into the permafrost since 1950. Downward infiltration of meteoric waters is controlled by the hydraulic conductivity of the frozen ground and the temperature gradient (Burn and Michel, 1988).

Studies in temperate regions have successfully applied natural tracers (such as ^3H, $\delta^{18}O, \delta^2H$) to quantify the contribution of precipitation versus subsurface water to stream runoff (Fritz *et al.*, 1976). Similar studies have been carried out in the High Arctic. Isotopical analysis of snowmelt runoff in the Apex River Watershed on Baffin Island indicates a 50% contribution of "old water" to peak runoff (Obradovic and Sklash, 1986); the reason for the high portion of "old water" could be the displacement of suprapermafrost groundwater by infiltrating snowmelt. Using the stable isotopes of oxygen for snowmelt runoff in the Imnavait Creek watershed in Alaska, Cooper *et al.* (1991) calculate that less than 14% of the stream water during the peak of snowmelt was derived from sources other than snow. Further isotope analysis was undertaken to determine interactions between atmospherically derived pollutants in the snowpack and the tundra soil and vegetation in the Imnavait Creek watershed in Alaska (Cooper *et al.*, 1991).

1.2.4. Impact of global warming on the permafrost environment

The effect of climatic change on permafrost hydrology is of great importance not only because of local effects but also in terms of possible global implications. So far it is still unknown whether climate warming has already started, or if the observed average global temperature increase of 0.5 °C since 1860 (Jones *et al.*, 1984) is within the range of natural climate variability. Evidence for recent climate change is given by temperature anomalies in boreholes in the permafrost of Alaska. Lachenbruch (1982) attributes these anomalies to a temperature increase of 4°C in the last 100 years. Climate change will occur worldwide, but GCM's indicate that high latitudes above 70°N, will be subject to the greatest change (Smith, 1986). Temperature increases of 4.5 to 11 °C during winter and 1.7 to 4.9 °C during the summer are predicted for the western Canadian High Arctic in a doubled carbon dioxide (2*CO2) world (Smith, 1986). Estimations of change in precipitation rates range from an 10 to 60% increase during the summer and 10 to 60% increase of snowfall during the winter (Smith, 1986). However, the large uncertainty with respect to timing and amount of summer precipitation and winter snow cover makes it very difficult to predict the thermal response of permafrost and the changes in the hydrological regime.

There are short term and long term responses of permafrost to climate warming (Smith, 1986); long term changes would affect the distribution of permafrost, shifting the southern limit of permafrost northward. However, the thermal stability of permafrost is influenced by buffering mechanism caused by the vegetation, snow cover and ice content. These factors which influence the microclimate have to be considered when climatic change effects are predicted on a local scale. Short term changes include melting of ground ice, increased thermokarst and solifluction activity, increased soil temperatures and deepening of the active layer over a prolonged summer period. Most hydrological processes occur in the active layer, consequently changes in the depth of this zone and the duration of the active layer development will affect the hydrology of northern watersheds. Generally, the potential for water movement and storage in the active layer would be increased and could result in an extended streamflow (baseflow) in fall. Hinzman and Kane (1992) present potential hydrological changes in an arctic watershed for a scenario of 4 °C warming with changes in precipitation of +15%, -15% and 0% over a period of 50 years. The results in all scenarios indicate an earlier snowmelt, however the predicted period of 7 to 8 days lies within the range of natural variability. Evaporation and runoff, which are both dependent on the timing and amount of precipitation, will increase with warmer temperatures and the 15% increase in precipitation scena.io (Hinzman and Kane, 1992).

The long term potential for change in water chemistry of high arctic ecosystems has been largely neglected in northern research. Climate change will enhance the terrestrial export of solute material and has consequences for the aquatic ecosystems and geomorphic environment. Deepening of the active layer and an increase in soil temperatures and higher moisture content will affect weathering rates. The timing and amount of precipitation in relation to the active layer thickness is also important because subsurface waters may have longer residence times in the active layer and consequently the export of ions during the summer months could be enhanced. Seasonal trends in the chemistry of subsurface and surface waters are reported by English *et al.* (1991) and Everett *et al.* (1989). They note an increase in ion transport from spring to fall which is attributed to different flowpaths of water. Lewkowicz and French (1982b) state that the removal of large quantities of solute material by the suprapermafrost groundwater plays an important role in the denudation process in arctic environments. Another factor, which would increase the transport of ions or change the structure and composition of soils, centres around strong weathered material often found as salt accumulations in the upper layer of the soil. These crusts result in areas where the evaporation is high and no transport via surface water takes place. If magnitude and intensity of precipitation increase, as predicted in the GCMs, leaching of dissolved material into the soil or into streams could occur. Stoner and Ugolini (1988) describe intensive leaching and break-down of particles in Spodosol soils in arctic Alaska, after a large summer rainstorm had occurred. They point out that high energetic events can play an important role in soil forming processes, especially in less stable geomorphic processes.

1.3. Previous research in the Colour Lake Basin

Research in the Expedition Fiord Area started 1959 with glaciologist and geographer Fritz Müller as scientific leader and with sponsorship of McGill University and later with the Geography Department of the ETH (Eidgenössische Technische Hochschule) in Zürich. Consequently, research has mainly focused on glaciology, but also included studies in meteorology, geology, geophysics, geomorphology, limnology and botany. Much of the data have been published in the form of graduate theses and an extensive bibliography of all research undertaken on Axel Heiberg Island is given in Ommanney (1987). Since 1985, more attention has been directed towards understanding the terrestrial catchment and its interaction with the hydrology and geochemistry of Colour Lake. Sources of the natural acidity of Colour Lake (mean pH of 3.7) were discussed by Schiff *et al.,* (1991). Seasonal differences in chemistry of spring and fall drainage waters were identified and possible interactions between lake and terrestrial catchment discussed (English *et al.*, 1991). The work of Boike *et al.* (1991) focused on the groundwater hydrology of Colour Lake and identified a local deep groundwater system associated with the talik beneath it. Physical and chemical properties of a rare second year ice cover of Colour Lake were examined by Adams *et al.* (1989). Hydrochemical fluxes during snowmelt in the wetland fed by the Colour Lake outflow and surrounding hillslopes were studied by Buttle and Fraser (1992).

1.4. Purpose and scope

The purpose of this study is to examine permafrost-water interactions in a small high arctic watershed located in the zone of continuous permafrost. To achieve this goal changes in the basin hydrogeochemistry from the snow dominated period (springmelt) to the active layer dominated period (fall) are monitored.
This research has the following objectives:

1. Identify spatial and seasonal variation in hydrology of the East Inflow (EIF) and West Inflow (WIF) basins' waters draining into Colour Lake and relate them to processes operating in the basins.

2. Identify spatial and seasonal variations in geochemistry of the waters draining into Colour Lake.

The study combines geochemical, hydrological and isotopical methods to identify surface and subsurface flowpaths and their seasonal changes related to the active layer development. A better understanding of the complex system hydrology-permafrost-climate may help to predict the impact of future climate changes and implications for the global ecosystem. In addition, an understanding of ecosystem response might be developed for predictive purposes at other High Arctic study sites.

1.5. Study location

Axel Heiberg Island is part of the Queen Elizabeth Islands in the Canadian High Arctic. The field work for this study was carried out in the Colour Lake Catchment (79°25'N; 90°45'W), which is located a distance of approximately 80 km from the Sverdrup Channel and 8 km inland from the Expedition Fiord (Fig.1.1). More than 50% of the island today is covered by ice caps (Müller Ice Cap and Steacie Ice Cap) and glaciers. Colour Lake is located in a today non-glaciated catchment in close proximity (approximately 3 km) to the White and Thompson glaciers (Fig.1.2).

1.6. Climate

The arctic climate is characterized by low mean annual temperatures (long, cold winters and short cool summers) and low annual precipitation. However, local variations in the arctic climate are caused by differences in altitude, topography, distance to the ocean, vegetation and snow and ice coverage. Because of the sparsity of climatic data and the need for further climate separations, a combination of criteria is used to characterize the high arctic climate. Tedrow (1977) suggested the term "polar desert" for the Queen Elizabeth Islands on the basis of climatic, biotic, geomorphic and pedologic factors. Bliss *et al.* (1984) add two more regions, polar semi desert and a complex region, based on soil moisture and vegetation

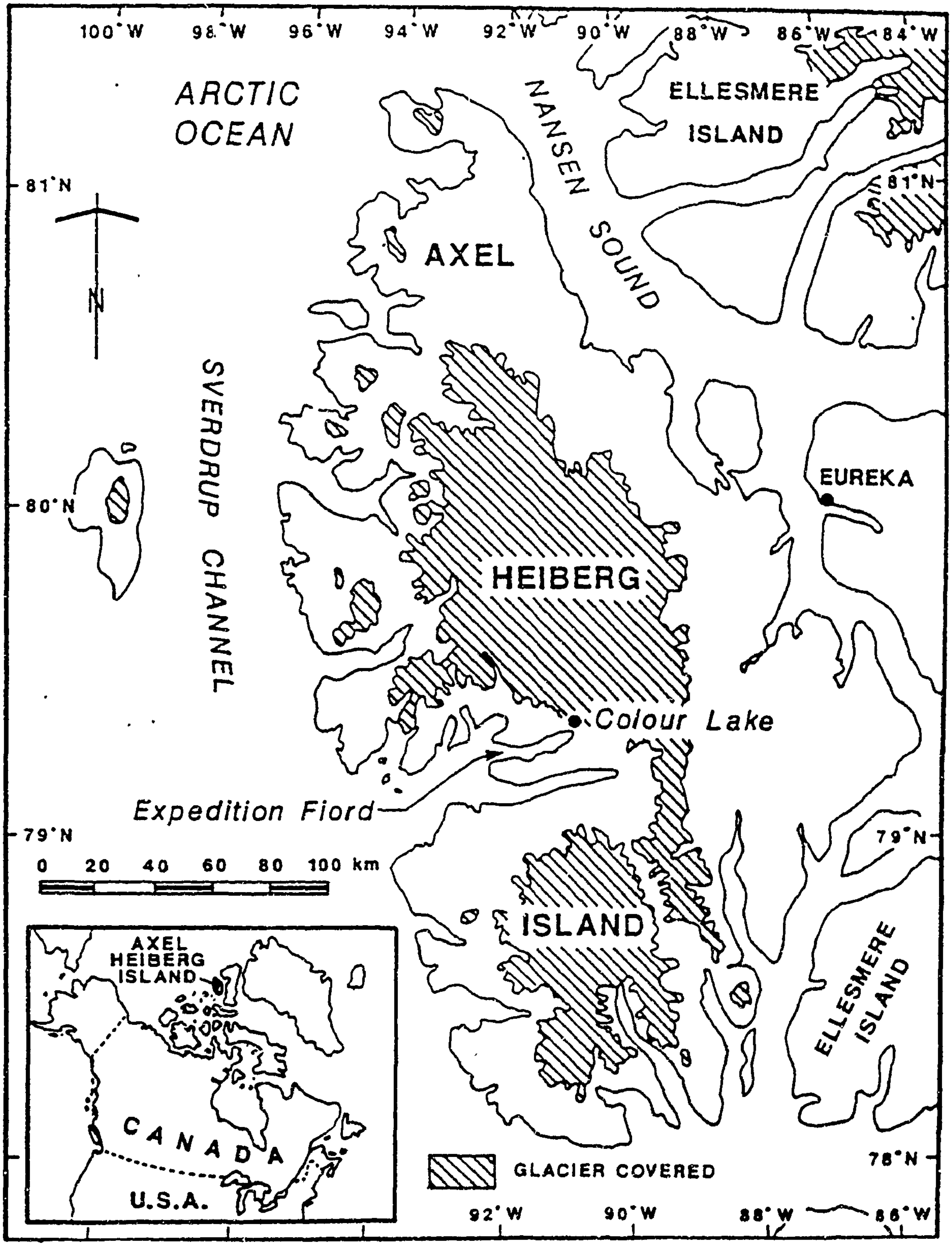

Figure 1.1. Colour Lake location map (source: Adams *et al.*, 1989).

Figure 1.2. Air photo showing the Colour Lake watershed and its environment. Scale at lake level is 1:25000 (Energy, Mines and Resources, National Air Photo Library, photo A24755-71, August 1977).

characteristics. The complex region is a combination of polar desert, polar semi desert and sedge meadows. Recently, Edlund and Alt (1989) divided the High Arctic in five bioclimatic zones based on the strong relationship between vegetation and summer climate. The Expedition Fiord area is placed into zone number two, which is the transition zone between the herbaceous zone and the prostrate shrub zone. This zone is characterized by an increase of species diversity, but still dominated by herbaceous species (Edlund and Alt, 1989).

There is no continuous, perennial climate record for the Expedition Fiord area on Axel Heiberg Island. However, since 1960, a sporadic climatological record (May-September) has been compiled by researchers as part of the aviation weather report. The closest permanent weather station with a perennial climate record since 1947 is located on Eureka (80°00'N; 85°56'W) on eastern Ellesmere Island, approximately 100 km ENE of Colour Lake. However, important climatic differences exist between these two stations. Due to the rain shadow effect of the Axel Heiberg and Ellesmere mountains, the climate of Eureka is more continental with lower precipitation rates and higher temperatures. The summer precipitation at Eureka in 1960 and 1961 was 30 and 51 mm; for these years summer precipitation at the Colour Lake Base Camp/Axel Heiberg Island was 78 and 111 mm, respectively (Nagel, 1979). From May to August 1991, a total precipitation of 146 mm was recorded at the Colour Lake base camp in contrast to only 49.8 mm recorded at Eureka. Therefore it was decided not to use the climatological record of Eureka as a surrogate for the climate at the Base Camp Station, Axel Heiberg Island.

Climatological work in the Expedition Fiord Area has been carried out by several researchers (Ohmura, 1972; Ohmura and Müller, 1977; Ohmura, 1982a, 1982b, 1982c; Nagel, 1979; Steffen and Müller, 1977). Ohmura (1972) summarizes the sequence of weather as follows: During April and May the air temperature is rising with increasing solar elevations. In June, high net-radiation inputs and higher air temperatures warm up the snowcover, thereby initiating snowmelt. With the break-up of the Arctic Ocean ice cover the frequency of cold, moist cyclones increases, dominating the weather from mid June to August. This period is characterized by rain and snow events and low temperatures. Anticyclones influence the weather in May/June and from mid August on. In mid/end August reduced solar elevation and decreasing air temperatures initiates the winter.

The following table summarizes mean air temperatures for the years with three months of continuous climate record:

	May	June	July	August
Mean monthly temp. (°C)	-10.6	-0.8	4.4	3.8
Mean monthly maximum temp.	-6.6	1.7	7.1	6.5
Mean monthly minimum temp.	-14.6	-3.3	1.3	0.7

Table 1.1. Mean monthly temperature and mean monthly maximum and minimum temperature for the years 1969, 1970 and 1972 at Base Camp, Axel Heiberg Island, N.W.T. (source: Ohmura and Müller, 1977).

Net-radiation is increasing from April and reaches its peak in mid July. July is the warmest month (Table 1.1) with highest solar elevation and 24 h sunlight. Of note is that despite the 24 h daylight there is a pronounced diurnal cycle in net-radiation and all energy balance elements (Ohmura, 1982b). The mean summer precipitation for the Expedition Fiord area for 17 years (1960 to 1976) is given as 95 mm (Ohmura, 1982a). The mean winter snow cover water equivalent on May 1 for seven year between 1966-1976 at the Base Camp is reported as 76 mm (Steffen and Müller, 1977), which makes a mean annual total precipitation of 170 mm (Ohmura, 1982a; Nagel, 1979). Daily rainfall intensities during the summer months are low, highest intensities recorded on Axel Heiberg Island are 26 mm/day (Nagel, 1979). However, rainstorms with high rainfall intensities are also recorded at other high arctic weather stations (50 mm/day at Vendom Fiord, Ellesmere Island, July 1973; Cogley and Mc Cann, 1976).

Evaporation rates in the Colour Lake Basin were calculated by using the aerodynamic profile, Bowen ratio energy balance methods and lysimeters (Ohmura, 1982a). Based on data collected in the years 1969, 1970 and 1972 he calculated a total annual evaporation of 140 mm. Approximately 85 % of the total annual precipitation is evaporated during the snow-free period (defined as time when area of snow cover becomes less than half of total area and end of August; Ohmura 1982a), therefore evaporation exceeds precipitation during this time. Ohmura (1982a) concludes that this is the reason for the low runoff during the snow-free period and that the snowmelt is the dominating runoff event. Water balance calculations at other high arctic sites also indicate that evaporation is a major component of the energy and water balance; a study site on polar desert soil near Resolute showed that water in the active layer was mainly lost by evaporation (Woo and Marsh, 1990). Evaporation accounts for a 34-66% loss of the total annual precipitation in a small watershed in Alaska (Kane *et al.*, 1990).

1.7. Geological setting

Axel Heiberg Island is part of the Sverdrup Basin Group. The Sverdrup strata overly rocks, known as the Franklin Geosyncline, an area of earlier sediment deposition between late Precambrian and Late Devonian (Plachut, 1971). After deformation, alternating marine and non-marine sediments of the Sverdrup Basin were continuously deposited from Carboniferous to the early Tertiary in two major phases (Plachut, 1971):

1. Carboniferous to lowermost Cretaceous
2. Lower Cretaceous to lower Tertiary

Tectonic movements in early Tertiary times resulted in strong faulting and folding of the area. During this time the formation of diapirs of Upper Palaeozoic evaporites (mainly consisting of anhydrite and gypsum) also took place (Fricker, 1963a). Hoen (1964) identifies about 40 diapirs on the central-western part of Axel Heiberg and suggests a tectonically and isostatically induced origin.

Sediment deposits in the Expedition Fiord Area are up to 11 km thick

(Fricker, 1963a). Thirteen formations were identified in the Expedition Fiord Area (Fricker, 1963a). The Colour Lake Catchment is underlain by the Heiberg, Savik and Awingak formation (Figure 1.3) with the characteristics shown in Table 1.2.

Formation	Time	Lithology	Medium	Notes
Awingak	Upper Jurassic	sandstone, shale	marine and non marine	mainly arenaceous deposits; carbonaceous matter
Savik	Lower, Middle and Upper Jurassic	shale, siltstone	marine	argillaceous deposits; calcareous; interbeds of siderite in lower part
Heiberg	Triassic and lowermost Jurassic	mainly sandstone; siltstone, shale	mainly non marine	predominance of quartz arenite

Table 1.2. Formations identified in the Colour Lake Catchment (source: Preliminary geological map of the Expedition Area, Fricker 1963a).

1.8. Glacial history and origin of Colour Lake

Reconstruction of the glacial history in the Expedition Fiord Area has been the subject of much research, yet there are still unknowns. Rudberg (1963) found more than thirty places, usually at low altitudes up to 240 m, where striae give

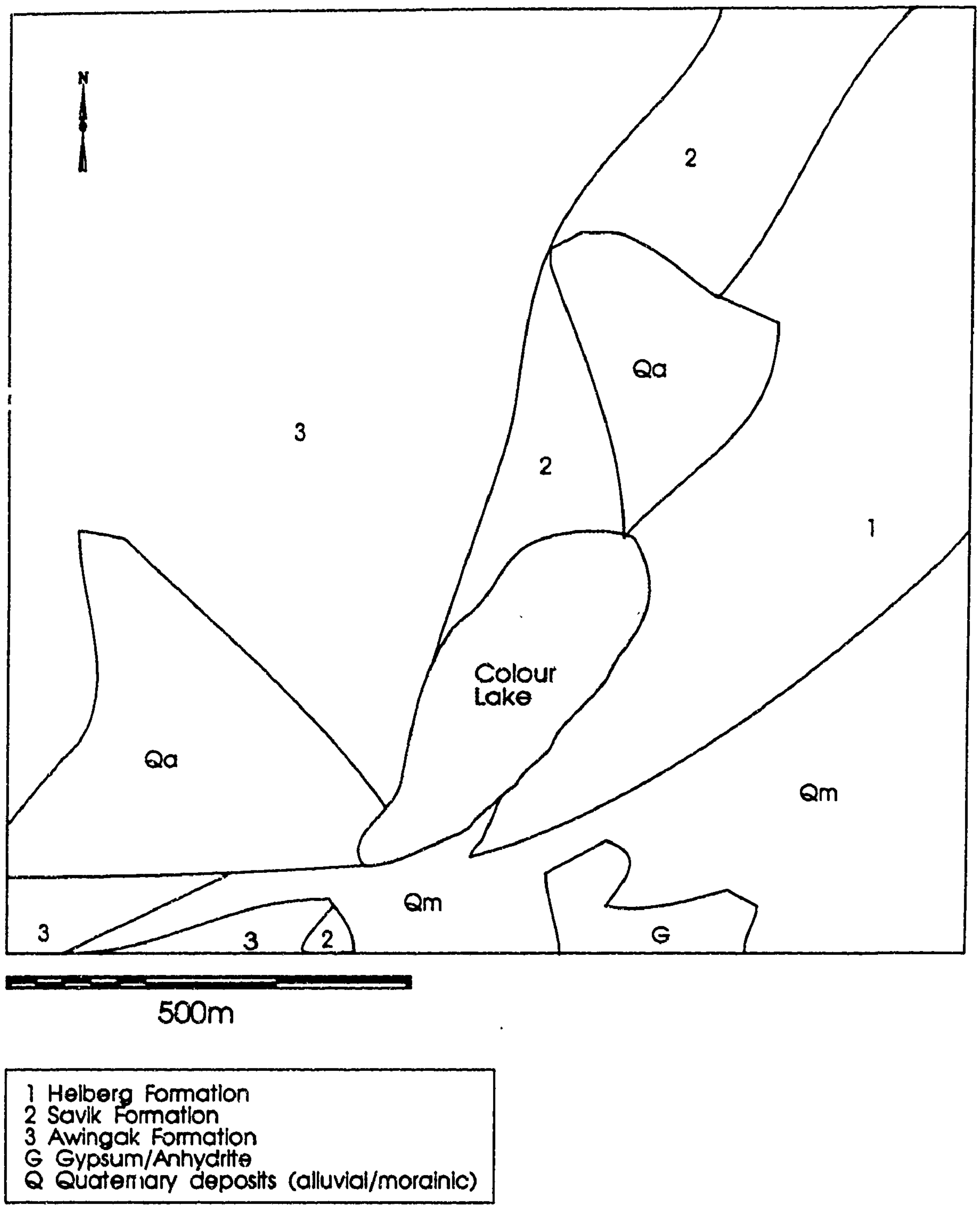

Figure 1.3. Geological map of the Base Camp area (after Fricker, 1963b).

evidence of glacial action. Boesch (1963) identifies two zones of glacial traces, a lower zone (up to 280 m a.s.l.), which he attributes to a younger, Wisconsinan glaciation and a higher (up to 680 m a.s.l.), older zone of pre-Wisconsinan age. However, Lemmen (1991) suggests that these two zones are attributed to glacier dynamics rather than to different glacial periods. ^{14}C dating of marine shells of the Expedition River valley terraces gives an age of 9000 B.P. (Müller, 1963). His conclusion is that in the last 9000 years the White and Thompson glacier did not advance more than a few hundred meters beyond their present position (Müller, 1963). A new approach of identifying glacial history is suggested by Lemmen *et al.* (1991). Using the marine sediment record of Expedition Fiord in combination with the terrestrial geomorphology of the area a significant expansion of local glaciers during Late Wisconsinan is proposed (Lemmen *et al.*, 1991).

The evidence of earlier glacierization of the Expedition Fiord area leads to the conclusion that Colour Lake was formed by glacial action. Müller (1963) suggests that during that time a south-west arm of the White Glacier occupied the valley. Melting of dead ice and/or glacial erosion created the deep Colour Lake basin, "an almost classical example of a glacial lake" (Müller, 1963).

CHAPTER 2 METHODS

2. Site Investigations

2.1. Introduction

The EIF and WIF sub basins in the Colour Lake Catchment were chosen for an intensive study for several reasons. Research on the streams draining into Colour Lake has been carried out since 1984. The results of this research made it possible to discuss and evaluate field techniques prior to the field season in 1991. Field work at Colour Lake started before the snowmelt began on 4 May, and finished on 21 August 1991. In addition, field work was carried out from 23 July to 24 August 1992.

The WIF/W stream (WIF/W) in the WIF basin and the EIF/W stream (EIF) in the EIF basin drain continuously from spring to fall into Colour Lake. The continuity in runoff is important because one of the objectives of this study is to look at their seasonal changes in hydrogeochemistry. Both basins are relatively easy to monitor because they are small in size and located in close proximity to each other. However, they show significant differences in their hydrology and geochemistry.

Field and laboratory activities in and around the Colour Lake catchment involved installing and reading instruments and taking samples from soil, surface and ground waters and bedrock. Some preliminary analyses of water samples and soils were done on site in the laboratory at the base camp.

2.1.2. Basin Characteristics and Topography

Colour Lake has a surface area of 102,070 m^2, a maximum depth of 24 m and a mean depth of 10 m (Allan *et al.*, 1987). The outflow at the south-west end of the lake is marshy, shallow and not well defined during snowmelt; later in the summer it becomes more restricted to a small, well defined channel. The south-east and north-west slopes (slope at MP3 from lake to top of ridge in 30 m intervals averages 14.8°; range 3° to 22°, n=7) adjacent to the lake are steep compared to the north-east and south-west shores (Figure 1.2). The south-east shore ("east slope" or "Sandstone Dome") is very steep (slope at MP6 from lake to top of ridge in 30 m intervals averages 26.4°; range 19° to 33°, n=5) and signs of material movement indicate the solifluction activity on this hillslope.

The Colour Lake catchment has a size of 790,000 m^2 and consists of six sub basins (Figure 2.1 and Table 2.1). Streams in the Colour Lake catchment are ephemeral; only the WIF/W and EIF streams flow continuously from spring to fall, contributing 99% of the total surface stream inflow into Colour Lake during springmelt and 100% during fall (English *et al.*, 1991). All other streams draining from the North Shore (Stream A and Gordon Creek), South Shore (Stream B and Knoff), WIF (WIF/2) and EIF basin (No Name Creek) only flow into the lake during snowmelt and after high precipitation events.

There are some major geomorphological differences between the WIF and EIF basin that are important for this study. Generally the WIF basin is the largest

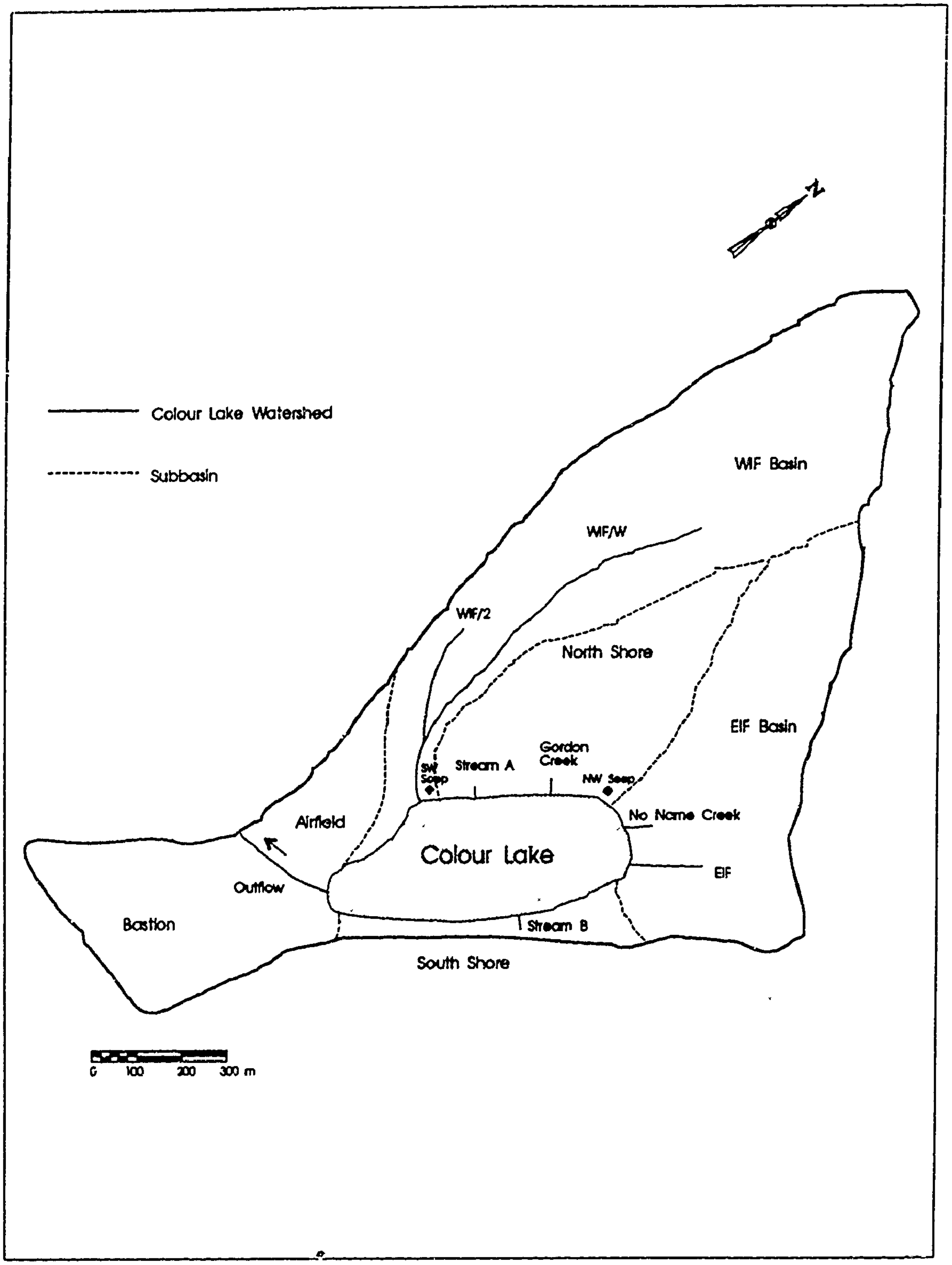

Figure 2.1. The Colour Lake catchment (after Allan *et al.*, 1987).

Location	Area (m^2)
Colour Lake Catchment (excluding lake)	790,000
Colour Lake surface area	102,070
WIF	319,471
EIF	201,940
Airfield	52,983
Bastion	108,510
North Shore	140,598
South Shore	33,909

Table 2.1. Size of the Colour Lake catchment and sub basins (m^2)
For location see Figure 2.1.

sub basin (319,471 m^2), has an elongated shape and extends to a greater altitude (Figure 2.2). Of note are two relatively deep valleys in the WIF basin, the rest of the basin is gradually sloped (Figures 2.2 and 2.3). Basically the WIF basin can be broken down into 2 major physiographic and hydrologic units: 1) the western part of the basin extending to the highest altitude, which supplies water for runoff in the WIF/2 stream and 2) the deep valleys in the eastern part, which supply water for the WIF/W stream. These valleys extend north along the north-western topographic divide adjacent to the North Shore and EIF basin. The WIF/W stream flows under large rocks at the bottom of the former valley before draining onto the alluvial fan (Figure 2.2). The stream gauging station is located in the alluvial fan area, approximately 25 m downstream from the point at which the stream discharges from beneath the large rocks in the lower valley. Below this location high water velocities

Figure 2.2. Air photo showing the sub basins of the Colour Lake catchment and geomorphological characteristics. Scale at lake level is 1:7831 (Energy, Mines and Resources, National Air Photo Library, photo A24755-71, August 1977).

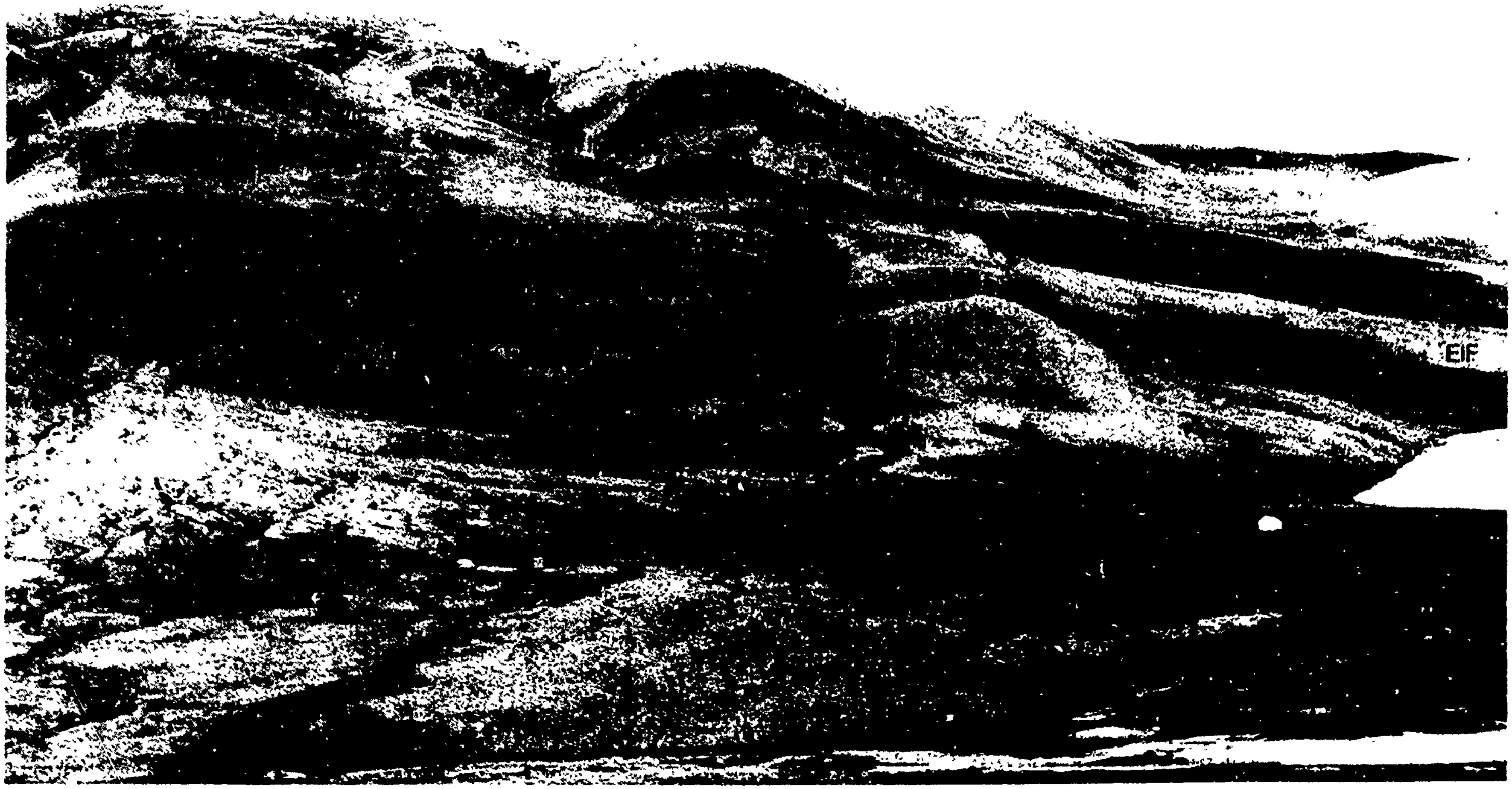

Figure 2.3. Photograph showing the deep valleys in the WIF basin in August, 1992. Note also the small,but relatively deep valley in the western part of the EIF basin. Height of white tent is approximately 2.5 metres.

have cut a well defined stream bed, approximately 20 cm deep. The other stream in the WIF basin, WIF/2, originates in the middle reaches of the alluvial fan and flows into the WIF/W stream (Figure 2.1). The stream bed is wider, shallower, rocky and is thought to be abandoned channel tributary of the stream which is presently not flowing into Colour Lake (Figure 2.2).

The EIF basin is the second largest sub basin in the Colour Lake catchment (201,940 m^2) and has a triangular shape. The centre part of the basin is relatively flat with a gradual slope (average slope of 30 m intervals measurements is 2.6°; range 2° to 4°, n=8) in comparison to the steep adjacent north-west and south-east slopes (Figure 2.2). In the western, upper part of the basin a small, but relatively deep valley is present (Figure 2.3). The EIF stream runs parallel to the south-west slope underneath rocks and becomes visible approximately 5 m before it drains into the lake.

2.1.3. Surficial geology, permafrost, soils

Low precipitation rates, low temperatures and the presence of permafrost are limiting factors for the weathering of bedrock and the development of soils. Hodgson (1989) reports that the depth of weathered bedrock, recorded from boreholes in several places on the Queen Elizabeth Islands, exceeds the active layer thickness for several metres.

Weathered bedrock is the most dominant surficial material in the Colour Lake catchment. Depending on the bedrock geology (Chapter 1) the weathered material ranges from clay to boulder size material. In the WIF basin, a ridge of weathered bedrock runs almost up to the top of the basin (Figure 2.2). Another important geomorphological feature in the WIF basin are felsenmeers in the "deep valleys", where rocks are extremely large (up to 2.5 m length). The north-west slope of the EIF is best described as frost-shattered blockfield. Dissaggregation of bedrock at the south-east slope (Sandstone Dome) has mainly created silt and sand fractions. In the lower part of the alluvial fan areas and at the base of slopes in the WIF and EIF basin, soil formation is favoured by the accumulation of fine-grain materials (clay) and the availability of water. Doran (1990) calculated that the stream at the north-eastern topographical divide of the WIF basin, which was flowing into Colour Lake and building up the large alluvial fan at the south-west end of the lake, left the basin 300 to 800 years B.P.. The alluvial fan in the EIF basin is much smaller in size compared to the alluvial fan in the WIF basin (Figure 2.2).

2.1.4. Vegetation

Plant growth in the high Arctic is limited by low temperatures, low moisture availability, shortage of nutrients and a short growing season. Vegetation studies can therefore be useful in identifying hydrological regimes (for example based on soil moisture content) within a catchment. In the Expedition Fiord area vegetation was mapped by Beschel (1963), but no studies have been carried out in the Colour Lake catchment.

The WIF basin can be divided into two vegetation zones: The upper "drier" part of the basin and a lower "wet" part, the latter being the alluvial fan areas where the WIF/W stream overflows during high flow periods and the suprapermafrost groundwater table is assumed to be high. Mainly mosses and lichens and a few scattered plants of *Dryas integrifolia, Salix arctica* and *Papaver radicatum* are found in the upper part, predominantly on rocks, where moisture is supplied from the melting of ground ice underneath. Further down in the alluvial fan area where the stream overflows, vegetation is abundant (vegetation cover > 80%) and plants of the wet sedge meadow community dominate (*Carex* species, especially *Carex aquatilis, Eriophorum scheuchzeri, Saxifraga tricuspidata*). In comparison, the lower part of the EIF basin (alluvial fan) is less abundant in vegetation (vegetation cover ≤ 80%). *Carex aquatilis* and other *Carex* species are the dominant plants and suggest a wet to mesic, sedge meadow community (Bliss and Svoboda, 1984). The adjacent north-west and south-east slopes have small patches of mosses and *Dryas integrifolia* and few scattered plants of *Papaver radicatum*.

2.1.5. General hydrology

Nagel (1979) describes the typical hydrological regime of a high arctic region. Over the arctic winter, snow accumulates. Snowmelt starts in May/June when the soil is still frozen and infiltration therefore limited. As a result, sheetlike surface runoff (overland flow) and high runoff in drainage channels occurs. Thawing of the frozen ground during the summer increases the soil storage capacity and the suprapermafrost groundwater flow in the active layer. Seeps develop where suprapermafrost groundwater discharges from the ground. Precipitation in July/August causes rapid throughflow resulting in peak runoff in streams. The hydrological year ends with the refreezing of the active layer and, subsequently, decreasing runoff.

2.2. Field Methods

2.2.1. Surface runoff

To estimate the water input into Colour Lake, discharge of the streams was measured as close to the lake as possible. Generally, surface runoff of the streams was measured at least three times a day, during snowmelt and during rainstorms at least 10 times a day. V-notch weirs made of plywood were used to monitor the discharge of the streams. The WIF/W weir was installed at a site before it confluences with the WIF/2, so that differences in the discharge could be recorded (Figure 2.4; Colour Print 2). Runoff in the WIF/2 only occurs during snowmelt and later in the season after rainstorms. Discharge from the WIF/W was therefore the only regular input from the WIF sub basin into Colour Lake. A standard stage board was fixed on the reservoir side of the V-notch weir. A stage-discharge relationship was established by taking the average of three to five measurements (taken manually

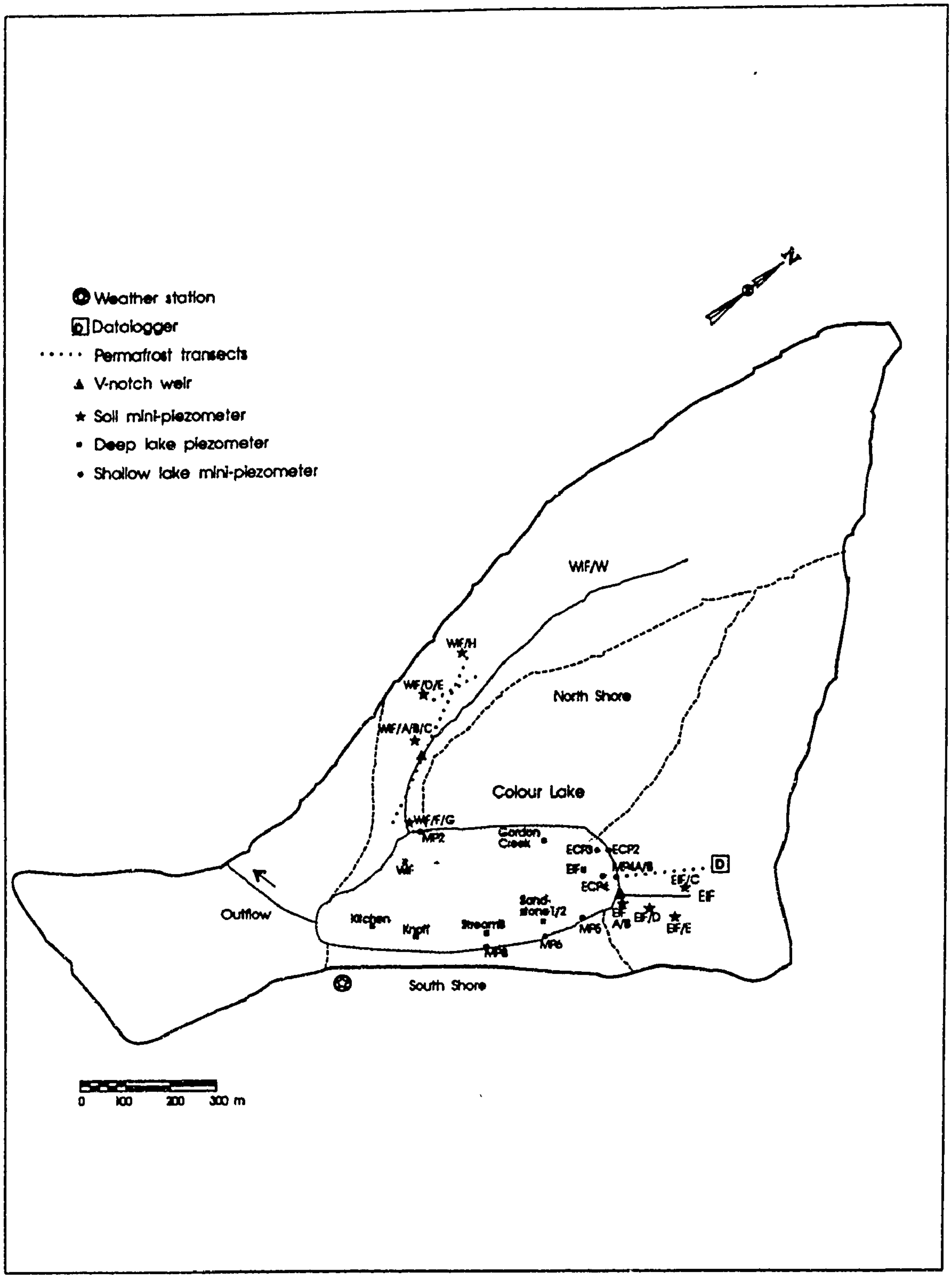

Figure 2.4. Instrumentation of the Colour Lake catchment.

with volumetric container and stopwatch) at the V-notch during different flow rates and plotting them against the stage (Appendix A). Injection of red dye into the pool above the EIF weir indicated leakage beneath the weir because of large gravel deposits in the stream bed (Colour Print 1). Therefore the first weir was removed and a second weir with plastic sheeting was installed. Discharge of the WIF/2 was measured by multiplying the cross-sectional area of the stream with the water velocity. To accomplish this, water depth and water velocity were recorded at regular intervals across the stream profile. The water velocity was measured, if possible, at two different depths using a Marsh McBirney electromagnetic water current meter Model 512 OEM. Total stream discharge was obtained by the summation of each discharge interval (product of interval area and water velocity) across the stream. After the discharge had decreased in the WIF/2, stream discharge was calculated from volumetric measurements over time; stop-watch readings were taken while a plastic bag was firmly pressed into the stream bed to record the volume of water ("baggy method"). This method and the area-velocity method outlined above were also used during high flow periods (snowmelt and after the rainstorm) when overland flow occurred. Additionally, a visual estimation of runoff was used when none of the methods mentioned above were satisfactory to estimate the total runoff.

2.2.2. Subsurface flow

Suprapermafrost groundwater flow in the active layer

Mini-piezometers (Lee and Cherry, 1978) were installed in the active layer of

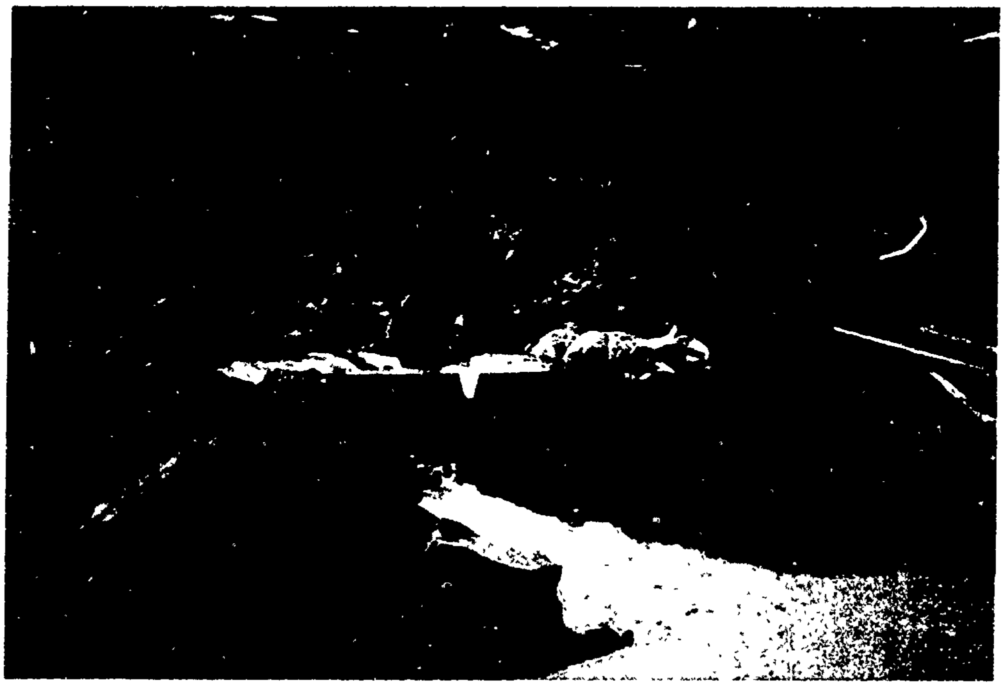

Colour Print 1. EIF stream weir, 8 June, 1991.

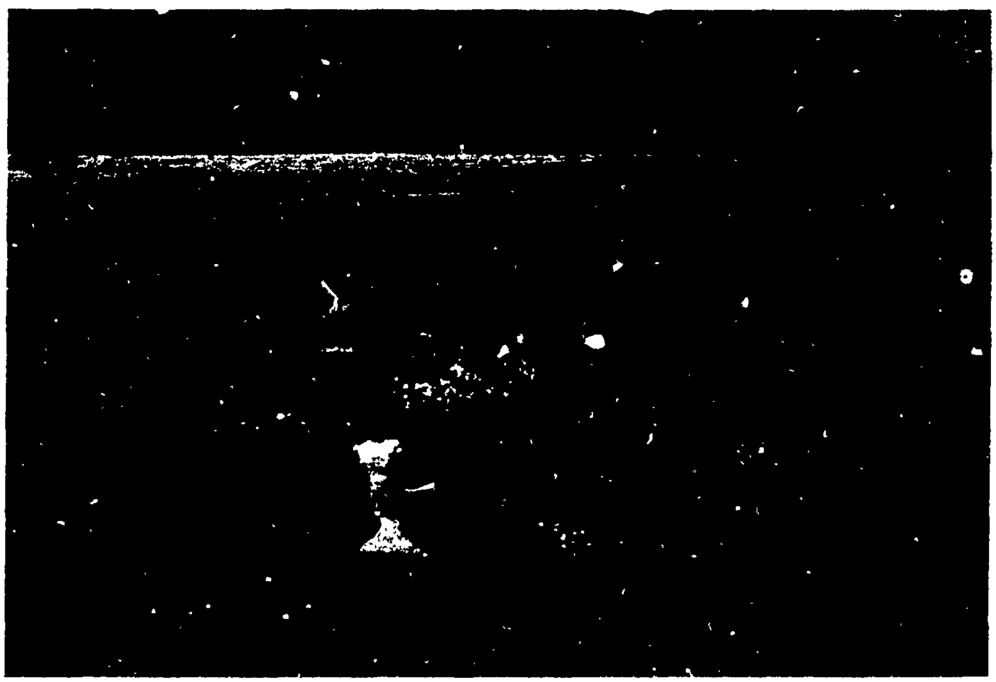

Colour Print 2. WIF/W stream weir, 19 July, 1991. Note cottongrass (*Eriophorum scheuchzeri*) along stream channel.

the sub basins and around the shoreline of Colour Lake in order to extract suprapermafrost groundwater for chemical analyses and to estimate the input of suprapermafrost groundwater input into Colour Lake (Figure 2.4). Mini-piezometers were installed in the soil at specific locations in the lower part of the EIF and WIF basin (Figure 2.4). At some sites, mini-piezometers were driven into the active layer at different depths ("multilevel piezometers") (Table 2.2).

Name (Location)	Depth of screened interval (cm)	Notes
WIF/A WIF/B WIF/C	21-31 15-25 5-15	All dry throughout the field season
WIF/2/D WIF/2/E	34-44 18-28	Nested piezometers; WIF/2/D not enough water to extract samples
WIF/F WIF/G	23-33 12-22	Nested piezometers; WIF/F not enough water to extract samples
WIF/H	0-10	
EIF/A EIF/B	7-17 21.5-31.5	
EIF/C	6.7-16.7	Not enough water to extract samples
EIF/D	13-23	
EIF/E	14-24	

Table 2.2. Depth of soil mini-piezometers in the WIF and EIF basins, 1991.

This was important for identifying the seasonal suprapermafrost groundwater flow and allowed water sampling at different depths. Not all of the soil mini-piezometers yielded enough water for chemistry analysis (Table 2.2). Other mini-piezometers in the shallow littoral zone around Colour Lake were installed in years prior to the summer field season of 1991 (Schiff *et al.*, 1991). Additional mini-piezometers at greater water and sediment depths (ECP2, ECP3, ECP4) were only successfully installed at sites close to the EIF basin (Figure 2.4). A summary of water depths, depths into sediment is presented in Table 2.3.

Seeps

Seeps are sites, where suprapermafrost groundwater discharges above the lake level. One seepage site (South-West seep) was located in the WIF basin close to the shoreline of Colour Lake in mid July (Figure 2.1). The North-West seep only discharged after the rainstorm in August had occurred. Discharge was measured at least twice a week with a plastic bag while recording the time ("baggy method"). To avoid sediment contamination, water samples were taken from a plastic sheeting imbedded into the soil around the seepage site.

Groundwater associated with the talik underlying Colour Lake

Drivepoint piezometers (Ingleton, in preparation) were installed in May 1991 in deeper parts of the lake (up to 14 m water depths). During installation the 2 m thick ice cover acted as a stable platform from where the piezometers could be driven into the lake sediments. As the ice cover began shifting later in the field season, the piezometer tubings were submerged under the ice. During July therefore,

Deep lake drivepoint piezometers									
Location	Gordon Creek	Sandstone 1	Sandstone 2	Stream B	Knoff	East Inflow	Kitchen	West Inflow	
Water depth (m)	5.8	5.8	5.8	9.78	9.37	14.8	8.9	8.14	
Depth in sediment (m)	1.5	1	0.5	1*	1.6	1*	1.8	1.65	
Mini-piezometers									
Location	ECP2	ECP3	ECP4	MP8	MP2	MP4A	MP4B	MP5	MP6
Water depth (m)	0.25	1.5	1.5	0.248	0.105	0.14	0.16	0.277	0.248
Depth in sediment (m)	0.64	1.08	1	0.694	0.67	0.745	0.359	0.58	0.578

*: could not be retrieved after ice off

Table 2.3. Installed deep and shallow piezometers in Colour Lake, 1991.

taking samples or readings was impossible. Reading of the deep piezometers' heads relative to lake level was recorded at least 3 times a week. Water levels in the mini-piezometers around the shoreline were first recorded in mid July. Readings from the drivepoint piezometers were taken regularly at least twice a week until the end of the field season in August.

2.2.3. Hydraulic head readings and hydraulic conductivity testing

Slug and bail tests (Freeze and Cherry, 1979) were performed on all shallow and deep lake piezometers to measure the hydraulic conductivity of the sediments. Problems occurred with the deep piezometers because the tubing had to be kept straight above the water during readings. To overcome this problem the tubing was attached to "floating platforms" built out of plywood, which kept the tubing straight and always at the same height above the water. A second piece of tubing, in which the lake level could be recorded, was attached to the piezometer tubing on the platform. The head of the piezometer was always read relative to the lake level in the second tubing. This increased accuracy of the readings by avoiding inaccuracies caused by capillary forces in the tubing and, in addition, measurements could be taken from the boat without moving the piezometer. The latter was necessary, because some piezometers had a very long equilibration time. Hydraulic heads relative to the lake level were read with an electronic water level tape. Small differences between the head of the lake and the piezometer made it necessary to stabilize the last one metre of the water level tape with a small stick.

2.2.4. Permafrost depth probing

With the seasonally thawing upper ground, a saturated zone (suprapermafrost groundwater) forms in the active layer. It was important to determine the frost table because this is the depth at which the groundwater movement becomes restricted.

Permafrost depth transects were established in the EIF and WIF basins close to the streams and soil piezometers in the lower parts of the WIF and EIF basins (Figure 2.4). On these transects point measurements were taken every 2 metres using a steel rod with a sharp tip pounded into the active layer until frozen ground was encountered. Accuracy was tested by comparison the thaw depth of the active layer in an excavated soil pit to the depth reading obtained with the steel rod whenever soil samples were taken.

2.2.5. Soil sampling

Soil samples from the EIF, WIF sub basin and Sandstone Dome were taken in June and July for chemical analysis. A soil pit was excavated until frozen ground was encountered. After a description of the soil horizons, 500 to 1000 g samples were taken from each horizon. A sub sample for determining soil moisture content was taken in a pre-weighted soil tin and sealed immediately. Soil handling and analysis are described in section 2.3.

2.2.6. Weather observations

Weather observations at the Colour Lake base camp were recorded twice a day at 7:00 and 19:00 CST as part of the Aviation Weather Report to the Polar Continental Shelf Project in Resolute Bay, N.W.T. Data collected for these reports include maximum and minimum air temperature, precipitation, wind speed and direction and sunshine hours. Air temperatures were read from standard alcohol thermometers in a Stevenson screen (Figure 2.4). Precipitation was sampled using a Standard Atmospheric Environment Service (Environment Canada) precipitation gauge. A wooden table lined with plastic sheeting was constructed close to the precipitation gauge to sample water and snow for chemical analysis. At the onset of a precipitation event, clean plastic Ziploc bags were also hung from a clothes line close to the Stevenson screen to ensure that enough water was available for chemical analysis. Total bright sunshine hours were measured with two Campbell-Stokes sunshine recorders. Wind speed was measured with a hand held anemometer and wind direction read from a standard wind vane. Incoming and outgoing solar radiation was measured hourly in the EIF basin using REBS (Radiation Energy Balance Systems) net radiometers and recorded on 21X Campbell Scientific dataloggers.

2.2.7. Snow Survey

In order to estimate the snow-water equivalent (SWE) of the EIF and WIF basins, snow surveys were conducted in early May on predetermined transects in the WIF basin and at random locations throughout the EIF basin before any runoff occurred (Figure 2.5). The topography of the EIF basin is more homogeneous and therefore sample sites were chosen randomly over the lower part of the basin (Figure 2.5). Five measurements of snow density and snow depth were taken at each sampling site along each transect. Total basin storage was calculated by extrapolating the mean snow density value and multiplying with mean snow depth. Air photos and pictures taken during the snow melt were also used to determine the mean snow depth and areal snow cover.

2.2.8. Sampling strategy

The focus of this research is to identify seasonal changes in the hydrochemistry of surface and subsurface waters. Therefore a regular sampling strategy was followed over the entire field season. Streams were sampled at the discharge measurement location at least once a day at the same time. Water from soil mini-piezometers and shallow lake mini-piezometers was taken once a week. As a result of the shifting lake ice cover during June and July, samples from the deep lake piezometers could only be taken in May and August. All piezometers were purged before samples were

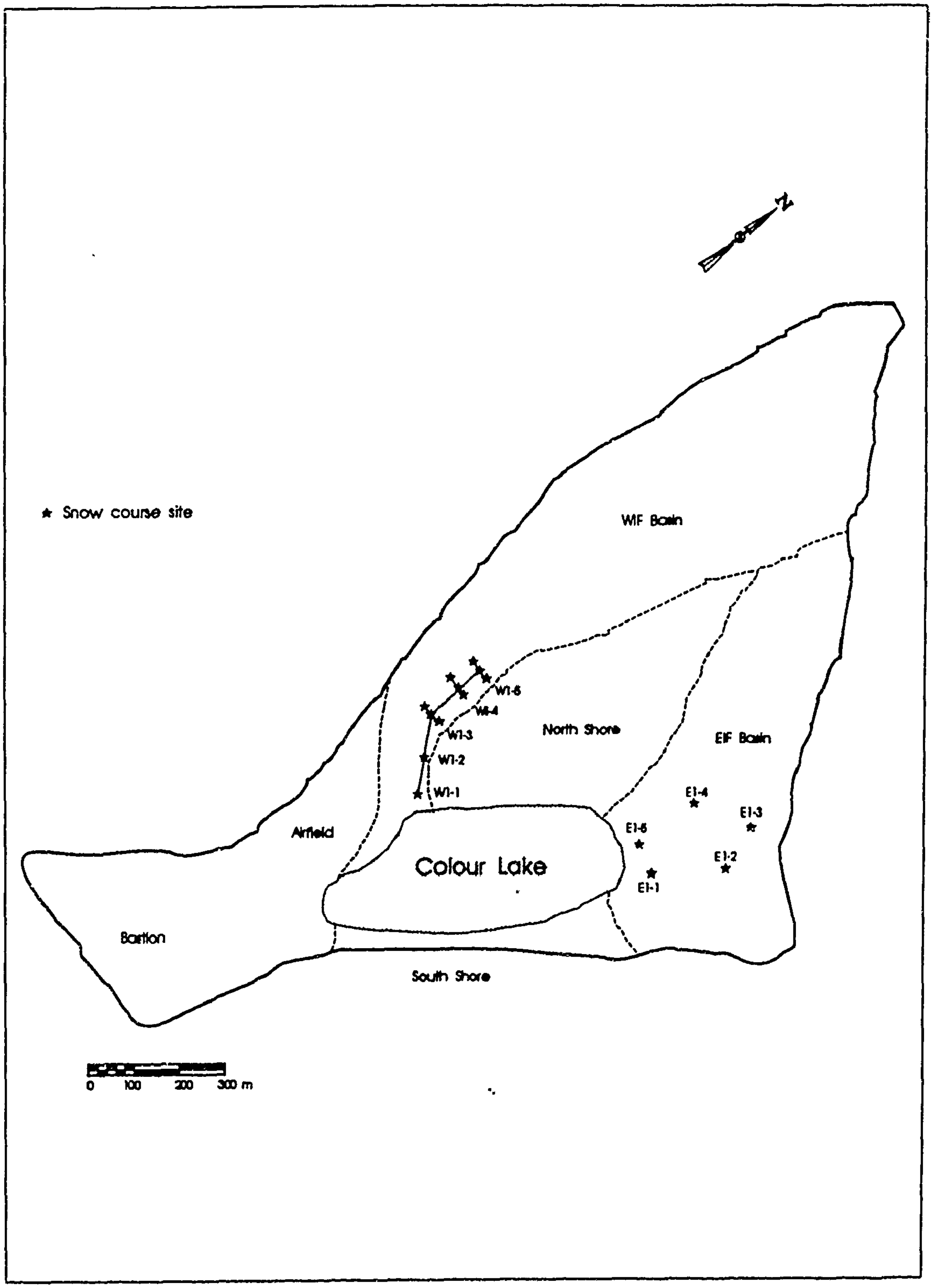

Figure 2.5. Snow survey sites in the EIF and WIF basins.

taken. Piezometers with low hydraulic conductivities of deep lake sediments were sampled several times over the day. Clean seep water samples were obtained biweekly from the plastic sheeting installed at the seepage site. Samples from different snow layers were taken from snowpits at various sites in the basins in May before snowmelt started. In order to estimate the chemical importance of precipitation for the stream chemistry it was necessary to sample every snowfall and rainfall during the field season.

2.3. Analytical and Laboratory Methods

2.3.1. Water sampling methods

In order to maximize sampling efficiency, two 250 ml plastic bottles were triple rinsed and filled to the top at each site. To avoid any contamination, the same two bottles were always used at the same sample location. One 250 ml sample was analyzed for pH and electrical conductivity (corrected to 25°C) at the lab facilities at the base camp, the other 250 ml sample was filtered through a 0.45 μm microfilter and stored in acid-prewashed, distilled water rinsed 20 ml (cation) and 125 ml (anion) sample bottles. Cation samples were acidified with concentrated HNO_3 to a pH below 2. All samples were kept cool outside the hut and transported to Waterloo in August.

Throughout this thesis reference is made to total dissolved solids (TDS). These TDS concentrations are calculated directly from the electrical conductivity using the formula:

$$\text{TDS (mg/l)} = \frac{[\text{initial conductivity } \mu S/cm]}{[1+0.02 \text{ (cell temp.}^{\circ}\text{C-25)}]} \times 0.666$$

Although the calculated TDS concentrations are not necessarily accurate estimates of the real TDS concentrations (calculated by the summation of anion and cation concentration), the calculated values provide an index of total dissolved solids. Furthermore, the statistical analysis (correlation and regression) is not influenced by the conversion.

Total alkalinity was determined biweekly on 25 ml stream sample aliquots using the Gran-Titration Method (Stumm and Morgan, 1981).

2.3.2. Soil preparation and analysis

Soil moisture was determined gravimetrically at the Base Camp by oven drying the soil sub sample at approximately 100°C (Hartge and Horn, 1989). Electrical conductivity and pH were also measured in the field using a sub sample of the bulk soil sample, which was taken to Waterloo for subsequent analysis. Electrical conductivity was measured in a 1:2 fresh soil-deionized water solution, since this method was applied for soil samples in 1985 on soils in the Colour Lake catchment (Allan *et al.*, 1987). The method for measuring soil pH in water is outlined in Peech (1965). Extracts of soil to water ratios of 1:5 were prepared from air dried soil samples (Bower and Wilcox, 1965) and analyzed for major cation and anions.

2.3.3. Cation and anion analysis

Analysis of major cations and metals (Na^+, K^+, Mg^{2+}, Ca^{2+}, Fe^{2+} and Al^{3+}) was performed with an Atomic Absorption Spectrometer (AAS) Model Perkin Elmer 3100 at the water chemistry lab, Wilfrid Laurier University, using standard methods outlined in Perkin Elmer (1982). Anions were analyzed using a 12 Dionex Ion chromatograph at Canada's Centre for Inland Waters, Burlington, in accordance with methods outlined by the same institute. The analytical uncertainty (precision) for all ions lies within ±5%. A further indication of the quality of ion analysis is given by charge balance calculations (Freeze and Cherry, 1979; Reardon, 1992):

$$\text{Charge imbalance } [\%] = \left| \frac{\Sigma\text{cations} - \Sigma\text{anions}}{\Sigma\text{cations} + \Sigma\text{anions}} \right| \times 100$$

where units are in equivalents. A charge imbalance within ±5% is assumed to be very good and above 10% usually unacceptable.

2.3.4. Tritium analysis

Isotopes of oxygen (^{18}O, ^{17}O, ^{16}O) and hydrogen (^{3}H, ^{1}H) are part of the water molecule and are therefore possible tracers for the study of water movement. For this study, the radioactive isotope tritium (^{3}H; $T_{1/2}=12.35$ years) was chosen. Concentrations of tritium are usually expressed in Tritium Units (T.U.), where 1 T.U.

unit corresponds to one tritium atom in 10^{18} hydrogen atoms (Fontes, 1980). Tritium samples were analyzed by direct scintillation counting at the Isotope Laboratory, University of Waterloo, with an uncertainty of ±8 T.U.'s.

2.3.5. Thin sections and description of rock samples

Three thin sections were prepared from the soil forming bedrock material on the "Sandstone Hillslope" to determine the main rock forming minerals. This was important in identifying the influence of this formation upon the local surface and subsurface water chemistry. In addition, nine rock samples were classified in accordance with standard methods by the Department of Geology, University of Freiburg, Germany. The description of rock samples includes: texture, sediment structure, grain size, components, porosity and carbonate content.

2.4. Statistical data treatment

Using the statistical package SPSS/PC, Version 3.2, basic statistics (arithmetic mean, median, standard deviation, maximum, minimum) were applied to the data set. Additionally, linear correlation, bivariate and multivariate regression were used to determine relationships between discharge and various chemical variables and discharge, air temperature and precipitation.

CHAPTER 3 THE SNOWMELT

3.1. Introduction: Climate and division into hydrological periods

The climate of west central Axel Heiberg Island was exceptional during the summer of 1991 because of a rainstorm that occurred in August. From 1 to 15 of August, a total rainfall of 117 mm was measured at the Colour Lake catchment, with highest intensities of 37.78 mm/day on 2 August (Table 3.1). In contrast, Eureka only recorded 20 mm for this time, which demonstrates the local occurrence of the storm (Table 3.1). In agreement with the data of Ohmura and Müller (1977) July was the warmest month at the Base Camp in 1991, with an average daily temperature of 6.3°C and maximum temperatures up to 19.5 °C.

Precipitation (mm)	May (5 to 31)	June	July	August (1 to 15)	$\sum_{5May-31Aug}$
Colour Lake	0	5.6	22.9	117	146
Eureka	0.6	16	12.4	20.8	49.8

Table 3.1. Precipitation at Colour Lake and Eureka, May to August 1991.

As a result of dominating climatic events (such as snowmelt, rainstorm and highest temperatures in July) and their effects on the stream discharge (Figure 3.1) this study identifies three hydrologic periods: 1. Snowmelt (1 to 11 June), 2. the period of active

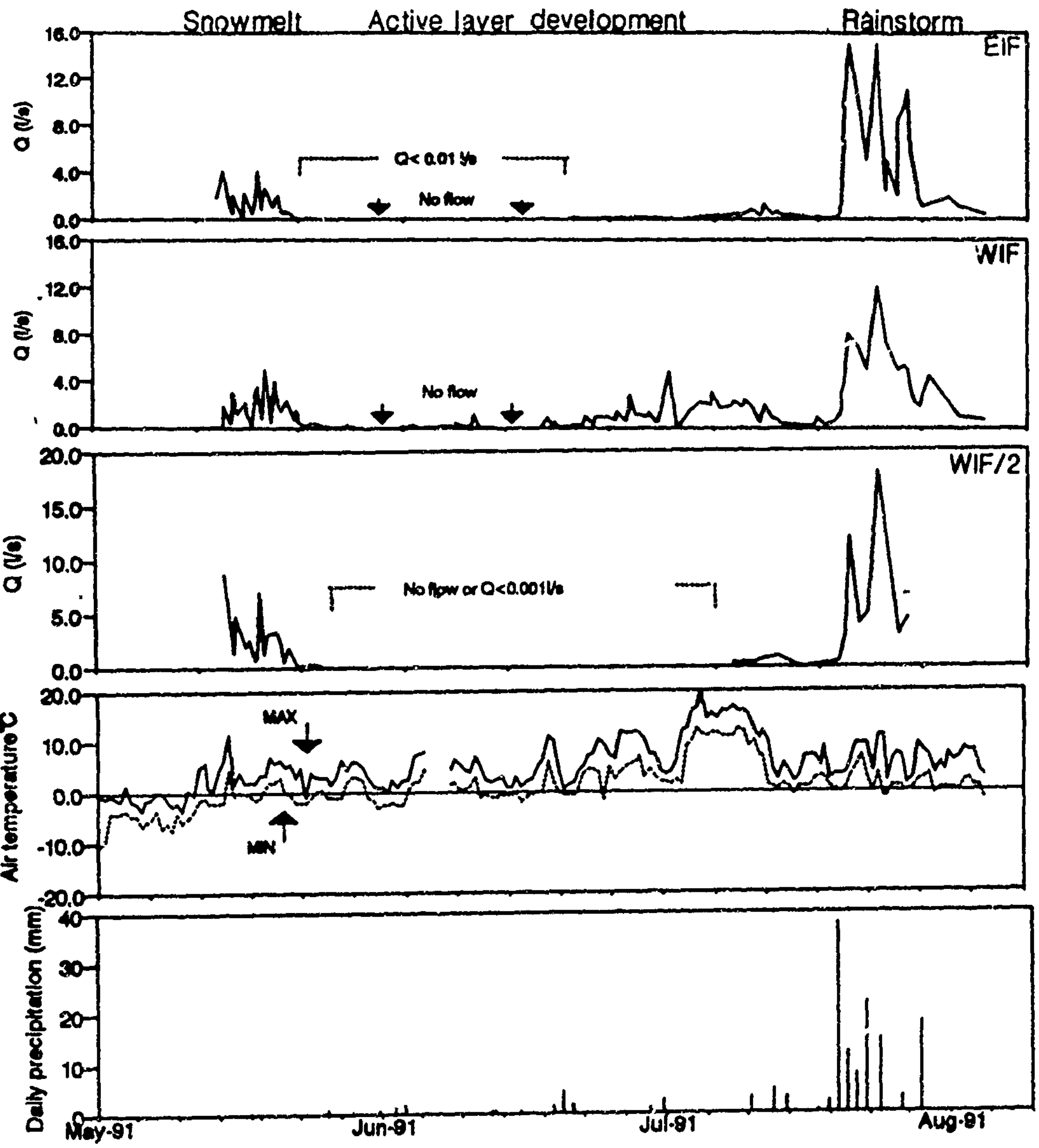

Figure 3.1. Precipitation, air temperatures and hydrographs for the EIF, WIF/W and WIF/2 for May to August, 1991.

layer development (12 June to 1 August) and 3. rainstorm (2 to 16 August). The end of the snowmelt period was defined by complete loss of the snow cover in the basin, the recession of streams to base flow and the lack of diurnal cycles in stream hydrographs. Further analyses of the relationship between discharge and TDS concentrations and ion concentrations in the streams indicate important changes in the terrestrial drainage system and suggest the division of the period of active layer development into three subperiods (Table 3.2).

	Snowmelt	Period of active layer development			Rainstorm
	(1-11 June)	1 (12 June-5 July)	2 (6-17 July)	3 (16 July-1 Aug.)	(2-10 Aug)
Total precip.(mm)	0.3	7.1	9.8	11.2	117
% precip. as Snow	100	94	70	42	0
% precip. as rain	0	6	30	58	100
Trace precip.*	5 times	7 times	1 time	1 time	0 times
Av.daily temp. °C **	1.9	2.1	5.1	8.8	3.9
Max.temp.	11.5 (3 June)	11.0 (4 July)	12.0 (17 July)	19.5 (19 July)	11.0 (6 Aug.)
Min.temp.	-1.5 (6 June)	-3.0 (18 June)	-1.5 (10 July)	-0.5 (28 July)	-1.0 (6 Aug.)

* trace precipitation < 0.1 mm

** calculated as: $\frac{7\text{ am } \Sigma\text{Min, Max temp.}/2 + 7\text{ pm } \Sigma\text{Min, Max temp.}/2}{2}$

Table 3.2. Summary of climatic characteristics for the hydrological periods, May to August 1991.

The following Chapters will address hydrological and geochemical characteristics of the EIF stream (EIF) and the WIF/W stream (WIF/W) for each of the defined periods separately. During the beginning of the period of active layer development, runoff in the WIF/2 stream (WIF/2) ceases (Figure 3.1) and therefore not data are available for a discussion of this period. However, the snowmelt and rainstorm periods will be included in the discussion to demonstrate hydrological and chemical characteristics of this intermittent stream.

3.2. The snowmelt period

3.2.1. Snow distribution and onset of snowmelt

Upon arrival in the Colour Lake catchment (19 May, 1991) the very inhomogeneous distribution of the snow cover was apparent. The snow cover was generally thin and only the relatively flat alluvial fan areas of the WIF and EIF catchments were completely snow covered. Estimations from photographic prints taken from air and ground on 27 May suggest a total snow coverage of approximately 80% in the WIF and approximately 95% in the EIF basin. Large snow free zones existed on the tops of ridges and steep slopes in contrast to high snow accumulations in the deep valleys of the WIF basin. Accumulation is attributed to wind-induced redistribution, where drifting snow was trapped in depressions, valleys and between the hummocks of the tundra. Further evidence of wind transport during the winter was given by a dirty snow layer. At the time of the first snow survey, snow thickness ranged from a low of 10 to 25 cm in the alluvial fan areas to a maximum of 65 cm in the lower, northerly extending valley of the WIF basin. Snow densities obtained from snow profiles ranged between 0.1 to 0.44 g/cm^3 (mean 0.23; Std.dev. 0.09, n=21), which is in agreement with values obtained from previous studies in the Colour Lake catchment (Adams, 1987; Steffen and Müller, 1977). Typically, a snow profile was characterized by an upper layer with low density (0.14 g/cm^3) followed by a snow layer of higher density (> 0.30 g/cm^3) and a layer of medium density (0.22-0.25 g/cm^3) on the bottom. The mean snow water equivalent (SWE) in early May before any melting had occurred was 82 mm for the WIF basin and 52 mm for the EIF basin. These numbers are in agreement with the mean winter SWE of 76 mm for seven years (1966-1976) by Steffen and Müller (1977). It is important to note that the higher SWE in the WIF basin is mainly attributed to the thick snowcover in the northerly extending valleys, resulting in a SWE of up to 22 mm at some sites. In comparison, the maximum SWE obtained in the alluvial fan area is only 9 mm.

Sublimation of snow during May 1991, when the radiation input was high may have reduced the SWE. Ohmura (1982a) reports an increase of the daily total evaporation in the Colour Lake catchment during the dry snow period (the period from April to early June, where no snow melting occurs) for the years 1969, 1970 and 1972 which he attributes to an increase of air temperature and net-radiation. From April to the beginning of June, the daily total evaporation increases from 0.03 mm to 0.6 mm, which results in 9 mm total evaporation from the snowpack (Ohmura, 1982a). Maximum daily sublimation of 2 mm/d were observed on May 27, 1969 under Föhn conditions (Ohmura, 1982a). Similar results are presented by Rydén

(1977) who reports an increase of the total daily evaporation from 0.03 mm to 0.8 mm for the dry snow period on Truelove Lowland/Devon Island. The second snow survey in the WIF basin undertaken at the end of May, after a period of long, bright sunshine hours, yielded a SWE of 72 mm. Although it could be argued that part of the 10 mm loss of SWE is the result of sublimation, the snow survey data suggest that site variabilities and different field methodologies account for the loss of 10 mm SWE (there is no consistent loss of SWE at the snow survey points over time; a ±50% variation of SWE is recorded at two snow survey points from the earlier to the later snow survey). By June 9, the majority of the snowcover had melted, only a few small patches remained (Table 3.3.).

Date	Snow coverage (%)	
	EIF-basin	WIF-basin
27 May 1991	90	75
1 June 1991	62	35
4 June 1991	20	20
9 June 1991	<1	<1

Table 3.3. Snow cover depletion during snowmelt in the WIF and EIF basin.

3.2.2. Snowmelt hydrology

Temperatures above 0°C were first recorded on May 24 and remained positive for most of the field season from May 31 on. On May 27, signs of snow melt were detected on south facing slopes in the Colour Lake catchment and on May 29, very wet, slush snow on the lake ice indicated rapid melting. By May 31, meltwater pools had developed in lower, alluvial fan areas of the catchment, but no runoff occurred in the streams. However, a soil pipe type feature (seep) with a flow rate of 3 ml/sec was found in the middle part of the WIF catchment at a site with a high gradient. Field observations (such as footprints left in the soft soil) reinforce the fact that a thin, unfrozen upper soil layer was present. This is attributed to the (observed) lack of snow at this site. Hence, one possible explanation for the soil pipe phenomenon is that the active layer enables quick infiltration and routing of snowmelt water at an upslope site and that this water is being discharged at a downslope site. Overland flow between the pools was observed on 31 May. At this time, very low flow rates of 1 ml/s in the WIF/W stream were probably induced by disturbance of the channel due to the construction of the weir. Stream runoff (with 1.8 l/sec) started first in the EIF on 2 June around 23:50. The earlier start of runoff in the EIF could be attributed to the south-west aspect of the EIF basin, thereby receiving a larger amount of solar radiation than the WIF basin. In addition, the thinner snowpack of the EIF basin is saturated quicker, which induces earlier discharge in the EIF stream. In the WIF basin, discharge was first noticed in the WIF/2 stream during the afternoon of June 3. Runoff was observed in the WIF/W stream on the following day. Hence, the difference in timing suggests that a different drainage network exists within the WIF basin. Considering the initial high discharge in the WIF/2 it is possible that the initial start and probably the peak of the snowmelt were missed by a few hours. In the WIF/W, the longer response of stream runoff to maximum net-radiation is related to the thick snowcover in the deep valley and also to the northerly aspect of this valley which equates, in this topographical setting, to a considerable period of shading. The lack of the initial discharge peak in the WIF/W stream suggests that either the energy input was not sufficient to generate high stream runoff or that the melting snow was refrozen on the cold substrate.

During snowmelt, widespread overland flow was observed in the low, alluvial fan areas and "channelized" overland flow (for example following microtopography) in the upper part of the basin. The limiting factor for the infiltration of snowmelt water is the low hydraulic conductivity of the frozen ground. Therefore quick saturation occurs in the shallow active layer and the watertable is forced above the ground surface, where the supply of water exceeds the drainage. Different thaw depths of the active layer result in an uneven permafrost table and local depressions in the permafrost table act as sinks for infiltrating snowmelt water, creating standing water conditions. Typically, water extracted from such a pool shows higher ion concentration than snow (TDS concentrations of water from pool: 22 mg/l; snow: 6 mg/l).

The hydrographs of all three streams (EIF, WIF/W, WIF/2) show a pronounced diurnal cycle (Figures 3.2., 3.3., 3.4.), which is caused by diurnal variations in net-radiation (Figure 3.5.). Even with 24 hours of continuous sunlight, net-radiation and all related energy balance elements show a pronounced diurnal cycle (Ohmura, 1982b). Given that three to five discharge measurements were taken daily, it is possible to estimate the time of peak runoff in the WIF/W and EIF.

Unfortunately, not enough discharge data for the WIF/2 are available for this analysis.

Date	Max.daily net-radiation		EIF		WIF/W	
	Time	Watts/ m^2	Q_{max} (l/s)	Time	Q_{max} (l/s)	Time
3 June	N.A.	N.A.	4	16:45	1.8	15:50
4 June	N.A.	N.A.	2	22:50	3	16:00
5 June	N.A.	N.A.	2.1	18:00	*	*
6 June	16:00, 20:00	229 201	4	22:50	3 3.5	16:00 22:30
7 June	11:00 15:00	319 279	2.5 2.3	16:40 23:30	5 3.4	16:30 22:30
8 June	14:00	307	1.9	22:30	4	14:30
9 June	16:00	272	*	*	2.3	17:12
10 June	15:00	314	*	*	1.5	17:42

N.A.: No data available
*: Not enough discharge data available to determine peak flow

Table 3.4. Hydrograph characteristics of the WIF/W and EIF streams during snowmelt, 1-10 June 1991.

In the WIF/W stream, maximum daily discharge occurs in the afternoon (Table 3.4) following the maximum daily net-radiation input. A double peak in net-radiation on 6 and 7 June (Figure 3.5) resulted in a double peak in discharge (Table 3.4). The discharge in the EIF stream during snowmelt consistently peaks later in the day (around 22:30) than that of the WIF/W. Possible reasons for the increased lag time between maximum net-radiation input and maximum discharge may be attributed to the earlier loss of snow in the lower part of the basin and resulting in slower transport of water in the fine grained sediments of the shallow active layer. Other possible factors centre around the stream channel development and the transport route of water towards the channel. It is important to note that a defined stream bed is only present in the lower part of the EIF basin and that this channel is filled with rocks, gravels and fine sediments (Colour Print 1). Therefore meltwater originating from the western, upper areas of the EIF basin travels in several flowpaths rather than in a defined channel, which possibly slows down the travel time. In addition, the low gradient of the well-vegetated and uneven alluvial fan is favourable for depression storage, thus retarding surface runoff. In contrast, the characteristics of the WIF/W drainage area in combination with the stream bed structure appear to provide a faster routing of meltwater downslope. Most of the drainage area of the WIF/W is covered by large boulders and rocks, where rapid seepage (into the bouldery material) of snowmelt water occurs. This water appears to flow over the bouldery bed which is partly covered by ice, which should reduce the channel roughness. In combination with a high gradient, water reaches a high velocity which was observed in the field. Compared to the EIF basin, depression storage is not an important lag factor in the alluvial fan area of the WIF/W basin since the channel is well developed, has no vegetation or rocks imbedded in the sediment and therefore allows water to travel at high speeds (Colour Print 2). During snowmelt (and also later on days with bright sunshine) the quick response of the WIF valley is noticed in the field. Flow started almost immediately at the onset of bright sunshine and rising air temperatures and was first detected by the sound of water travelling underneath the boulders of the felsenmeer. Woo (1976) identifies a lag time of 12 hours between the highest net-radiation input and maximum discharge in the Umingmak basin on Ellesmere Island which he attributes to the slow seepage of meltwater into the sandy/silty active layer and retarded channel flow caused by channel characteristics. His results demonstrate how basin and stream characteristics influence the surface and subsurface transport of water and therefore the shape of the hydrograph. It could be argued, however, that the potential for water taking the subsurface route in the active layer is low since the active layer at the time of snowmelt is very shallow.

The highest discharge during the study period was recorded in the WIF/2 at the beginning of snowmelt (8.77 l/s; 3 June at 14:30) and again on 7 June at 16:30 with 6.6 l/s. The same pattern is reflected in the EIF hydrograph, peak discharges are recorded at the onset (3 June 16:40 with 4.1 l/s) and middle (6 June 22:53 with 4.1 l/s) of the snowmelt. Clearly, the timing of peak discharge follows the maximum air temperature of 11.5 °C recorded on 3 June (at 19:00). In comparison, only one maximum discharge event (5 l/s) occurred in the WIF/W during snowmelt on June 7 at 16:30. The lack of the initial high discharge pulse could either be the result of insufficient energy input or the refreezing of the meltwater at the base of a cold substrate such as boulders of a felsenmeer. Figure 3.6 shows the air temperature at different depths at a WIF felsenmeer site during snowmelt. Clearly, the air temperatures at 30 and 50 cm depth do not show diurnal variations up to 9 June, as it is the case for the surface mosses. Furthermore, the temperatures close to the base of the boulders (at 50 cm depth) stay continuously below 0 °C. Thus it can be assumed that part of the infiltrating snowmelt water freezes and therefore is not available for runoff. Figures 3.3 and 3.4 show that the two streams draining the WIF basin have an extended snowmelt compared to the EIF/W. As previously noted the WIF basin has a larger basin area and higher snow storage capacities than the EIF basin, which results in a higher SWE.

3.3. Chemistry

3.3.1. Snow chemistry

The chemistry of the premelt snowpack in the Colour Lake catchment is shown in Table 3.5.

Site	pH	Na^+ mg/l	K^+ mg/l	Ca^{2+} mg/l	Mg^{2+} mg/l	Cl^- mg/l	SO_4^{2-} mg/l	NO_3^- mg/l	% imbalance*
W3	5.58	0.24	0.02	1.1	0.11	0.27	1.37	0	35
E5	5.78	0.2	0.0	0.5	0.04	n.a.	n.a.	n.a.	n.a.
E1-1	5.9	0.2	0.02	1.3	0.07	0.19	0.77	0.05	58
B2	5.47	0.99	0.20	1.31	0.17	0.32	1.94	0	44

* Charge imbalance [%] = $\left| \frac{\Sigma cations - \Sigma anions}{\Sigma cations + \Sigma anions} \right| \times 100$ (units in equivalents)

Table 3.5. Premelt snow chemistry in the Colour Lake catchment in 1991. B2 is located in the Bastion sub basin (Figure 2.5).

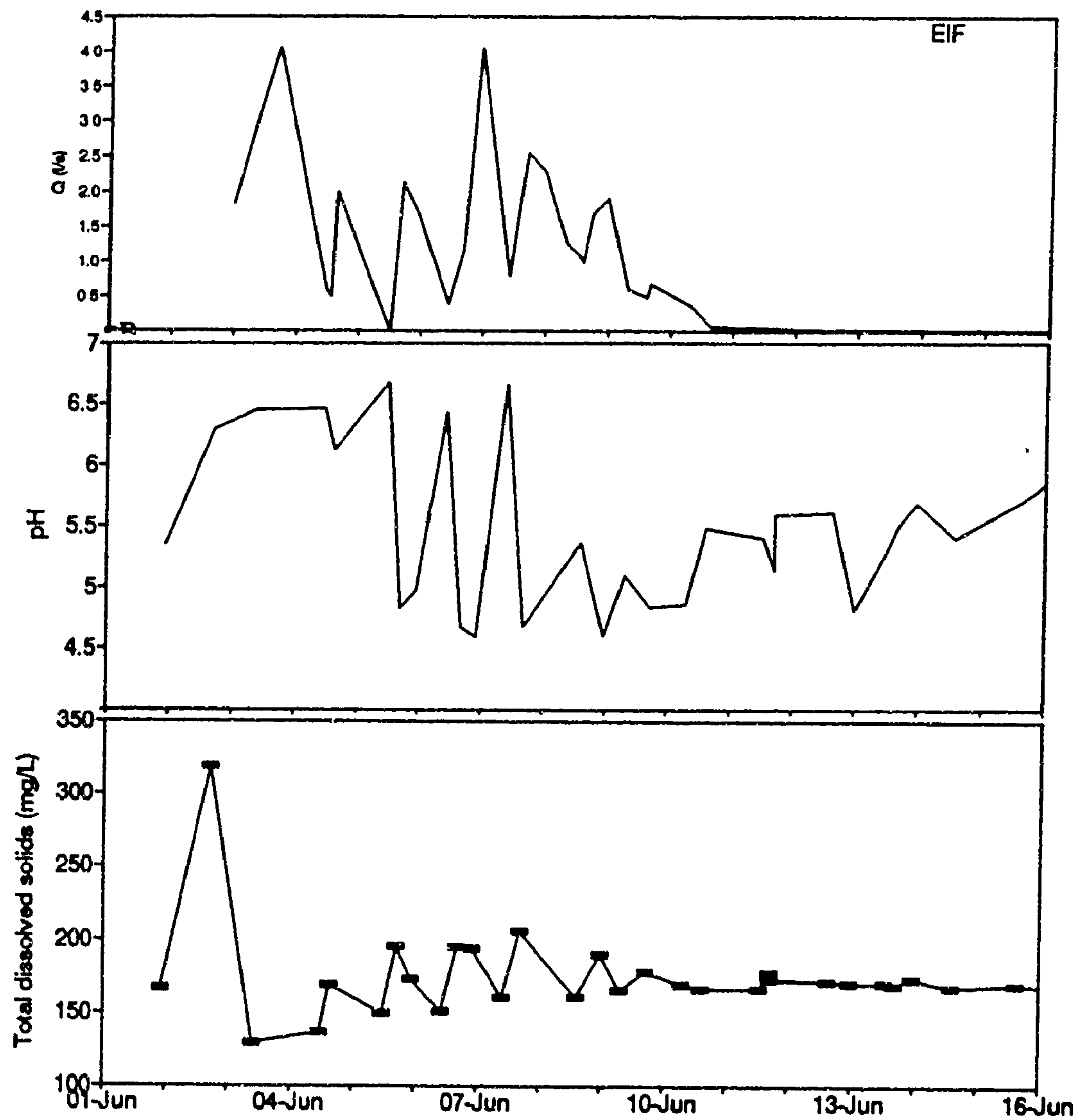

Figure 3.2. Discharge, pH and TDS concentrations in the EIF stream during snowmelt, 1-11 June, 1991.

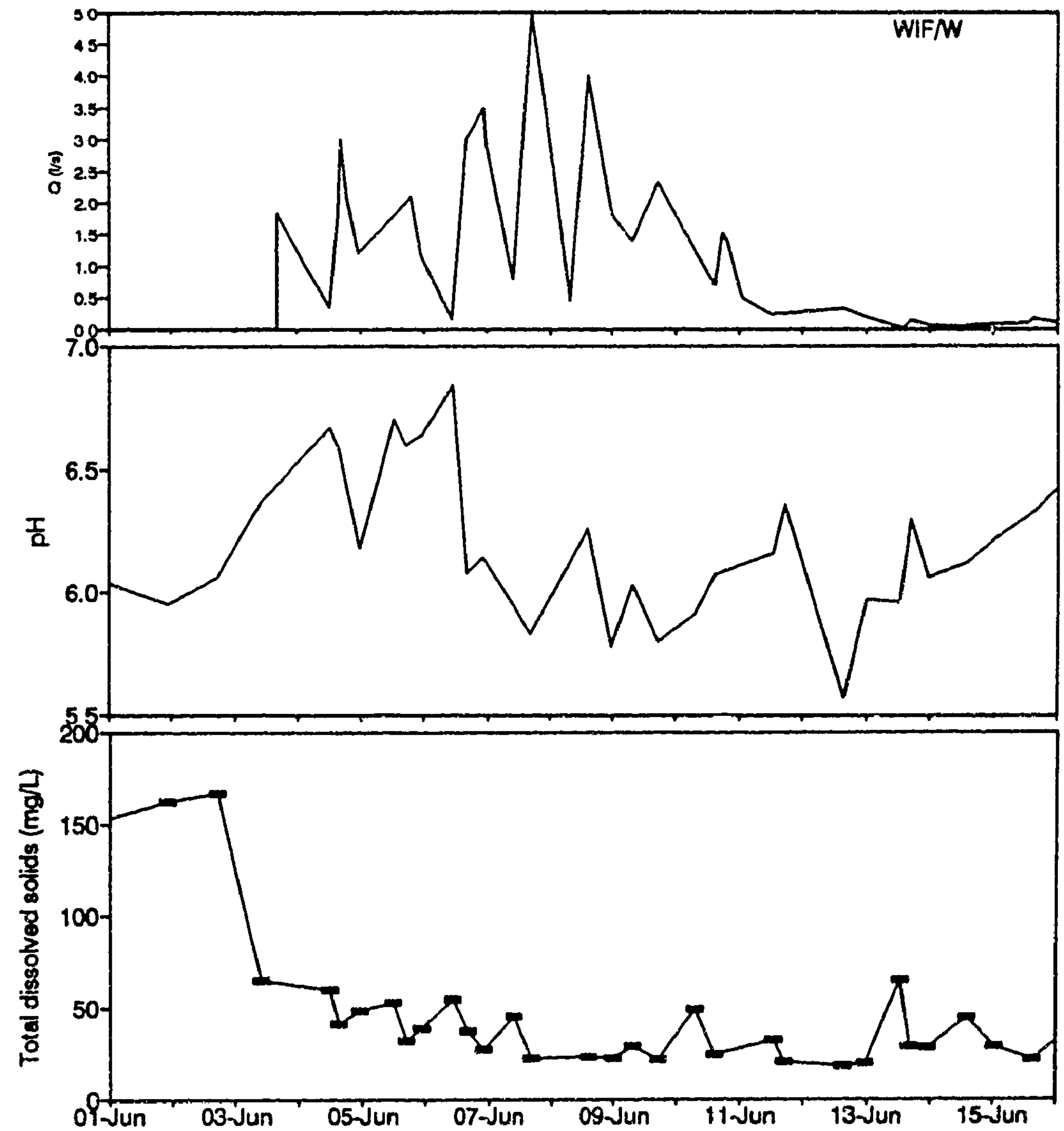

Figure 3.3. Discharge, pH and TDS concentrations in the WIF/W stream during snowmelt, 1-11 June, 1991.

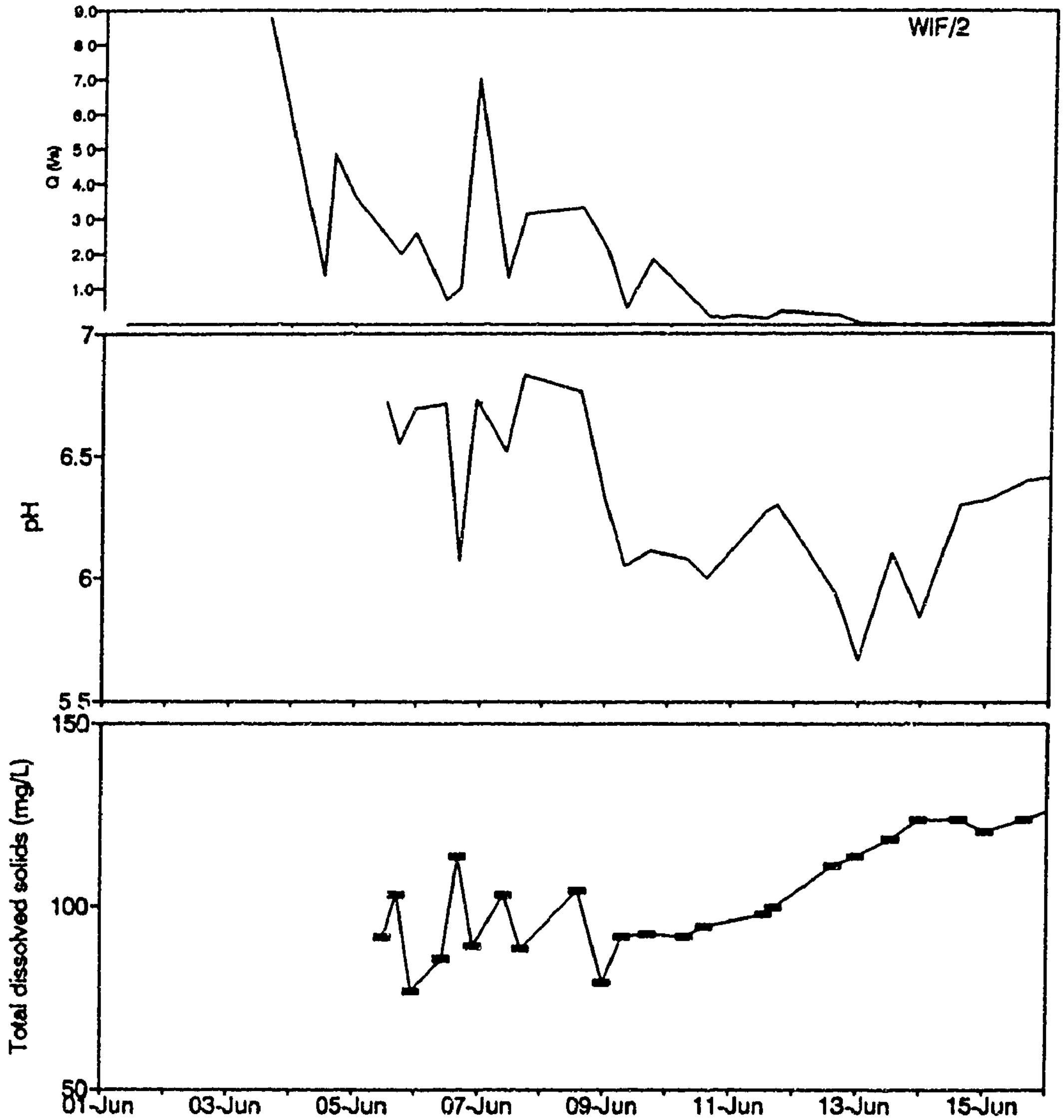

Figure 3.4. Discharge, pH and TDS concentrations in the WIF/2 stream during snowmelt, 1-11 June, 1991.

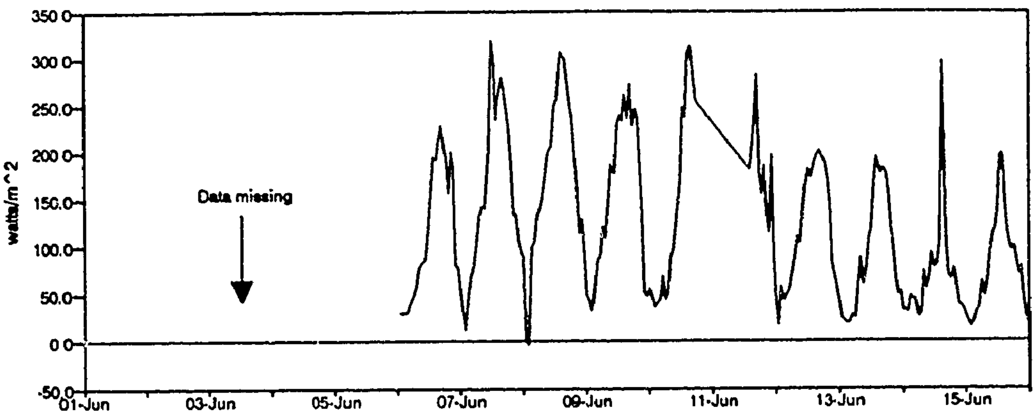

Figure 3.5. Daily variation in net-radiation recorded from 6 to 19 June, 1991 on datalogger in EIF basin (Figure 2.4).

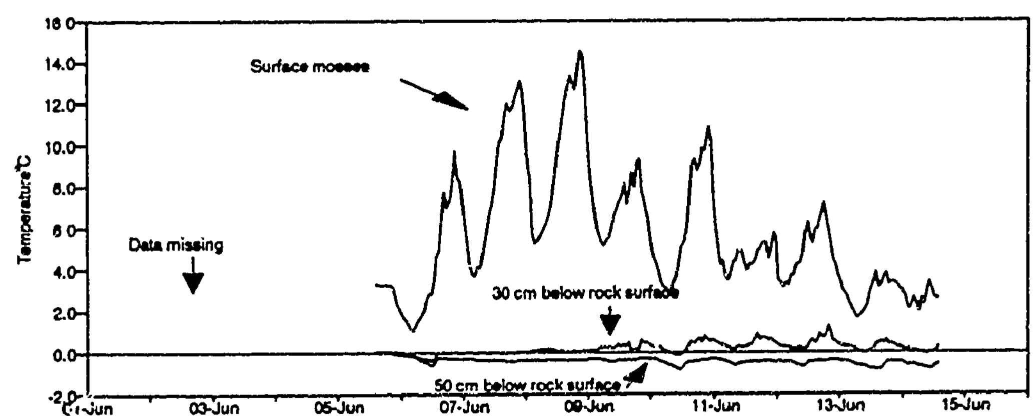

Figure 3.6. Air temperatures at 30 and 50 cm depth and in surface mosses recorded at a felsenmeer site, upper WIF basin, during snowmelt, 1-11 June, 1991. (Note: thermistors were installed in the bouldery material without contacting water or ground ice).

Generally, snow samples have low total dissolved solid (TDS) concentrations and are dominated by Ca^{2+} and SO_4^{2-} ions. The variability in snowpack chemistry could be influenced by the particulate matter content of the snowpack, which is a result of wind redistribution and entrapping of material. Overall, the strong positive charge imbalance of the snow samples is likely the result of the absence of HCO_3^- data in the charge balance calculations, as alkalinity was not determined on snow samples.

3.3.2. Snowmelt chemistry

The chemical composition of the surface water is a result of the chemical composition of snowmelt water interacting with surface materials (frozen or unfrozen) and provides information about the flowpath of water. To determine the relationship between discharge and ion concentrations correlation analyses is used throughout the defined hydrological periods. Linear correlation coefficients (r) between discharge and H^+ concentrations (referred to as acidity; AC) and discharge and TDS concentrations can be used to infer relationships between meltwater flowpaths and sediment-water interactions. For example, a strong inverse relationship between discharge and TDS in the surface stream could indicate a rapid routing of dilute meltwater. Correlation analysis between TDS concentrations and ion concentrations explains changes in TDS concentrations by changes in the concentration of specific ions. And finally, correlation analysis between discharge and ion concentrations determines the change of ion concentrations with increasing and decreasing discharge, thereby demonstrating dilution and concentration of ions in the water. Throughout this thesis, a correlation coefficient between two variables is presented as rX_1/X_2 (i.e. rQ/TDS is the correlation coefficient between discharge and TDS concentrations).

Generally, the water of the EIF/W stream is more acidic and the range of pH fluctuations is higher than that of the waters draining the WIF basin (Figures 3.2, 3.3 and 3.4). The mean pH of samples of the EIF/W during snowmelt is 5.07, with a minimum pH of 4.59 (Table 3.6). The streams draining the WIF basin are very weakly acidic; the mean pH of the WIF/W stream is 6.12 and of the WIF/2 stream is 6.33 (Tables 3.6). All three streams show strong fluctuations in stream pH, with decreasing amplitude as the snowmelt progresses (Figures 3.2, 3.3, 3.4). This is especially pronounced for the EIF; the range of fluctuation in stream pH decreases from 1.5 pH units during the early melt to 0.5 pH units during the later melt.

During snowmelt, no significant relationship between acidity and discharge is apparent in all streams (Table 3.7).

Generally, all streams have higher ionic concentrations than the snow; ion concentrations in the WIF/W stream are six to forty seven times those in the snow, the WIF/2 twenty two to thirty three times and the EIF/W thirty seven to ninety times the ion concentration of the snowpack. In comparison, the concentration of ions in Imnavait Creek, Alaska, are four to nine times the concentration of the snowpack (Everett *et al.*, 1989). Total dissolved solid concentrations in samples taken during snowmelt are highest in the EIF stream (mean TDS concentrations = 176 mg/l;

	EIF					WIF/W					WIF/2				
	n	Mean	Std. dev.	Max.	Min.	n	Mean	Std. dev.	Max.	Min.	n	Mean	Std. dev.	Max.	Min.
pH[a]	21	5.07	0.75	6.67	4.59	23	6.12	0.32	6.84	5.78	16	6.33	0.3	6.83	6.0
TDS (mg/l)	21	176	37	316	128	23	53	43.8	166	20.5	16	94.1	9.55	114	76.9
Q (l/s)	20	1.3	1.22	4	0.03	20	1.52	1.47	5.0	0	15	1.82	1.77	7.02	0.17
Na^+ (mg/l)	11	2.73	2.24	9.25	1.22	10	2.04	2.37	8.35	0.45	9	1.52	0.37	2.15	1.01
K^+ (mg/l)	11	1.96	1.0	4.92	1.33	10	1.76	1.63	5.79	0.47	9	1.32	0.16	1.51	1.05
Ca^{2+} (mg/l)	11	33.2	7.27	48.3	19.5	10	13.1	9.33	27.1	4.33	9	14.3	1.39	16.9	12.8
Mg^{2+} (mg/l)	11	7.73	4.3	20.5	5.46	10	3.78	3.32	8.79	0.96	9	7.29	1.22	9.6	5.25
Fe^{2+}(mg/l)	2	0.3	0.12	0.38	0.21	n.a.	n.a.	n.a.	n.a.	n.a.	n.a.	n.a.	n.a.	n.a.	n.a.
Al^{3+}(mg/l)	2	1.21	1.53	2.29	0.13	n.a.	n.a.	n.a.	n.a.	n.a.	n.a.	n.a.	n.a.	n.a.	n.a.
Cl^- (mg/l)	11	1.61	1.12	4.95	1.03	11	2.06	2.06	7.27	0.35	9	1.18	0.3	1.92	0.84
SO_4^{2-} (mg/l)	11	127	37.3	220	74.3	11	32.9	32.9	87.3	8.9	9	58.3	10.4	76.5	43.9

a: Mean calculated from $[H^+]$ concentrations and reconverted to pH

Table 3.6. Mean, maximum and minimum values of chemical characteristics of the EIF, WIF/W and WIF/2 streams during snowmelt, 1 to 11 June, 1991.

Table 3.6) and lowest in the WIF/W stream (mean TDS concentrations=53 mg/l; Table 3.6).

With the start of snowmelt, the concentrations of TDS in the WIF/W and EIF peak followed by a sudden drop in TDS concentrations (Figures 3.2 and 3.3). Assuming the same TDS pattern for the WIF/2, where the initial snowmelt was unfortunately not sampled, it is possible that the peak in TDS concentrations may have been missed. All streams show fluctuations in TDS concentrations, which are most pronounced in the WIF/W and least pronounced in the WIF/2 stream indicated by the range of fluctuation and standard deviation (Table 3.6 and Figures 3.2 to 3.4). During the first days of snowmelt, TDS concentrations in the EIF increase while concentrations in the WIF/W decrease. Linear correlation analysis between discharge and TDS concentrations identifies a significant inverse relationship in the WIF/W, TDS concentrations decrease with increasing discharge ($r=-0.53$; $p < 0.01$, $n=20$). There is no significant linear relationship between discharge and TDS concentrations in the EIF, since TDS concentrations in the EIF are more or less constant with increasing discharge; a similar pattern is also found in the WIF/2 (Figure 3.7 and Table 3.7).

The dominant ions in all streams are Ca^{2+} and SO_4^{2-} (Table 3.6). A significant relationship between TDS and K^+, Ca^{2+}, Mg^{2+}, Cl^- and SO_4^{2-} concentrations supports the observation that variations in TDS concentrations in the EIF and WIF/W can mainly be explained by variations of all ions except Na^+ ($0.81 < r < 0.99$ for rTDS/K^+, Ca^{2+}, Mg^{2+}, Cl^-, SO_4^{2-}; $0.01 < p < 0.001$, $n=10$;

Appendix B). Differences in the relationship of discharge and TDS concentration are also reflected in the relationship between discharge and ions. Only Ca^{2+} and SO_4^{2-}concentrations have a significant, inverse relationship with discharge in the WIF/W ($rQ/Ca^{2+} = -0.75$, $p < 0.01$; $rQ/SO_4^{2-} = -0.74$, $p < 0.01$, $n = 10$). No significant relationship exists between ion concentrations and discharge in the EIF and WIF/2 (Appendix B).

	EIF	WIF/W	WIF/2
Q-TDS	0.19	-0.53*	-0.23
Q-AC[a]	0.39	0.25	-0.52
Sample size	20	20	15
a : calculated from $[H^+]$ concentrations * : r value significant at 0.01 level			

Table 3.7. Linear correlation coefficients (r) for discharge and TDS and discharge and acidity for the three streams during snowmelt, 1-11 June, 1991.

It is of note that the EIF stream has elevated concentrations of aluminum (Table 3.6). The solubility of aluminum increases with decreasing pH; in waters below a pH of 5, Al^{3+}, $Al(OH)^{2+}$ and $Al(OH)_{2+}$ are the predominant aluminum species (Stumm and Morgan, 1981). This explains the higher aluminum concentrations on 8 June in the EIF stream (2.29 mg/l at pH of 4.6 on 8 June, 1991; 0.13 mg/l at pH of 6.29 on 2 June, 1991).

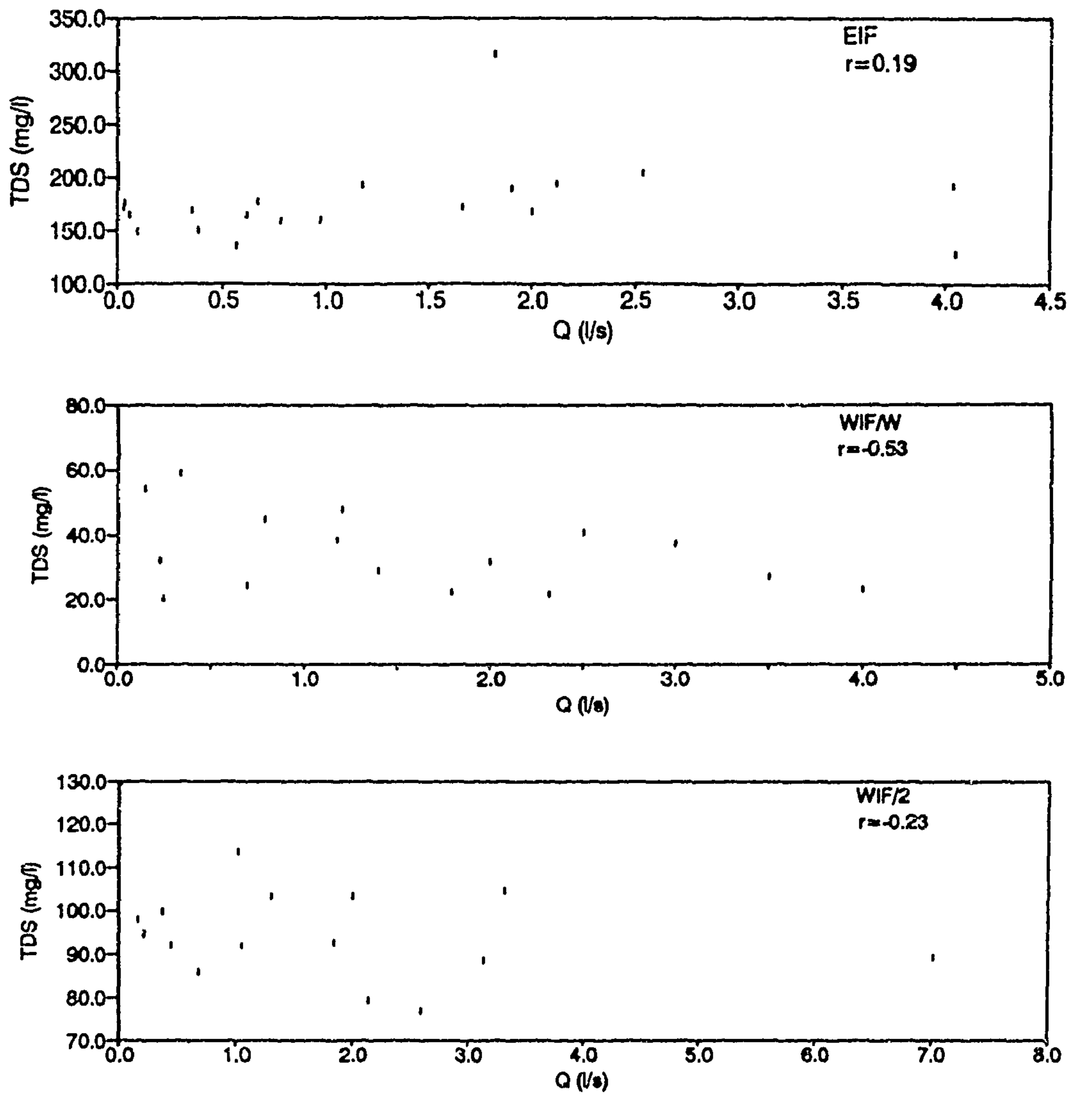

Figure 3.7. Discharge against TDS concentrations and linear correlation coefficent (r) for the three streams during snowmelt, 1991. Significance level (p) and sample size (n) are listed in Table 3.7.

3.4. Discussion

There are several possibilities to explain the hydrological and geochemical processes during snowmelt. The initial low pH recorded in the WIF/W and EIF stream could be the result of a preferential elution process. Snowmelt studies carried out in temperate regions show fractionation and enrichment of ions (notable H^+, SO_4^{2-} and NO_3^-) during the early melt period (Semkin and Jeffries, 1986). Johannessen and Henriksen (1978) report from their study in Norway that the fractionation of pollutants is responsible for a sharp pH drop during the initial snowmelt. The low pH water exchanges with ions that are weakly bound on dissolved or suspended material. This is one possibility for explaining the high TDS concentrations of all ions in the WIF/W and EIF streams during the onset of snowmelt. Highest concentration of all ions at the onset of snowmelt in combination with a low pH are also reported by Everett *et al.* (1989) and Everett and Ostendorf (1988) from Imnavait Creek in Alaska.

The second and most likely explanation is that initial TDS peak concentrations in the stream waters are the result of standing water conditions. Before any runoff occurs, pools of water are observed in the EIF and WIF basins. These conditions are favourable for the meltwater to dissolve weathered and leached surface material, especially when soluble salts are present on top of the soil. Such a surface soil layer could be formed by the exsolution of ions during the last years' refreezing of the active layer or the result of high evaporation rates during the previous summers.

Colour Print 3. Salt crusts on east slope of EIF basin, 9 June, 1991.

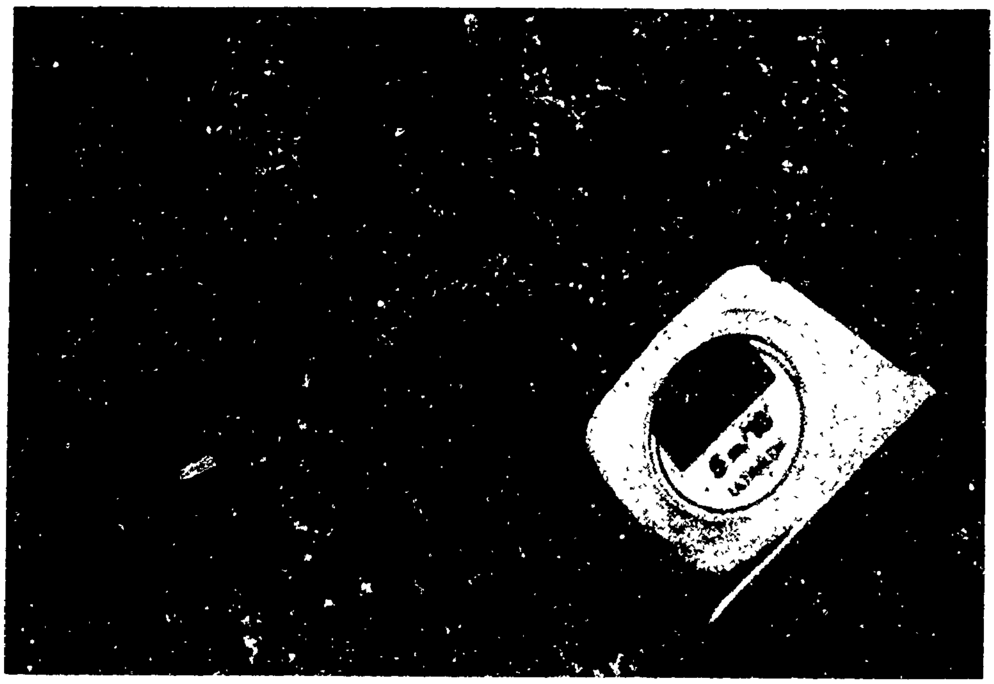

Colour Print 4. Close-up of east slope salt crusts, 9 June, 1991.

Evidence for the latter is given by visible salt crusts on the eastern slope of the EIF basin ("Sandstone Dome"), which were observed during several field seasons (Colour Prints 3 and 4).

The spatial distribution of snow has an important effect in determining the discharge regime and the chemistry of the streams during snowmelt. Large accumulations of snow in the WIF catchment control the release of meltwater in the WIF valleys and prolong the melt period. This also explains the inverse relationship of discharge and TDS concentration in the WIF/W stream. Similar to a glacial regime, high discharge is correlated with low ion concentration as a result of release and quick transport of dilute meltwater. This is not the case for the WIF/2 stream, as large snow storage facilities in the form of deep valleys are lacking and a defined stream channel providing quick water transport downslope is only developed in the lower part of the alluvial fan area. Hence, a combination of processes and factors such as transport through the active layer, depression storage, the lack of a well defined stream channel and geomorphological characteristics of the drainage area influence the travel time and therefore also the concentration of TDS.

Table 3.8 demonstrates the thawing of the frozen upper ground during snowmelt. At least three conclusions can be drawn: 1. a thin and uneven active layer was already present before any runoff occurred 2. a considerable amount of active layer development occurs during snowmelt 3. the active layer development occurs slower in the EIF basin, but at the end of the snowmelt both basins show approximately the same depth of thaw (Table 3.8).

Time	Basin	Mean active layer depth (cm)	n	Range	Std.Dev.
28 May 1991	WIF	2.9	18	0-9	1.8
	EIF	1.3	6	0-6	1.8
30 May 1991	WIF	4.4	25	0-12	3.9
	EIF	2.3	6	0-6	2.4
1 June 1991	WIF	8.2	25	0-20	5.4
	EIF	3.5	6	0-7	2.4
3 June 1991	WIF	13.1	25	0-25	6.7
	EIF	4.7	6	0-11	3.8
5 June 1991	WIF	16.7	25	0-26	5.6
	EIF	9.6	6	0-13	3.9
7 June 1991	WIF	22.5	16	8-29	5.4
	EIF	16.2	6	0-30	8.9
12 June 1991	WIF	25	18	15-40	5.2
	EIF	23.2	6	11-30	6.3

Table 3.8. Development of the active layer in the EIF and WIF basins from 28 May to 12 June, 1991. Mean active layer depth is calculated from all permafrost transect sites (Figure 2.4).

It is possible that the thawing of the upper few centimetres of the seasonally frozen ground is enhanced by the infiltration of meltwater (the first signs of snow melting in the catchment were observed on May 27); infiltration of meltwater into frozen soil is possible because of pore-pressure and gravitational gradients (Kane and Stein, 1983).

Saturated transport in the thin active layer or in the lower snowpack could therefore "smooth" the effects of diurnal discharge inputs (which is the case for the WIF/2). A similar scenario can be applied for the EIF stream. The interaction of snowmelt water with the active layer, either by infiltration and displacement or by surface scouring is important to explain the higher TDS concentrations and the change in pH of the snowmelt water. These pH changes of surface water relative to snow meltwater substantiate the importance of hydrological flowpaths and geological material on the stream water pH. The fact that the pH of the EIF is considerably lower than the snowmelt water suggests that the geological material is a source of H^+ ions. The geological material of the WIF basin appears to be a sink for H^+, since the pH is elevated relative to the snowmelt water. However, the positive relationship between discharge and pH in the WIF/2 indicates the ability of the snowmelt water to rapidly interact with the sediments. In the WIF/W, the interaction between the icy, bouldery bed and the meltwater is limited and hence, the pH of the stream water stays more or less constant or decreases with increasing flow.

It is important to note that another source of ions other than atmospheric deposition must exist, creating much higher stream ion concentrations in comparison to the snow ion concentrations. In fact, Cooper *et al.* (1991) show that 66% of the atmospherically deposited sulphur (in the snowpack) is retained in the tundra of the arctic watershed "Imnavait Creek". Assuming that the Colour Lake watershed behaves the same way, the sulphate in the streams must originate from sources other than the atmosphere most likely the active layer.

The dynamic melting process of the upper part of the ground seems to be a source of additional ions, either by allowing the meltwater to infiltrate into the ground or by the release of high concentrated waters stored in the seasonally frozen ground. This "old groundwater" (water stored in the catchment prior to snowmelt) could become available from the melting of ground ice (below boulders) or the thawing of the active layer. Furthermore, "old groundwater" in the form of highly concentrated water pockets included in the seasonally frozen ground could become flushed out by infiltrating meltwater. These highly concentrated water pockets are formed by exclusion and concentration during the refreezing of the previous fall active layer (Anisimova, 1978; van Everdingen, 1990). If highly concentrated "old water " is subsequently released with the thawing of the seasonally frozen ground, stream ion concentrations are expected to be more or less consistent with increasing discharge, which is the case for the EIF. Figure 3.2 and Table 3.8 demonstrate that the peak in concentration (after the initial peak at the start of the snowmelt) in the EIF stream occurs simultaneously with most rapid active layer development.

Further evidence of "old groundwater" contribution is provided by tritium data from snowmelt samples (Table 3.9).

	EIF	WIF/W	WIF/2
^3H (T.U.)	34 (±8)	12 (±8)	25 (±8)

Table 3.9. Tritium concentrations (T.U.) in the three streams during snowmelt, 7 June, 1991.

Although caution has to be exercised in interpreting the tritium concentrations (due to the high analytical error of ±8 T.U. relative to the low tritium concentrations in the streams) it can be stated that tritium concentrations are higher in the EIF stream than in the WIF/W (Table 3.9). Since tritium concentrations of the snowpack are low (range = 9 to 20 ±8 T.U., n=2) and high in the waters extracted from the frozen active layer at 41 cm depth (52 ±8 T.U.), the data suggest that the contribution of "old groundwater" to runoff is highest in the EIF. On the other hand, the WIF/W has little or almost no contribution of "old water" to runoff, which is in agreement with the chemical data. Other snowmelt studies carried out in a small high arctic watershed on Baffin Island indicate a 50% contribution of old water to the snowmelt runoff (Obradovic and Sklash, 1986). In contrast, Cooper *et al.* (1991) report that only 14% of Imnavait Creek in Alaska was derived from "old water" due to the limited soil-water mixing.

Nevertheless, there must be another important factor responsible for creating the chemical differences in the streams of the two basin. This factor centres around the geological material of the two catchments which should also be reflected in the chemistry of the "old groundwater". Soils in the EIF basin have to be more acidic and higher concentrated compared to soils in the WIF basin. The geological material of the eastern slope of the EIF basin (Heiberg Formation) seems to be considerably different in chemical and mineral characteristics from the geological material underlying the western part of the EIF basin and the WIF basin (Savik and Awingak Formation, Figure 1.3). A detailed discussion about these mineralogical differences and their effect on the stream water chemistry is provided in Chapter 6.

2

PM-1 3½"x4" PHOTOGRAPHIC MICROCOPY TARGET
NBS 1010a ANSI/ISO #2 EQUIVALENT

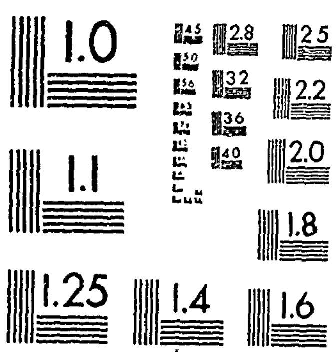

PRECISION[SM] RESOLUTION TARGETS

In conclusion, a combination of water transport mechanism, basin characteristics (such as surface cover), chemical characteristics of active layer and geological material is responsible for the observed hydrological and chemical differences in the EIF and WIF basins during snowmelt.

CHAPTER 4- THE PERIOD OF ACTIVE LAYER DEVELOPMENT

4.1. Introduction

This chapter discusses the hydrology and chemistry for the period 12 June to 1 August 1991, when the active layer development was most pronounced. Based on differences in the climatological record (precipitation, air temperature) and resulting stream hydrographs, this period is further divided into three subperiods (Figure 4.1). Average daily air temperatures and amount of precipitation are increasing from the first to the third period of active layer development. Of note is that the percentage of rain of the total precipitation increases from subperiod one (6% as rain) to almost 60% in the third subperiod (Table 3.2).

4.2. Period of active layer development: subperiod 1 (12 June to 5 July, 1991)

4.2.1. Hydrology

Figure 4.1 shows the hydrographs of the WIF/W and EIF stream in combination with daily air temperature and precipitation. Generally, this is the period with the lowest average discharge in both streams, the average discharge in the WIF is 0.22 l/s and in the EIF 0.01 l/s (Table 4.1). Runoff ceases twice in both streams during cold periods, when minimum temperatures stay below 0°C (Figure 4.1). The mean daily temperature of 2.1 °C recorded during this period is only

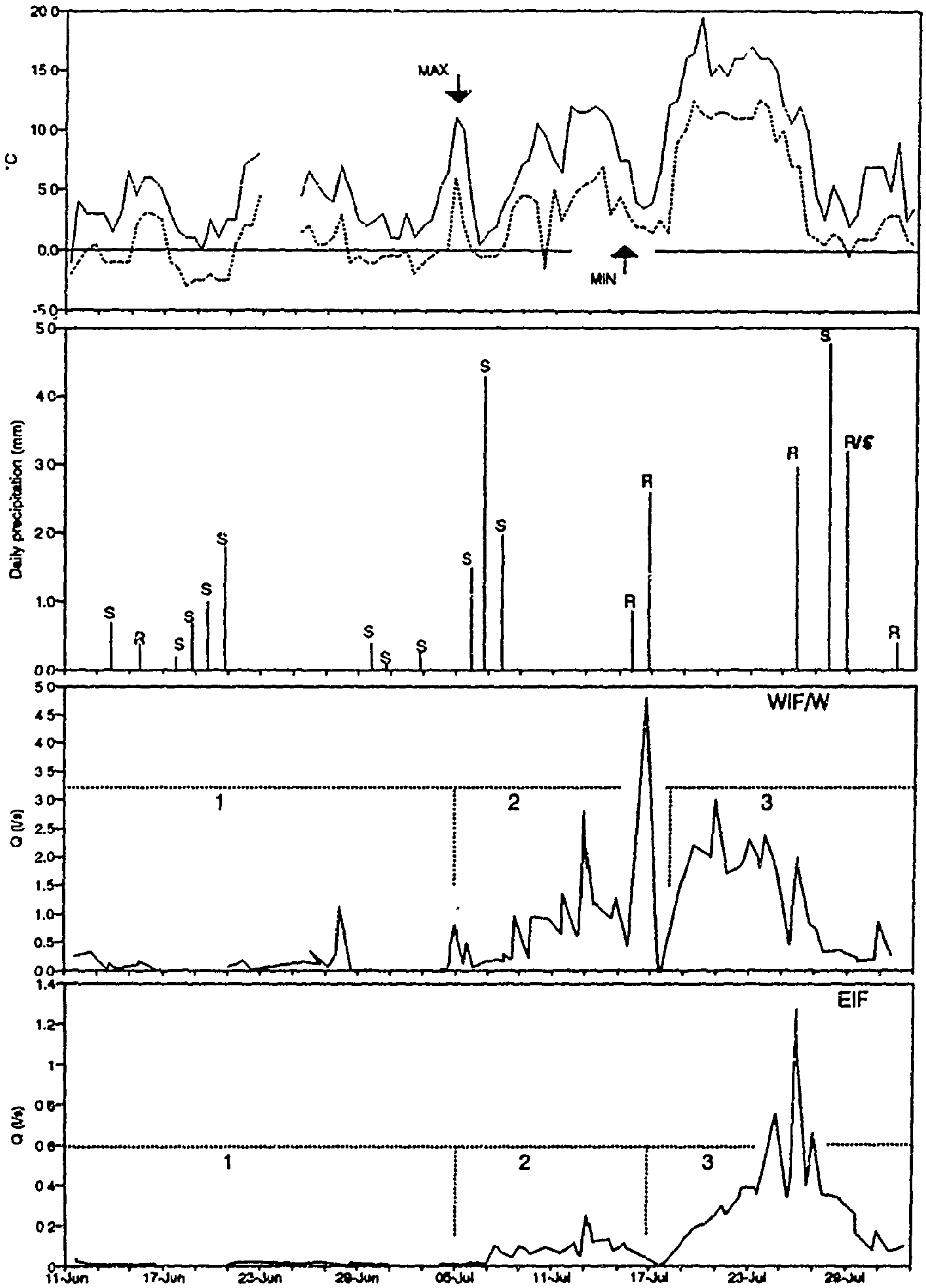

Figure 4.1. Air temperature, precipitation (as snow: S, as rain: R) and hydrographs of the EIF and WIF/W streams during the period of active layer development, 12 July to 2 August, 1991.

	EIF					WIF/W				
	n	Mean	Std. dev.	Max.	Min.	n	Mean	Std. dev.	Max.	Min.
pH^a	34	5.52	0.26	6.03	4.8	39	6.12	0.21	6.56	5.57
TDS (mg/l)	34	164.15	7.91	180.18	148.5	39	44.93	15.42	81.18	18.48
Q (l/s)	28	0.01	0.0	0.02	0.0	37	0.22	0.23	0.8	0.0
Na^+ (mg/l)	7	3.83	3.04	9.03	1.37	13	2.26	2.47	8.44	0.34
K^+ (mg/l)	7	1.18	0.07	1.25	1.05	13	0.67	0.14	0.87	0.44
Ca^{2+} (mg/l)	7	30.03	2.19	32.36	27.07	13	8.53	2.8	13.43	3.53
Mg^{2+} (mg/l)	7	9.25	8.44	28.35	5.34	13	2.9	2.09	9.3	0.9
Fe^{2+}(mg/l)	1	0.23	n.a.	n.a.	n.a.	n.a.	n.a.	n.a.	n.a.	n.a.
Al^{3+}(mg/l)	1	0.0	n.a.	n.a.	n.a.	n.a.	n.a.	n.a.	n.a.	n.a.
Cl^-(mg/l)	7	0.74	0.38	1.29	0.05	13	0.67	0.34	1.65	0.33
SO_4^{2-}(mg/l)	7	108.21	6.14	116.08	98.77	13	23.14	9.0	38.21	7.88
a: Mean calculated from $[H^+]$ concentrations and reconverted to pH										

Table 4.1. Mean, maximum and minimum values of chemical characteristics of the EIF and WIF/W stream during the period of active layer development, subperiod 1, 12 June to 5 July, 1991.

slightly higher compared to snowmelt (mean Temp. = 1.9°C) (Table 3.2). During these cold periods active layer development is inhibited and perhaps refreezing of the active layer occurs in the WIF basin as is suggested in Figure 4.2. Most of the precipitation falls as snow and does not generate runoff in the streams; however, the WIF/W stream responds to precipitation during flow periods, such as the snowfall on 13 June and rain on 15 June, 1991 (Figure 4.1). Considering the amount of snow and the increase in air temperature it is possible that the peak in discharge on 15 June and 4 July in the WIF/W stream is the result of a sudden release of snowmelt water. After runoff ceases for a second time, both streams begin flowing again on 4 July as a result of increasing air temperatures.

In order to identify whether air temperature and precipitation have a significant influence on the generating of runoff, linear bivariate and multivariate regression analyses were applied on the data. This information can be used to ascertain the type and behaviour of the hydrological storage in the basin (such as ground ice, groundwater). Linear regression analysis was applied on the entire data set of the period of active layer development (subperiod 1+2+3) and, in addition, for the three subperiods separately (Table 4.2). During the entire period of active layer development (subperiods 1+2+3) the total daily discharge of the WIF/W is significantly correlated to the mean daily air temperature in the WIF/W ($r=0.9$, $p < 0.001$, $n=41$), as well as in the EIF ($r=0.47$, $p < 0.05$, $n=41$) (Table 4.2). However, according to a Fisher-Z test (Steiger, 1980) performed on these two correlation coefficients, there is a statistically significant difference in predicting total

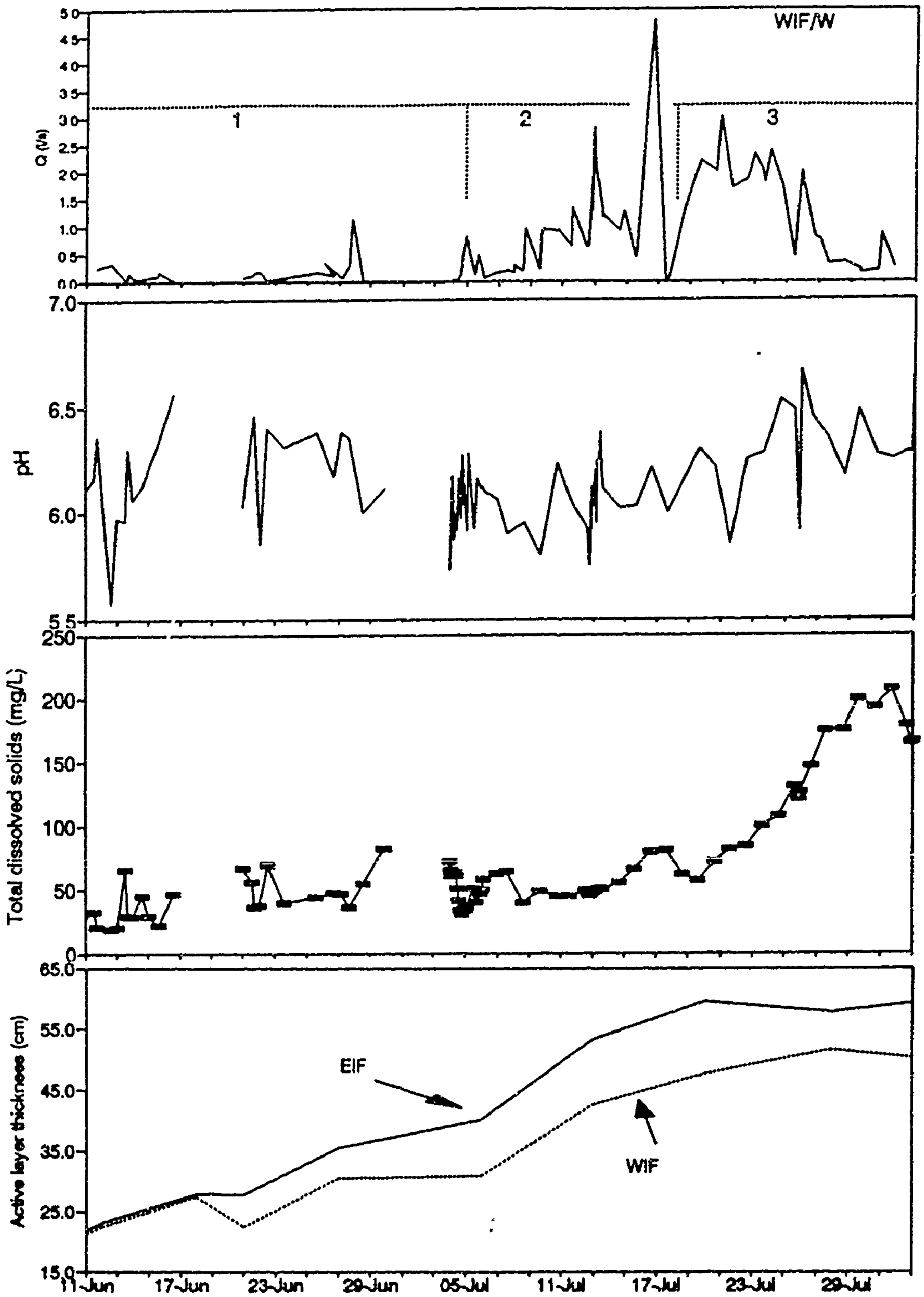

Figure 4.2. Discharge, pH and TDS concentrations of the WIF/W stream and active layer development in the EIF and WIF basins during the period of active layer development, 12 July to 2 August, 1991.

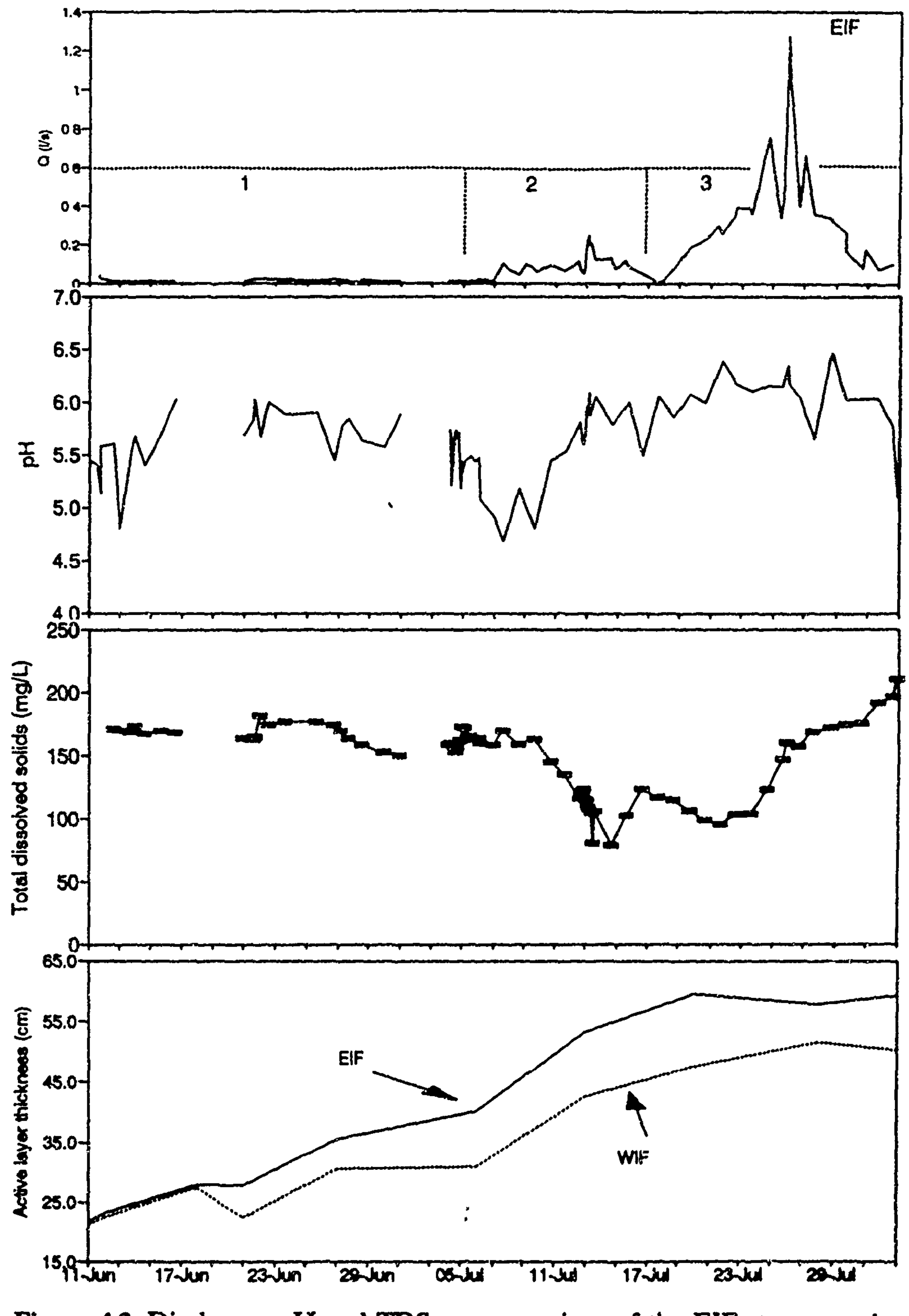

Figure 4.3. Discharge, pH and TDS concentrations of the EIF stream and active layer development in the EIF and WIF basins during the period of active layer development, 12 July to 2 August, 1991.

daily discharge by mean daily temperature between the EIF and WIF stream. The combination of air temperature and precipitation (multivariate regression) increases the observed relationship significantly only for the EIF ($r=0.68$, $p < 0.001$, $n=41$) (Table 4.2).

r	Active layer period 1 n=15		Active layer period 2 n=11		Active layer period 3 n=15		Active layer period 1+2+3 n=41	
	EIF	WIF	EIF	WIF	EIF	WIF	EIF	WIF
mean daily temperature (x_1)	0.33	0.41	0.4	0.81**	0.14[a]	0.95**	0.47+	0.90**
Daily precipitation (x_2)	0.15	0.24	0.24	0.56	0.38	0.36	0.29	0.18
mean daily temp. and precip.(x_1,x_2)	0.33	0.6	0.44	0.84**	0.5	0.96**	0.68**	0.92+
+ : r value significant at 0.05 level * : r value significant at 0.01 level ** : r value significant at 0.001 level	a: r=0.43 for one day time lag (x_1= mean daily temperature $_{Q+1day}$) r=0.68* for two days time lag (x_1=mean daily temperature $_{Q+2days}$) r=0.77+ for two days time lag (x_1=mean daily temperature $_{Q+2days}$) and precipitation (x_{2Q})							

Table 4.2. Summary of bivariate and multivariate regression analysis among discharge (dependent variable, y), mean daily temperature and daily precipitation (independent variables, x_1 and x_2) for the period of active layer development, 1991.

For this first period of active layer development, no significant relationship could be identified between discharge and/or precipitation in either basin (Table 4.2, Figure 4.9).

4.2.2. Chemistry

Generally, the pH of the EIF stream is more acidic and average TDS concentrations are four times the concentration of the WIF/W stream. Chemical results show that the dominant ions are SO_4^{2-}, Ca^{2+} and Mg^{2+} and, in addition, Na^+

in the WIF/W (Table 4.1). Variations in TDS concentrations in the WIF/W stream are strongly related to variations in K^+, Ca^{2+} and SO_4^{2-} (rTDS/K^+,Ca^{2+},SO_4^{2-} > 0.96, $p < 0.001$, n=13) (Appendix B). These ions also exhibit a significant negative relationship to discharge in the WIF/W (rQ/=-0.75, $p < 0.01$, n=13; rQ/Ca^{2+},SO_4^{2-} > -0.8, $p < 0.001$, n=13) (Appendix B). In the EIF, only Ca^{2+} concentration is significantly correlated to TDS concentrations (rTDS/Ca^{2+} =0.92, $p < 0.01$, n=7) and consequently, no significant dilution for a specific ion is found with increasing discharge (Appendix B). The relationship between TDS concentrations and discharge in subperiod 1 is demonstrated in Figures 4.4b and 4.5b: TDS concentrations vary from 148 mg/l to 172 mg/l over a given discharge (0.01 l/s) in the EIF stream (Figure 4.5b), while TDS concentrations in the WIF decrease significantly with increasing discharge (r=-0.53, $p < 0.001$, n=37; Figure 4.4b). For the WIF/W, three observations indicate that this period resembles the snowmelt period: 1. a large variation of TDS concentration from 20 mg/l to 75 mg/l (snowmelt: 20 mg/l to 166 mg/l) 2. low average TDS concentration of 53 mg/l (snowmelt: 53 mg/l) 3. a significant, negative correlation coefficient for TDS and discharge of r=-0.53 (snowmelt: r=-0.53) and 4. a mean discharge of 1.28 l/s (snowmelt: 1.52 l/s). Unlike the WIF/W, similarities to snowmelt are not observed in the EIF. The differences between flow systems in the WIF/W and EIF basins suggest that the WIF/W stream received a considerable amount of water from the melting of snow ("prolonged snowmelt"). On 11 June, large patches of snow still existed in the lower WIF/W valley. By this time, all snow had melted in the EIF

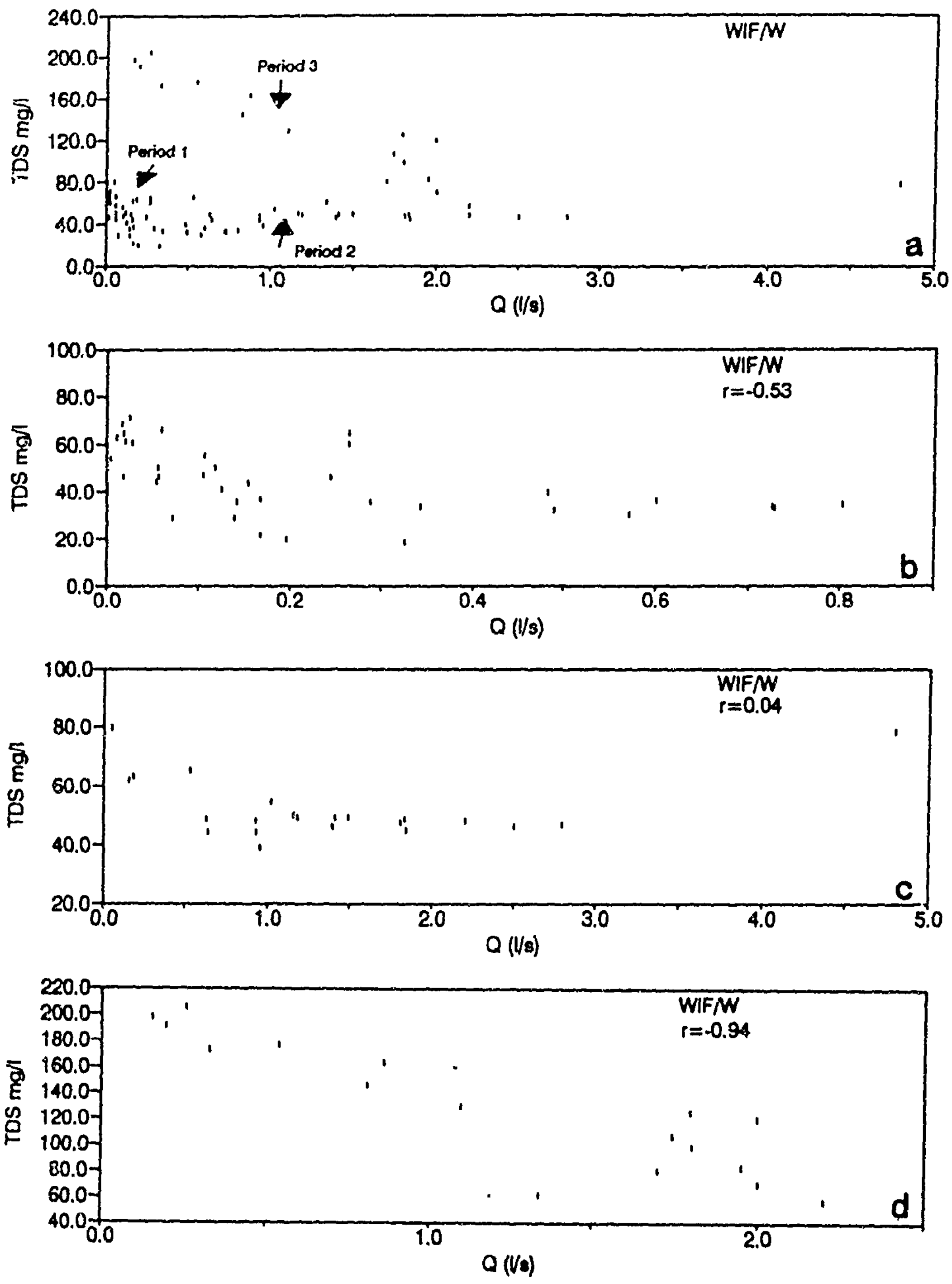

Figure 4.4. Discharge against TDS concentrations and linear correlation coefficient (r) for the WIF/W stream during the period of active layer development (a), subperiod 1 (b), subperiod 2 (c) and subperiod 3 (d), 1991.

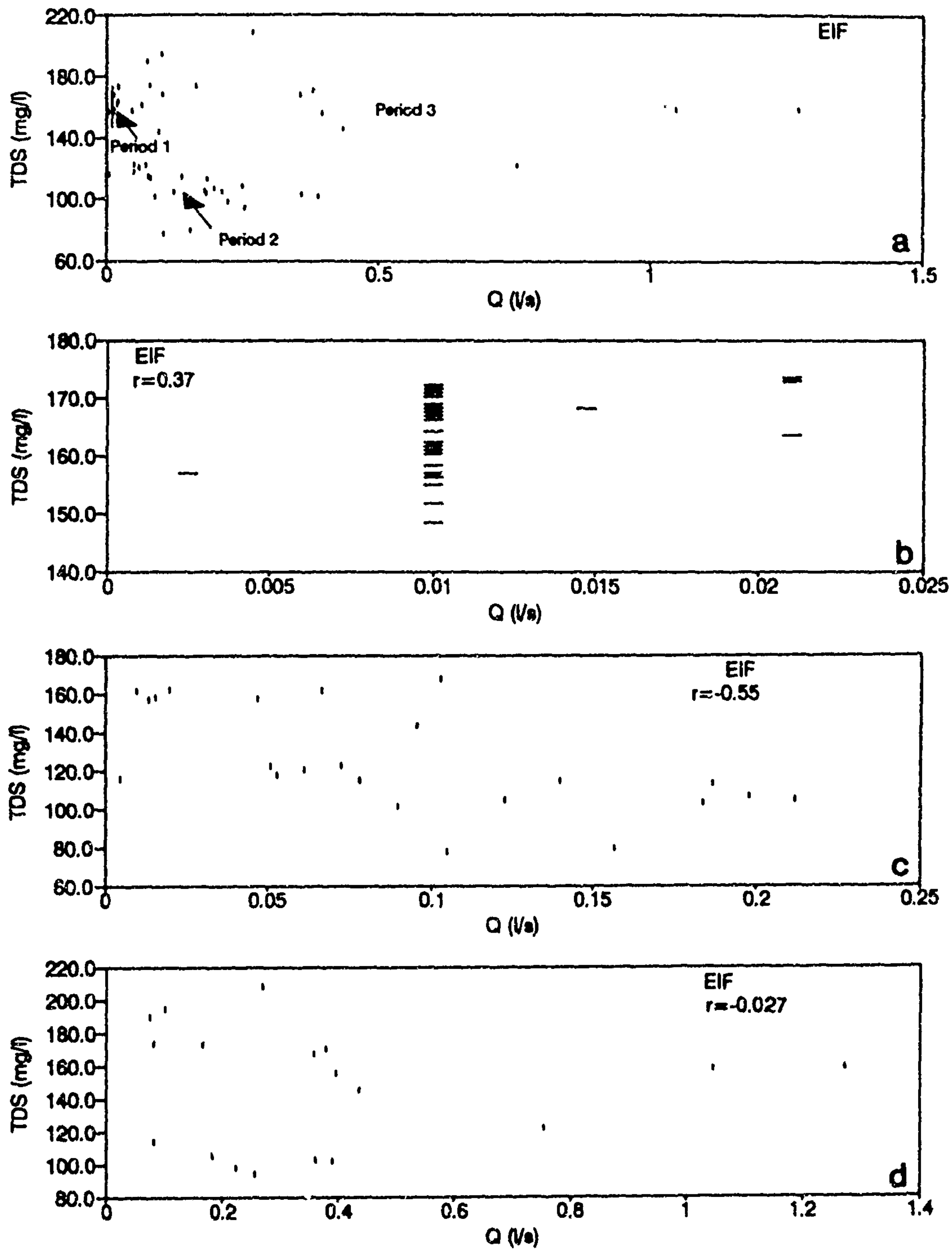

Figure 4.5. Discharge against TDS concentrations and linear correlation coefficient (r) for the EIF stream during the period of active layer development (a), subperiod 1 (b), subperiod 2 (c) and subperiod 3 (d), 1991.

basin. No relationship between discharge and acidity is observed in either stream (Table 4.3).

	EIF	WIF/W
Q-TDS	0.37	-0.53**
Q-AC[a]	-0.16	0.04
Sample size	28	37
a : calculated from $[H^+]$ concentrations ** : r value significant at 0.001 level		

Table 4.3. Linear correlation coefficients (r) for discharge and TDS and discharge and acidity for the EIF and WIF streams during the period of active layer development, subperiod 1, 1991.

4.3. Period of active layer development: subperiod 2 (6 July to 17 July, 1991)

4.3.1. Hydrology

This period of comparatively rapid active layer development (Figure 4.2) is characterized by warmer daily mean temperatures (mean temp.= 5.1 °C) than recorded in period one. Rainfall on 15 and 16 June results in peak discharge in the WIF/W on 16 June, but has no effect on the hydrograph of the EIF stream. Overall, the hydrographs of both streams are very different; the discharge of the WIF/W, especially, fluctuates over a large range (Table 4.4). A further assessment of the timing of diurnal peak discharge is given by bi-hourly sampling on 12 and 13 July (Figures 4.6 and 4.7). Peak discharge occurs in the WIF stream on 12 July between 23:00 and 24:00 hours and in the EIF stream later on 13 July around 3:00 to 4:00

	EIF					WIF/W				
	n	Mean	Std. dev.	Max.	Min.	n	Mean	Std. dev.	Max.	Min.
pH	24	6.12	0.42	6.09	4.68	25	6.06	0.15	6.38	5.75
TDS (mg/l)	24	124	25.9	168	77.9	25	52.9	10.3	79.9	38.9
Q (l/s)	23	0.10	0.07	0.25	0.0	25	1.28	1.05	4.8	0.05
Na^+ (mg/l)	7	4.03	1.38	5.83	1.38	6	5.75	2.97	9.96	3.53
K^+ (mg/l)	7	0.94	0.08	1.08	0.83	6	0.73	0.05	0.81	0.69
Ca^{2+} (mg/l)	7	22.4	4.93	32.1	17.5	6	9.53	1.73	12.7	7.89
Mg^{2+} (mg/l)	7	3.89	0.47	4.77	3.48	6	2.89	0.53	3.91	2.43
Cl^- (mg/l)	7	0.36	0.15	0.65	0.24	6	0.52	0.36	0.78	0.05
SO_4^{2-} (mg/l)	7	78.1	20.4	109	57.1	6	28.3	7.0	42.0	22.9

a: Mean calculated from $[H^+]$ concentrations and reconverted to pH

Table 4.4. Mean, maximum and minimum values of chemical characteristics of the EIF and WIF/W streams during the period of active layer development, subperiod 2, 6-17 July, 1991.

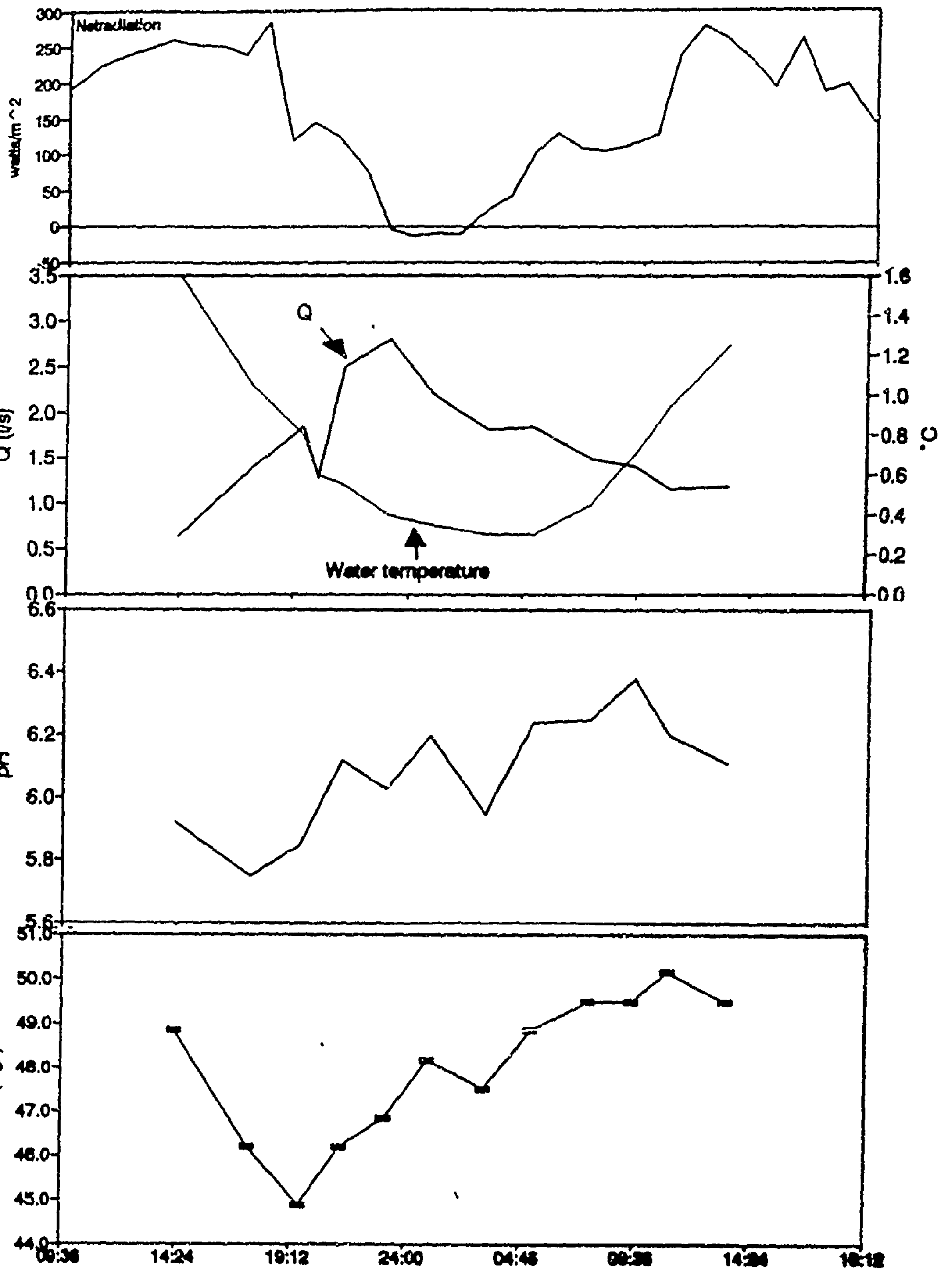

Figure 4.6. Diurnal variations in net-radiation, discharge, water temperature, pH and TDS concentrations in the WIF/W stream, 12 to 13 July, 1991.

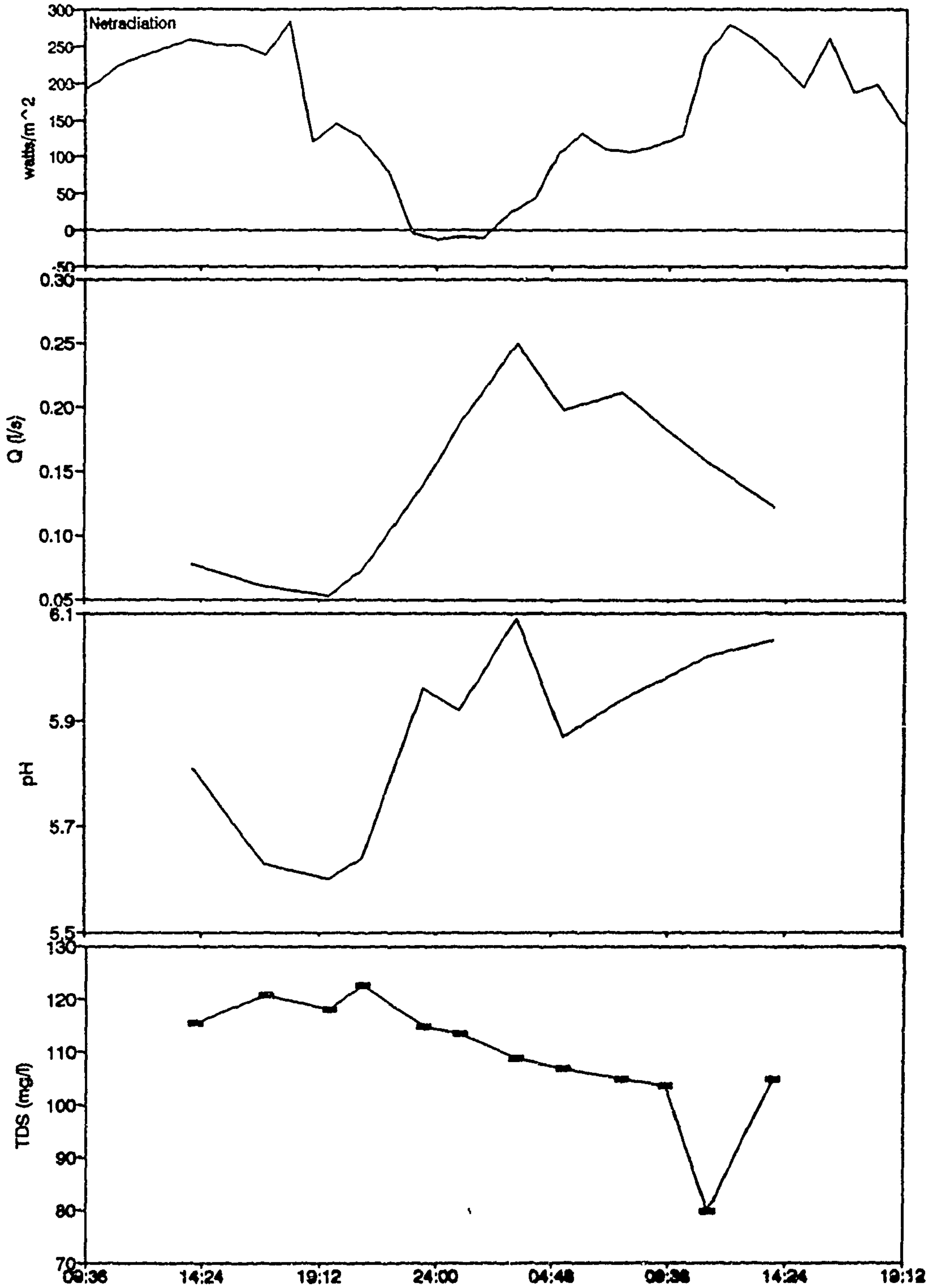

Figure 4.7. Diurnal variations in net-radiation, discharge, pH and TDS concentrations in the EIF stream, 12 to 13 July, 1991.

hours, when net-radiation reaches the daily minimum. It was also noted in the field that the sun shines directly from the northwest into the north extending valleys of the WIF/W and EIF basin between 1:00 and 2:00 hours. In comparison to snowmelt, the lag time between maximum net radiation and peak discharge is increased considerably (approximately five to seven hours) as a result of active layer drainage characteristics, ice and snow storage characteristics and changing flowpaths. Figure 4.6 demonstrates that, with increasing discharge in the WIF/W stream, the stream water temperature decreases, reaching a minimum of 0.3 °C approximately three hours later than the peak in discharge. These daily water temperature fluctuations in the WIF/W stream persist throughout the entire summer period (Figure 4.8). Unfortunately, such a temperature record is not available for the EIF stream. However, EIF stream data recorded from 30 June to 5 July reveal some interesting results (Figure 4.8): 1. EIF stream water temperatures also fluctuate on a daily basis and 2. the water of the EIF is considerably warmer than in the WIF.

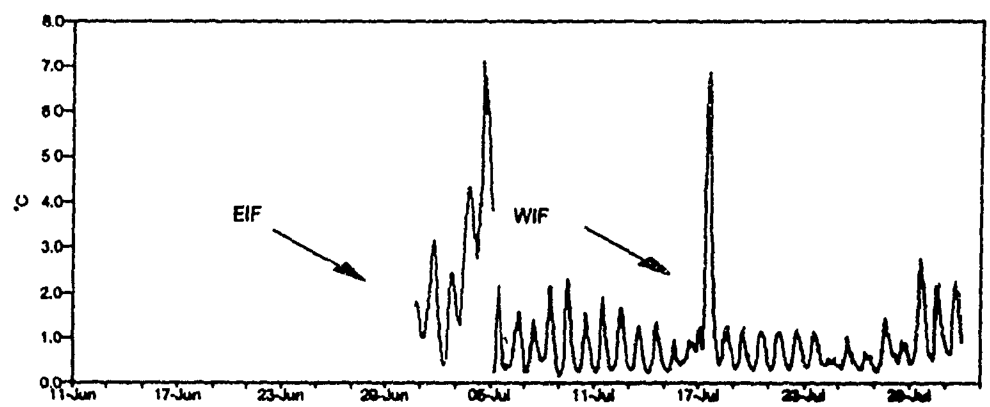

Figure 4.8. Water temperatures of the EIF (30 June to 5 July) and WIF/W streams (5 July to 1 August), 1991.

The sharp increase of stream water temperature in the WIF on 17 July could be the result of rain on 16 July.

Total daily discharge and average daily temperature display a strong, positive relationship in the WIF/W stream ($r=0.81$, $p < 0.001$, $n=11$; Figure 4.9 and Table 4.2); however, a similar relationship is not observed in the EIF stream.

4.3.2. Chemistry

Mean TDS concentrations of the EIF stream are more than twice the concentrations of the WIF stream (Table 4.4). In the EIF stream, TDS concentrations decrease significantly with increasing discharge ($rQ/TDS=-0.55$, $p < 0.01$, $n=24$; Table 4.5 and Figure 4.5), but a significant correlation between discharge and specific ions is not found (Appendix B).

	EIF	WIF/W
Q-TDS	-0.55*	0.04
Q-AC[a]	-0.35	-0.21
Sample size	24	25
a : calculated from $[H^+]$ concentrations * : r value significant at 0.01 level		

Table 4.5. Linear correlation coefficients (r) for discharge and TDS and discharge and acidity for the EIF and WIF streams during the period of active layer development, subperiod 2, 1991.

In the WIF stream, TDS concentrations stay relatively constant with increasing discharge (Figure 4.4c). The fact that high discharge does not coincide with low TDS concentrations is also demonstrated by diurnal sampling undertaken July 12 and 13, 1991 (Figures 4.6 and 4.7).

4.4. Period of active layer development: subperiod 3 (18 to 1 August)

4.4.1. Hydrology

This subperiod is characterized by the highest mean daily air temperature (8.8°C) and highest amount of precipitation recorded (11.2 mm) throughout the entire period of active layer development (Table 3.2).

In comparison to the other two periods, the mean discharge is highest in both streams during this period (Tables 4.1, 4.4 and 4.7). Diurnal variations in discharge are reflected in the shape of the hydrographs; peak discharge in the WIF/W stream occurs shortly before midnight. Associated with diurnal variation in discharge are diurnal variations in water temperature (Figure 4.8). Of note during this high flow period is the fact that stream water temperature of the WIF/W stream is lower than in previous periods.

A linear regression analysis applied on the WIF/W data for the third period of active layer development supports the observation of a significant positive correlation between total daily discharge and mean daily air temperature ($r=0.95$, $p < 0.001$, $n=15$; Table 4.2); mean daily air temperature explains as much as 90%

of the observed variability in total discharge (Figure 4.9c). This is the highest correlation coefficient between discharge and mean, daily temperature for all periods of active layer development (Table 4.2) and underlines the strong, positive relationship between these two variables.

In comparison, the EIF stream exhibits no significant relationship between average daily temperature and total daily discharge (Table 4.2). One reason for the lack of a significant relationship is the paucity of data (Table 4.2). However, peak discharge in the EIF stream occurs between midnight and 6:00 hours the following morning. This time lag makes it necessary to regress the total daily discharge with the temperature of the previous day (for example total daily discharge on 18 July against the daily average temperature of 17 July). Using this method, a significant correlation is identified for a 48 hour delay between mean daily temperature and time of peak discharge ($r=0.68$; $p < 0.01$, $n=15$; Table 4.2).

Following the precipitation on 25 July (3 mm of rain), both streams show a peak in discharge (Figure 4.1). Subsequent precipitation events (snow on 27 July, rain on 28 July) only have an effect on the EIF stream. This, in addition to the fact that the magnitude of the discharge peak after the rain on 25 July is much higher in the EIF, indicates that response to precipitation is different in the EIF and WIF/W basins possibly indicating different levels of saturation of the active layer. Multivariate regression analysis for mean daily temperature, precipitation and total daily discharge illustrates that precipitation is only significant for predicting the total daily discharge of streams in combination with mean air temperature (Table 4.2).

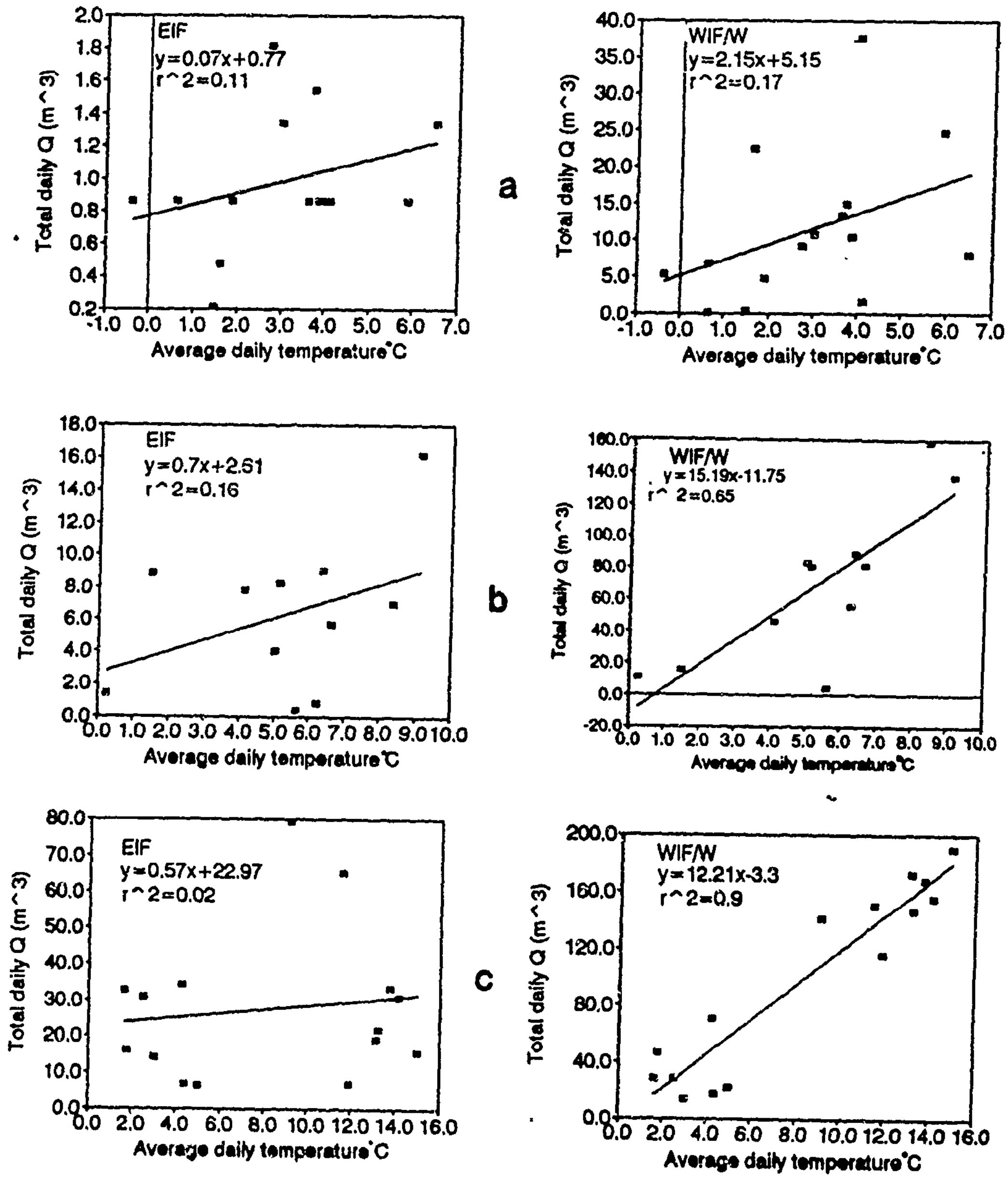

Figure 4.9. Linear regression analysis for mean daily temperature (independent) and total daily discharge (dependent) for the EIF and WIF/W streams during the period of active layer development, subperiod 1 (a), subperiod 2 (b) and subperiod 3 (c), 1991.

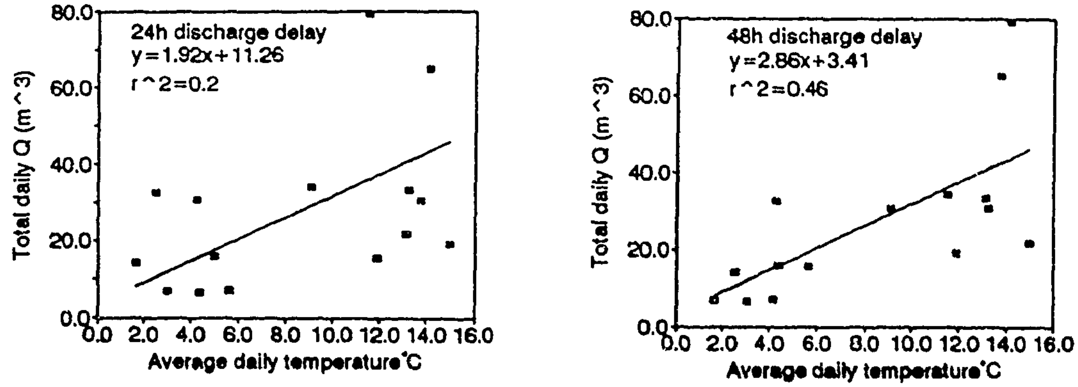

Figure 4.10. Linear regression analysis for mean daily temperature and 24 and 48 hours delay in discharge of the EIF stream during the third period of active layer development.

Overland flow was observed in the lower, alluvial fan areas in both basins during this time. In the WIF basin, this phenomenon is caused by high discharge in the WIF/W stream channel forcing the WIF/W stream to overflow first when it exits the lower, WIF/W valley (Figure 2.3) and a second time downstream at the weir site. As a result, widespread overland flow occurs in microtopographic channels (between hummocks) towards the lake below the weir.

Seepage areas (known as "seeps"; Chapter 2; Figure 2.1) are an interesting phenomena that appear to be connected to surface runoff. Further observations and spatial sampling were undertaken to investigate this phenomenon (Figure 4.11). The WIF/W stream overflows shortly after exiting the valley and flows towards the SW seep. After approximately 10 metres, the stream disappears into the ground, similar to a sinkhole of a karst system. The water reappears 41 metres downslope in the form of one large seep (SW seep) and several minor seeps. It appears that a thermokarstic system in combination with large grained soil material enables infiltration and fast routing of water. The residence time of the water is unknown (a dye tracer test failed), however field observations suggest it is short because the discharge rate seemed to be directly proportional to the WIF/W overflow and infiltration rate. In addition, tritium concentrations of the SW seep and the WIF/W stream are essentially the same and tritium concentrations of the frozen active layer considerably higher (Table 4.6), which indicates no mixing of the infiltration water.

	EIF 23 July	WIF/W 23 July	WIF/2 23 July	SW seep 25 July	Ground ice* 23 July	Snowpack 10 May	Active layer** 23 July	Snow 19 June
T.U.	33 (± 8)	27 (± 8)	34 (± 8)	28 (± 8)	13-16 (± 8)	9 (± 8) (B2) 20 (± 8) (W3)	52 (± 8)	33 (±8)

* taken from solid ice at the base of boulders at felsenmeer site in EIF basin
** extracted from frozen, active layer at 41-42 cm depth

Table 4.6. Tritium concentrations from selected sites during the period of active layer development, 1991.

In the EIF basin, areas with overland flow were observed on the western and eastern steep slopes beneath felsenmeers (Figure 2.2). In contrast to the WIF basin, discharge in the EIF is not sufficient to generate overland flow in the lower alluvial fan area. At the base of the slope, surface water infiltrates into the active layer. As a result of this saturation, relatively wet areas are created on the base of the slopes and in parts in the upper and middle alluvial fan area. These highly saturated areas can be distinguished easily by the type, colour and density of vegetation (Colour Print 5), since wetter areas support mosses and sedges. Overland flow was also observed in the upper and middle reaches of the WIF/2 catchment (Figures 2.2 and 4.12).

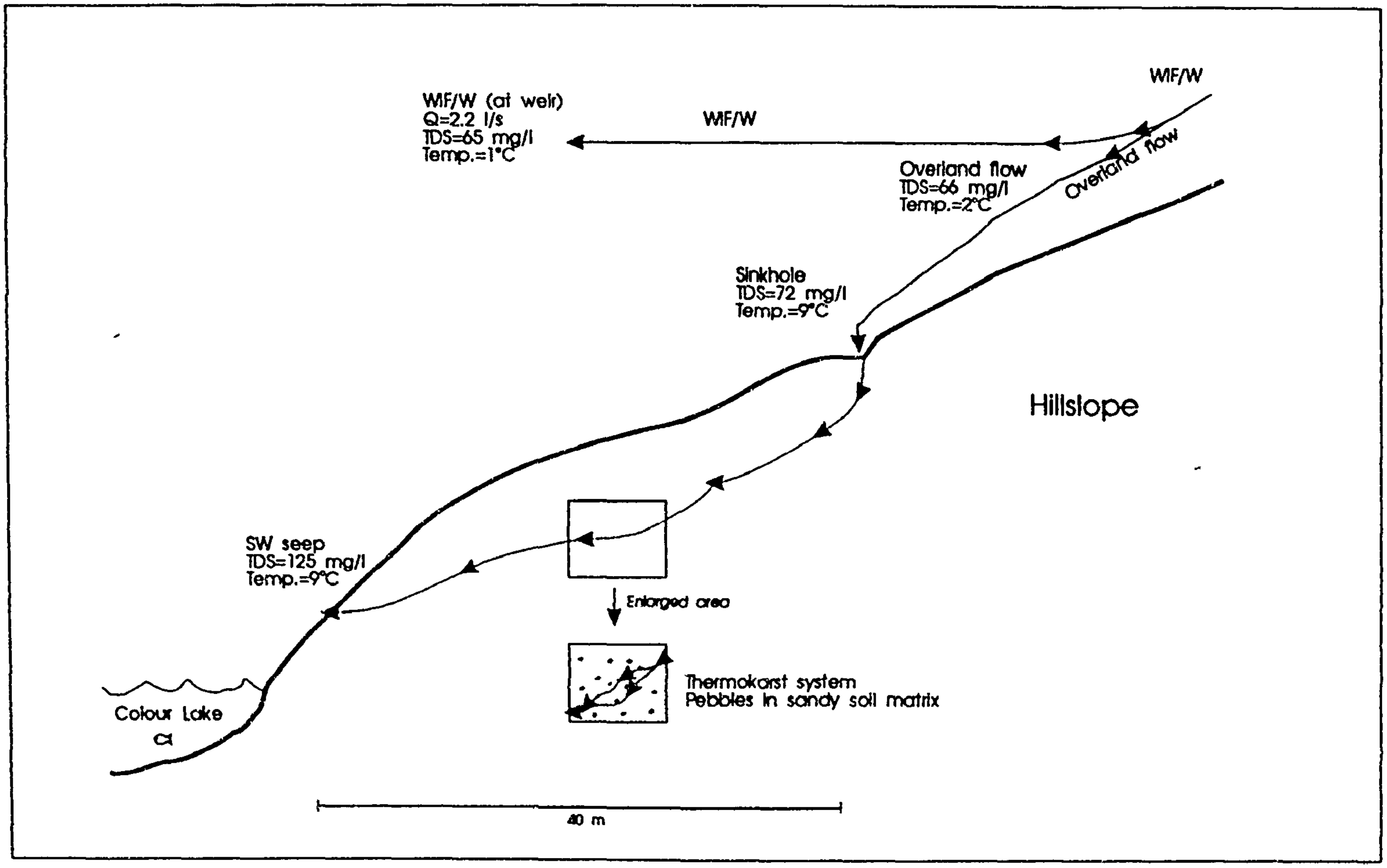

Figure 4.11. Spatial sampling to investigate the source of the SW seep, 19 July, 1991.

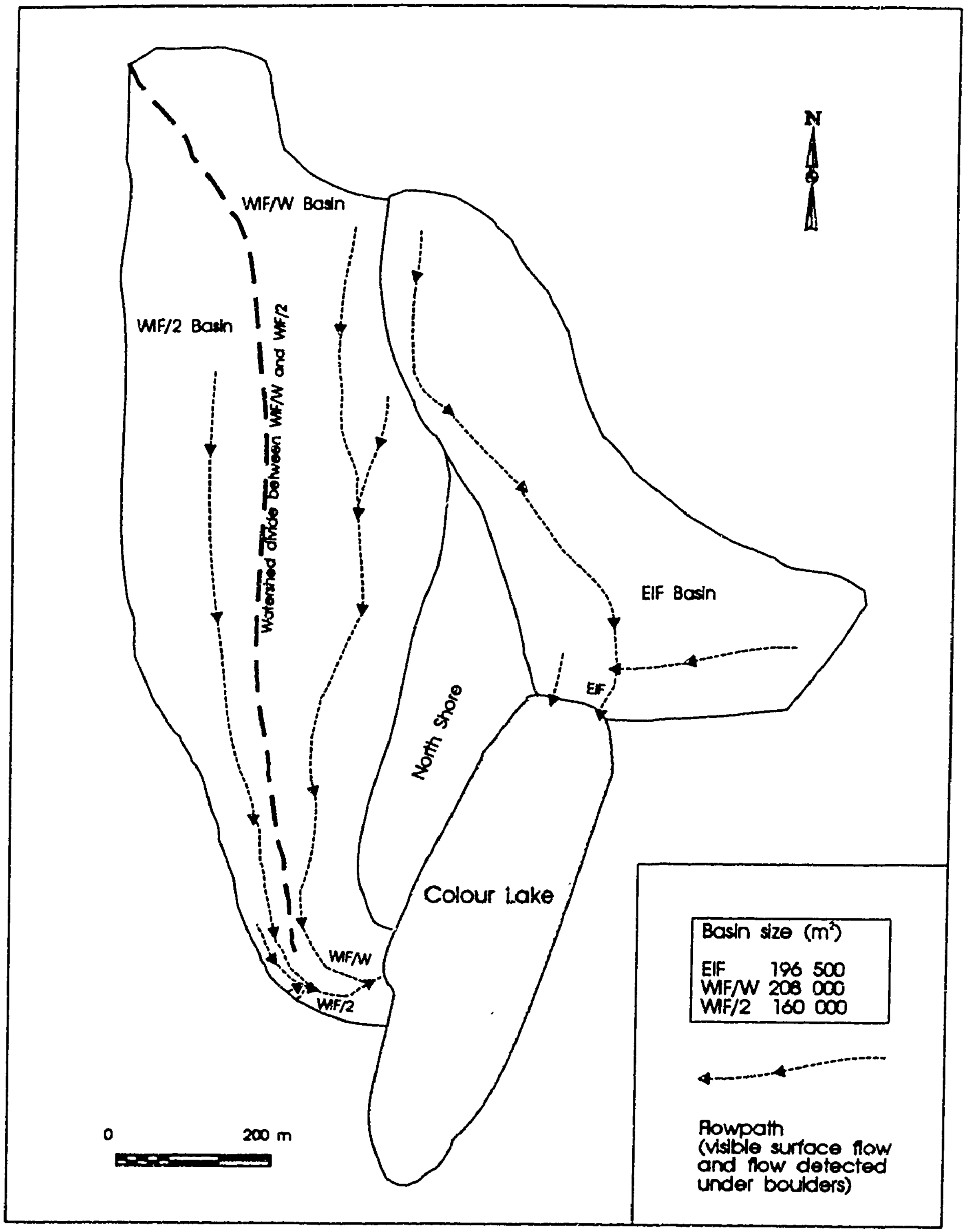

Figure 4.12. Water flowpaths identified in the EIF and WIF basins and division of the WIF basin into the WIF/W and WIF/2 sub watersheds.

Colour Print 5. EIF basin on 3 August, 1991. Higher ground saturated zones in the basin can be distinguished by the lighter colour of the vegetation.

	EIF					WIF/W				
	n	Mean	Std. dev.	Max.	Min.	n	Mean	Std. dev.	Max.	Min.
pH[a]	18	6.12	0.31	6.47	5.09	17	6.3	0.2	6.67	5.85
TDS (mg/l)	18	147	37.0	209	94.4	17	135	47.5	205	56.8
Q (l/s)	18	0.38	0.33	1.27	0.08	16	1.22	0.75	2.2	0.16
Na^+ (mg/l)	4	3.23	1.05	4.05	1.78	6	3.34	2.2	7.02	0.98
K^+ (mg/l)	5	1.14	0.18	1.41	0.92	7	1.12	0.13	1.27	0.9
Ca^{2+} (mg/l)	5	28.4	6.74	36.3	17.84	7	24.3	5.66	33.0	15.3
Mg^{2+} (mg/l)	5	5.07	1.06	5.88	3.3	7	7.77	2.09	11.27	5.22
Fe^{2+}(mg/l)	3	0.06	0.03	0.09	0.04	1	0.03	n.a.	n.a.	n.a.
Al^{3+}(mg/l)	3	0.28	0.04	0.32	0.25	1	0.42	n.a.	n.a.	n.a.
Cl^- (mg/l)	4	0.5	0.26	0.74	0.24	6	1.44	1.63	4.76	0.68
SO_4^{2-}(mg/l)	5	94.1	29.3	130	51.1	7	84.2	23.6	123	84.5

a: Mean calculated from $[H^+]$ concentrations and reconverted to pH

Table 4.7. Mean, maximum and minimum values of chemical characteristics of the EIF and WIF/W stream during the active layer period, subperiod 3, 18 to 1 August, 1991.

Water running beneath boulders and fractured bedrock enters the alluvial fan area and travels from there as surface flow or saturated groundwater flow in the active layer towards the lake. Field observations such as this made it possible to define the sub watersheds of the WIF/W and WIF/2 streams (Figure 4.12). As a result of saturated active layer conditions in large parts of the lower alluvial area and, in addition, rain on 15 and 16 July, the WIF/2 stream starts to flow on 21 July and continues to flow to 30 July.

4.4.2. Chemistry

Mean TDS concentrations in the WIF/W during this period (135 mg/l) are more than double the TDS concentrations of the previous period (53 mg/l) and reach mean TDS concentrations of the EIF stream (147 mg/l). This increase is due to an increase in the concentration of Ca^{2+}, Mg^{2+} and SO_4^{2-} (Table 4.7). Of note is that the pH in the EIF is slightly decreased (mean pH=6.12) compared to the second period of active layer development (mean pH=6.6), which results in low Al^{3+} concentrations (Table 4.7).

Linear correlation analysis performed on WIF/W data supports the observation of a significant relationship between discharge and TDS concentrations ($r=-0.94$, $p < 0.001$, $n=16$) (Table 4.8). With increasing discharge, a significant dilution of Ca^{2+}, Mg^{2+} and SO_4^{2-} concentrations occurs ($rQ/Ca^{2+}=-0.86$, $p < 0.01$; $rQ/Mg^{2+}=-0.91$, $p < 0.001$; $rQ/SO_4^{2-}=-0.92$, $p < 0.001$; all $n=7$).

	EIF	WIF/W
Q-TDS	-0.03	-0.94**
Q-AC[a]	-0.18	0.3
Sample size	18	17

a : calculated from $[H^+]$ concentrations
* : r value significant at 0.01 level
** : r value significant at 0.001 level

Table 4.8. Linear correlation coefficients (r) for discharge and TDS and discharge and acidity for the EIF and WIF streams during the period of active layer development, subperiod 3, 1991.

An interesting result of the correlation analyses between ion concentrations is that this is the first period where Na^+ concentrations in both stream waters exhibit a significant, positive relationship to Cl^- ($rNa^+/Cl^-=0.99$, $p < 0.001$, $n=7$), suggesting the dissolving of an NaCl rich layer or mineral (such as halite). Anisimova (1978) reports from his observations in Siberian permafrost areas and laboratory experiments that a concentrated, chloride salt layer is formed between the upper permafrost and the frozen active layer by cryogeneous processes. During the last stages of active layer freezing, chloride salts migrate via diffusion through the interconnected liquid film system towards the permafrost induced by gravitational and thermal gradients (Anisimova, 1978). This hypothesis of ion migration and subsequent formation of ion concentrated layers is further supported by Ugolini and Anderson (1973) and Qiu *et al.* (1988). Therefore it seems possible that the significant correlation between Na^+ and Cl^- in both streams indicates the dissolving of a NaCl rich layer between the upper permafrost and thawed active layer; by the end of this period, the depth of thaw of the active layer had reached the seasonal maximum of 0.55 m which was close to the permafrost table.

Precipitates of iron oxy-hydroxides found in the EIF stream bed adjacent to the soil-piezometer site EIF/D and EIF/E (Figure 2.1), possibly identify areas of suprapermafrost groundwater discharge. Water samples extracted from soil mini-piezometer EIF/D are exceptionally high in total iron (up to 22.3 mg/l) in comparison to other water samples extracted from soil-piezometers in the EIF and WIF basin (Appendix C). Further evidence of discharge of highly concentrated groundwater into the stream is given by spatial stream sampling conducted on 19 July, 1991 (Figure 4.13). The data suggest that between sampling points 5 and 7 no surface flow enters the stream, but an increase in TDS concentrations from 88 to 120 mg/l indicates a source of highly concentrated groundwater. Moreover, spatial stream sampling undertaken on 12 August, 1992 suggests that this concentrated groundwater, originating from the eastern slope of the EIF basin, is highly acidic (Figure 4.15).

Rain and snow events appear to have little effect on the streamflow chemistry. Of note is an increase in TDS concentrations and a decrease in pH in all streams (including WIF/2; Appendix C) during the rising limb of the hydrograph. The only exception to these observations is a pH increase in the WIF/W after the rain on 16 July (Figure 4.2). Since ion concentrations are very low in precipitation (Table 4.9), a dilution would be expected in the streams. According to Everett *et al.* (1989) pH decrease can in some cases be tied to an increase in total dissolved organic carbon

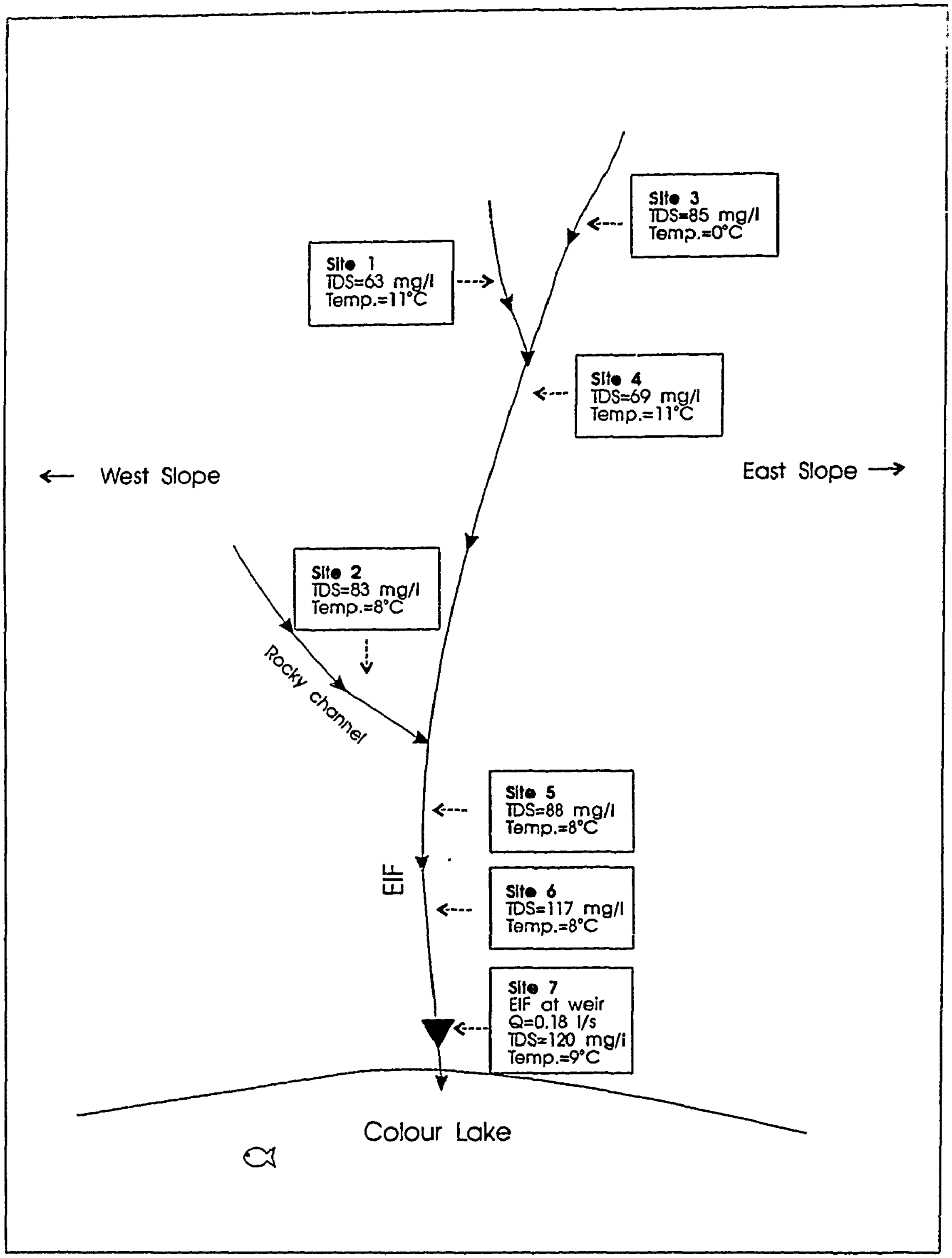

Figure 4.13. Spatial stream sampling in EIF basin, 19 July 1991.

Date	Type	pH	TDS (mg/l)	Na^+ (mg/l)	K^+ (mg/l)	Ca^{2+} (mg/l)	Mg^{2+} (mg/l)	Cl^- (mg/l)	SO_4^{2-} (mg/l)	NO_3 (mg/l)	% imb.x
13-Jun-91	Snow	5.76	2.6	0.24	0.11	0.11	0.04	0.16	0.47	0.08	21
14-Jun-91	Rain	4.97	4.6	n.a.	n.a.	n.a.	n.a.	n.a.	n.a.	n.a.	n.a.
18-Jun-91	Snow	5.36	n.a.	1.06	0.43	1.89	0.1	n.a.	n.a.	n.a.	n.a.
19-Jun-91	Snow	5.11	9.2	0.88	0.41	0.61	0.03	0.75	1.07	0.18	31
29-Jun-91	Snow	5.33	7.3	0.57	0.40	0.65	0.04	0.88	0.4	n.a.	36
15-Jul-91	Rain	5.11	4	n.a.	n.a.	n.a.	n.a.	n.a.	n.a.	n.a.	n.a.
16-Jul-91	Rain	5.57	5.9	n.a.	n.a.	n.a.	n.a.	n.a.	n.a.	n.a.	n.a.
01-Aug-91	Rain	n.a.	n.a.	1.53	0.48	1.12	0.07	0.92	0.78	n.a.	54
02-Aug-91	Rain	5.72	7.26	*	0.23	1.66	0.14	*	2.07	0.11	n.a.

* sample was contaminated with NaCl

x Charge imbalance [%] = $\left| \frac{\sum cations - \sum anions}{\sum cations + \sum anions} \right| \times 100$ (units in equivalents)

Table 4.9. Summary of precipitation chemistry, 1991.

(DOC) and organic acids. However, as the DOC concentration is low in both streams (Schiff *et al.*, 1991), other factors must be responsible for the pH depression associated with increased TDS concentrations. Another possible interpretation is the contribution of highly concentrated suprapermafrost groundwater to the stream. Rainwater potentially mixes with water in the phreatic (suprapermafrost groundwater) and vadose zone and this mixture is pushed out during the onset of the rain event ("flushing"). This is supported by higher total ion concentrations in the suprapermafrost groundwaters relative to stream water (Chapter 6).

4.5. Discussion

The classification of the period of active layer development into three subperiods identifies the effects of environmental variables such as precipitation, air temperature, net-radiation and active layer development on the hydrological regime.

Data collected during the first period of active layer development suggest that the temperature has to rise above a critical point (for example mean daily temperature > 0.8 to 1°C) to have a positive effect on runoff and that storage in the relatively thin active layer is insufficient to generate runoff. This period could be classified as "low flow period". During the second period the fast developing active layer provides an enhanced storage potential for precipitation ("replenishment/saturation of active layer period"). In the third subperiod, total discharge in the WIF/W and EIF is largely determined by the melting of ground ice (stored under large boulders, typically felsenmeer or fractured bedrock) and flow routing of the meltwater ("ground ice melt period"). During this period, the strong causal connection between discharge and average daily temperature in the WIF/W stream enables reasonably accurate prediction of total daily discharge by average daily air temperature. Throughout the entire summer period, no such accurate function can be developed to predict discharge in the EIF. The greater time required for a response to maximum daily net radiation and air temperature in the EIF basin indicates different flowpaths and water storage mechanism in the two basins.

A combination of several observations and analyses suggest that the melting of ground ice is a potential source of stream water. Throughout this thesis the term ground ice refers to the basal ice layer underneath boulders and shattered bedrock material and should not be mistaken with the seasonally thawing of the active layer. This basal ice layer is typically formed by meltwater refreezing on the base of a cold substrate (Woo *et al.*, 1982) and was found in the basin (Colour Print 6 and Figure 4.14). Results presented in Chapter 3 suggest that cold temperatures at the base of felsenmeers and boulders induce the refreezing of snowmelt water and therefore the formation of the basal ice. In addition, the ground ice is preserved in the deep valleys by the lack of the direct sunlight and diurnal air temperature variations. Surface flow is typically detected in areas with a high potential for the development of ground ice; the WIF/W runs adjacent to the area of highest ground ice potential (Figure 4.14). Similar to a glacial system, high discharge is yielded on

Colour Print 6. Ground ice under boulders (soil zone 4) in EIF basin, June 1991.

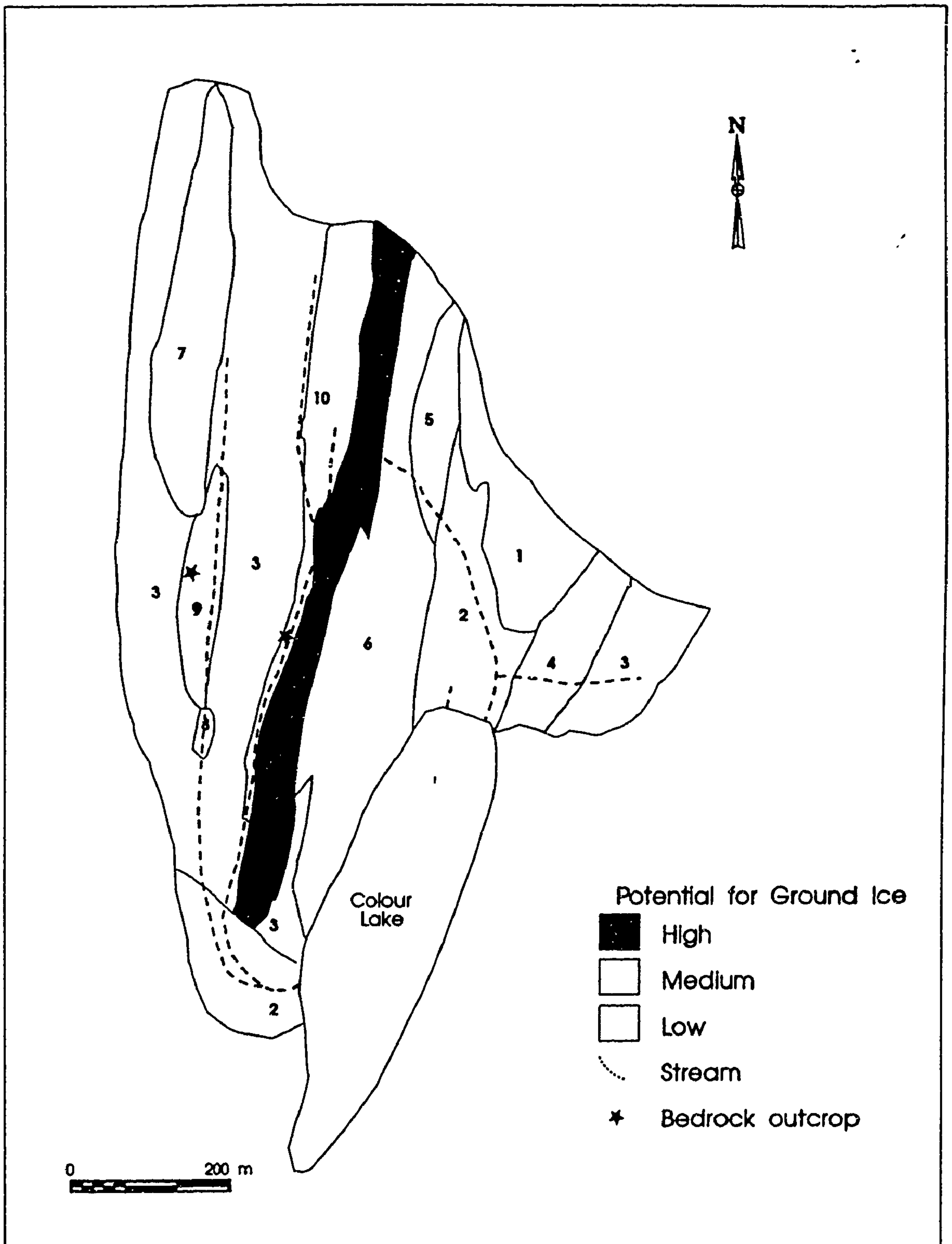

Figure 4.14. Areas with high potential for ground ice in the EIF and WIF basins. For description of geomorphology zones 1 to 10 see following page.

Zone	Vegetation cover (%)	Average grain size (m), % coverage, material	Classification	Notes
1	>80 (Mosses, lichens)	20% rock cover	Alluvial fan	-
2	60-80 (Carex, Willow, Cassiopea spp.)	Sandy loam with pebbles	Alluvial fan	Wet to mesic meadow vegetation
3	<10	0.05-0.25, 50-80% coverage on sandy soil Sandstone on EIF slope, Sandstone and Shale in WIF basin	?	Slumping Abundant salt crusts on east slope of EIF basin
4	<30 >70 moss cover in lower parts adjacent to stream	0.2-0.7, 80% coverage Sandstone, shale	Felsenmeer?	Slumping
5	<10	0.25-0.5, 10-30% coverage (?) Fine weathered shale soil matrix	?	Slumping
6	<1-5	0.2-0.5, 90-100% coverage Sandstone	Shattered blockfield	-
7	<1	0.5-2.0, 100 % coverage Sandstone	Felsenmeer	Area with highest potential* for ground ice
8	>70-80	0.1-0.5, <20 % coverage Sandy loam with pebbles	?	Vegetation abundant close to stream; wet sedge meadow vegetation
9	<1 (Papaver radicatum)	80% coverage Sandstone	Shattered bedrock ridge	Slumping
10	<1-5	0.1-1.5, 90% coverage Sandstone	Felsenmeer, partly covered by slumps	Large slumping sites partly vegetated

* potential meaning here the quantitative amount of ground ice below boulder material (classified into three zones: high, medium, low) determined by field observations and geomorphological and vegetation characteristics

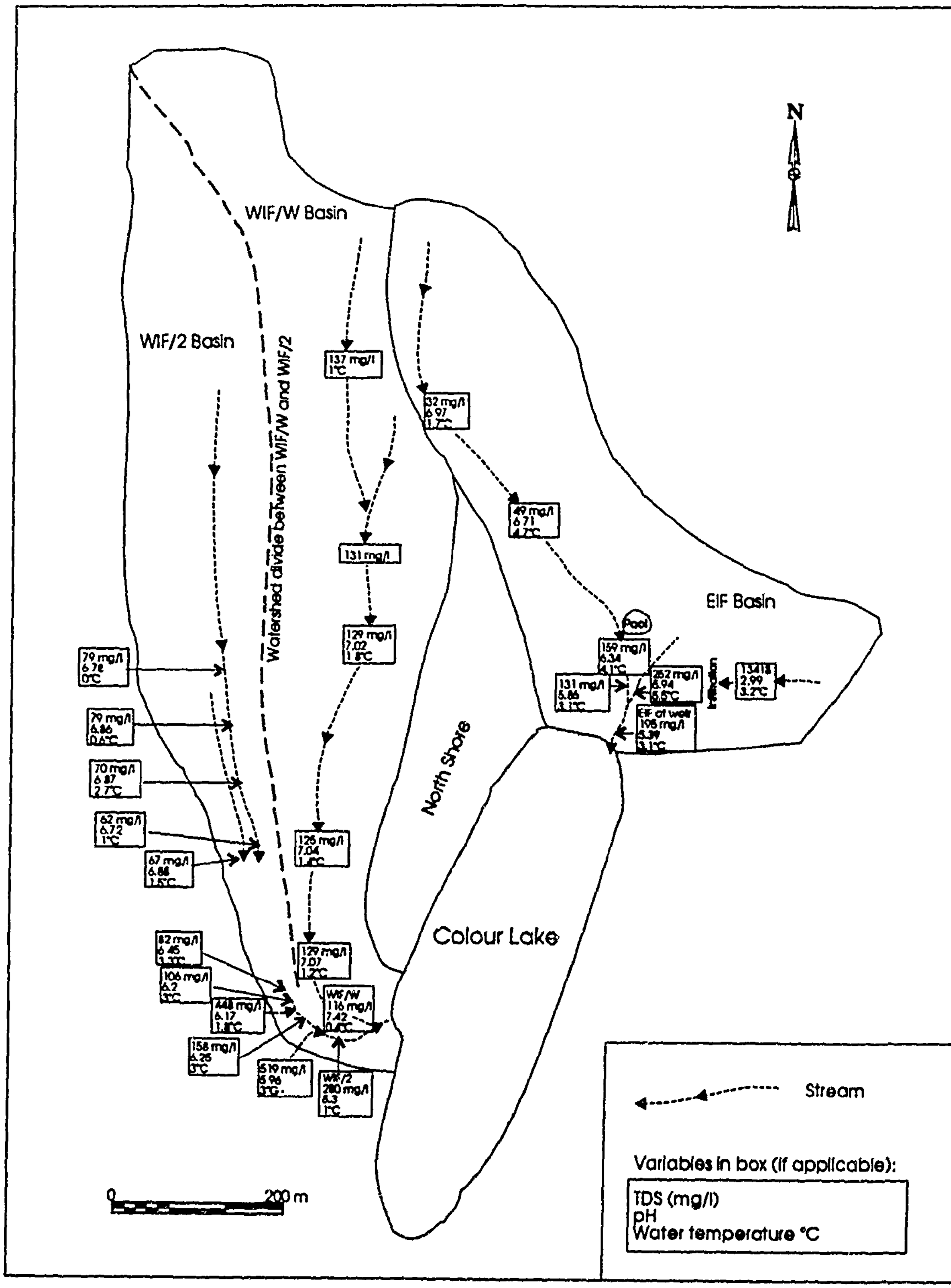

Figure 4.15. Spatial stream sampling of waters in the WIF and EIF basins, 12 August, 1992.

warmer days within short response times. Further evidence of the release of cold meltwater in the WIF/W is given by daily fluctuations in stream water temperature and minimum temperatures at the time of highest discharge. In the EIF, ground ice is found on the lower eastern hillslope and in the upper western valley. In contrast to the WIF/W, a generally smaller ground ice storage capacity reduces the amount of meltwater (Figure 4.14). Additionally, the lack of a defined stream channel results in increased transport of water through the saturated layer which is reflected by the increased lag time between discharge and maximum net-radiation and mean daily temperatures. Since the sediments in the alluvial fan area are mainly comprised of sandy loams, the hydraulic conductivity is estimated in the order of $K=10^{-5}$ to 10^{-3} cm/s (Freeze and Cherry, 1979).

The water temperatures of the EIF stream recorded from 1 to 5 July are considerably higher than the WIF/W. This could either be the result of discharge of warm suprapermafrost groundwater into the stream or the lack of the cooling effect of water travelling on ground ice. Figure 4.15 shows that water discharging into the stream after travelling in the active layer is considerably warmer than water emerging from felsenmeer sites (for example, the temperature of surface water entering the alluvial fan from the WIF/2 basin increases from 1.5 to 3.3°C and in the EIF basin from 1.7 to 4.7 °C; Figure 4.15).

Multivariate regression analysis for temperature and precipitation versus discharge for both streams indicates that the effects of precipitation on discharge are only significant in combination with air temperature during the three periods of active layer development. Differences in antecedent moisture conditions and thickness of the active layer in the basins affect the streams in different ways. For example, heavy rainfall on 15 and 16 July shows no effect on the EIF stream which could be the result of greater thaw depth of the active layer in the EIF basin (Figure 4.3) and therefore increased storage potential for precipitation. An interesting result is the seasonal changing response of discharge to precipitation in the EIF stream. While there is no response to precipitation during the first and second period of active layer development, a significant increase of discharge occurs after precipitation during the third period of active layer development. This supports the observation, that the saturation of the active layer increases during the first and second period of active layer development and as a result, precipitation has a significant influence on runoff in the EIF stream during the third period of active layer development.

Antecedent moisture conditions and the amount of precipitation are important factors in generating stream flow, as is exhibited by the intermittent WIF/2 stream. Although this assessment of antecedent moisture condition is entirely based on field observations and hydrograph analysis, it gives a rough indication about the spatial and temporal changes of the saturation of the active layer. Chapter 5 discusses this topic in greater detail.

Results from chemical and isotopic analyses give further evidence of the differences in flow regimes of the EIF and WIF basin. The first important result centres around the formation of ground ice. Using tritium analysis, Chizkov *et al.* (1983) identify the source of ground ice as refrozen snowmelt water in rock glaciers and other unconsolidated deposits. In agreement with their results, tritium concentrations of the snowpack and the ground ice lie in the same range in the Colour Lake catchment, thereby the origin of ground ice could be snowmelt water (Table 4.6). It is possible that older ground ice (which was formed in previous years and could possibly be identified by higher tritium concentrations) exists in the basin, but no data are available to support this. Higher tritium concentrations are detected in samples extracted from the frozen active layer at 41 cm depth (Table 4.6). Considering the results of tritium analyses for the three streams it appears that stream runoff is generated in different ways. The WIF/W has the lowest tritium concentrations of all three streams which suggests reduced mixing between meltwater from ground ice and the active layer and/or a faster transport of water in a bouldery, icy bed structure. The isotopic results are in agreement with the chemical data; higher TDS concentrations in the EIF and WIF/2 stream reflect a longer residence time of the water in the soil and/or a higher mixing rate with the suprapermafrost groundwater. The diurnal fluctuations in TDS, which are related to discharge variations in the WIF (similar to a glacial regime), are not found in the EIF/W stream. However, melting of ground ice is also an important factor in generating stream flow runoff. Evidence for this is given by 1. field observations (overland flow below zones where the potential for ground ice is high) (Figure 4.14), 2. a significant relationship for discharge and air temperature (for two days delay in discharge) during the third period of active layer development.

Since the meltwater from the western part of the EIF is higher in pH than the eastern slope, the proportion of this source is higher relative to the more acidic water from the eastern slope. The spatial and temporal variation of surface water flow suggest two chemically different sources within the EIF basin. This is investigated in detail in Chapter 6.

CHAPTER 5 THE RAINSTORM

5.1. Introduction

In the literature, the high arctic is often described with the term "polar desert" due to low precipitation rates and intensities (Tedrow, 1977; Bliss *et al.*, 1984). However, rainstorms with high rainfall intensities up to 50 mm/day are recorded at several high arctic weather stations (Table 5.1). The occurrence of such events is rare and takes place every 10 to 20 years, for some stations the return period might even exceed 25 to 50 years (Cogley and McCann, 1976).

Date	Location	Total precipitation event	Maximum, daily intensities	Source
21-24 July, 1973	Vendom Fiord (Ellesmere Is.)	55.5	49.4	Cogley and McCann, 1976
21-24 July, 1973	Cape Herschel (Ellesmere Is.)	63.9	47.2	Cogley and McCann, 1976
21-24 July, 1973	Coburg Island	34.6	30	Cogley and McCann, 1976
2-4 August, 1978	Oobloyah Valley (Ellesmere Is.)	35.4	26.2	Flügel, 1981
5-27 July, 1961	Colour Lake Camp (Axel Heiberg Is.)	81.6	21.7	Müller and Roskin-Sharlin, 1967
1-13 August, 1991	Colour Lake Camp (Axel Heiberg Is.)	117	38	This study

Table 5.1. Examples of exceptional precipitation events recorded from stations in the high arctic.

Between 1 and 11 August 1991, a total precipitation of 117 mm was recorded in the Colour Lake catchment with maximum intensities of 38 mm/day on 2 August. A second peak in rain occurred on 5 and 6 August, when a total precipitation of 35 mm fell in 24 hours. In between high rainfall intensities, several smaller events were recorded (Figure 5.1). Since this event is exceptional, this chapter will discuss in detail the effects on the hydrology and chemistry of streams draining into Colour Lake.

5.2.1. Hydrology

During the event, widespread overland flow was observed in the lower alluvial areas in the catchment (Colour Print 7). Ephemeral streams and seeps that had ceased during the summer started flowing again (No Name Creek, Gordon Creek, stream A and B, NW seep, SW seep; Figure 2.1). Overland flow on the eastern and westerns steep slopes (Gordon Creek and Stream B) carried a large amount of sediment and created small sediment deltas in the lake (Colour Print 8). On the eastern slope seepage of suprapermafrost groundwater into the lake (below the lake level) was identified by plumes of yellow-brownish sediment (close to MP5; Colour Print 9). Further observations were undertaken to investigate the origin and flowpaths of water. For example, the origin of the SW seep could be identified as WIF/W stream water by following the WIF/W stream from the point where it leaves the stream bed to the SW seep site (Figure 4.11). Streams in the WIF basin could

Colour Print 7. Overland flow at WIF/W during the rainstorm, 7 August 1991.

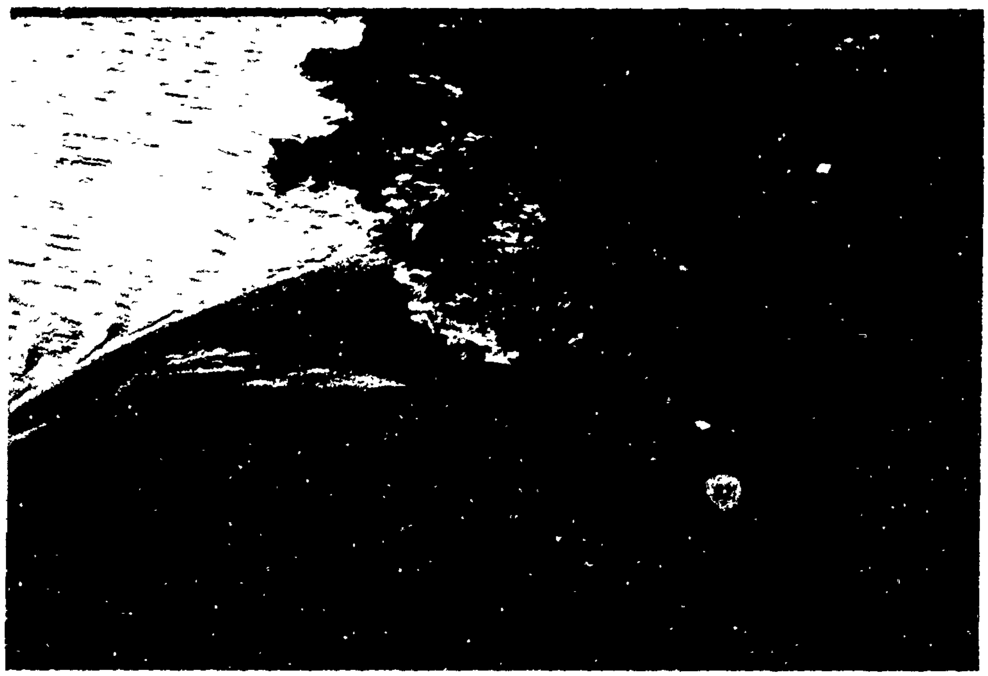

Colour Print 8. Sediment delta at Gordon Greek during rainstorm, 3 August 1991.

Colour Print 9. Discharge of suprapermafrost groundwater into Colour Lake at mini-piezometer MP5 during rainstorm, 3 August 1991.

	EIF					WIF/W					WIF/2				
	n	Mean	Std. dev.	Max.	Min.	n	Mean	Std. dev.	Max.	Min.	n	Mean	Std. dev.	Max.	Min.
pH[a]	20	4.63	0.59	5.76	4.12	19	6.29	0.19	6.71	5.83	19	6.31	0.11	6.55	6.12
TDS (mg/l)	20	224	59.21	334	135	19	126	29.9	164	70.6	19	227	84.9	381	73.9
Q (l/s)	17	5.13	5.08	15	0.38	18	4.31	2.95	12	0.96	14	4.4	4.8	18.0	0.75
Na^+ (mg/l)	12	2.37	1.34	5.23	1.22	9	1.45	0.86	3.38	0.81	10	2.81	1.32	4.8	1.0
K^+ (mg/l)	12	1.02	0.14	1.19	0.78	9	1.01	0.11	1.15	0.82	10	1.23	0.24	1.66	0.82
Ca^{2+} (mg/l)	12	38.57	9.01	53.9	24.09	9	19.6	4.02	24.3	12.9	10	25.2	7.7	38.71	13.58
Mg^{2+} (mg/l)	12	6.29	1.22	7.9	3.7	9	6.2	1.7	8.38	3.39	9	16.47	9.24	31.8	5.89
Fe^{3+}(mg/l)	12	0.76	1.75	6.31	0.14	1	0.05	n.a.	n.a.	n.a.	1	0.01	n.a.	n.a.	n.a.
Al^{3+}(mg/l)	12	2.22	2.31	6.36	0.0	1	0.46	n.a.	n.a.	n.a.	1	0.36	n.a.	n.a.	n.a.
Cl^- (mg/l)	12	0.5	0.48	1.65	0.2	9	0.72	0.2	1.17	0.39	10	0.37	0.24	0.66	0.03
SO_4^{2-}(mg/l)	12	154	50.5	223	79.4	9	65.7	16.7	87.3	38.7	10	118	50.4	221	52.3

a: Mean calculated from $[H^+]$ concentrations and reconverted to pH

Table 5.2. Mean, maximum and minimum values of chemical characteristics of the EIF, WIF/W and WIF/2 streams during the rainstorm, 2 to 13 August, 1991.

be followed up to the upper parts of the basin along water tracks outlined in Figure 4.12.

Figures 5.1 to 5.3 demonstrate the hydrographs of the EIF, WIF/W and WIF/2 streams and the rainfall record for the storm event. Detailed, bi-hourly readings and chemistry analyses were undertaken during the first 26 hours of the event. Overall, the three streams show maximum discharge peaks (up to 18 l/s; Tables 5.2) after highest precipitation intensities of 38.8 mm/12 hours on 2 August and 35.5 mm/24 hours on 5 and 6 August. In contrast to the EIF stream, where both discharge peaks have the same peak value, the first discharge peak is lower than the second in the WIF/W and WIF/2 streams. Another difference is the sharper rising limb of the first peak of the EIF stream and an additional third pronounced peak as a result of only minor rainfall (<5mm) on 8 August. These hydrograph characteristics can give an indication about antecedent saturation conditions in the active layer. Although the active layer was thicker in the EIF than in the WIF basin (Table 5.3), hence the storage potential for incoming precipitation increased, the hydrographs suggest "wetter" antecedent active layer conditions in the EIF basin.

Time	Basin	Mean active layer depth (cm)	n	Range	Std.Dev.
6 August, 1991	WIF	50	17	37-90	12.5
	EIF	60.3	6	24-77	23.9

Tables 5.3. Active layer thickness in the EIF and WIF basins during the rainstorm, 6 August 1991.

Only one measurement of the saturation level of the active layer was taken on 2

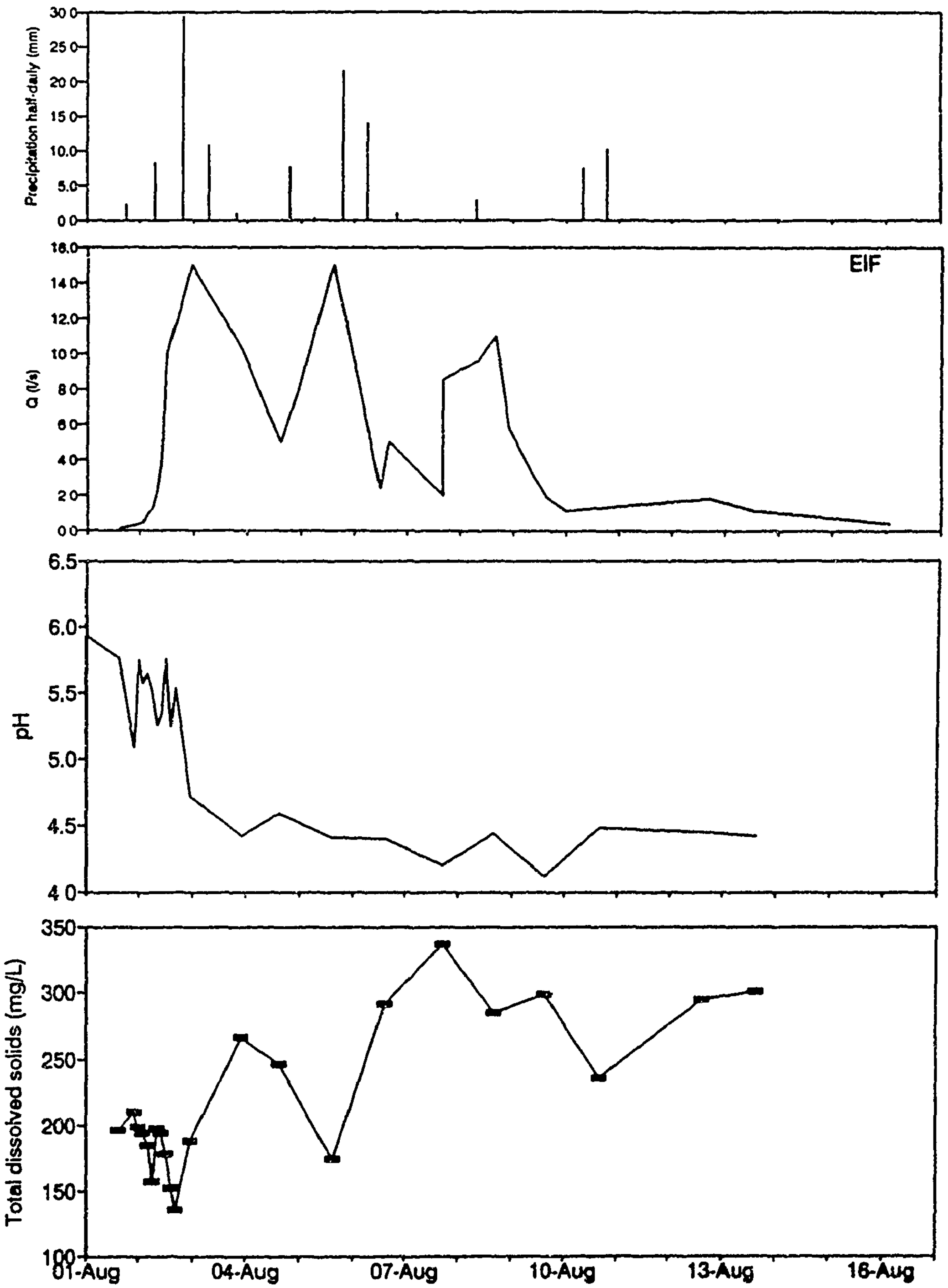

Figure 5.1. Precipitation record and discharge, pH and TDS concentrations for the EIF stream during the rainstorm, 2 to 10 August, 1991.

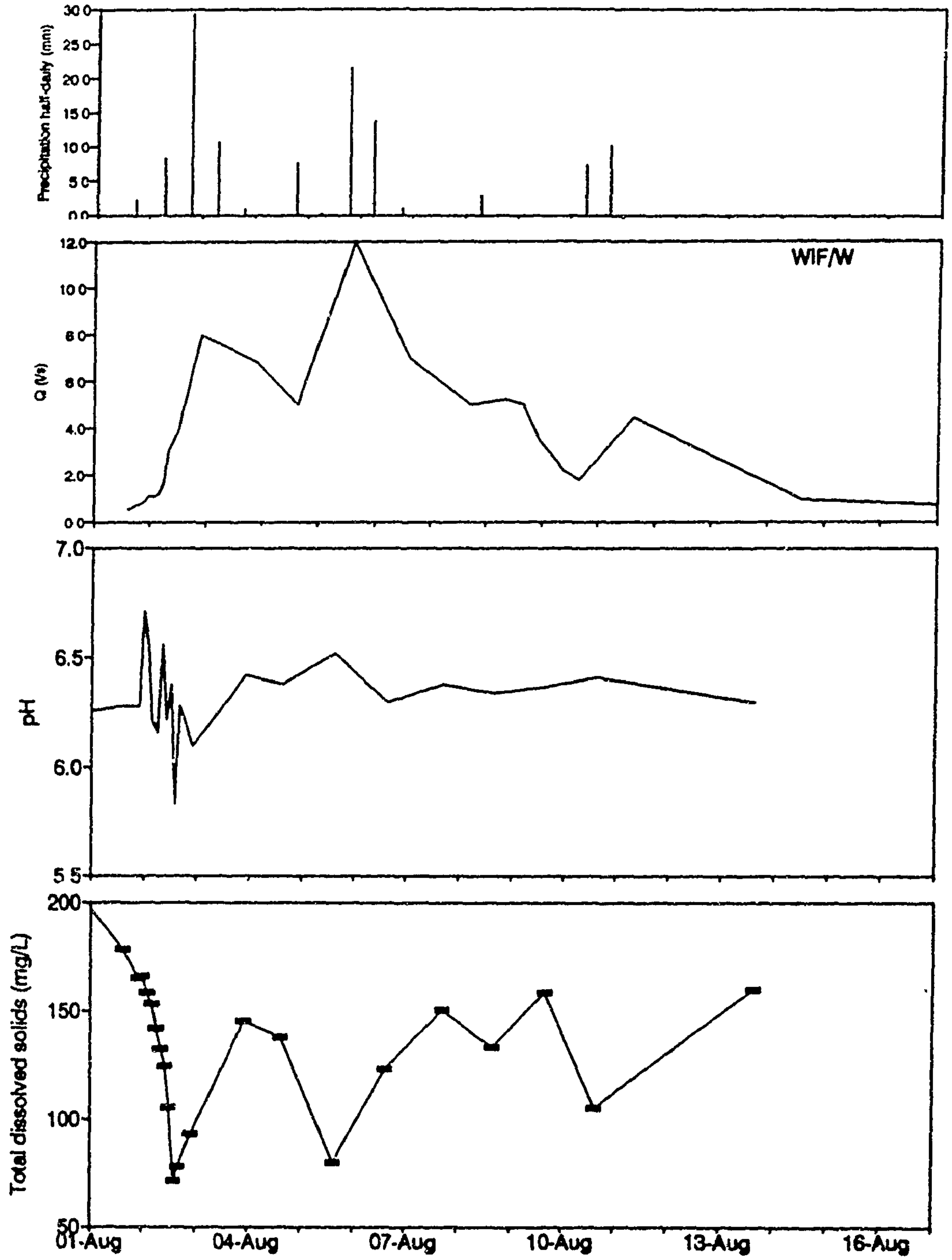

Figure 5.2. Precipitation record and discharge, pH and TDS concentrations for the WIF/W stream during the rainstorm, 2 to 10 August, 1991.

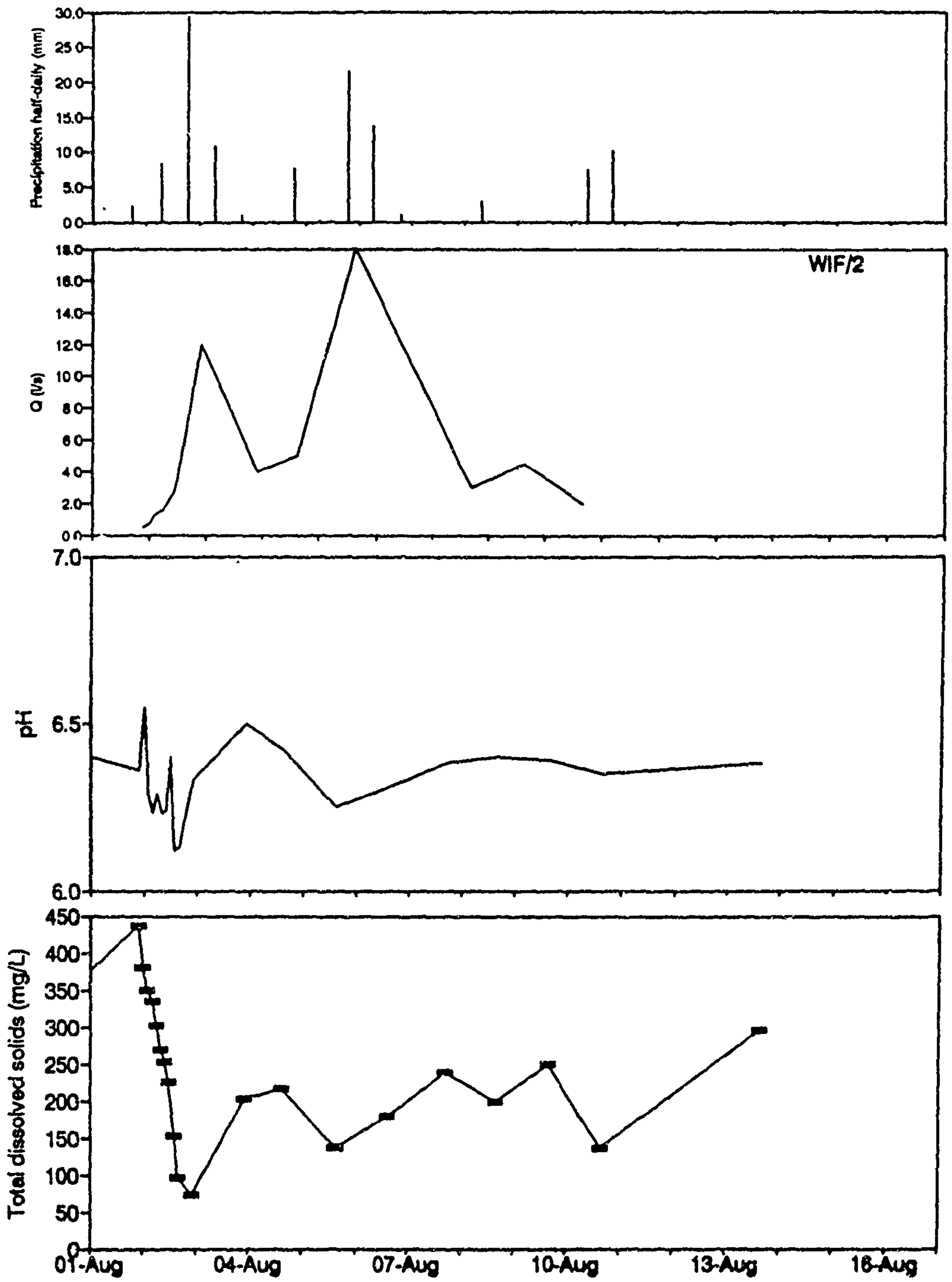

Figure 5.3. Precipitation record and discharge, pH and TDS concentrations for the WIF/2 stream during the rainstorm, 2 to 10 August, 1991.

August at a site in the EIF catchment close to mini-piezometers MP4 A/B. At this time, the water level in the active layer at this site was detected at 2.7 cm depth below the surface. Although no other water level depths are available for comparison this value demonstrates that the water level was close to the surface in the lower, alluvial fan area of the EIF catchment.

A further assessment of antecedent moisture conditions is given by the analysis of runoff coefficients, calculated by the total basin runoff volume (output) versus the total basin precipitation volume (input) (Table 5.4). A low runoff coefficient indicates that less runoff is produced relative to incoming precipitation, hence it can be concluded that a greater proportion of water is absorbed by the unsaturated zone.

Date (day/hours)	Rain intensity (mm/12 hours)	Net basin precipitation input (m^3)		
		EIF	WIF/W	WIF/2
1 to 2 August (19:00 to 7:00)	8.4	61643	1743	1341
2 August (7:00 to 19:00)	29.4	5762	6115	4704
2 to 3 August (19:00 to 7:00)	10.8	2117	2246	1728

Table 5.4. Rain intensity, net basin precipitation input during rainstorm, 1 to 3 August, 1991.

Since detailed bi-hourly discharge measurements were only taken during the first 36 hours of the event and precipitation was recorded at 7:00 and 19:00 hours, runoff coefficients are calculated for 12 hour intervals for the time period 1 August 19:00 hours to 3 August 7:00 (Table 5.4).

Figure 5.4 presents the temporal change of runoff coefficients for the EIF, WIF/W and WIF/2 basin during the first 36 hours of the event. Of note are the low runoff coefficients for all basins with the onset of the event (2 August 7:00 hours) and the rapid increase after 2 August 19:00 as a result of exceptional high rain intensity (29.4 mm/12 hours). The increase of the runoff coefficient is most pronounced in the EIF basin, thereby suggesting wetter antecedent moisture conditions in the EIF basin compared to the WIF/2 and WIF/W basins.

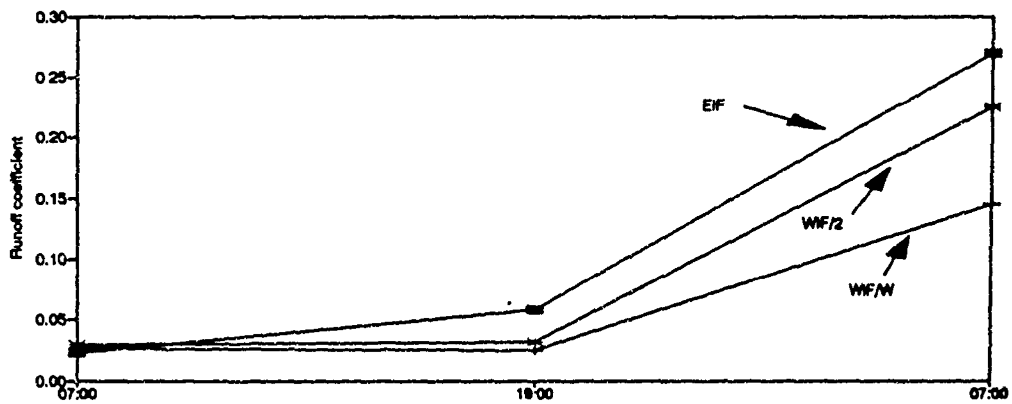

Figure 5.4. Runoff coefficients (precipitation volume/runoff volume) for the three basins from 2 to 3 August, 1991. For net basin precipitation input see Table 5.4.

5.2.2. Chemistry

With the onset of the precipitation event, TDS concentrations peak in the

WIF/2 and EIF streams while concentration decrease in the WIF/W (Figures 5.1 to 5.3). Only in the WIF/W and WIF/2 streams TDS concentrations have a significant, inverse relationship to discharge, TDS concentrations decrease with increasing discharge ($rQ/TDS_{WIF/W}$ = -0.75, $p < 0.001$, n=18; $rQ/TDS_{WIF/2}$=-0.8, $p < 0.001$, n=14; Figure 5.5). No relationship between discharge and acidity is found for any streams (Table 5.5).

	EIF	WIF/W	WIF/2
Q-TDS	-0.18	-0.75**	-0.8**
Q-AC[a]	0.11	0.05	0.18
Sample size	17	18	14
a : calculated from $[H^+]$ concentrations ** : r value significant at 0.001 level			

Tables 5.5. Linear correlation coefficients for discharge and TDS and discharge and acidity for the three streams during the rainstorm, 2 to 13 August, 1991.

Of note is a significant pH drop in the EIF stream after the first discharge peak on 2 and 3 August (Figure 5.1). In comparison to the mean pH of the WIF/W (mean pH=6.29) and WIF/2 streams (mean pH=6.31), the water of the EIF stream is acidic (mean pH=4.63; Table 5.2). The low pH water increases the mobility of Al^{3+} resulting in elevated aluminum concentrations (Tables 5.2); in low pH waters (below pH 5) the dominant aluminum species are Al^{3+}, $Al(OH)_{2+}$ and $AL(OH)^{2+}$ (Stumm and Morgan, 1981). Linear correlation analysis applied on EIF data supports the observation that changes in TDS concentrations are mainly related to changes in the

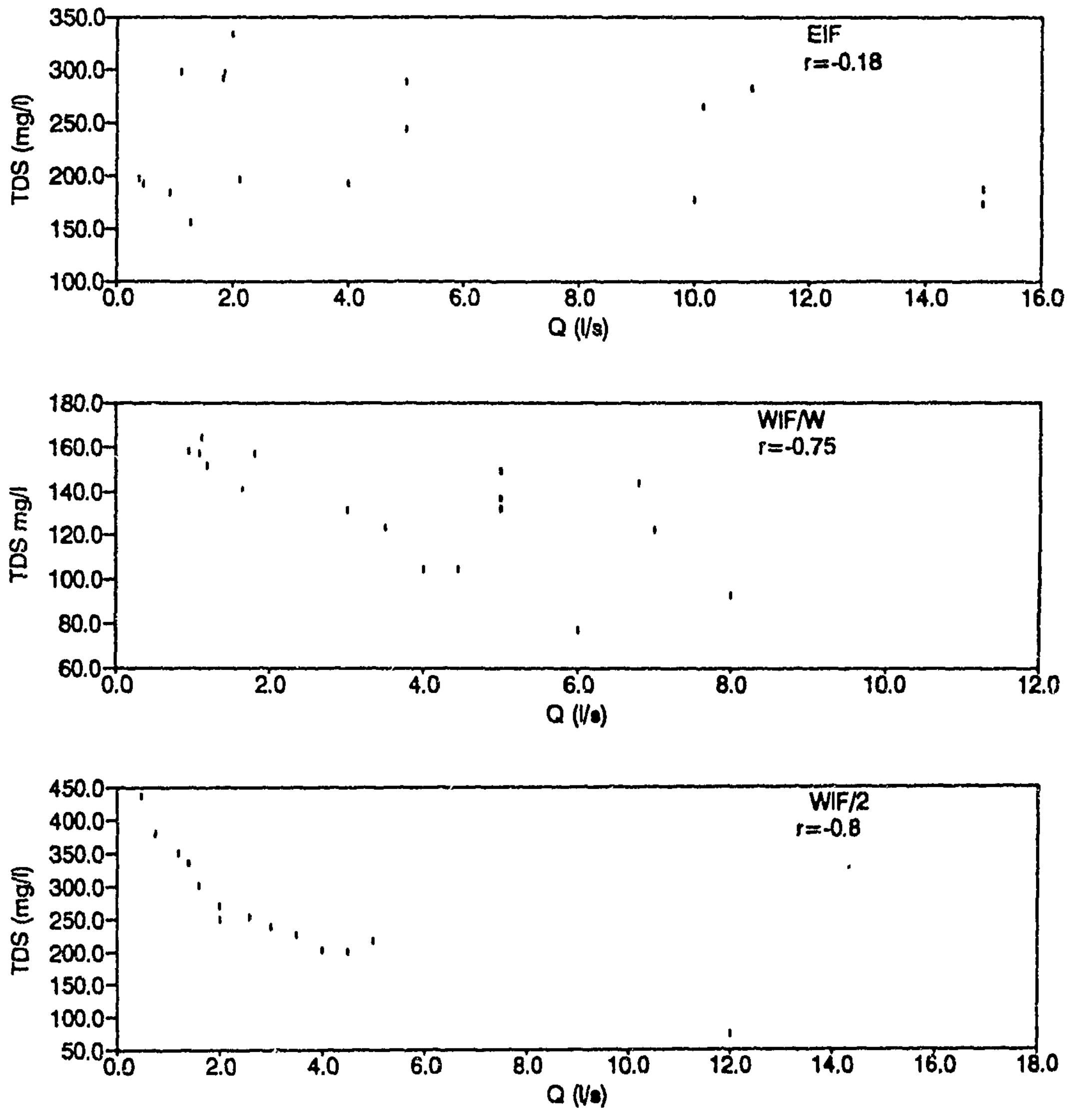

Figure 5.5. Discharge against TDS concentrations and linear correlation coefficient for the three streams during the rainstorm, 2 to 10 August, 1991.

concentration of Ca^{2+}, Mg^{2+}, SO_4^{2-} and Al^{3+} (rTDS/Ca^{2+},Mg^{2+},SO_4^{2-} > 0.91, p<0.001, n=10; rTDS/Al^{3+} =0.8, $p < 0.01$, n=10). In the WIF/W concentrations of all ions but Na^{+} and Cl^{-} increase with increasing TDS concentrations (rTDS/K^{+},Ca^{2+},Mg^{2+},SO_4^{2-} > 0.99, $p < 0.001$, n=9) and in the WIF/2, mainly Ca^{2+} concentrations increase with increasing TDS concentrations (rTDS/Ca^{2+} =0.95, $p < 0.001$, n=9) (Appendix B).

5.2.3. Discussion

Field observations of this episodic, high energy rainstorm demonstrate the strong effect on the terrain and basin hydrology and chemistry. Mass movement, slope instability and slope erosion were observed throughout the catchment and surrounding areas and the transport of sediment and solutes towards the lake was greatly enhanced.

Generally, this rainfall event produced peak discharge in streams and overland flow due to the limited infiltration and storage capacity of the ground. The magnitude of precipitation-induced peak flow in a high arctic setting is a function of 1. depth of thaw of the active layer (with increasing thaw depth the storage potential is enhanced simply by a greater volume) 2. antecedent moisture conditions (a "dry" basin with highly unsaturated soil can absorb more water) 3. hydraulic conductivity (K) of the soil (at sites with higher hydraulic conductivities precipitation infiltrates more rapidly into the soil than at sites with low hydraulic conductivities) and 4.

precipitation intensity.

Although caution should be exercised in interpreting the runoff coefficients (since the calculation comprises only the start of the event), the analysis gives an indication of antecedent saturation conditions in the basins and identifies highest saturation of the active layer in the EIF basin prior to the event. This is in agreement with field observations in the lower, alluvial fan areas of the basins before and during the event ("wet" conditions are indicated by ponding of water, overland flow and rapid filling of footprints with water). However, relatively low runoff coefficients in this high arctic catchment, in comparison to runoff coefficients in a temperate, humid catchment (for example, runoff coefficients in the Harp 4-21 catchment located in the Canadian Shield range from 0.07 to 0.37; MacLean, 1992), indicate that basins have a significant ability to absorb a great portion of the precipitation. This is an interesting result since the loss of precipitation by groundwater recharge (sub- and intrapermafrost groundwater) can only account for small amounts of precipitation; therefore it appears that the ability to store a great portion of the incoming precipitation is a result of extensive unsaturated active layer conditions.

The higher saturation of the EIF basin can be related to two processes : 1. a greater proportion of the EIF basin is covered with sediments of smaller grain sizes compared to the WIF/W basin (Figure 4.14); at sites with smaller grain sizes, the suprapermafrost groundwater table rises higher due to lower storage capacity and lower hydraulic conductivity (Woo and Steer, 1982) and 2. the slow flow routing of water in the active layer compared to the fast routing of water in the WIF/W channel.

Although there are important differences in groundwater flow between an arctic catchment (groundwater movement is essentially confined to the active layer and permafrost is regarded as an aquitard) and a catchment located in temperate climates, the variable source area/subsurface stormflow concept (Hewlett and Nutter, 1970; Dunne and Black, 1970) could be applied for this event. This concept combines the subsurface stormflow concept, which relies on the rapid transfer of event water downslope through the upper soil layer and the variable source area concept, which relies on an expanding channel network as a result of rising water table. In a high arctic catchment, the limiting factor for the absorbtion of rainfall is the frost table; the storage capacity of the ground increases with the depth of the unfrozen ground. The second important difference is that the storage capacity for incoming precipitation increases exponentially upslope in a temperate slope. The storage capacity of an arctic slope increases linearly, since the depth of frozen ground is more or less constant over the slope. Despite these differences, the variable source area/subsurface stormflow concept has applicability in high arctic catchments.

According to this concept, runoff water could potentially be a mixture of event water, suprapermafrost groundwater ("phreatic water") and vadose water in the active layer. Results of the chemical analysis of the WIF/2 and EIF streams suggest that higher concentrated suprapermafrost groundwater mixes with incoming precipitation and that this water is discharged into the streams at the beginning of the event. The fact that TDS concentrations peak at the onset of the rainstorm in the WIF/2 and EIF streams is an indication of this. Further information about the source of stream water (event water, suprapermafrost groundwater or vadose water) is given by tritium concentrations of stream and event waters (Table 5.6). Tritium units of streams and precipitation lie in the same range, which indicates that the streams are primarily fed by event water or old water with the same tritium concentrations (for example from prior rain events). However, one should keep in mind that the samples were taken at the end of the storm and therefore it is assumed that the active layer is highly saturated, hence reducing the potential mixing between precipitation and suprapermafrost groundwater.

	EIF	WIF/W	WIF/2	Precipitation
^3H (T.U.)	26 (+/-8)	26 (+/-8)**	29 (+/-8)	27 (+/-8)
** average of two sample runs (20 and 32 T.U.)				

Table 5.6. Tritium concentrations in the three streams during the rainstorm, 13 of August, 1991.

A further assessment of water flowpaths during the event is given by examining TDS concentrations and pH of the streams and precipitation. In contrast to the rain, which is characterized by low ion concentrations (TDS=7.3 mg/l) and a weak to moderate acidic pH (5.72; Table 4.9), all streams have a high concentration of TDS and pH is considerably lower in the EIF (mean pH=4.63), higher in the WIF/W (mean pH=6.24) and WIF/2 (mean pH=6.31) streams (Table

5.2). A possible explanation is that water travels as overland flow and shallow throughflow in the active layer and, despite a short residence time dissolves readily available ions. The flow regimes of the WIF/W and WIF/2 are characterized by a significant, inverse relationship between TDS and discharge and therefore exhibit dilution as a result of large input of low concentrated rainwater and fast routing downslope. This is supported by the surficial geology of the WIF basin, where a large proportion is covered by felsenmeer and watertracks are confined to these areas (Figure 4.14).

In the EIF stream, the lack of a significant relationship between discharge and TDS concentrations and in addition, high concentrations of ions and a low mean pH indicate a complicated flow regime. One important process could be the dissolving of highly weathered material in form of salt crusts on the eastern slope of the EIF basin (Colour Prints 3 and 4). Colour Print 3 also shows that the areal distribution of these salt crust on the slope is highly variable. With respect to the variable source area subsurface stormflow concept, the expanding channel system potentially reaches highly weathered material in upslope areas. As a result, shallow throughflow and overland flow become concentrated within areas of high salt accumulations. Considering also two contributing hydrological and chemical source areas in the EIF basin (Chapter 6), the EIF stream water is a mixture of relative low ion concentrated and high pH water from the western slope and high acidic, high ion concentrated water draining the east slope.

CHAPTER 6 SUMMARY AND DISCUSSION: SEASONAL HYDROLOGY AND CHEMISTRY

6.1. Introduction

Based on the data presented in the Chapters 3 to 5, this chapter presents a scheme to relate the seasonal changes in chemistry and hydrology of the streams to hydrological processes operating in the catchment.

6.1.1. Classification of arctic streamflow regimes and application for the streams in the Colour Lake catchment

According to Church (1974), three classifications of arctic hydrological regimes exist: 1. arctic nival regime, 2. proglacial regime 3. muskeg regime. The arctic nival regime is dominated by the snowmelt; after snowmelt, streamflow recesses to base flow or ceases completely with occasional peaks in runoff generated by rainstorms. The proglacial regime experiences peak flow during the snowmelt as well, but during the summer increasing discharge and high flows are due to the input of glacial meltwater. Woo (1990) points out that the separation between a proglacial regime and a regime fed by perennial snowbanks is not always clear, since streamflow is generated in similar ways (snowbanks will release more meltwater during warm days and can maintain discharge throughout the summer). The muskeg regime, also called "wetland" regime by Woo (1990), is different to the nival regime in the sense that summer flow is of lower intensity. This is due to the fact that the muskeg vegetation has a high water retaining capacity and that the irregular, hummocky terrain provides a natural resistance against surface runoff. The following paragraph will discuss the application of the arctic streamflow regimes for the EIF, WIF/W and WIF/2 streams.

The division of the 1991 spring to fall runoff into three hydrological periods (snowmelt, period of active layer development and rainstorm) allows elucidation of detailed hydrological and chemical responses of surface waters to meteorological factors and terrestrial properties. Table 6.1 contains a summary of the main hydrological and chemical processes for the streams in each period. Considering that discharge is increasing in the WIF/W towards the end of the summer and that a significant relationship exists between discharge and air temperature, the flow regime of the WIF/W stream is similar to the proglacial regime. However, it is suggested that the term "proglacial regime" should be modified by the term "melting ground ice regime", since the stream runoff on warm days is derived by the melting of ground ice (not by glacier melt). The flow regime of the WIF/2 exhibits typical characteristics of the arctic nival regime; after snowmelt, flow ceases and is induced again by a series of rain events at the end of July. A more complicated regime is demonstrated by the EIF; surface water from the melting of ground ice on the east and west slopes infiltrates to a great extent at the base of the slopes. From this point, water moves as surface flow above the active layer when the suprapermafrost

	Snowmelt	Period of active layer development			Rainstorm	Classification of regime
		1- Low flow period	2- Active layer saturation period	3- Ground ice melt period		
General observations in catchment	-depth of thaw of active layer at end of period:0.22m -shallow frost table limits storage capacity producing overland flow -diurnal cycle in Q, TDS and pH	-depth of thaw of active layer at end of period:0.36m -flow in intermittent streams ceases -SW seep starts to flow	-depth of thaw of active layer at end of period:0.50m -suprapermafrost groundwater input starts in EIF basin (MP4B)	-depth of thaw of active layer at end of period:0.55m -overland flow -suprapermafrost groundwater input starts in WIF basin (MP2)	-depth of thaw of active layer on 6 August:0.55m -precipitation intensity >> storage capacity causing overland flow -intermittent streams and seeps start flowing again	
EIF	-peak in TDS at onset of melt -formation of ground ice	-no significant relationship for Q and TDS -flow ceases twice as a result of cold air temperatures -lowest mean Q of all periods	-rQ/TDS=-0.55* -no significant relationship between Q and air temperature -contribution of water from western part of basin predominates over eastern part -decrease of Ca^{2+} and SO_4^{2-}	-no significant relationship for Q and TDS -rQ/Temp.=0.68* (two days delay in discharge) -highest mean Q of three periods of active layer development -seasonal increase of Ca^{2+} and SO_4^{2-}	-no significant relationship for Q and TDS -peak in TDS with rising hydrograph -pH drop to 4.12 -Al^{3+} and Fe^{2+} concentrations elevated	-"modified melting ground ice regime" (ground ice is source for runoff, but slow routing of water results in significant lag of discharge)
WIF/W	-rQ/TDS=-0.53* -peak in TDS at onset of melt -formation of ground ice	-rQ/TDS=-0.53** -prolonged snowmelt -flow ceases twice as a result of cold air temperatures -lowest mean Q of all periods	-no significant relationship between Q and TDS -rQ/Temp.=0.81** -increase of Ca^{2+}, SO_4^{2-} and Mg^{2+}	-rQ/TDS=-0.94** -rQ/Temp.=0.95** -highest mean Q of three periods of active layer development -seasonal increase of Ca^{2+}, SO_4^{2-} and Mg^{2+}	-rQ/TDS=-0.75* -dilution of TDS with rising hydrograph	-"melting ground ice regime" (proglacial characteristics, but fed by melting of ground ice)
WIF/2	-formation of ground ice	-flow ceases after snowmelt and start to flow again at the end of the third active layer development period due to precipitation input			-rQ/TDS=-0.8** -peak of TDS with rising hdyrograph	-arctic nival

* : significant at 0.01 level
**: significant at 0.001 level

Table 6.1. Summary of seasonal hydrological and chemical characteristics of the three streams, May to August 1991.

groundwater table is above the ground (overland flow) or as suprapermafrost groundwater within the active layer; in both cases the travel time is significantly longer than the fast routing of water in the WIF/W. In addition, the total coverage of area with a medium and high potential for ground ice is considerably smaller in the EIF than in the WIF/W basin, hence the potential to yield water is reduced (Figure 4.14). In light of these characteristics, the flow regime of the EIF could be classified as "modified melting ground ice regime".

6.1.2. Seasonal changes in stream chemistry

Figures 6.1 to 6.3 demonstrate the seasonal trends in discharge, TDS concentrations and pH for the three streams from May to August, 1991. Highest TDS concentrations occur in the EIF streams with the onset of snowmelt and during the rainstorm at the beginning of August. This peak, at the beginning of snowmelt, which is also detected in the WIF/W stream, is caused by all ions but Na^+ (Figures 6.4 and 6.5). A seasonal decreasing trend of TDS concentrations in the EIF is observed during the second period of active layer development, and a seasonal increasing trend in the third period of active layer development. Figure 6.4 shows that these changes in TDS concentrations are attributed to changes in concentrations of Ca^{2+} and SO_4^{2-}; Mg^{2+}, Cl^- and K^+ only show a weak decrease or increase in concentration. The pH increases over time through summer and drops to the lowest level during the rainstorm (pH of rain = 5.72, minimum pH in EIF = 4.12) (Figure 6.1).

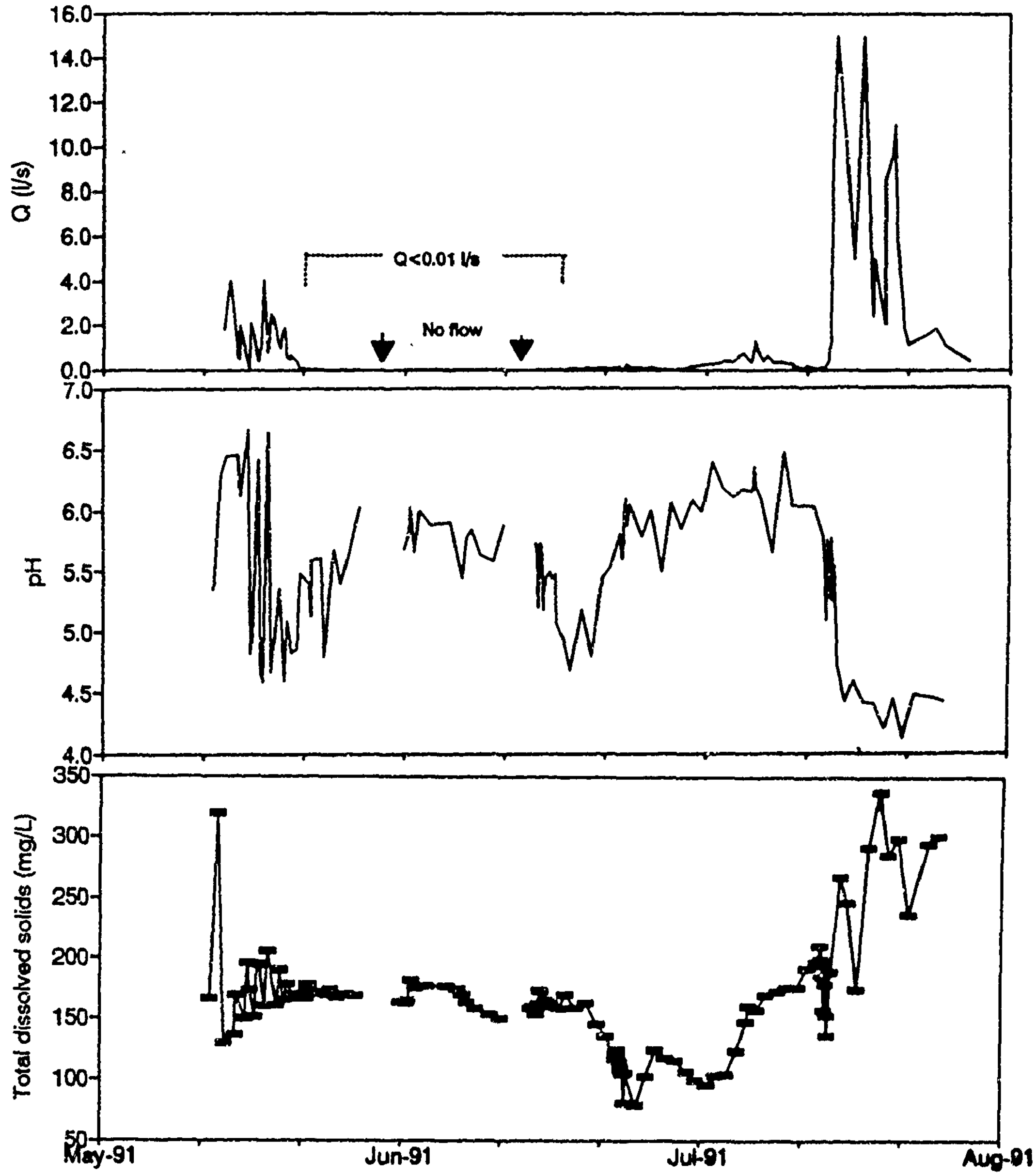

Figure 6.1. Discharge, pH and TDS of the EIF stream from May to August, 1991.

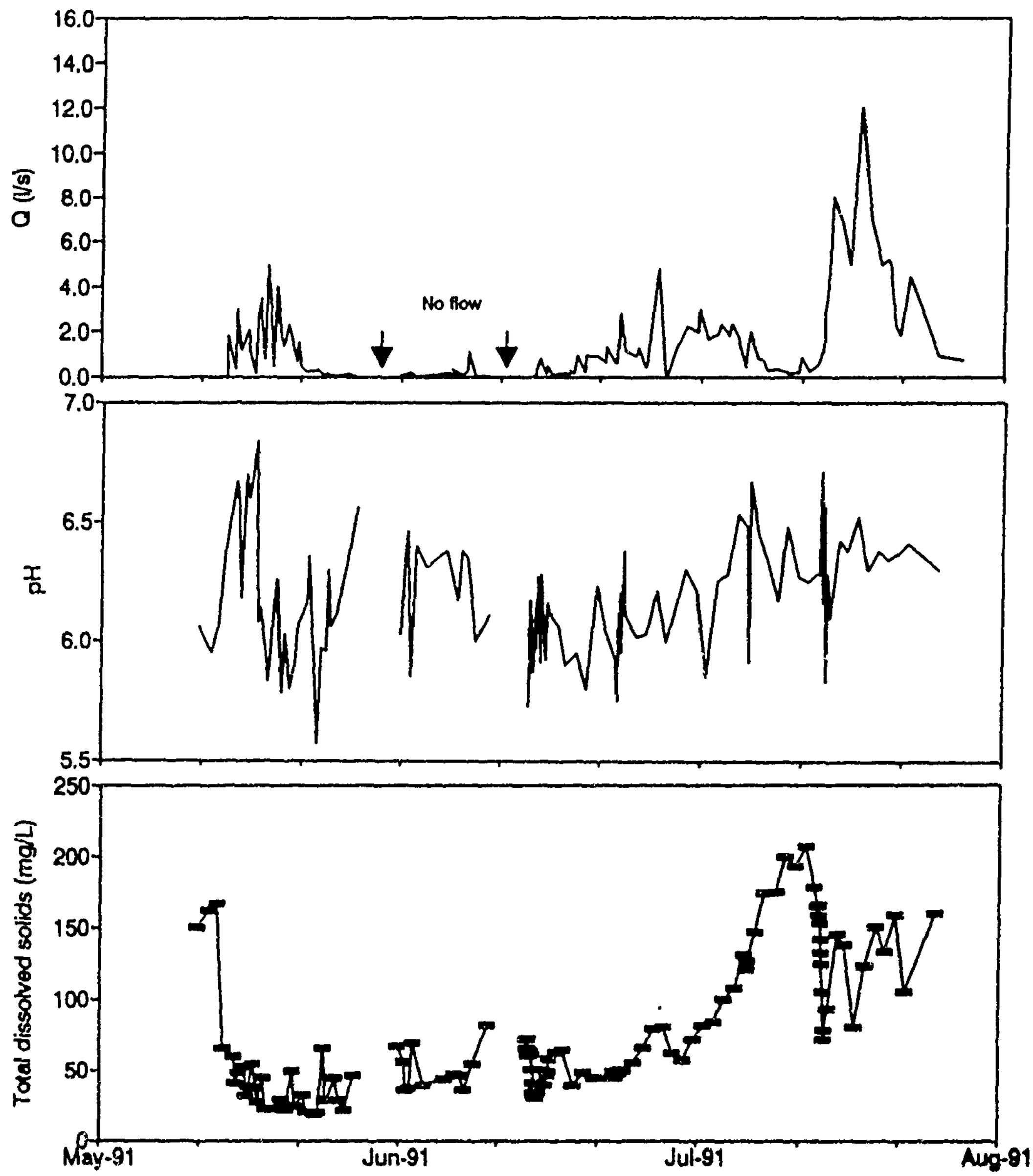

Figure 6.2. Discharge, pH and TDS of the WIF/W stream from May to August, 1991.

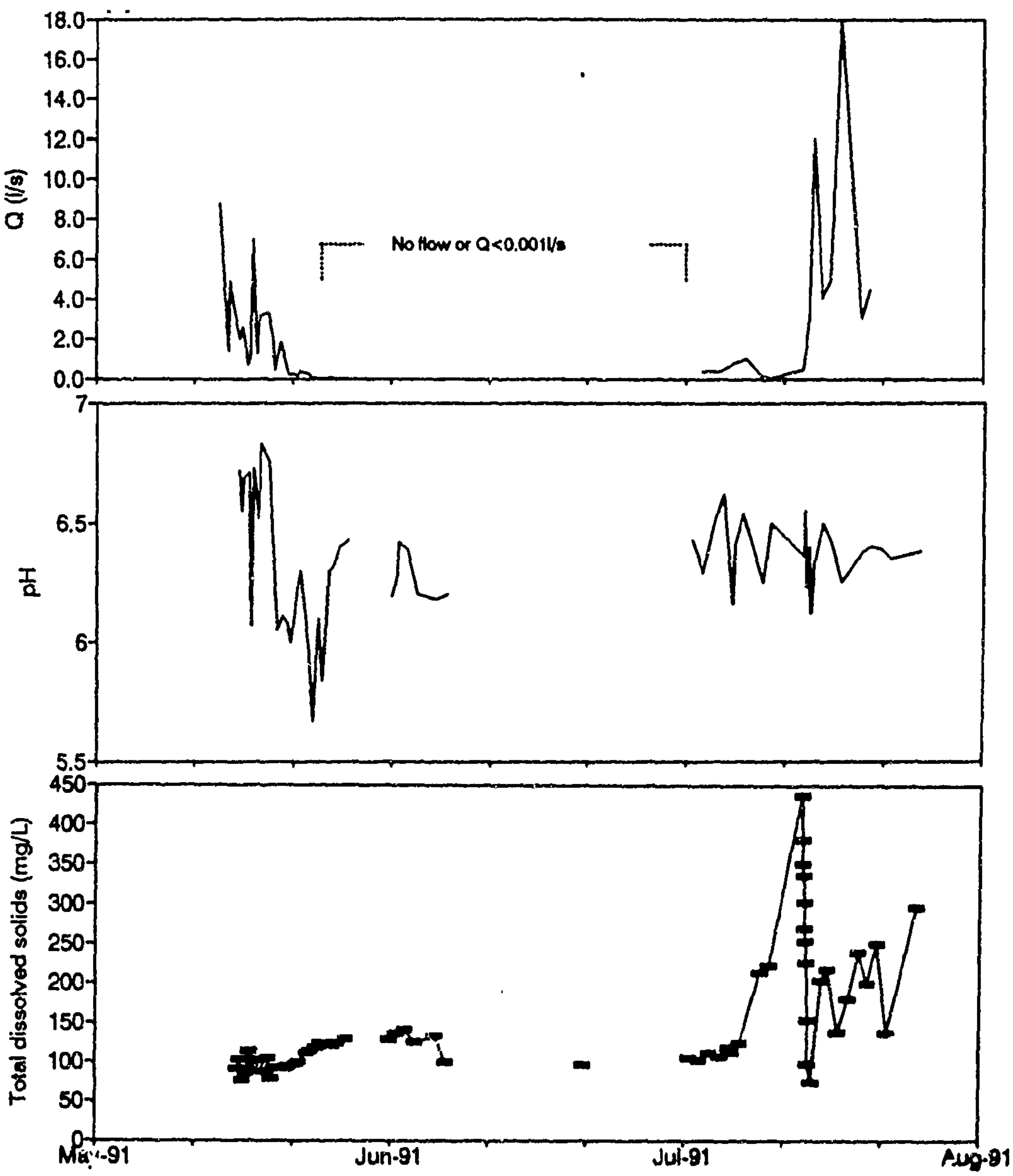

Figure 6.3. Discharge, pH and TDS of the WIF/2 stream from May to August, 1991.

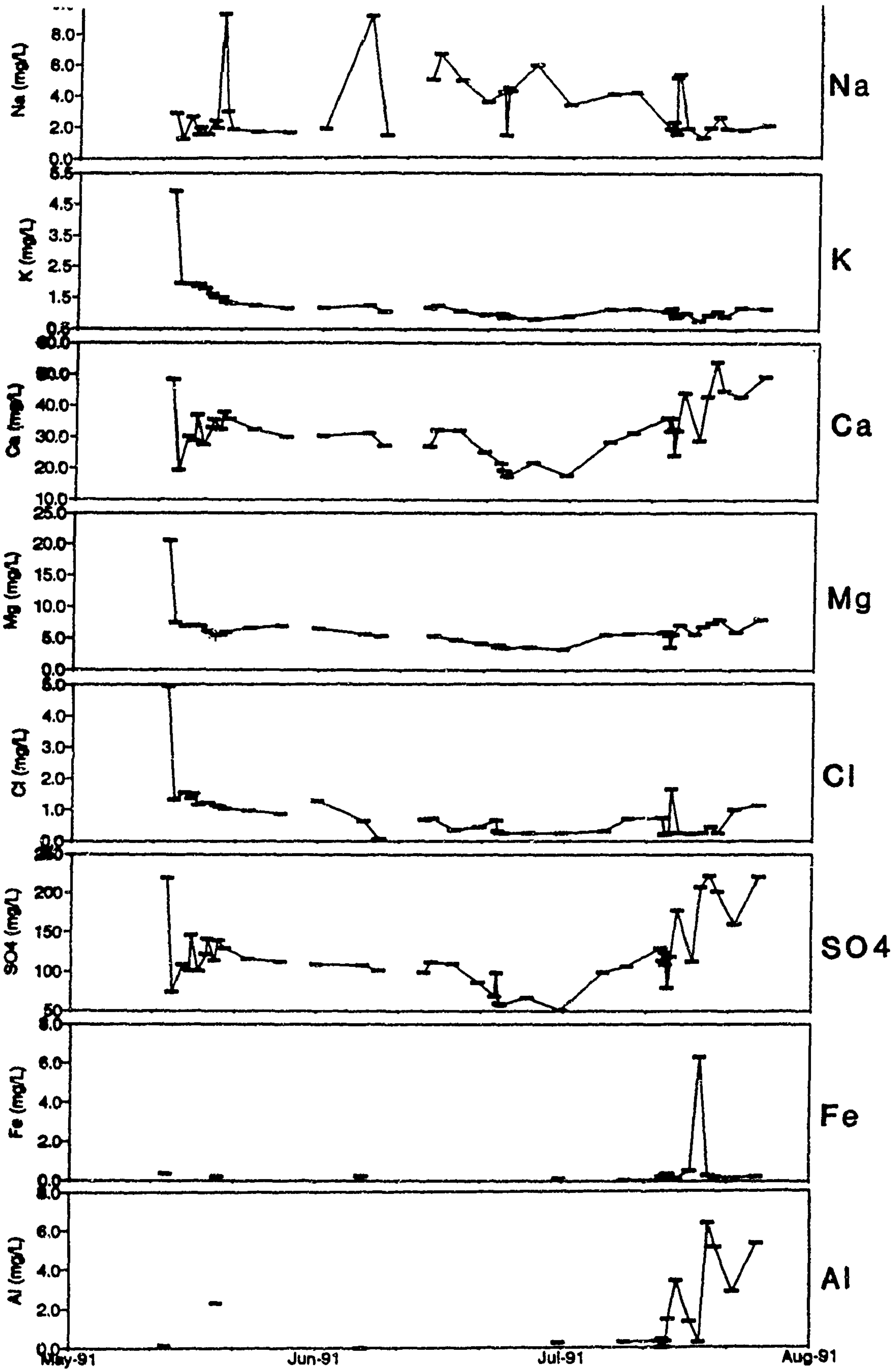

Figure 6.4. Ion concentrations of the EIF stream from May to August, 1991.

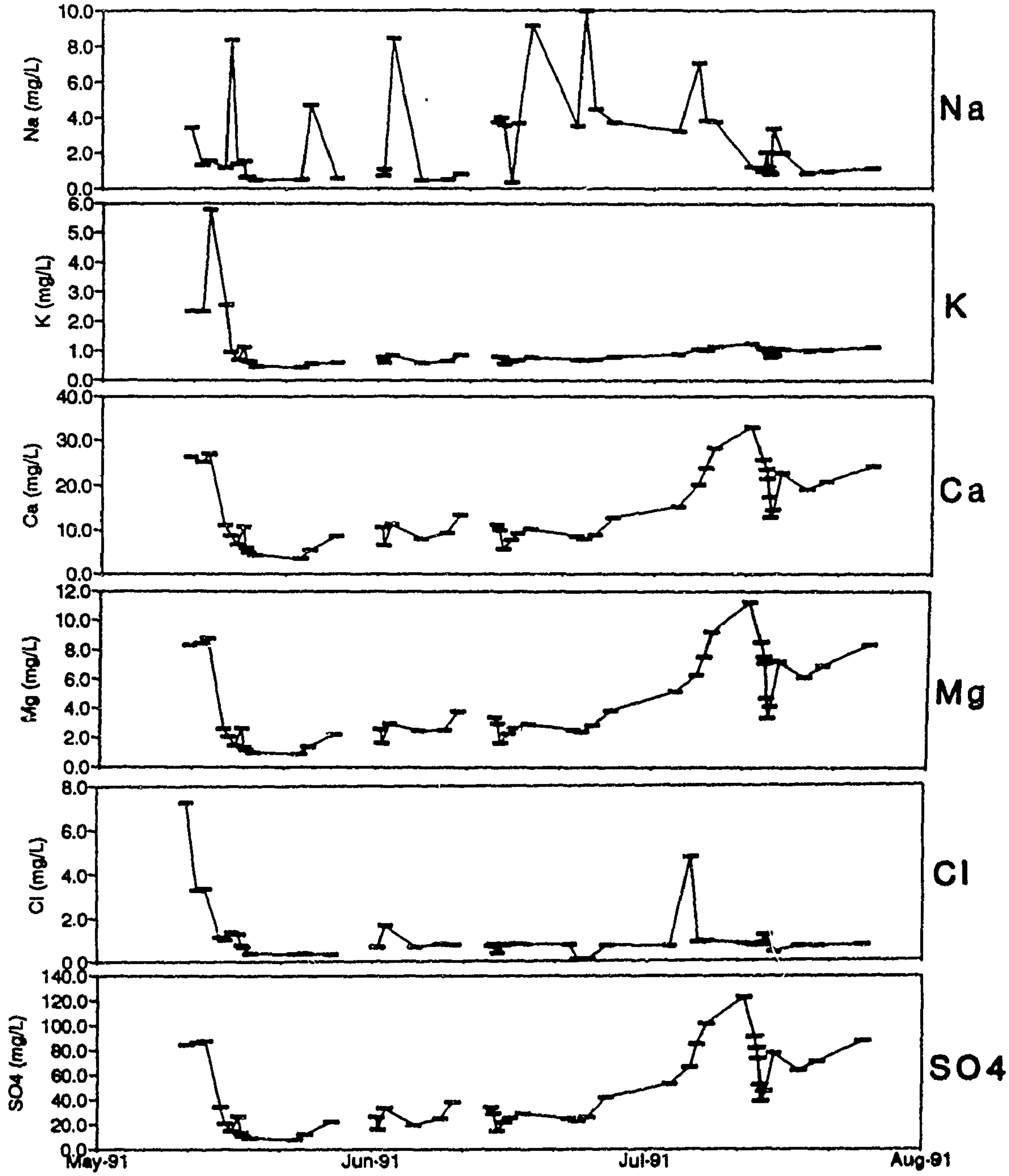

Figure 6.5. Ion concentrations of the WIF/W stream from May to August, 1991.

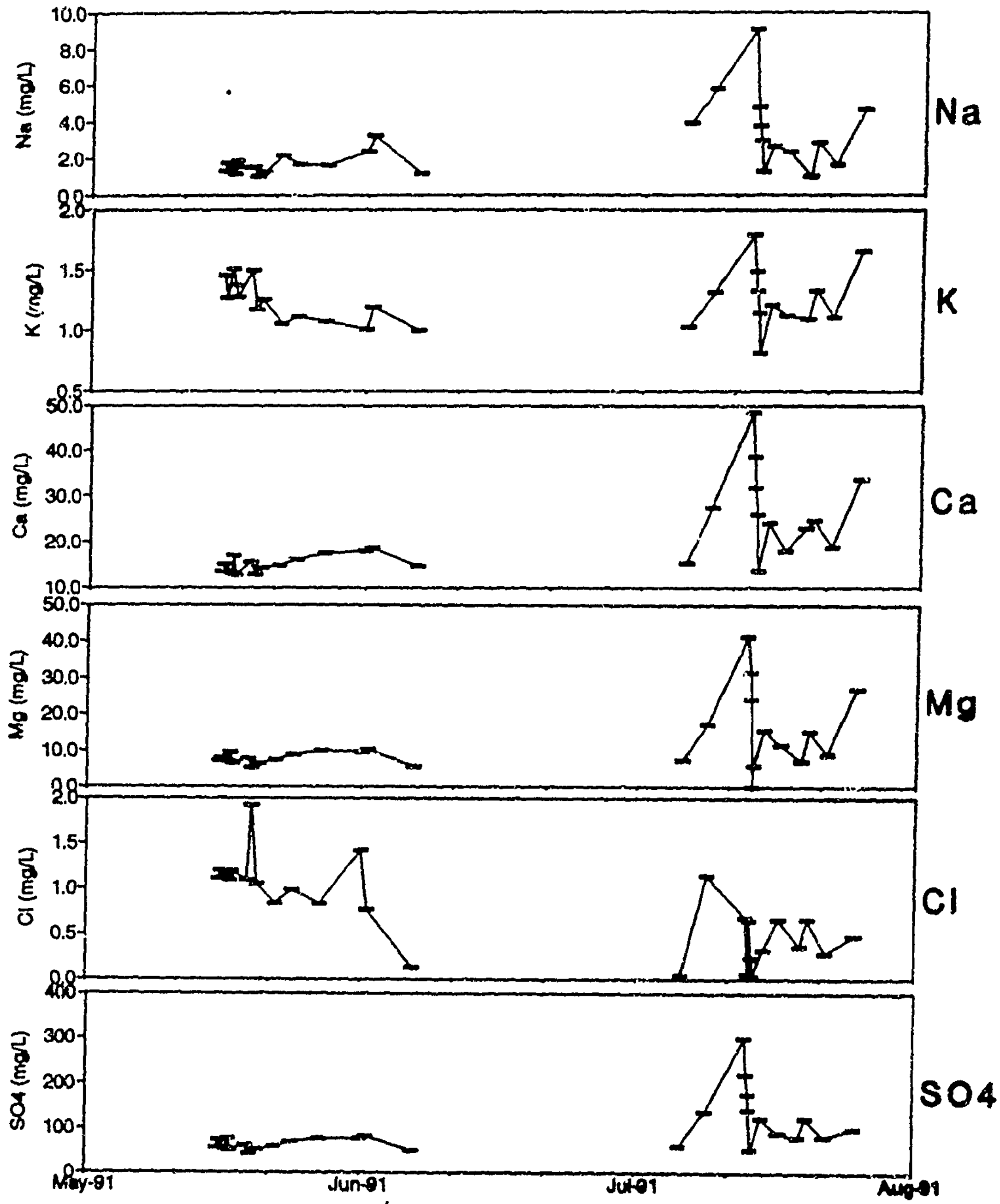

Figure 6.6. Ion concentrations of the WIF/2 stream from May to August, 1991.

In addition, elevated concentrations of Al^{3+} and Fe^{2+} are measured during the rainstorm when the pH drop is most pronounced (Figures 6.1 and 6.4).

As already mentioned in Chapters 4 and 5, two (chemically and hydrologically) different contribution areas of the EIF basin are considered as an important factor determining the seasonal changes in water chemistry of the EIF stream. During the second period of active layer development, the proportion of water from the western part of the catchment is higher relative to the water draining the east slope. Evidence for this is given by 1. field observations (overland flow was identified on the west slope) and 2. a decrease of TDS concentrations and increase in pH in the EIF stream water. Possible reasons for the higher melt rate of ground ice on the west slope are a greater exposure to direct sunlight and the lack of vegetation (Figures 2.2. and 2.3). The felsenmeer on the eastern slope is partly covered by a thick moss mat, which insulates the ice underneath (soil zone 4; Figure 4.14).

EIF alkalinity concentrations during low flow (6 and 28 July) and high flow (21 July) indicate differences between contributing areas (Table 6.2).

Date	Alkalinity (μeq/l)		
	EIF	WIF/W	WIF/2
26 June, 1991	8	93	199
5 July, 1991	n.a.	118	n.a.
6 July, 1991	16	130	n.a.
21 July, 1991	187	140	n.a.
28 July, 1991	85	201	199
6 August, 1991	14	183	n.a.

Table 6.2. Alkalinity of the EIF, WIF/W and WIF/2 stream waters, 1991.

From the limited data it appears that alkalinity concentrations are much lower during low flow than during high flow. These results suggest that the high acidity of the east slope water is overshadowed by the high pH water of the west slope during high flow.

In the WIF/W, TDS concentrations peak with the onset of snowmelt and during the third period of active layer development (Figure 6.2). TDS concentrations start to increase from the second period of active layer development, which is mainly caused by an increase in concentration of SO_4^{2-}, Ca^{2+} and Mg^{2+}, and only minor increases in K^+ (Figure 6.5). The question arises, what are the governing factors that cause the seasonal increase of Ca^{2+}, Mg^{2+} and SO_4^{2-} in the WIF/W and why is the increase of those ions is most pronounced during the third period of active layer development.

6.1.3. Suprapermafrost groundwater flow in the active layer

The seasonal thawing of the frozen ground and therefore the increase in storage capacity from spring to fall enables the infiltration of precipitation and/or water derived from the melting of ground ice. As a result, a saturated zone develops and the potential for water moving via the subsurface groundwater route is enhanced (suprapermafrost groundwater flow). In order to obtain information about the physical and chemical characteristic of this seasonal suprapermafrost groundwater flow, mini-piezometers were installed in the terrestrial part of the catchment and in the shallow littoral zone of Colour Lake (Table 2.2 and 2.3; Figure 2.4).

Interestingly, the mini-piezometers at greater depth (WIF/2/D and WIF/F) at the nested piezometer sites (Table 2.2) did not yield enough water for sample extraction throughout the entire summer. In addition, some of the mini-piezometers installed in the terrestrial catchment did not yield water at all (WIF/A/B/C, EIF/C). The hydraulic conductivity values and hydraulic heads recorded from mini-piezometers in the shallow, littoral zone vary considerably over short distances. For example, MP4/A and ECP2, both installed in the littoral zone of the EIF basin at approximately the same sediment depth, have a difference of ten orders of magnitude in hydraulic conductivity and a difference of several centimetres of hydraulic head (Table 6.3 and Figure 6.7). In addition, strong fluctuations in hydraulic heads are recorded in mini-piezometer ECP2 in contrast to more or less steady hydraulic conditions in mini-piezometers MP4/B and MP2 (Figure 6.7).

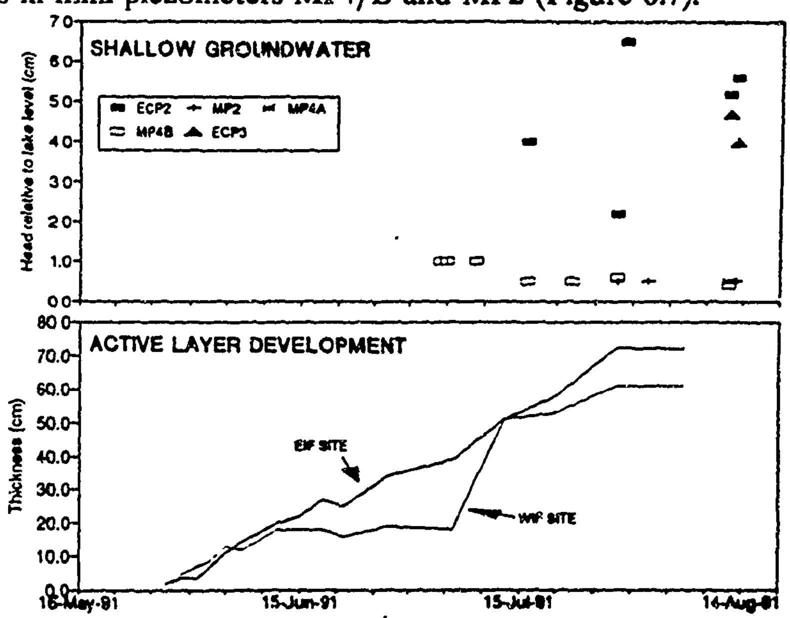

Figure 6.7. Shallow groundwater piezometric head and the development of the active layer from May to August, 1991.

Figure 6.7. Shallow groundwater piezometric head and the active layer development (at lake end of each permafrost transect) from May to August, 1991.

Location	ECP1	ECP3	ECP4	ECP2	MP2	MP4A	MP4B	MP5	MP6	MP8
Water depth[a] (m)	1.5	1.5	1.5	0.25	0.11	0.14	0.16	0.28	0.25	0.25
Depth in sediment[b] (m)	0.92	1.08	1	0.64	0.67	0.75	0.36	0.58	0.58	0.69
K (cm/s)	X• 10^{-2}	3.4• 10^{-6}	5.9• 10^{-5}	1.1• 10^{-4}	2• 10^{-3}	3.6• 10^{-3}	2.4• 10^{-3}	8.6• 10^{-4}	2.5• 10^{-3}	1.1• 10^{-3}

X : estimated
a : depth from lake sediment to lake water level
b : depth of bottom of piezometer in lake sediment

Table 6.3. Water depth, depth in sediment and hydraulic conductivity of shallow, lake mini-piezometers, 1991.

These observations suggest a complex flowpath system ("fingering of flow") within a heterogeneous aquifer rather than a widespread, lateral flow system. Woo and Steer (1986; 1982) report the movement of water on a high arctic hillslope close to Resolute, Cornwallis Island. According to their results, the observed large variations of the water table and differences in subsurface drainage on a single slope are related to the source area of water, hydraulic conductivity and storage capacity of the sediment, the microtopography of the frozen ground and vegetation cover. A higher hydraulic conductivity in combination with high storage capacity in gravely soil produces only a thin saturated active layer. Conversely, the water table is higher in bog soil with low hydraulic conductivity and low storage capacity. Although these physical parameters were not determined on soils in the Colour Lake catchment (only for lake mini-piezometers), the large heterogeneity of the active layer was noticed during the excavation of soil pits. Therefore the results of the soil and lake mini-piezometer can give an indication of the heterogeneity of the terrestrial sediments.

Figure 6.7 illustrates the hydraulic head of the mini-piezometers in the shallow, littoral zone of the lake over the time period May to August 1991. The temporal relationship between active layer development and the suprapermafrost groundwater is demonstrated by data recorded at mini-piezometers MP4/A, MP4/B and MP2 (Figure 2.4). MP4/A and MP4/B were installed at the same site at 0.75 m and 0.35 m respectively (Table 6.3). Water levels were first recorded in the shallow standpipe of this piezometer nest on 1 July 1991 when the active layer adjacent to the lake reached a depth of 0.38 m. On 15 August 1991, standing water was first recorded in the deeper MP4/A piezometer when the active layer was measured at 0.70 m below ground surface. In mid August when the active layer reached 0.60 m at the WIF permafrost-depth sampling site standing water was first recorded in nearby mini-piezometer MP2 which was installed to a depth of 0.67 m (Figure 6.7). This demonstrates that the suprapermafrost flow system develops with the seasonal thawing of the active layer. However, the earlier start of suprapermafrost groundwater discharge into the lake in the EIF basin is largely a function of the higher saturation level of the active layer (discussed in Chapter 4 and 5) despite the fact that the storage potential for incoming water is higher in the EIF basin than in the WIF basin (the mean depth of active layer thaw in the EIF basin is greater than in the WIF basin; Figure 4.2).

Table 6.4 demonstrates the chemistry of waters extracted from two representative soil mini-piezometers in the EIF and WIF catchment (additional

Locat -ion	Date	pH	TDS (mg/l)	Na^+ (mg/l)	K^+ (mg/l)	Ca^{2+} (mg/l)	Mg^{2+} (mg/l)	Fe^{2+} (mg/l)	Al^{3+} (mg/l)	Cl^- (mg/l)	SO_4^{2-} (mg/l)	imbalance % [a]
EIF/D	10-Jul-91	3.97	119	5.05	0.84	37.1	2.02	0.50	2.61	0.87	132	-1.6
EIF/D	11-Jul-91	3.72	215	n.a.	n.a.	n.a.	n.a.	n.a.	n.a.	n.a.	n.a.	n.a.
EIF/D	12-Jul-91	4.08	207	5.36	0.58	37.2	2.05	0.23	2.63	1.33	135	-3.6
EIF/D	15-Jul-91	3.87	248	n.a.	n.a.	n.a.	n.a.	n.a.	n.a.	n.a.	n.a.	n.a.
EIF/D	20-Jul-91	3.96	243	4.71	0.65	40.5	2.41	0.88	3.69	0.87	157	-4.4
EIF/D	26-Jul-91	4.06	357	5.50	0.74	68.4	4.64	n.a.	n.a.	0.66	285	-17.9
EIF/D	31-Jul-91	3.91	406	3.76	0.73	77.7	4.51	0.16	9.35	0.84	324	-9.4
EIF/D	02-Aug-91	4.01	444	114	0.99	107	4.03	0.21	8.03	33.8	338	18.7
EIF/D	09-Aug-91	3.79	593	n.a.	n.a.	n.a.	n.a.	n.a.	n.a.	n.a.	n.a.	n.a.
EIF/D	13-Aug-91	3.87	540	2.72	0.62	121	4.20	0.28	10.86	0.79	426	-6.1
WIF/E	29-Jun-91	6.15	83	1.32	1.23	15.3	5.87	n.a.	n.a.	0.67	53.4	8.4
WIF/E	04-Jul-91	6.07	104	4.29	1.26	15.7	6.07	n.a.	n.a.	0.21	54.8	13.4
WIF/E	12-Jul-91	6.27	94	6.47	1.19	14.4	5.04	n.a.	n.a.	0.15	49.8	16.3
WIF/E	26-Jul-91	6.32	81	3.83	0.93	12.9	4.31	n.a.	n.a.	0.14	42.6	14.2
WIF/E	02-Aug-91	6.53	137	3.86	0.75	9.9	3.16	0.04	0.59	0.68	31.7	19.5

Table 6.4. Seasonal chemistry of suprapermafrost groundwaters extracted at two sites in the EIF and WIF basin, 1991. For location see Figure 2.2.

chemical results of all soil and lake mini-piezometer waters are provided in Appendix C). Generally, the chemical results show that TDS concentrations of all suprapermafrost groundwaters exhibit a seasonal increase (Table 6.4 and Appendix C). This could be the result of longer residence time of water in the soil as the season progresses under enhanced conditions for chemical weathering, such as a deeper unfrozen active layer, higher soil temperatures and the availability of water in form of precipitation or meltwater from ground ice. A greater availability of weathered material (demonstrated by salt crusts on the east slope; Colour Prints 3 and 4) or the chemical properties of the geological material of the east slope in the EIF basin appear to be the important factors for the considerably higher seasonal increase of TDS concentrations in suprapermafrost groundwater compared to the suprapermafrost groundwater in the WIF basin. Of note is that TDS concentrations of suprapermafrost groundwater in the WIF catchment are generally lower and pHs are higher than in the suprapermafrost water in the EIF catchment (Table 6.4). The pH of waters extracted from all soil mini-piezometers in the EIF basin is strongly acidic, resulting in high concentrations of Al^{3+} (Table 6.4). Dominant ions in the EIF soil mini-piezometers are SO_4^{2-} and Ca^{2+}, and in the WIF basin: SO_4^{2-}, Ca^{2+}, Na^{+} and Mg^{2+}.

Ionic ratios of samples from the EIF and WIF suprapermafrost groundwaters can be visualized by plotting the relative percentage of cations and anions on triangular coordinates (Figure 6.8). The cation triangle shows that the suprapermafrost groundwaters from the EIF and WIF basin plot in two different groups; the suprapermafrost groundwaters from the WIF basin have a higher percentage of Mg^{2+} than the ones in the EIF. It should be noted that the chemical composition of water extracted from soil mini-piezometers in the EIF is not representative for the entire basin, since all soil mini-piezometers were located on the base of the east slope (EIF/C on the west side of the stream did not yield water). However, the chemical composition of suprapermafrost groundwater draining from the west slope is given by waters extracted from the littoral mini-piezometer MP4/B. Like waters from the WIF/W basin, the suprapermafrost groundwater from the west slope of the EIF basin is characterized by a higher pH and a higher relative percentage of Mg^{2+} (Figure 6.8). This supports the observation of two chemically different source areas of water in the EIF basin.

The ionic composition of the EIF stream water (Figure 6.9) plots between the data groups of suprapermafrost groundwaters from the east and west slope thus suggesting that both suprapermafrost groundwaters (and surface waters) contribute to the stream. This is further supported by the tritium content of the EIF stream (33 ±8 T.U.), which suggest mixing between suprapermafrost groundwater (EIF/E: 40 ±8 T.U.), precipitation (33 ±8 T.U.) and/or meltwater from ground ice (13-16 ±8 T.U.) (Table 6.5).

	EIF 23 July	WIF/W 23 July	WIF/2 23 July	WIF/E 20 July	EIF/E 20 July	Ground ice 23 July	Frozen active layer** 23 July	Snow 19 June
T.U.	33 (± 8)	27 (± 8)	34 (± 8)	35 (± 8)	40 (± 8)	13-16 (± 8)	52 (± 8)	33 (±8)

* for location see Figure 2.5
** extracted from 41-42 cm depth

Table 6.5. Tritium concentrations from selected sites, 1991.

Evidence for highly concentrated input of suprapermafrost groundwater from the east slope is given by the results of spatial chemistry sampling (Figure 4.13). Furthermore, precipitates of iron oxy-hydroxides found in the EIF stream bed adjacent to the soil-piezometer site EIF/D and EIF/E possibly identify areas of suprapermafrost groundwater discharge, since the total iron content is high in some suprapermafrost groundwater samples (EIF/D). The bed structure of the EIF stream channel, characterized by a high proportion of gravels and rocks, is favourable for the fast routing of subsurface water similar to flow in a macropore (groundwater discharge into the stream was observed during the installation of the weir). A similar channel bed structure is also present in the upper, alluvial reaches of WIF/W stream.

The seasonally increasing concentrations of ions in the stream waters could therefore be explained by two processes: 1. increasing contribution of suprapermafrost groundwater to the stream runoff as a result of higher storage capacities of the active layer towards the end of the summer and 2. seasonally increasing ion concentrations of suprapermafrost groundwater with a longer residence time of water in the soil and increasing depth of thaw of the active layer.

6.1.4. Discussion of charge imbalances

Generally, a high positive charge imbalance in the WIF/W (mean charge balance error=14.2%, Std. dev.=9.9, n=45) could indicate that HCO_3^- is an important anion in the charge balance (Appendix C). This is further supported by the "good" charge balances of the WIF/2 (mean charge balance error=6.7%, Std. dev.=8.3, n=27) and EIF (mean charge balance error=5.7%, Std. dev.=5.6, n=42), since the same analytical technique was applied for all water samples. Furthermore, concentrations of NO_3^- and F^- are thought to be low, since no signal of either ion was detected on the Ion Chromatograph. Alkalinity concentrations are considerably higher in the WIF/W and WIF/2 than in the EIF (Table 6.2). Calculating the charge balance inclusive HCO_3^- concentrations, the positive imbalance for the WIF/W and WIF/2 is decreased up to 50% (Appendix C). Of note is the seasonal change of the charge imbalance of the WIF/W; the charge imbalance decreases by the end of the third period of active layer development (after 26 July) and reaches minimum values during the rainstorm (mean charge imbalance during rainstorm=6.9%, Std. dev.=1.8, n=9). This could indicate lower concentrations of HCO_3^- caused by the shorter transport time of water and thus a reduced contact with the sediments. However, this does not explain the observed high charge imbalance of WIF/W samples during snowmelt (mean charge imbalance error=16.8%, Std. dev.=9.8, n=10). These differences can possibly be attributed to considerably higher HCO_3^- concentration in snow or to different geochemical processes operating during the snowmelt in early June and the rainstorm in early August.

6.1.5. Geological sources for the chemistry of waters in the EIF and WIF basin

To interpret the hydrogeochemistry of the surface and groundwaters a triangular plot is used (Figures 6.9 and 6.10). These figures show that all streams are generally dominated by Ca^{2+} and SO_4^{2-}, but that the percentage of Mg^{2+} and HCO_3^- is higher in the WIF/W and WIF/2 than the EIF stream (Figures 6.9 and 6.10). This supports the assertion that geochemical weathering of a calcite, magnesium-calcite or silicate mineral is a possible source of alkalinity in the WIF basin. In the EIF, the ability to neutralize H^+ concentration is reduced by low alkalinities. To further explain the observed differences in geochemistry of the waters in the EIF and WIF basin, information on the mineralogical composition of the sediments is required. Field observations of the east slope (reddish colour, salt accumulations) indicate different sediment characteristics compared to the WIF basin. Using thin sections and a description of the rocks for texture, sediment structure, grain size and components allows a further classification of rock type and important minerals. All rocks can be classified as quartz-sandstones with grain sizes ranging from fine to medium sand. The binding matrix is predominantly calcite and silicate and all samples are without biogenic components.

The important factor that influences the water chemistry is the high pyrite (FeS_2) content of the rocks. Six of the eight analyzed rock samples of the east slope include pyrite, with a total volume percentage of up to 10% (grain size of pyrite minerals up to 0.5 cm; Colour Print 10). The weathering of pyrite is most pronounced at the exposed surface of the rock but can proceed as far as to the core of the rock (Colour Print 11). The weathering is enhanced by a high intergranular porosity, allowing water to migrate in the interconnected porous media (Colour Print

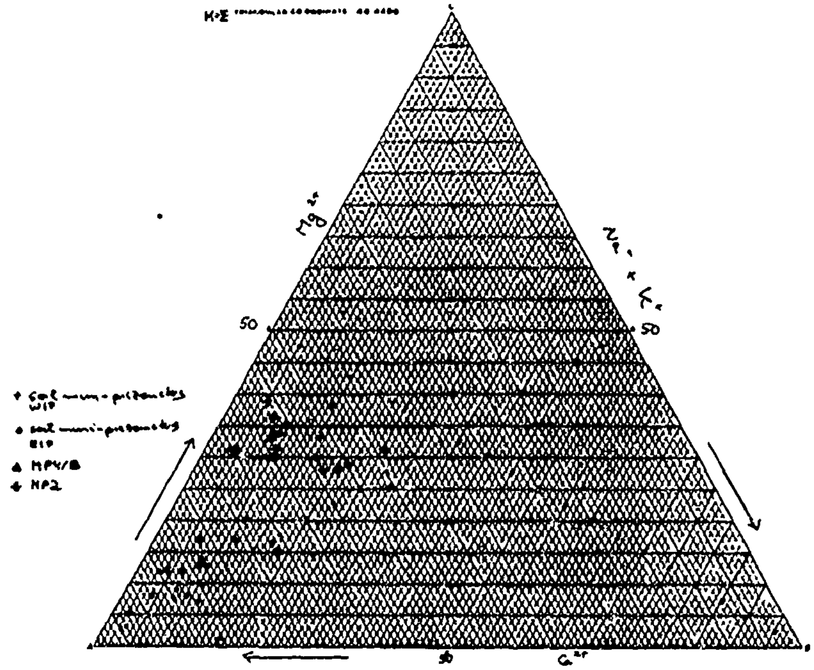

Figure 6.8. Cation ratios of suprapermafrost groundwaters of the EIF and WIF basin, 1991.

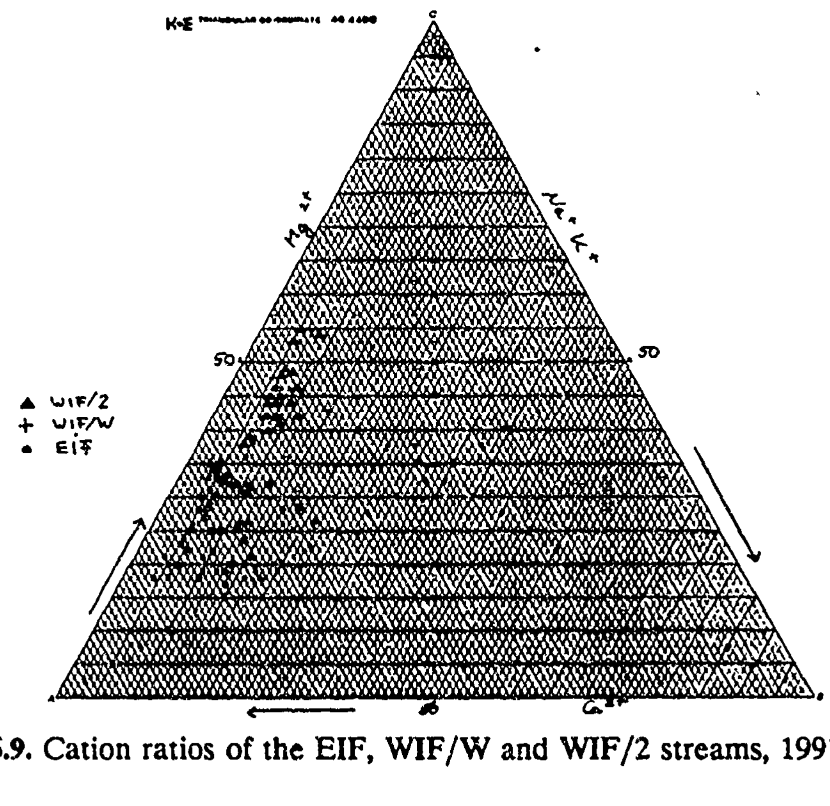

Figure 6.9. Cation ratios of the EIF, WIF/W and WIF/2 streams, 1991.

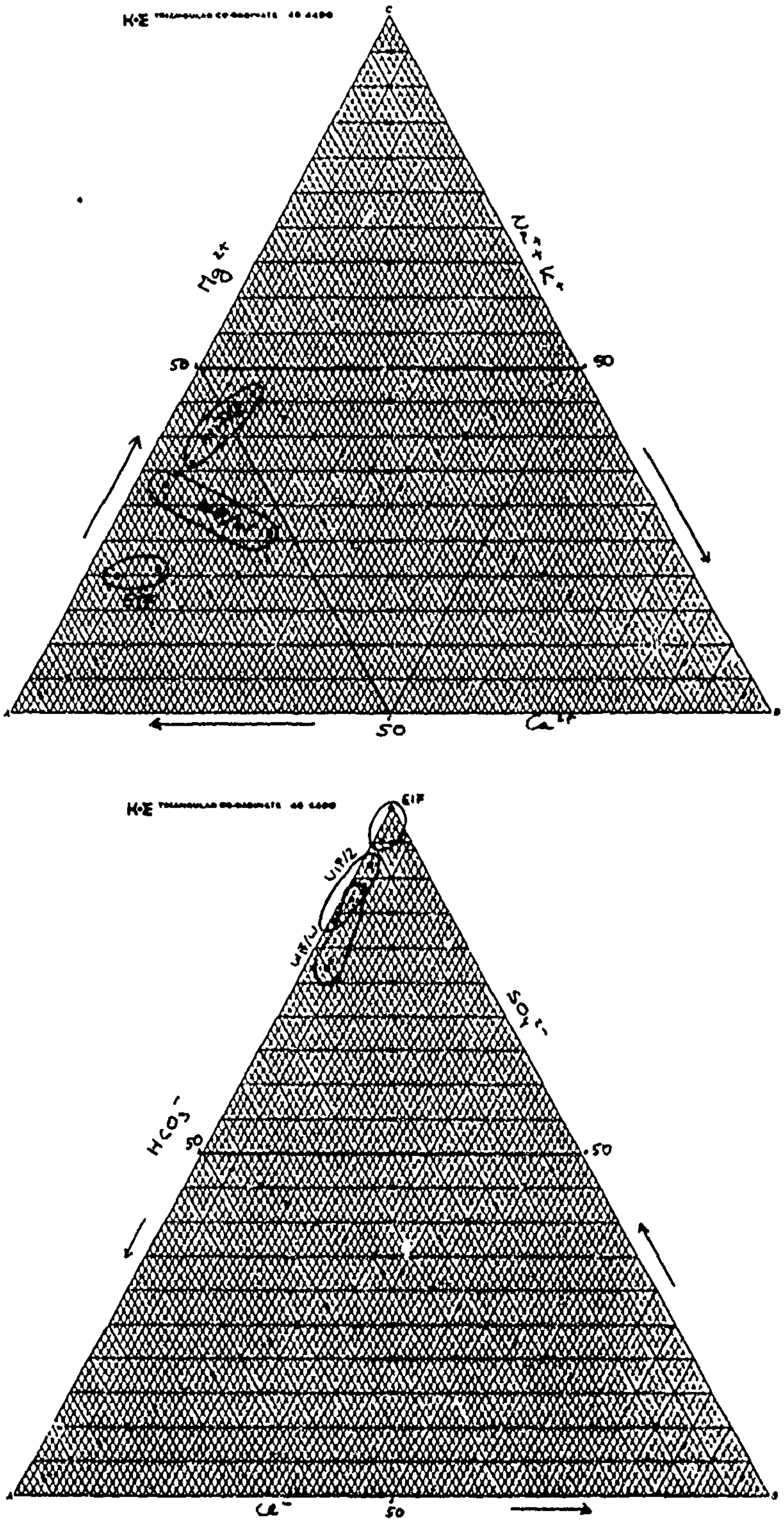

Figure 6.10. Cation and anion ratios of EIF, WIF/W and WIF/2 streams, 1991.

12). The only rock sample taken from the WIF basin can be classified as a quartz-sandstone as well. Signs of chemically weathered minerals (possibly Feldspar) are present, but in contrast to the rock samples from the east slope this sample does not contain pyrite. According to Fricker (1963a), the Awingak formation which underlies the WIF basin is mainly comprised of sandstone and shale (Figure 1.3). The predominance of sandstone in the WIF basin is also in agreement with results of the soil map (Figure 4.14).

Taking into consideration, that the suprapermafrost groundwater chemistry from the east slope in the EIF basin is characterized by a low pH and dominance of Ca^{2+} and SO_4^{2-} it seems plausible, that the weathering of pyrite has an important influence on the water chemistry. The oxidation of pyrite generates acidity in the following way:

$$(1)\ \ FeS_2 + 3.75O_2 + 3.5H_2O = Fe(OH)_3 + 4H^+ + 2SO_4^{2-} \ \text{(Drever, 1982)}$$

High concentrations of Ca^{2+} and SO_4^{2-} could be either produced by the oxidation of pyrite and following reaction with calcite:

$$(2)\ \ FeS_2 + 3.75O_2 + 3.5H_2O = Fe(OH)_3 + 4H^+ + 2SO_4^{2-}$$

$$4H^+ + 2CaCO_3 = 2Ca^{2+} + 2H_2CO_3$$

or the dissolution of gypsum ($CaSO_4{*}2H_2O$) or anhydrite ($CaSO_4$):

(3) $CaSO_4 * 2H_2O = Ca^{2+} + SO_4^{2-} + 2H_2O$ (Drever, 1982)

Using the sulphur isotope $^{34}\delta$, Schiff *et al.* (1991) suggest a sedimentary-pyrite or reduced sulfur (S) source for the western part of the Colour Lake catchment (including WIF stream) and an evaporite and reduced S source for the eastern part (including EIF stream). Since only one rock of the WIF basin was classified (which does not contain pyrite), it is not possible to assume that pyrite is not a source for sulphate in WIF basin. The higher pH of WIF waters suggests that pyrite weathering is not as prevalent in comparison to the east slope of the EIF basin or, the acidity is being consumed by another geochemical process, for example the dissolution of calcite. Higher Mg^{2+} and HCO_3^- concentrations of waters in the WIF basin relative to the EIF might be indicators for the greater presence of a Ca^{2+}/Mg^{2+} mineral in the WIF basin relative to the EIF basin. In the EIF, the high content of pyrite in rocks and visible signs of weathering on the east slope strongly suggest pyrite weathering as the reduced S source of sulphate (in addition to the dissolution of gypsum or anhydrite) and the source of high acidity.

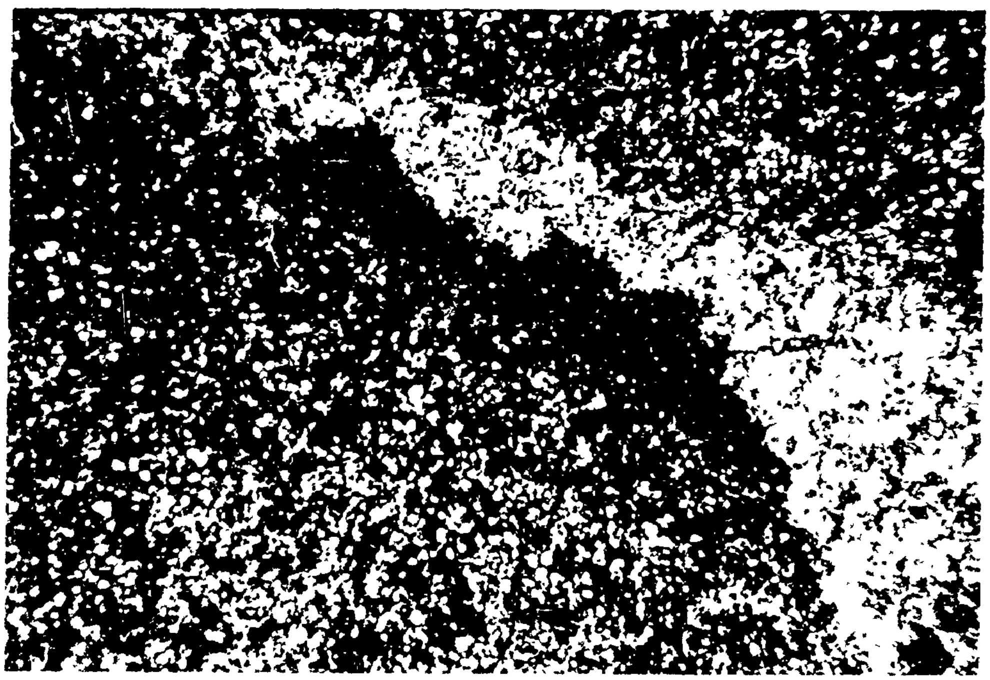

Colour Print 10. Thin section of quartz-sandstone of the Heiberg Formation (Colour Lake east slope) in polarized light. Rock contains up to 10 volume% pyrite (black minerals are pyrite, coloured minerals are quartz).

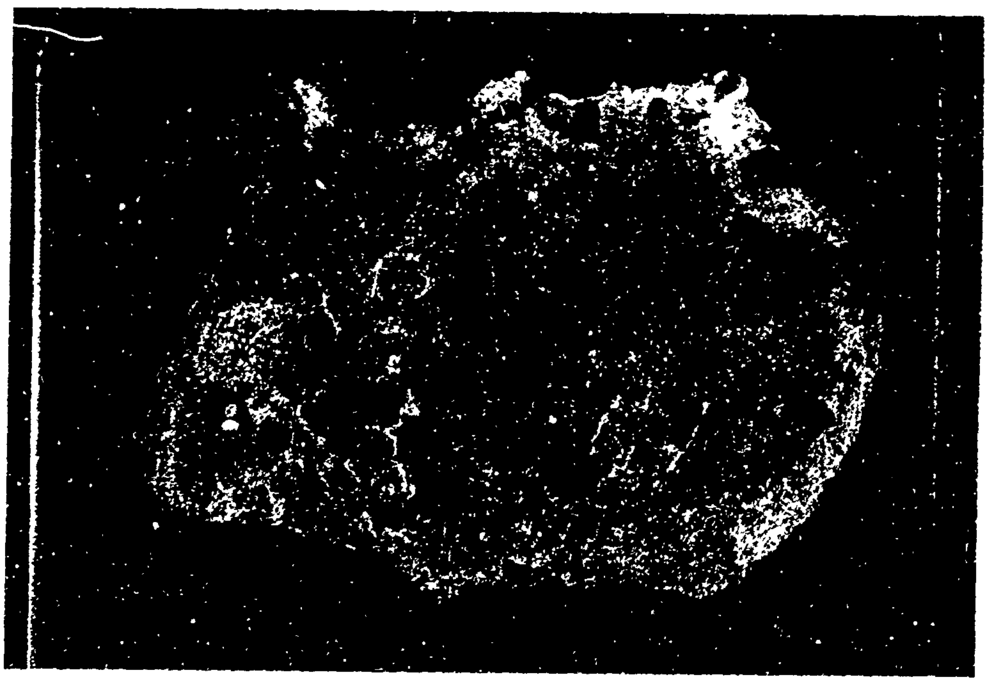

Colour Print 11. Thin section of quartz-sandstone of Heiberg Formation (Colour Lake east slope). Note high pyrite content and strong signs of chemical weatering of exposed rock surface and inside the rock.

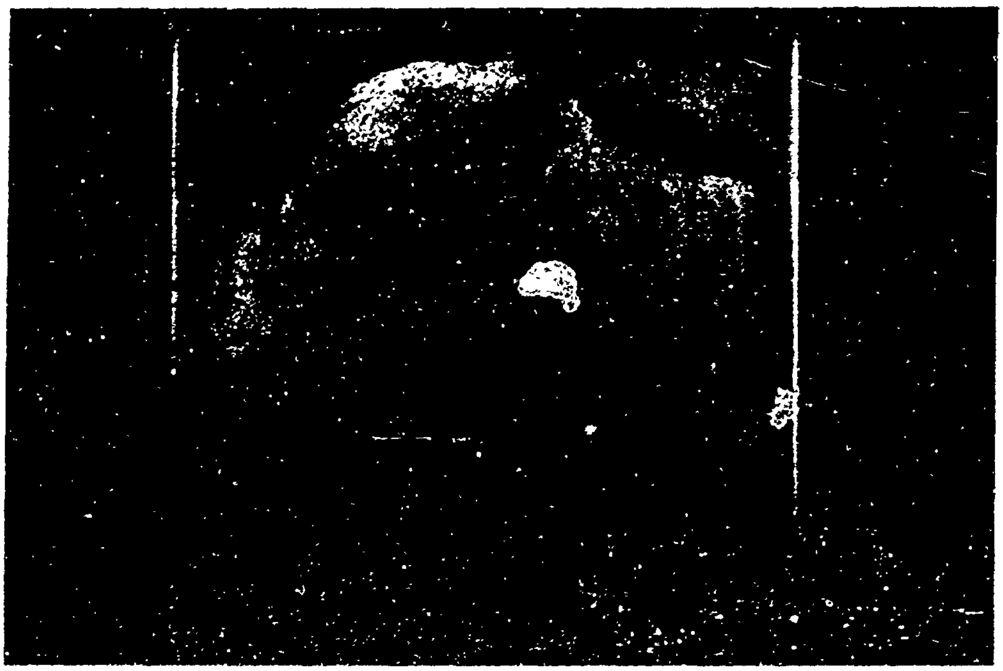

Colour Print 12. Thin section of quartz-sandstone of Heiberg Formation (Colour Lake east slope). Note high pyrite content and high intergranular porosity, which enables water to travel in interconnected, porous system.

6.2. Total export of ions from the watersheds

To understand the surface transfer of dissolved ions and water from land to the aquatic system, the total load and total discharge exported from each watershed is calculated. Figure 6.11 demonstrates the seasonal total load of TDS (mg/s) for the three streams from May to August, 1991. Clearly, the highest amount of TDS is exported during the rainstorm. Tables 6.6 contains the total load of TDS calculated for each stream during the three defined hydrological periods. The highest total amount of TDS is exported from the EIF stream. Although the WIF/2 does not flow for a long time during the summer, it transports the second highest amount of TDS to the lake. The WIF/W has the highest total discharge from all streams, but the total transport of TDS is the lowest compared to the WIF/2 and EIF streams (Table 6.6).

Major differences between the hydrology of the EIF, WIF/W and WIF/2 are further illustrated by the total discharge per drainage area (m^3/km^2) calculated for the entire runoff period May to August, 1991 (Table 6.6). While the EIF and WIF/2 produce approximately the same amount of discharge (EIF: 34 941 m^3/km^2, WIF/2: 32 781 m^3/km^2), the WIF/W produces a greater total amount of 40 202 m^3/km^2 (Table 6.6). This supports the observation that a higher ground ice storage in the bouldery material of the felsenmeer in the WIF/W basin is the important factor for higher discharge in the WIF/W compared to the EIF and WIF/2.

Assessment of the total loads shows that the importance of the second and

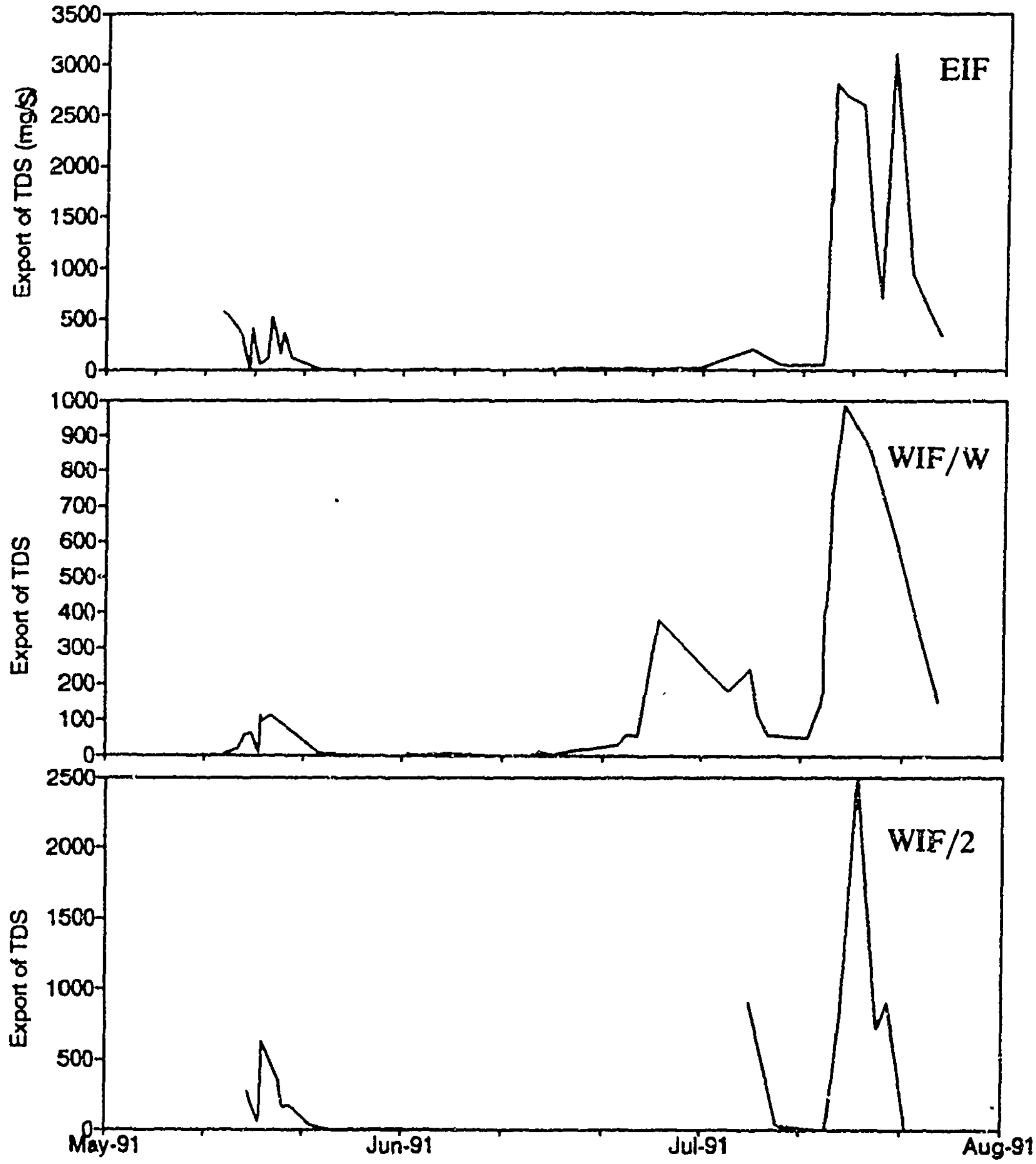

Figure 6.11. Load of TDS (mg/s) for the EIF, WIF/W and WIF/2 streams from May to August, 1991.

third period of active layer development is most pronounced in the WIF/W. This is also illustrated by TDS concentrations for each of the defined periods (ratio of total export of TDS (kg) to total discharge (m^3)) (Table 6.8). A constant, seasonal increase of TDS concentration is only found in the WIF/W stream, where TDS concentrations increase relative to discharge. No seasonal pattern is apparent in the EIF/W stream, however, highest export of TDS relative to discharge takes place during snowmelt and the rainstorm.

Table 6.7 gives the percentage of the total export of TDS for cations and anions of the streams. These numbers are calculated using the mean ion concentration and the total TDS export of each period (Table 6.6), since TDS concentrations were analyzed much more frequently than ion concentrations (Appendix C). As a result of different sampling frequency, the export calculations based on TDS concentrations gives a more accurate estimate of the total load (the total load calculated from ion concentrations overestimates the export value obtained from TDS concentrations up to 100%).

Sulphate is the ion with the highest export rate for all streams. In the EIF, the sum of Ca^{2+} and SO_4^{2-} is more than 90% of the total TDS exported. In the WIF/W, the percentage of Ca^{2+} and SO_4^{2-} exported is increasing seasonally from 83 to 90%. Considering the rainstorm in August as a rare event, the importance of the total transport of ions for each period requires a further assessment. Excluding the rainstorm in the calculation, the dominant event in the EIF and WIF/2 is the snowmelt and in the WIF/W the period of active layer development (Table 6.6).

	EIF				WIF/W				WIF/2			
Period	Total Export (kg)	Daily Export (kg/d)	Total Q (m^3)	Daily Q (m^3/d)	Total Export (kg)	Daily Export (kg/d)	Total Q (m^3)	Daily Q (m^3/d)	Total Export (kg)	Daily Export (kg/d)	Total Q (m^3)	Daily Q (m^3/d)
Snowmelt	226	23	1234	123	32	3.9	1185	148	91	13	984	141
Active layer 1	2.9	0.1	17	0.7	6.9	0.3	187	7.8				
Active layer 2	9.2	0.8	74	6.2	69	5.8	1173	98	37	*	286	*
Active layer 3	58	3.9	415	28	146	9.7	1468	98				
Rainstorm [a]	1216	135	5126	597	513	57	4349	483	731	81	3975	331
Σ all periods	1512	-	6866	-	749	-	8362	-	858	-	5245	-
Σ periods excl.storm	296	-	1740	-	254	-	4012	-	128	-	1270	-
Σ all periods/km^2	7695	-	34941	-	3601	-	40202	-	5363	-	32781	-

[a] calculation based for time period 2 to 10 of August, 1991
* intermittent streamflow
Basin sizes: EIF=196 500 m^2, WIF/W=208 000 m^2 and WIF/2=160 000 m^2

Table 6.6. Total export and daily normalized rates of TDS and discharge for the three streams during the hydrological periods, 1991.

	EIF								WIF/W						WIF/2					
	% of total ions exported*								% of total ions exported						% of total ions exported					
Period	Na^+	K^+	Ca^{2+}	Mg^{2+}	Fe^{2+}	Al^{3+}	Cl^-	SO_4^{2-}	Na^+	K^+	Ca^{2+}	Mg^{2+}	Cl^-	SO_4^{2-}	Na^+	K^+	Ca^{2+}	Mg^{2+}	Cl^-	SO_4^{2-}
Snow-melt	1.6	1.1	18.9	4.4	0.2	0.7	0.9	72.3	3.7	3.2	23.5	6.8	3.7	59.1	1.8	1.6	17.0	8.7	1.4	69.5
Active layer 1	2.5	0.8	19.6	6.0	0.2	0	0.5	70.5	5.9	1.8	22.4	7.6	1.8	60.6						
Active layer 2	3.7	0.9	20.5	3.6	0	0	0.3	71.1	12.0	1.5	19.9	6.05	1.1	59.3	2.5	0.8	14.9	9.4	0.5	72
Active layer 3	2.4	0.9	21.4	3.8	0.1	0.2	0.4	70.9	2.7	0.9	19.8	6.34	1.3	68.7						
Rain-storm	1.2	0.5	18.7	3.1	0.4	1.1	0.3	74.9	1.5	1.1	20.6	6.5	0.8	69	1.7	0.8	15.3	10	0.2	72

* calculated as percentage of total export of TDS (kg) accounted for by the mean ion concentration for each of the defined periods

Table 6.7. Percentage of ions of total export exported from the three streams *during the hydrological* periods, 1991.

	[Total load of TDS (kg)] / [Total Q (m^3)]		
Period	EIF	WIF/W	WIF/2
Snowmelt	0.18	0.03	0.09
Active layer 1	0.16	0.04	n.a.
Active layer 2	0.12	0.06	n.a.
Active layer 3	0.14	0.1	n.a.
Rainstorm	0.25	0.12	0.18

Table 6.8. Ratio of total load of TDS (kg) and total discharge (m^3) during the hydrological periods for the three streams, 1991.

This is surprising, since the dominating events take place during a time when the depth of thaw of the active layer is minimal (EIF during snowmelt) and maximal (WIF/W during third period of active layer development) and indicates different hydrological and chemical processes. The WIF/W exhibits a flow system where seasonal changes of flowpaths result in increased total export of ions (higher contribution of suprapermafrost groundwater with deeper thaw of active layer). In the EIF and WIF/2, the interactions between frozen and unfrozen ground and meltwater result in the highest total export of ions during snowmelt.

6.3. Conclusions

This study identifies three different arctic hydrological regimes in the Colour Lake catchment: Arctic nival (WIF/2), "melting ground ice regime with proglacial characteristics" (WIF/W) and "modified melting ground ice regime" (EIF).

With the seasonally thawing of the upper ground and concomitant saturation by precipitation or meltwater from ground ice, the potential for suprapermafrost groundwater flow above the frost table is increased. Results indicate that this flow system in the active layer is very complex as a result of the heterogeneous aquifer. Spatial and temporal variations of the suprapermafrost groundwater are due to the heterogeneity and properties of the active layer sediments and the surface topography of the frost table. The seasonally changing flowpaths of water with increasing thaw depth of the active layer, in combination with higher weathering rates, are thought to be the important process responsible for the increasing ion concentrations in surface and subsurface waters. On one hand, the ionic strength of suprapermafrost groundwaters increases with time due to longer residence times; on the other hand the subsurface flowpath is enhanced by the seasonally thawing ground. This process is evident in the WIF/W in light of the seasonally increasing TDS concentration. In contrast, a clear, seasonally increasing trend of ions is not found in the flow regime of the EIF as a result of two chemically and hydrologically different contributing areas of water in the EIF catchment. These areas have been identified by the results of the chemical analysis and mapping of the local geology; the area eastward of the EIF stream (soil zones 3 and 4) generates high acidity and high ion concentrations, the west slope (westward of the EIF stream including soil zones 1, 2, 5, 7; Figure 4.14) generates low acidity and low ion concentrations.

Generally, the mineralogical properties of the geological material determine the chemical characteristics of surface and subsurface waters and are one important cause for the chemical difference of waters in the EIF and WIF basin. A significant high content of pyrite has been identified in the Heiberg Formation, which is part of the east slope of the EIF catchment. The weathering of pyrite is suggested to be the main source of acidity and the reduced S source of sulphate for the suprapermafrost groundwaters draining the east slope and for the EIF stream. The chemistry of the waters in the WIF basin suggests the presence of a calcite-magnesium mineral. Future classification of minerals in the WIF basin could identify the source of Ca^{2+}/Mg^{2+} ions and give further indication about the reduced S source of sulphate.

CHAPTER 7 CONCLUSIONS

This research provides a detailed overview of geochemical and hydrological processes operating in a small high arctic catchment. On a relatively small spatial scale, important differences in hydrological and geochemical characteristics of waters in adjacent sub-basins have been identified. These results underline that the catchment hydrological system can only be understood within the framework of surface and soil (mineral and physical) properties, topography, vegetation cover and meteorological conditions. Despite the diversity of arctic environments, in general, active layer processes play a major role in the hydrology of arctic catchments. By achieving an improved understanding of the role of permafrost and active layer processes in basin hydrology, this small scale study allows the extrapolation of general processes to a larger scale.

Better understanding of the "short term" effects of the formation and melting of ground ice is given by the results of this research. In this study, ground ice is an important storage factor and its changes over time should be considered in water balance calculations. Moreover, the melting of ground ice during the summer has a considerable influence on the hydrological regime. The term "proglacial regime" is insufficient to describe catchments where streamflow is generated by melting of ground ice or perennial snowbanks, since it includes only the contribution of glacier meltwater. It is therefore suggested that the term "arctic, proglacial regime" should be refined either by subdividing the proglacial regime by source areas of water (glacier, ground ice, snowbanks) or by the introduction of a new hydrological regime.

Given a good understanding of the natural, unaffected conditions within a hydrological system (as for an intensively studied catchment), anthropogenic effects such as pollution and climate change can be estimated. General circulation models (GCM's) predict that high latitudes above 70°N will be subject to the greatest change in the event of global climate change, with potential temperature increases of 4.5 to 11°C during winter and 1.7 to 4.9°C during summer (Smith, 1986). Assuming that this projection is valid, this process may substantially influence the hydrological and geochemical system. From this study at least three important conclusions can be drawn:

1. Most of the GCM's predict an increase in summer precipitation from 10 to 60% (Smith, 1986). This study has shown that the dominant event in terms of total export of ions and sediments is the rainstorm. It can therefore be concluded that the occurrence of high intensity rainstorms will probably have a tremendous effect on the unstable, geomorphic permafrost environment resulting in high transport rates of sediment and ions. Moreover, as exemplified by the EIF stream, the pH of the water may drop to the lowest seasonal level during the rainstorm. Since the lake is not covered by ice during this time, the runoff water potentially mixes with the lake water and the effects upon the aquatic system could be significant. Effects of acidic, terrestrial snowmelt runoff are intensively studied in northern and temperate catchments; acid runoff can mobilize aluminum, which is toxic for fish habitat and

3 of/de 3

PM-1 3½"x4" PHOTOGRAPHIC MICROCOPY TARGET
NBS 1010a ANSI/ISO #2 EQUIVALENT

1.0 1.1 1.25 1.4 1.6 1.8 2.0 2.2 2.5 2.8 3.2 3.6 4.0 4.5 5.0 5.6 6.3 7.1

affects microbiological metabolism in soil (Mancinelli, 1986). Furthermore, higher frequencies of increased ion and sediment loading could alter the nutrient budget of aquatic systems.

2. Higher air temperatures and therefore an increased thaw depth would result in a higher potential for water movement and storage in the active layer. In addition, higher soil temperatures and increased moisture content would increase weathering rates. These processes would intensify the seasonal transport of ions in stream and groundwaters towards aquatic systems. Lewkowicz and French (1982b) state that the removal of large quantities of solute material by suprapermafrost groundwater plays an important role in the denudation process in arctic environments.

3. As this study shows, ground ice is an important factor for sustaining streamflow during the summer. Higher air and ground temperatures could deplete the short and long term water storage in form of ground ice and therefore changes in the hydrological regimes could occur.

Nevertheless, one should keep in mind that these changes are hypothetical, since many factors are unknown. Large uncertainties include, for example, the timing, intensity and amount of summer precipitation, which are essential to predict changes in evaporation and runoff.

Another focus of polar research is to study biochemical and hydrological cycles in "hostile" environments. Although hydrological processes are more or less confined to a relatively short season during the summer, the supply of water is important for sustaining the arctic ecosystem. Even under extreme polar desert conditions, many forms of life (fauna, flora and microorganism) exist. One of the long term objectives of studies carried out by the NASA is to assess the possibilities of life on other planets (especially Mars). Missions to Mars have revealed that the martian crust, with temperatures down to -60°C, could bear substantial amounts of water and other materials for the start of a biochemical cycle (McKay and Haynes, 1990). Thus, permafrost studies in extreme polar conditions (carried out by the NASA in the polar deserts of the high Arctic and in the Dry Valleys in the Antarctic) could likely give information about "permafrost" conditions on Mars and the potential for the existence or genesis of life forms.

Tedrow's (1977) bioclimatic classification of the Queen Elizabeth Islands as "polar desert" is too general for the Colour Lake catchment since it neglects the diversity and abundant vegetation in some areas of the catchment. However, Edlund and Alt's (1989) recent classification of the high Arctic into five bioclimatic zones, which places the Expedition Fiord Area under the transition zone between herbaceous and prostrate shrub zone, is much more applicable to the actual conditions. This reinforces the need for detailed, integrated small scale studies including climatic, biotic, geomorphic and pedologic factors for the classification of high Arctic bioclimatic zones.

And last, this study gives only a small piece of hydrological and chemical information concerning a largely unstudied region. Further research in high Arctic regions is needed to understand hydrological and geochemical processes on a larger spatial and temporal scale. Future studies should therefore include year to year variations in hydrology and chemistry, to identify long term processes operating in the catchment and between the terrestrial and aquatic system. The Colour Lake catchment is potentially suitable for this research, since intensive research has focused since 1959 on a variety of topics such as meteorology, limnology, geology and hydrology. Integrating these results would give a better understanding of the linkages between the hydrological, chemical and climatic systems. Only given these preconditions will it be possible to assess the impact of humans on the high Arctic ecosystem.

REFERENCES

Adams, W.P.(ed.) 1987. Field research on Axel Heiberg Island, N.W.T.Canada. McGill University, Axel Heiberg Island Research Report, Misc.Papers No.2. McGill University, pp. 67-189.

Adams, W.P., Doran, P.T., Ecclestone, C.M., Kingsbury, C.M. and C.J.Allan (1989). A rare second year-lake ice cover in the Canadian high arctic. *Arctic* 42(4), pp. 299-306.

Allan, C., S.L. Schiff, D. Pierson, M.C. English, M. Ecclestone and P. Adams (1987). Colour Lake, Axel Heiberg Island, N.W.T., a naturally acidic, high arctic lake-data report. *In:* Adams, W.P.(ed.) 1987. Field research on Axel Heiberg Island, N.W.T., Canada. McGill University, Axel Heiberg Island Research Report, Misc.Papers No.2. McGill University, pp. 67-189.

Anisimova, N.P. (1978). Cryogenous metamorphization of chemical composition of subsurface water (exemplified in central Yakutia). *Proceedings Second International Conference*, USSR Contributions. National Academy of Sciences, Washington DC, pp. 365-374.

Beschel, R.E. (1963). Geobotanical studies on Axel Heiberg in 1962. *In*: Axel Heiberg Island Research Reports, Preliminary Report 1961-1962. McGill University, Montreal, pp. 199-215.

Bliss, L.C. and J.Svoboda (1984). Plant communities and plant production in the western Queen Elizabeth Islands. *Holarctic Ecology* 7, pp. 325-344.

Bliss, L.C., Svoboda J. and D.I. Bliss (1984). Polar deserts , their plant cover and plant production in the Canadian High Arctic. *Holarctic Ecology* 7, pp. 301-320.

Boesch, H. (1963). Notes on the geomorphological history. *In*: Axel Heiberg Island Research Reports, Preliminary Report 1961-1962. McGill University, Montreal, pp. 163-168.

Bower, C.A. and L.V.Wilcox (1965). Soluble salts. *In*: Black, C.A. and R.C.Dinauer (ed.), Methods of Soil Analysis, Part 2: Chemical and microbiological properties. American Society of Agronomy, Madison, Wisc., pp. 933-951.

Boike, J.B., English, M.C., Schiff, S.L., Rau, S., MacLean, R.A., Elgood, R.J. and M.J.Hinton (1991). Preliminary investigations of groundwater hydrology of a high arctic lake. *Proceedings of the Third National Student Conference on Northern Studies*. The Musk-Ox (in press).

Burn, C.R. and F.A.Michel (1988). Evidence for recent temperature-induced water migration into permafrost from the tritium content of ground ice near Mayo, Yukon Territory, Canada. *Canadian Journal of Earth Science* 25, pp. 909-915.

Buttle, J.M. and K.E.Fraser (1992). Hydrochemical fluxes in a high arctic wetland basin during spring snowmelt. *Arctic and Alpine Research* 24(2), pp. 153-164.

Caflisch, T. (1972). Limnological investigations of Colour and Phantom Lake. *In:* Axel Heiberg Island Research Reports. Miscellaneous Papers McGill University, pp. 67-189.

Cheng, G. and E.J.Chamberlain (1988). Observation of moisture migration in frozen soils during thawing. *Proceedings of the Fifth International Conference of Permafrost*, Trondheim.. Norway, pp. 308-312.

Chizhov, A.B., Chizhova, N.I., Morkovkina, I.K. and V.V.Romanov (1983). Tritium in permafrost and in ground ice. *Proceedings of the Fourth International Conference on Permafrost*, Fairbanks, Alaska, pp. 147-151.

Church, M. (1974). Hydrology and permafrost with reference to northern North-America. *In*: Permafrost Hydrology, Proceedings of Workshop Seminar 1974. Canadian Nationa Committee for the International Hydrological Decade, Ottawa, Ontario, pp. 7-20.

Cogley, J.G. and S.B. McCann (1976). An exceptional storm and its effects in the Canadian Arctic. *Arctic and Alpine Research* 8(1), pp. 105-110.

Cooper, L.W., Olsen, C.R., Solomon, D.K., Larsen, I.L., Cook, R.B. and J.M. Grebmeier (1991). Stable isotopes of oxygen and natural and fallout radionuclides used for tracing runoff during snowmelt in an Arctic watershed. *Water Resources Research* 27(9), pp. 2171-2179.

Dionex Corp. (1982). Dionex Ion Chromatography System 2010i operator's manual.

Doran, P. (1990). Sedimentology and paleolimnology of Colour Lake, Axel Heiberg Island, a naturally acidic high arctic lake. Unpubl. MSc.Thesis, Department of Geography, Queen's University, Kingston, Ontario, 172 pp.

Drever, J.I. (1982). The geochemistry of natural waters. Englewood Cliffs, N.J.: Prentice-Hall, 388 pp.

Dunne, T. and R.D.Black (1970). An experimental investigation of runoff production in permeable soils. *Water Resources Research,* 6(2), pp. 478-490.

Edlund, S.A., Woo, M.K. and K.L.Young (1990). Climate, hydrology and vegetation patterns Hot Weather Creek, Ellesmere Island, Arctic Canada. *Nordic Hydrology* 21, pp. 273-286.

Edlund, S.A. and B.Taylor Alt (1989). Regional congruence of vegetation and summer climate patterns in the Queen Elizabeth Islands, N.W.T., Canada. *Arctic* 42(1), pp. 3-23.

English, M.C., Schiff, S.L, Ecclestone, M., Adams, W.P., Hinton, M., Pezzuto, L., Elgood, R., Allan, C. and D. Pierson (1991). Seasonal changes in the hydrochemistry of land drainage: Colour Lake Catchment, Axel Heiberg Island, N.W.T. *In*: Prowse, T.D. and C.S.L. Ommanney (ed.). Northern Hydrology: Selected Perspectives, NHRI Science Report No.2, National Hydrology Research Institute, Environment Canada, Saskatoon, Saskatchewan, pp. 75-88.

Everett, K.R., Marion, G.M. and D.L. Kane (1989). Seasonal geochemistry of an arctic tundra drainage basin. *Holarctic Ecology* 12, pp. 279-289.

Everett, K.R. and B.Ostendorf (1988). Hydrology and geochemistry of a small drainage basin in upland tundra, northern Alaska. *Proceedings of the Fifth International Conference of Permafrost*, Trondheim, Norway, pp. 574-579.

Flügel, W.A. (1981). Hydrologische Studien zum Wasserhaushalt hocharktischer Einzugsgebiete im Bereich des Oobloyah Tals, N-Ellesmere Island, N.W.T., Kanada. *Heidelberger Geographische Arbeiten* 69, pp. 311-382 (in german).

Fontes, J.C. (1980). Environmental isotopes in groundwater hydrology. *In*: Fritz, P. and J.Ch.Fontes (ed.). Handbook of Environmental Isotope Geochemistry, Vol.1. Elesvier Scientific Publishing, Amsterdam, pp. 75-140.

Freeze, R.A. and J.A. Cherry (1979). Groundwater. Englewood Cliffs, N.J.: Prentice-Hall, 558 pp.

Fricker,P.E. (1963a). Geology of the Expedition Fiord Area, Western Central Axel Heiberg Island, Canadian Arctic Archipelago. *In:* Axel Heiberg Island Research Reports, Geology No.1. McGill University, Montreal, 156 pp.

Fricker,P.E. (1963b). Geological work in the Expedition Area. *In*: Axel Heiberg Island Research Reports, Preliminary Report 1961-1962. McGill University, Montreal, pp. 127-132.

Fritz, P., Cherry, J.A., Weyer, K.U. and M.Sklash (1976). Storm runoff analysis using environmental isotopes and major ions. *Proceedings of the advisory group* *meeting on interpretation of environmental isotopes and hydrochemical data in groundwater hydrology.* International Atomic Energy Agency, Vienna, pp. 111-129.

Gold, L.W. and A.H.Lachenbruch (1973). Thermal conditions in permafrost-a review of North American literature. *Proceedings Second International Conference on Permafrost*, North American Contribution, pp. 3-23.

Harris, S.A. (1988). Observations on the redistribution of moisture in the active layer and permafrost. *Proceedings of the Fifth International Conference of Permafrost*, pp. 364-368.

Hartge, K.H. and R.Horn (1989). *Die physikalische Untersuchung von Böden*. -2., völlig neu bearb. Aufl. Ferdinand Enke Verlag, Stuttgart, 175 pp. (in german).

Hewlett, J.D. and W.L.Nutter (1970). The varying source area of streamflow from upland basins. Paper presented at Symposium of Interdisciplinary Aspects of Watershed Management. Mont. State Univ.

Hinzman, L.D. and D.L. Kane (1992). Potential response of an arctic watershed during a period of global warming. *J. of Geophysical Research* 97(3), pp. 2811-2820.

Hodgson, D.A. (1989). Quaternary geology of the Queen Elizabeth Islands. *In*: Quaternary Geology of Canada and Greenland, R.J.Fulton (ed.). Geological Survey of Canada, Geology of Canada, no.1., pp. 443-476.

Ingleton, B., Drive point piezometers for groundwater quality monitoring. Waterloo Centre for Groundwater Research, in preparation.

Intergovernmental Panel on Climate Change (1990). Climate change- the IPCC scientific assessment (ed. J.T.Houghton, G.J.Jenkins and J.J.Ephraums). Report prepared for IPCC by working group 1. Cambridge University Press, Cambridge, Great-Britain, 365pp.

Johannessen, M. and A.Henriksen (1978). Chemistry of snow meltwater: changes in concentration during melting. *Water Resources Research* 14(4), pp. 615-619.

Jones, P.D., Wigley, T.M.L. and P.B.Wright (1984). Global temperature variations between 1861 and 1984. *Nature* 322(6077), pp. 430-434.

Kane, D.L. and J.Stein (1983). Water movement into seasonally frozen soils. *Water Resources Research* 19(6), pp. 1547-1557.

Kane, D.L. and L.D.Hinzmann (1988). Permafrost hydrology of a small arctic watershed. *Proceedings of the Fifth International Conference of Permafrost*, Trondheim, Norway, pp. 590-595.

Kane, D.L. and C.W.Slaughter (1973). Recharge of a central Alaska lake by subpermafrost groundwater. *Proceedings Second International Conference*, North American Contribution, pp. 458-462.

Kane, D.L., Fox, J.D., Seifert, R.D. and G.S.Taylor (1978). Snowmelt infiltration and movement in frozen soils. *Proceedings Third International Conference on Permafrost*, 10-13 July, Edmonton, Alberta, Vol.1, pp. 201-206.

Kane, D.L., Hinzman, L.D., Benson, C.S. and K.R. Everett (1989). Hydrology of Imnavait Creek, an arctic watershed. *Holarctic Ecology* 12, pp. 262-269.

Kane, D.L., Gieck, R.E. and L.D. Hinzmann (1990). Evapotranspiration from a small alaskan arctic watershed. *Nordic Hydrology* 21, pp. 253-272.

Kondrat'yev, K.Ya. and V.M.Kotlyakov, V.M. (1991). The polar regions and their contribution to climate change. *Polar Geography and Geology* 15(1), pp. 70-84.

Lachenbruch, A.H. and B.V.Marshall (1986). Changing climate: Geothermal evidence from permafrost in the Alaskan Arctic. *Science* 234, pp. 689-696.

Lee, D.R. and J.A.Cherry (1978). A field exercise on groundwater flow using seepage meters and mini-piezometers. *J. of Geological Education* 27, pp. 6-10.

Lemmen, D.S., Gilbert, R. and A.E.Aitken (1991). Quaternary investigations in the Expedition Fiord Area, west-central Axel Heiberg Island, N.W.T. *In*: Current Research, Part B, Geological Survey of Canada, Paper 91-1B, pp. 1-7.

Lewkowicz, A.G. and H.M. French (1982a). The hydrology of small runoff plots in an area of continuous permafrost, Banks Island, N.W.T. *Proceedings Fourth Canadian Permafrost Conference*, pp. 151-162.

Lewkowicz, A.G. and H.M. French (1982b). Downslope water movement and solute concentrations within the avtive layer, Banks Island, N.W.T. *Proceedings Fourth Canadian Permafrost Conference*, pp. 163-172.

Lewkowicz, A.G. and K.L Young (1991). Hydrological Processes in a small catchment containing a perennial snowbank, Melville Island, N.W.T. *In*: Prowse, T.D. and C.S.L. Ommanney (ed.). Northern Hydrology: Selected Perspectives, NHRI Science Report No.2, National Hydrology Research Institute, Environment Canada, Saskatoon, Saskatchewan, pp. 237-251.

Mancinelli, R.L. (1986). Alpine tundra soil bacterial responses to increased soil loading rates of acidic precipitation, nitrate and sulfate, Front Range, Colorado, USA. *Arctic and Alpine Research* 18, pp. 269-275.

Marsh, P. (1986). Modelling water levels for a lake in the Mackenzie Delta. *Proceedings of the Cold Regions Hydrology Symposium*, 22-25 July, Fairbanks, Alaska. American Water Resources Ass., Technical Publ. Series No.TPS-86-1, Betheseda, Maryland, pp. 23-29.

Marsh, P. and M.K.Woo (1977). The water balance of a small pond in the high arctic. *Arctic* 30(2), pp. 109-117.

McKay, C.P. and R.H.Haynes (1990). Should we implant life on Mars? *Scientific American* 263(6), pp. 144.

MacLean, R.A. (1992). The role of the vadose zone in the generation of runoff from a headwater basin in the Canadian Shield. M.A.Thesis, Department of Geography, Wilfrid Laurier University, 158 pp.

Michel, F.A. and P.Fritz (1978). Environmental isotopes in permafrost related waters along the Mackenzie Valley Corridor. *Proceedings Third International Conference on Permafrost*, Edmonton, Alberta, Vol.1, pp. 207-211.

Michel, F.A. and P.Fritz (1982). Significance of isotope variations in permafrost waters in Illisarvik, N.W.T. *Proceedings Fourth International Conference on Permafrost*, Calgary, Alberta, Vol.2, pp. 207-211.

Müller, F. (1963). Depth sounding projects. *In*: Axel Heiberg Island Research Reports, Preliminary Report 1961-1962. McGill University, Montreal, pp. 103-108.

Müller, F. (1963). Radiocarbon dates and notes on the climatic and morphological history. *In*: Axel Heiberg Island Research Reports, Preliminary Report 1961-1962. McGill University, Montreal, pp. 169-172.

Müller, F. and N.Roskin-Sharlin (1967). A high arctic climate study on Axel Heiberg Island. Part 1: General Meteorology. *In*: Axel Heiberg Island Research Reports, Meteorology No.3. McGill University, Montreal, 82 pp.

Munter, J.A. (1986). Evidence of groundwater recharge through frozen soils at Anchorage, Alaska. *Proceedings of the Cold Regions Hydrology Symposium*, 22-25 July, Fairbanks, Alaska. American Water Resources Ass., Technical Publ. Series No.TPS-86-1, Betheseda, Maryland, pp. 245-252.

Nagel, G. (1979). Untersuchungen zum Wasserkreislauf in Periglazialgebieten. *In*: Müller-Wille, L. und H. Schroeder-Lanz (Ed.). Kanada und das Nordpolargebiet. *Trierer Geographische Studien*, Sonderheft 2, pp. 157-178 (in german).

National Research Council Canada (1988). Glossary of permafrost and related ground-ice terms. N.R.C.C, Ottawa, 156 pp.

Obradovic, M.M. and M.G. Sklash (1986). An isotopic and geochemical study of snowmelt runoff in a small arctic watershed. *Hydrological Processes* 1, pp. 15-30.

Ohmura, A. (1972). Some climatological notes on the Expedition Area. *In:* Axel Heiberg Island Research Report, McGill University, Montreal, Quebec. International Geographical Union, Field Tour Ea2: Arctic Archipelago I, 22nd International Geographical Congress, Miscellaneous Papers by F. Müller and Members of the Expedition, August 5-13, pp. 5-14.

Ohmura, A. and F.Müller (1977). Die mesoklimatische Verteilung von Lufttemperatur und Niederschlag über der hocharktischen Tundra von Axel Heiberg Island, N.W.T., Kanada. *Geographica Helvetica* 4, pp. 185-193 (in german).

Ohmura, A. (1982a). Evaporation from the surface of the arctic tundra on Axel Heiberg Island. *Water Resources Research* 18(2), pp. 291-300.

Ohmura, A. (1982b). Regional water balance on the arctic tundra in summer. *Water Resources Research* 18(2), pp. 301-305.

Ohmura, O. (1982c). Climate and energy balance on the arctic tundra. *Journal of Climatology* 2, pp. 65-84.

Ommanney, C.S.L. (1987). Axel Heiberg Island bibliography. *In:* Adams, W.P.(ed.)1987. Field research on Axel Heiberg Island, N.W.T.Canada. McGill University, Axel Heiberg Island Research Report, Misc.Papers No.2. McGill University, pp. 5-55.

Peech, M. (1965). Hydrogen-ion activity. *In*: Black, C.A. and R.C.Dinauer (ed.), Methods of Soil Analysis, Part 2: Chemical and microbiological properties. American Society of Agronomy, Madison, Wisc., pp. 914-925.

Perkin Elmer (1982). Analytical Methods for Atomic Absorption Spectrometry. Perkin Elmer Corp., Norwalk, Connecticut, U.S.A.

Plauchut, B.P. (1971). Geology of the Sverdrup Basin-Summary. *Proceedings of the Second International Symposium on Arctic Geology*, February 1-4, 1971, San Francisco, California, pp. 76-82.

Qiu, G., Sheng, W., Huang, C. and K.Zheng (1988). Direction of ion migration during cooling and freezing processes. *Proceedings of the Fifth International Conference of Permafrost*, Trondheim, Norway, pp. 442-447.

Reardon, E.J. (1992). Course Notes: Chemical Modeling of Rock/Water Interaction. University of Waterloo, Department of Earth Science, 145 pp.

Rudberg, S. (1963). Geomorphological processes in a cold semi-arid region. *In*: Axel Heiberg Island Research Reports, Preliminary Report 1961-1962. McGill University, Montreal, pp. 139-150.

Rydén, B.E. (1977). Hydrology of Truelove Lowland. *In*: Bliss, L.C. (ed.). Truelove Lowland, Devon Island, Canada: A High Arctic Ecosystem. *University of Alberta Press,* Edmonton, pp. 107-136.

Schiff, S.L, English, M.C.,Ecclestone, M., Elgood, R., Hinton, M. and L. Pezzuto, (1991). Constraints on the origin of acidity in Colour Lake, Axel Heiberg Island (79° 25'N). *In*: Prowse, T.D. and C.S.L. Ommanney (ed.). Northern Hydrology: Selected Perspectives, NHRI Science Report No.2, National Hydrology Research Institute, Environment Canada, Saskatoon, Saskatchewan, pp. 303-318.

Semkin, R.G. and D.S.Jeffries (1986). Storage and release of major ionic contaminants from the snowpack in the Turkey Lakes Watershed. *Water, Air, and Soil Pollution* 31, pp. 215-221.

Smith, M. (1986). The significance of climate change for the permafrost environment. *Proceedings of a Canadian Climate Program Workshop*, March 3-5, Geneva Park, Ontario (ed.H.M.French), pp. 67-81.

Steffen, K. and Müller, F. (1977). Lokale Schneeverteilung auf Axel Heiberg Island, N.W.T. *Geographica Helvetica* 4, pp. 195-202 (in german).

Steiger, J.H. (1980). Tests for comparing elements of a correlation matrix. *Psychological Bulletin* 87(2), pp. 245-251.

Stoner, M.G. and F.G. Ugolini (1988). Arctic pedogenesis: 2. Threshold-controlled subsurface leaching episodes. *Soil Science* 145(1), pp. 46-51.

Stuiver, M., Yang, I.C. and G.H.Denton (1976). Permafrost oxygen isotope ratios and chronology of three cores from Antarctica. *Nature* 261, pp. 547-550.

Stumm, W. and J.J. Morgan (1981). Aquatic Chemistry: An Introduction Emphasizing Chemical Equilibria in Natural waters. Second edition, John Wiley and Sons, New York, 780 pp.

Tedrow, J.C.F.(1977). Soils of the Polar Landscapes. Rutgers University Press, New Jersey, 638 pp.

Ugolini, F.C. and D.M.Anderson (1973). Ionic migration and weathering in frozen Antarctic soils. *Soil Science* 115(6), pp. 461-470.

Vaikmäe, R. (1991). Oxygen-18 in permafrost ice. Proceedings of the International Symposium on the Use of Isotope Techniques in Water Resources Development, Vienna, March 11-15. International Atomic Energy Agency, paper IAEA-SM-319/34, 29 pp.

van Everdingen, R.O. (1990). Ground water hydrology. *In*: Prowse T.D. and C.S.L. Ommanney (ed.). Northern Hydrology: Canadian Perspectives. NHRI Science Report No.1, National Hydrology Research Institute, Environment Canada, Saskatoon, Saskatchewan, pp. 77-101.

Washburn, A.L. (1979/1980). Permafrost features as evidence of climatic change. *Earth-Science Reviews* 15, pp. 327-402.

Williams, P.J. and M.Smith (1989). *The Frozen Earth: Fundamentals of Geocryology.* Cambridge University Press, Cambridge, Great Britain, 306pp.

Woo, M.K., Heron, R. and P.Marsh (1982). Basal ice in high arctic snowpacks. *Arctic and Alpine Research* 14(3), pp. 251-260.

Woo, M.K. (1976). Hydrology of a Small Canadian High Arctic Basin during the Snowmelt Period. *Catena* 3, pp. 155-168.

Woo, M.K. and P.Steer (1983). Slope hydrology as influenced by thawing of the active layer, Resolute, N.W.T. *Canadian Journal of Earth Science* 20, pp. 978-986.

Woo, M.K. and P.Steer (1982). Occurrence of flow on arctic slopes, southwestern Cornwallis Island. *Canadian Journal of Earth Science* 19, pp. 2368-2377.

Woo, M.K. and P.Steer (1986). Runoff regime of slopes in continuous permafrost areas. *Canadian Water Resources Journal* 11(1), pp. 58-68.

Woo, M.K. (1990). Permafrost hydrology. *In*: T.D. Prowse and C.S.L. Ommanney (ed.). Northern Hydrology: Canadian Perspectives. NHRI Science Report No.1, National Hydrology Research Institute, Environment Canada, Saskatoon, Saskatchewan, pp. 63-76.

Woo, M.K. and P.Marsh (1990). Response of soil moisture change to hydrological processes in a contiuous permafrost environment. *Nordic Hydrology* 21, pp. 235-252.

Woo, M.K., Marsh, P. and P.Steer (1983). Basin water balance in a continuous permafrost environment. *Proceedings Fourth International Conference on Permafrost*, Fairbanks, Alaska, pp. 1407-1411.

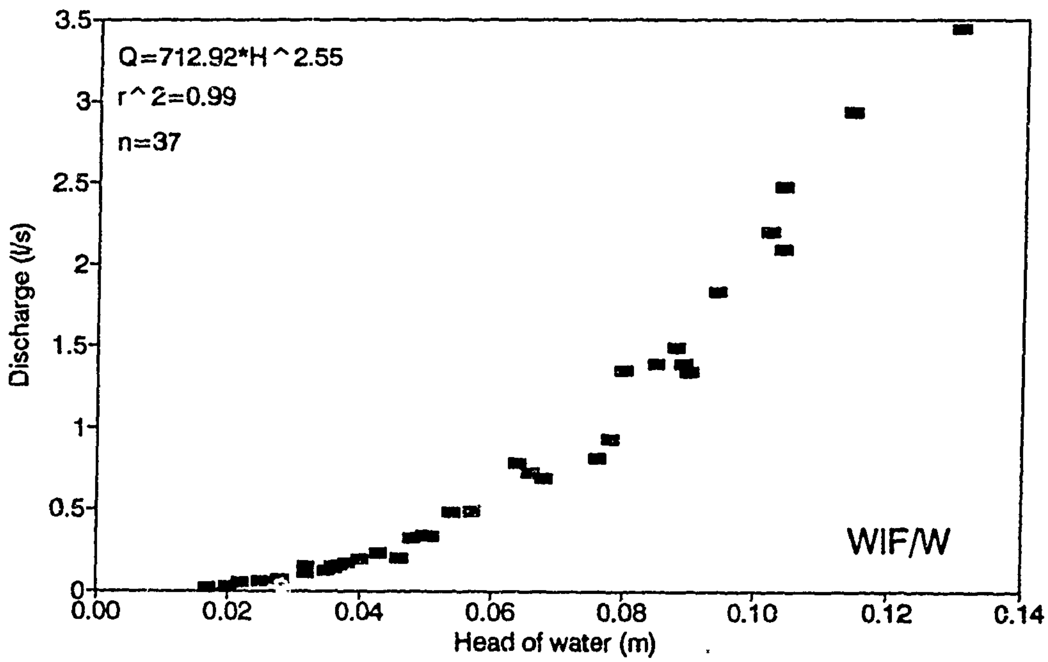
Q=712.92*H^2.55
r^2=0.99
n=37
WIF/W
Discharge (l/s)
Head of water (m)
0 0.5 1 1.5 2 2.5 3 3.5
0.00 0.02 0.04 0.06 0.08 0.10 0.12 0.14

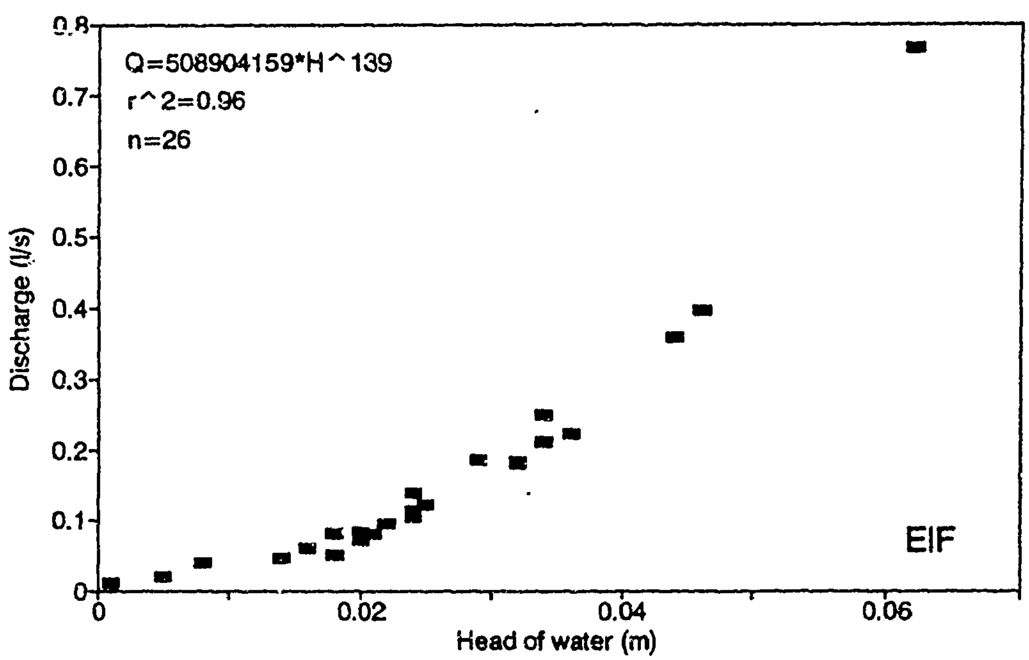
Q=508904159*H^139
r^2=0.96
n=26
EIF
Discharge (l/s)
Head of water (m)
0 0.1 0.2 0.3 0.4 0.5 0.6 0.7 0.8
0 0.02 0.04 0.06

APPENDIX B- CORRELATION MATRIXES

Q (l/s)
TDS (mg/l)
Ions (mg/l)
ACID=ACIDITY=10^{-pH}
EIF- SNOWMELT

Correlations:	TDS	Q	NA	K	CA	MG
TDS	1.0000	.0819	.0199	.8238**	.9049**	.8469**
Q	.0819	1.0000	-.1733	.1315	-.1708	.1099
NA	.0199	-.1733	1.0000	-.0604	.1517	-.0735
K	.8238**	.1315	-.0604	1.0000	.5648	.9946**
CA	.9049**	-.1708	.1517	.5648	1.0000	.5994
MG	.8469**	.1099	-.0735	.9946**	.5994	1.0000
CL	.8812**	.1174	-.0196	.9916**	.6548	.9927**
SO4	.9779**	-.0222	.0596	.7300*	.9671**	.7580*
ACID	.1526	.1927	-.0421	-.3759	.3613	-.3290

Correlations:	CL	SO4	ACID
TDS	.8812**	.9779**	.1526
Q	.1174	-.0222	.1927
NA	-.0196	.0596	-.0421
K	.9916**	.7300*	-.3759
CA	.6548	.9671**	.3613
MG	.9927**	.7580*	-.3290
CL	1.0000	.8006*	-.2885
SO4	.8006*	1.0000	.2436
ACID	-.2885	.2436	1.0000

N of cases: 11 1-tailed Signif: * - .01 ** - .001

Correlations:	ACID	Q	TDS
ACID	1.0000	.3853	.2357
Q	.3853	1.0000	.1901
TDS	.2357	.1901	1.0000

N of cases: 20 1-tailed Signif: * - .01 ** - .001

EIF- PERIOD OF ACTIVE LAYER DEVELOPMENT, SUBPERIOD 1

Correlations:	TDS	Q	NA	K	CA	MG
TDS	1.0000	.6830	.4861	.8174	.9246*	-.5477
Q	.6830	1.0000	.7283	.7589	.5333	.0109
NA	.4861	.7283	1.0000	.5664	.2583	.1144
K	.8174	.7589	.5664	1.0000	.8324	-.0705
CA	.9246*	.5333	.2583	.8324	1.0000	-.5813
MG	-.5477	.0109	.1144	-.0705	-.5813	1.0000
CL	.3347	.4489	-.1212	.5447	.5492	-.0316
SO4	.8173	.3220	-.0851	.6314	.9226*	-.6441
ACID	.5510	.2980	.7029	.5601	.5192	-.3027

Correlations:	CL	SO4	ACID
TDS	.3347	.8173	.5510
Q	.4489	.3220	.2980
NA	-.1212	-.0851	.7029
K	.5447	.6314	.5601
CA	.5492	.9226*	.5192
MG	-.0316	-.6441	-.3027
CL	1.0000	.5666	-.1446
SO4	.5666	1.0000	.2096
ACID	-.1446	.2096	1.0000

N of cases: 7 1-tailed Signif: * - .01 ** - .001

Correlations:	ACID	Q	TDS
ACID	1.0000	-.1620	.1244
Q	-.1620	1.0000	.3684
TDS	.1244	.3684	1.0000

N of cases: 28 1-tailed Signif: * - .01 ** - .001

EIF- PERIOD OF ACTIVE LAYER DEVELOPMENT, SUBPERIOD 2

Correlations:	TDS	Q	NA	K	CA	MG
TDS	1.0000	-.4528	.0507	.6100	.9319*	.9219*
Q	-.4528	1.0000	.0808	.1462	-.3100	-.2771
NA	.0507	.0808	1.0000	.0798	.2692	-.0680
K	.6100	.1462	.0798	1.0000	.7574	.7481
CA	.9319*	-.3100	.2692	.7574	1.0000	.9345*
MG	.9219*	-.2771	-.0680	.7481	.9345*	1.0000
CL	.2206	-.3610	-.1434	.4627	.2222	.1815
SO4	.8458*	-.4675	-.3786	.5030	.7420	.8989*
ACID	.7942	-.1579	.2612	.7196	.9111*	.8759*

Correlations:	CL	SO4	ACID
TDS	.2206	.8458*	.7942
Q	-.3610	-.4675	-.1579
NA	-.1434	-.3786	.2612
K	.4627	.5030	.7196
CA	.2222	.7420	.9111*
MG	.1815	.8989*	.8759*
CL	1.0000	.1201	-.0378
SO4	.1201	1.0000	.7338
ACID	-.0378	.7338	1.0000

N of cases: 7 1-tailed Signif: * - .01 ** - .001

Correlations:	ACID	Q	TDS
ACID	1.0000	-.3459	.7659**
Q	-.3459	1.0000	-.5541*
TDS	.7659**	-.5541*	1.0000

N of cases: 23 1-tailed Signif: * - .01 ** - .001

EIF- PERIOD OF ACTIVE DEVELOPMENT, SUBPERIOD 3

Correlations:	TDS	Q	NA	K	CA	MG
TDS	1.0000	-.0333	-.4008	.0174	.9186	.8895
Q	-.0333	1.0000	.2452	.4642	.0629	.2992
NA	-.4008	.2452	1.0000	.8582	-.0113	-.0936
K	.0174	.4642	.8582	1.0000	.3979	.4032
CA	.9186	.0629	-.0113	.3979	1.0000	.9431*
MG	.8895	.2992	-.0936	.4032	.9431*	1.0000
CL	-.3815	.2262	.9993**	.8556	.0080	-.0852
SO4	.9785*	.0590	-.2114	.2230	.9783*	.9482*
ACID	.6845	-.4260	-.2703	-.2196	.5932	.3576

Correlations:	CL	SO4	ACID
TDS	-.3815	.9785*	.6845
Q	.2262	.0590	-.4260
NA	.9993**	-.2114	-.2703
K	.8556	.2230	-.2196
CA	.0080	.9783*	.5932
MG	-.0852	.9482*	.3576
CL	1.0000	-.1928	-.2346
SO4	-.1928	1.0000	.6280
ACID	-.2346	.6280	1.0000

N of cases: 5 1-tailed Signif: * - .01 ** - .001

Correlations:	ACID	Q	TDS
ACID	1.0000	-.1842	.4716
Q	-.1842	1.0000	-.0266
TDS	.4716	-.0266	1.0000

N of cases: 18 1-tailed Signif: * - .01 ** - .001

EIF- RAINSTORM

Correlations:	TDS	Q	NA	K	CA	MG
TDS	1.0000	-.4040	-.0944	.1330	.9773**	.9036**
Q	-.4040	1.0000	.2437	-.8653**	-.4733	-.3448
NA	-.0944	.2437	1.0000	-.0609	-.1016	-.1908
K	.1330	-.8653**	-.0609	1.0000	.2739	.1391
CA	.9773**	-.4733	-.1016	.2739	1.0000	.8953**
MG	.9036**	-.3448	-.1908	.1391	.8953**	1.0000
FE	.2800	-.1107	-.0940	-.2114	.1159	.0630
AL	.7932*	-.1414	.0295	.0281	.8360*	.8473**
CL	.0147	.1829	.8353*	.0023	.0313	.0006
SO4	.9886**	-.3794	-.1217	.1005	.9532**	.9273**
ACID	.8011*	.0099	-.0516	-.3375	.7339*	.6758

Correlations:	FE	AL	CL	SO4	ACID
TDS	.2800	.7932*	.0147	.9886**	.8011*
Q	-.1107	-.1414	.1829	-.3794	.0099
NA	-.0940	.0295	.8353*	-.1217	-.0516
K	-.2114	.0281	.0023	.1005	-.3375
CA	.1159	.8360*	.0313	.9532**	.7339*
MG	.0630	.8473**	.0006	.9273**	.6758
FE	1.0000	-.3000	-.1518	.3257	.2193
AL	-.3000	1.0000	.2075	.7734*	.7593*
CL	-.1518	.2075	1.0000	.0429	.0478
SO4	.3257	.7734*	.0429	1.0000	.7856*
ACID	.2193	.7593*	.0478	.7856*	1.0000

N of cases: 10 1-tailed Signif: * - .01 ** - .001

Correlations: ACID Q TDS

ACID	1.0000	.1079	.8216**
Q	.1079	1.0000	-.1812
TDS	.8216**	-.1812	1.0000

N of cases: 17 1-tailed Signif: * - .01 ** - .001

EIF- PERIOD OF ACTIVE LAYER DEVELOPMENT, SUBPERIODS 1, 2 AND 3

Correlations:	TDS	Q	NA	K	CA	MG
TDS	1.0000	-.0346	-.1847	.5534*	.9425**	.2515
Q	-.0346	1.0000	.4237	.2461	.0583	-.1340
NA	-.1847	.4237	1.0000	.5307*	.0713	-.0435
K	.5534*	.2461	.5307*	1.0000	.7413**	.2848
CA	.9425**	.0583	.0713	.7413**	1.0000	.1888
MG	.2515	-.1340	-.0435	.2848	.1888	1.0000
CL	-.1708	.4251	.9888**	.5271	.0808	-.0520
SO4	.9440**	-.0648	-.1269	.5902*	.9071**	.2348
ACID	.3651	-.1912	-.1130	-.0058	.3840	-.0659

Correlations:	CL	SO4	ACID
TDS	-.1708	.9440**	.3651
Q	.4251	-.0648	-.1912
NA	.9888**	-.1269	-.1130
K	.5271	.5902*	-.0058
CA	.0808	.9071**	.3840
MG	-.0520	.2348	-.0659
CL	1.0000	-.0930	-.1362
SO4	-.0930	1.0000	.3430
ACID	-.1362	.3430	1.0000

N of cases: 19 1-tailed Signif: * - .01 ** - .001

APPENDIX B- CORRELATION MATRIXES

Correlations:	ACID	Q	TDS
ACID	1.0000	-.2298	.3218*
Q	-.2298	1.0000	-.1440
TDS	.3218*	-.1440	1.0000

N of cases: 69 1-tailed Signif: * - .01 ** - .001

WIF- SNOWMELT

Correlations:	TDS	Q	NA	K	CA	MG
TDS	1.0000	-.7216*	.0681	.8055*	.9948**	.9977**
Q	-.7216*	1.0000	-.2966	-.6342	-.7545*	-.7072
NA	.0681	-.2966	1.0000	-.0299	.0912	.0646
K	.8055*	-.6342	-.0299	1.0000	.8045*	.7905*
CA	.9948**	-.7545*	.0912	.8045*	1.0000	.9965**
MG	.9977**	-.7072	.0646	.7905*	.9965**	1.0000
CL	.8138*	-.5956	.1616	.5046	.8505**	.8413*
SO4	.9970**	-.7368*	.0617	.8016*	.9976**	.9967**
ACID	.2556	.4304	-.0941	.0536	.2008	.2646

Correlations:	CL	SO4	ACID
TDS	.8138*	.9970**	.2556
Q	-.5956	-.7368*	.4304
NA	.1616	.0617	-.0941
K	.5046	.8016*	.0536
CA	.8505**	.9976**	.2008
MG	.8413*	.9967**	.2646
CL	1.0000	.8367*	.1671
SO4	.8367*	1.0000	.2286
ACID	.1671	.2286	1.0000

N of cases: 10 1-tailed Signif: * - .01 ** - .001

APPENDIX B- CORRELATION MATRIXES

Correlations:	ACID	Q	TDS
ACID	1.0000	.2463	.0399
Q	.2463	1.0000	-.5267*
TDS	.0399	-.5267*	1.0000

N of cases: 20 1-tailed Signif: * - .01 ** - .001

WIF- PERIOD OF ACTIVE LAYER DEVELOPMENT, SUBPERIOD 1

Correlations:	TDS	Q	NA	K	CA	MG
TDS	1.0000	-.8006**	.2365	.9579**	.9796**	.2932
Q	-.8006**	1.0000	-.1478	-.7457*	-.8176**	-.1885
NA	.2365	-.1478	1.0000	.3870	.1710	-.1364
K	.9579**	-.7457*	.3870	1.0000	.9523**	.1993
CA	.9796**	-.8176**	.1710	.9523**	1.0000	.3209
MG	.2932	-.1885	-.1364	.1993	.3209	1.0000
CL	.6063	-.5033	.5893	.6970*	.5909	.2002
SO4	.9973**	-.8037**	.2530	.9621**	.9851**	.2844
ACID	-.2035	.4069	-.1236	-.2680	-.3164	-.2777

Correlations:	CL	SO4	ACID
TDS	.6063	.9973**	-.2035
Q	-.5033	-.8037**	.4069
NA	.5893	.2530	-.1236
K	.6970*	.9621**	-.2680
CA	.5909	.9851**	-.3164
MG	.2002	.2844	-.2777
CL	1.0000	.6219	-.2606
SO4	.6219	1.0000	-.2168
ACID	-.2606	-.2168	1.0000

APPENDIX B- CORRELATION MATRIXES

N of cases: 13 1-tailed Signif: * - .01 ** - .001

Correlations:	ACID	Q	TDS
ACID	1.0000	.0388	.0144
Q	.0388	1.0000	-.5297**
TDS	.0144	-.5297**	1.0000

N of cases: 37 1-tailed Signif: * - .01 ** - .001

WIF/W- PERIOD OF ACTIVE LAYER DEVELOPMENT, SUBPERIOD 2

Correlations:	TDS	Q	NA	K	CA	MG
TDS	1.0000	.7701	-.1881	.8741	.9853**	.9577*
Q	.7701	1.0000	-.2659	.6146	.7883	.8745
NA	-.1881	-.2659	1.0000	.0335	-.2763	-.3415
K	.8741	.6146	.0335	1.0000	.8983*	.8402
CA	.9853**	.7883	-.2763	.8983*	1.0000	.9729**
MG	.9577*	.8745	-.3415	.8402	.9729**	1.0000
CL	.4196	.0241	-.3545	.4661	.4936	.3178
SO4	.9585*	.8878*	-.3130	.8561	.9817**	.9903**
ACID	-.3095	-.5893	.0317	.0887	-.2222	-.3120

Correlations:	CL	SO4	ACID
TDS	.4196	.9585*	-.3095
Q	.0241	.8878*	-.5893
NA	-.3545	-.3130	.0317
K	.4661	.8561	.0887
CA	.4936	.9817**	-.2222
MG	.3178	.9903**	-.3120
CL	1.0000	.3839	.3673
SO4	.3839	1.0000	-.3162

ACID	.3673	-.3162	1.0000

N of cases: 6   1-tailed Signif: * - .01 ** - .001

Correlations:	ACID	Q	TDS
ACID	1.0000	-.2098	-.1289
Q	-.2098	1.0000	.0380
TDS	-.1289	.0380	1.0000

N of cases: 25   1-tailed Signif: * - .01 ** - .001

WIF/W- PERIOD OF ACTIVE LAYER DEVELOPMENT, SUBPERIOD 3

Correlations:	TDS	Q	NA	K	CA	MG
TDS	1.0000	-.9283*	-.4748	.4909	.9211*	.9913**
Q	-.9283*	1.0000	.4274	-.4021	-.8556*	-.9146*
NA	-.4748	.4274	1.0000	.5045	-.1003	-.3714
K	.4909	-.4021	.5045	1.0000	.7834	.5839
CA	.9211*	-.8556*	-.1003	.7834	1.0000	.9557**
MG	.9913**	-.9146*	-.3714	.5839	.9557**	1.0000
CL	-.4501	.4109	.9989**	.5258	-.0750	-.3453
SO4	.9780**	-.9171*	-.2908	.6417	.9779**	.9940**
ACID	-.1228	.4171	-.3272	-.2259	-.2451	-.1588

Correlations:	CL	SO4	ACID
TDS	-.4501	.9780**	-.1228
Q	.4109	-.9171*	.4171
NA	.9989**	-.2908	-.3272
K	.5258	.6417	-.2259
CA	-.0750	.9779**	-.2451
MG	-.3453	.9940**	-.1588

CL	1.0000	-.2658	-.3337
SO4	-.2658	1.0000	-.2159
ACID	-.3337	-.2159	1.0000

N of cases: 7 1-tailed Signif: * - .01 ** - .001

Correlations:	ACID	Q	TDS
ACID	1.0000	.2966	-.2908
Q	.2966	1.0000	-.9433**
TDS	-.2908	-.9433**	1.0000

N of cases: 16 1-tailed Signif: * - .01 ** - .001

WIF/W- RAINSTORM

Correlations:	TDS	Q	NA	K	CA	MG
TDS	1.0000	-.6243	-.0531	.9879**	.9935**	.9887**
Q	-.6243	1.0000	.2938	-.6646	-.6493	-.6175
NA	-.0531	.2938	1.0000	-.1909	-.0982	-.1155
K	.9879**	-.6646	-.1909	1.0000	.9904**	.9875**
CA	.9935**	-.6493	-.0982	.9904**	1.0000	.9864**
MG	.9887**	-.6175	-.1155	.9875**	.9864**	1.0000
CL	-.5630	.1996	.5232	-.6050	-.6003	-.5499
SO4	.9963**	-.6359	-.0545	.9837**	.9921**	.9945**
ACID	-.3208	.2739	.6760	-.4139	-.4094	-.3895

Correlations:	CL	SO4	ACID
TDS	-.5630	.9963**	-.3208
Q	.1996	-.6359	.2739
NA	.5232	-.0545	.6760
K	-.6050	.9837**	-.4139

CA	-.6003	.9921**	-.4094
MG	-.5499	.9945**	-.3895
CL	1.0000	-.5427	.7115
SO4	-.5427	1.0000	-.3442
ACID	.7115	-.3442	1.0000

N of cases: 9 1-tailed Signif: * - .01 ** - .001

Correlations:	ACID	Q	TDS
ACID	1.0000	.0542	-.2388
Q	.0542	1.0000	-.7506**
TDS	-.2388	-.7506**	1.0000

N of cases: 18 1-tailed Signif: * - .01 ** - .001

WIF- PERIOD OF ACTIVE LAYER DEVELOPMENT, SUBPERIODS 1, 2 AND 3

Correlations:	TDS	Q	NA	K	CA	MG
TDS	1.0000	.1913	.1204	.9181**	.9860**	.8646**
Q	.1913	1.0000	.2522	.2704	.2082	.1470
NA	.1204	.2522	1.0000	.4376	.2628	.1137
K	.9181**	.2704	.4376	1.0000	.9526**	.7690**
CA	.9860**	.2082	.2628	.9526**	1.0000	.8650**
MG	.8646**	.1470	.1137	.7690**	.8650**	1.0000
CL	.1417	.2255	.9791**	.4410	.2915	.1581
SO4	.9942**	.2130	.1948	.9275**	.9946**	.8677**
ACID	-.3221	-.1168	-.1919	-.3632	-.3596	-.3736

Correlations:	CL	SO4	ACID
TDS	.1417	.9942**	-.3221

Q	.2255	.2130	-.1168
NA	.9791**	.1948	-.1919
K	.4410	.9275**	-.3632
CA	.2915	.9946**	-.3596
MG	.1581	.8677**	-.3736
CL	1.0000	.2200	-.1915
SO4	.2200	1.0000	-.3301
ACID	-.1915	-.3301	1.0000

N of cases: 26 1-tailed Signif: * - .01 ** - .001

Correlations:	ACID	Q	TDS
ACID	1.0000	-.0762	-.3068*
Q	-.0762	1.0000	.0562
TDS	-.3068*	.0562	1.0000

N of cases: 78 1-tailed Signif: * - .01 ** - .001

WIF/2- SNOWMELT

Correlations:	TDS	Q	NA	K	CA	MG
TDS	1.0000	-.1748	.7876*	.1135	.9586**	.9261**
Q	-.1748	1.0000	-.1143	.0093	-.3176	-.2778
NA	.7876*	-.1143	1.0000	-.3538	.6749	.7001
K	.1135	.0093	-.3538	1.0000	.0970	.3177
CA	.9586**	-.3176	.6749	.0970	1.0000	.8695*
MG	.9261**	-.2778	.7001	.3177	.8695*	1.0000
CL	-.5860	.1686	-.6448	-.1209	-.4413	-.5812
SO4	.9216**	-.2602	.7075	.1649	.8747*	.9547**
ACID	.3386	-.3660	.2228	-.3882	.5042	.2092

Correlations: CL SO4 ACID

TDS	-.5860	.9216**	.3386
Q	.1686	-.2602	-.3660
NA	-.6448	.7075	.2228
K	-.1209	.1649	-.3882
CA	-.4413	.8747*	.5042
MG	-.5812	.9547**	.2092
CL	1.0000	-.4562	-.0561
SO4	-.4562	1.0000	.2549
ACID	-.0561	.2549	1.0000

N of cases: 9 1-tailed Signif: * - .01 ** - .001

Correlations:	ACID	Q	TDS
ACID	1.0000	-.5201	.2703
Q	-.5201	1.0000	-.2262
TDS	.2703	-.2262	1.0000

N of cases: 15 1-tailed Signif: * - .01 ** - .001

WIF/2- PERIOD OF ACTIVE LAYER DEVELOPMENT, SUBPERIODS 1, 2 AND 3

Correlations:	TDS	Q	NA	K	CA	MG
TDS	1.0000	.4304	.9287**	.9819**	.9986**	.9986**
Q	.4304	1.0000	.6203	.3804	.4071	.4217
NA	.9287**	.6203	1.0000	.9260**	.9324**	.9181**
K	.9819**	.3804	.9260**	1.0000	.9819**	.9799**
CA	.9986**	.4071	.9324**	.9819**	1.0000	.9957**
MG	.9986**	.4217	.9181**	.9799**	.9957**	1.0000
CL	.1045	-.4895	.0348	.1022	.1326	.1251
SO4	.9996**	.4204	.9250**	.9819**	.9981**	.9995**
ACID	-.2388	-.4407	-.3472	-.2468	-.2329	-.2388

APPENDIX B- CORRELATION MATRIXES

Correlations:	CL	SO4	ACID
TDS	.1045	.9996**	-.2388
Q	-.4895	.4204	-.4407
NA	.0348	.9250**	-.3472
K	.1022	.9819**	-.2468
CA	.1326	.9981**	-.2329
MG	.1251	.9995**	-.2388
CL	1.0000	.1245	.3489
SO4	.1245	1.0000	-.2361
ACID	.3489	-.2361	1.0000

N of cases: 8 1-tailed Signif: * - .01 ** - .001

Correlations:	ACID	Q	TDS
ACID	1.0000	-.2824	-.1882
Q	-.2824	1.0000	.1909
TDS	-.1882	.1909	1.0000

N of cases: 20 1-tailed Signif: * - .01 ** - .001

WIF/2- RAINSTORM

Correlations:	TDS	Q	NA	K	CA	MG
TDS	1.0000	-.7835	.6295	.7085	.9524**	.1910
Q	-.7835	1.0000	-.3135	-.4598	-.6921	-.2503
NA	.6295	-.3135	1.0000	.8756*	.8337*	.3044
K	.7085	-.4598	.8756*	1.0000	.8569*	-.0505
CA	.9524**	-.6921	.8337*	.8569*	1.0000	.2309
MG	.1910	-.2503	.3044	-.0505	.2309	1.0000
CL	-.6247	.4949	-.2996	-.2265	-.5357	-.4450
SO4	.8234	-.5309	.9568**	.8751*	.9535**	.3316

ACID	.3600	.2159	.5285	.4432	.4491	-.1069

Correlations:	CL	SO4	ACID
TDS	-.6247	.8234	.3600
Q	.4949	-.5309	.2159
NA	-.2996	.9568**	.5285
K	-.2265	.8751*	.4432
CA	-.5357	.9535**	.4491
MG	-.4450	.3316	-.1069
CL	1.0000	-.4647	.1267
SO4	-.4647	1.0000	.4921
ACID	.1267	.4921	1.0000

N of cases: 7 1-tailed Signif: * - .01 ** - .001

Correlations:	ACID	Q	TDS
ACID	1.0000	.1775	.0014
Q	.1775	1.0000	-.7976**
TDS	.0014	-.7976**	1.0000

N of cases: 14 1-tailed Signif: * - .01 ** - .001

APPENDIX C- CHEMICAL DATA SUMMARY

All concentrations (Na^{+}, K^{+}, Ca^{2+}, Mg^{2+}, AL^{3+}, Fe^{2+}, Cl^{-}, SO_4^{2-}) in mg/l
Missing values indicated by -99.0 or empty box
TDS (total dissolved solids) in mg/l
a: charge balance including HCO_3^{-} concentrations

EIF

Day	Time	pH	TDS	Q l/s	Na^{+}	K^{+}	Ca^{2+}	Mg^{2+}	Fe^{2+}	Al^{3+}	Cl^{-}	SO_4^{2-}	%
02-Jun-91	23:00	6.29	316	1.82	2.85	4.92	48.3	20.52	0.38	0.13	4.95	219.8	-3.6
03-Jun-91	09:18	6.45	128	4.05	1.22	1.95	19.5	7.48	-99.00	-99.00	1.34	74.3	3.2
04-Jun-91	13:00	6.46	135	0.57	-99.00	-99.00	-99.0	-99.00	-99.00	-99.00	-99.00	-99.0	-99.0
04-Jun-91	22:49	6.12	168	2.00	2.64	1.95	30.2	6.92	-99.00	-99.00	1.56	109.2	-1.7
05-Jun-91	11:58	6.67	149	0.10	1.49	1.86	28.8	7.08	-99.00	-99.00	1.39	101.9	-0.6
05-Jun-91	17:58	4.82	194	2.12	1.94	1.93	36.9	7.07	-99.00	-99.00	1.52	146.1	-9.0
05-Jun-91	23:49	4.97	172	1.66	-99.00	-99.00	-99.0	-99.00	-99.00	-99.00	-99.00	-99.0	-99.0
06-Jun-91	10:40	6.42	150	0.39	1.51	1.80	27.5	6.96	-99.00	-99.00	1.16	100.7	-1.8
06-Jun-91	17:00	4.67	193	1.18	-99.00	-99.00	-99.0	-99.00	-99.00	-99.00	-99.00	-99.0	-99.0
06-Jun-91	22:53	4.59	193	4.04	-99.00	-99.00	-99.0	-99.00	-99.00	-99.00	-99.00	-99.0	-99.0
07-Jun-91	10:14	6.65	159	0.79	2.34	1.61	32.8	6.11	-99.00	-99.00	1.23	121.7	-5.9
07-Jun-91	16:43	4.67	204	2.54	1.93	1.51	35.5	5.92	-99.00	-99.00	1.22	141.1	10.7
08-Jun-91	13:49	5.36	160	0.97	9.25	1.50	32.5	5.51	-99.00	-99.00	1.14	114.4	2.1
08-Jun-91	22:29	4.6	189	1.90	2.95	1.36	37.9	5.46	0.21	2.29	1.11	139.5	-2.4
09-Jun-91	12:31	5.09	164	0.62	-99.00	-99.00	-99.0	-99.00	-99.00	-99.00	-99.00	-99.0	-99.0
09-Jun-91	17:12	4.83	177	0.67	1.84	1.33	35.8	5.97	-99.00	-99.00	1.03	129.4	-6.2

10-Jun-91	07:29	4.86	168	0.37	-99.00	-99.00	-99.0	-99.00	-99.00	-99.00	-99.00	-99.0	-99.0
10-Jun-91	13:59	5.48	165	-99.00	-99.00	-99.00	-99.0	-99.00	-99.00	-99.00	-99.00	-99.0	-99.0
11-Jun-91	15:14	5.4	165	0.06	-99.00	-99.00	-99.0	-99.00	-99.00	-99.00	-99.00	-99.0	-99.0
11-Jun-91	12:30	5.13	176	0.04	-99.00	-99.00	-99.0	-99.00	-99.00	-99.00	-99.00	-99.0	-99.0
11-Jun-91	17:13	5.59	172	0.03	-99.00	-99.00	-99.0	-99.00	-99.00	-99.00	-99.00	-99.0	-99.0
12-Jun-91	17:00	5.61	170	0.01	1.66	1.25	32.4	6.59	-99.00	-99.00	0.97	116.1	-3.8
12-Jun-91	22:17	4.8	169	-99.00	-99.00	-99.00	-99.0	-99.00	-99.00	-99.00	-99.00	-99.0	-99.0
13-Jun-91	12:59	5.32	169	0.01	-99.00	-99.00	-99.0	-99.00	-99.00	-99.00	-99.00	-99.0	-99.0
13-Jun-91	17:29	5.51	168	0.01	-99.00	-99.00	-99.0	-99.00	-99.00	-99.00	-99.00	-99.0	-99.0
13-Jun-91	23:29	5.68	172	0.01	-99.00	-99.00	-99.0	-99.00	-99.00	-99.00	-99.00	-99.0	-99.0
14-Jun-91	22:29	5.4	166	0.01	-99.00	-99.00	-99.0	-99.00	-99.00	-99.00	-99.00	-99.0	-99.0
15-Jun-91	15:28	5.7	168	0.01	-99.00	-99.00	-99.0	-99.00	-99.00	-99.00	-99.00	-99.0	-99.0
16-Jun-91	13:14	6.03	167	0.01	1.60	1.15	30.0	6.92	-99.00	-99.00	0.87	112.0	-4.2
20-Jun-91	21:44	5.68	162	0.01	1.84	1.17	30.3	6.54	-99.00	-99.00	1.29	108.9	-3.1
21-Jun-91	12:28	5.82	162	-99.00	-99.00	-99.00	-99.0	-99.00	-99.00	-99.00	-99.00	-99.0	-99.0
21-Jun-91	16:59	6.02	164	0.02	-99.00	-99.00	-99.0	-99.00	-99.00	-99.00	-99.00	-99.0	-99.0
22-Jun-91	00:14	5.66	180	-99.00	-99.00	-99.00	-99.0	-99.00	-99.00	-99.00	-99.00	-99.0	-99.0
22-Jun-91	12:00	6	174	0.02	-99.00	-99.00	-99.0	-99.00	-99.00	-99.00	-99.00	-99.0	-99.0
23-Jun-91	14:00	5.88	176	-99.00	-99.00	-99.00	-99.0	-99.00	-99.00	-99.00	-99.00	-99.0	-99.0
25-Jun-91	14:00	5.9	176	-99.00	-99.00	-99.00	-99.0	-99.00	-99.00	-99.00	-99.00	-99.0	-99.0
26-Jun-91	16:53	5.45	173	0.02	9.03	1.24	31.2	5.66	0.23	0.00	0.64	108.3	3.9
27-Jun-91	03:59	5.77	168	0.01	-99.00	-99.00	-99.0	-99.00	-99.00	-99.00	-99.00	-99.0	-99.0
27-Jun-91	15:30	5.84	162	-99.00	-99.00	-99.00	-99.0	-99.00	-99.00	-99.00	-99.00	-99.0	-99.0

28-Jun-91	13:00	5.64	157	0.00	1.37	1.05	27.1	5.34	-99.00	-99.00	0.05	101.4	-5.8
29-Jun-91	15:00	5.58	152	0.01	-99.00	-99.00	-99.0	-99.00	-99.00	-99.00	-99.00	-99.0	-99.0
30-Jun-91	17:58	5.88	149	0.01	-99.00	-99.00	-99.0	-99.00	-99.00	-99.00	-99.00	-99.0	-99.0
04-Jul-91	02:19	5.73	157	0.01	4.92	1.17	27.1	28.35	-99.00	-99.00	0.67	98.8	30.8
04-Jul-91	04:00	5.63	157	0.01	-99.00	-99.00	-99.0	-99.00	-99.00	-99.00	-99.00	-99.0	-99.0
04-Jul-91	06:00	5.2	158	0.01	-99.00	-99.00	-99.0	-99.00	-99.00	-99.00	-99.00	-99.0	-99.0
04-Jul-91	10:00	5.7	156	0.01	-99.00	-99.00	-99.0	-99.00	-99.00	-99.00	-99.00	-99.0	-99.0
04-Jul-91	12:00	5.73	152	0.01	-99.00	-99.00	-99.0	-99.00	-99.00	-99.00	-99.00	-99.0	-99.0
04-Jul-91	14:00	5.65	152	0.01	-99.00	-99.00	-99.0	-99.00	-99.00	-99.00	-99.00	-99.0	-99.0
04-Jul-91	16:00	5.71	155	0.01	-99.00	-99.00	-99.0	-99.00	-99.00	-99.00	-99.00	-99.0	-99.0
04-Jul-91	19:59	5.18	160	0.01	-99.00	-99.00	-99.0	-99.00	-99.00	-99.00	-99.00	-99.0	-99.0
04-Jul-91	21:00	5.44	161	0.01	-99.00	-99.00	-99.0	-99.00	-99.00	-99.00	-99.00	-99.0	-99.0
04-Jul-91	23:00	5.33	172	0.01	6.55	1.25	32.2	5.38	-99.00	-99.00	0.72	112.1	0.3
05-Jul-91	02:00	5.44	171	0.01	-99.00	-99.00	-99.0	-99.00	-99.00	-99.00	-99.00	-99.0	-99.0
05-Jul-91	12:00	5.49	164	0.01	-99.00	-99.00	-99.0	-99.00	-99.00	-99.00	-99.00	-99.0	-99.0
05-Jul-91	17:29	5.44	162	0.01	-99.00	-99.00	-99.0	-99.00	-99.00	-99.00	-99.00	-99.0	-99.0
06-Jul-91	01:00	5.47	162	0.02	-99.00	-99.00	-99.0	-99.00	-99.00	-99.00	-99.00	-99.0	-99.0
06-Jul-91	03:30	5.07	158	0.02	-99.00	-99.00	-99.0	-99.00	-99.00	-99.00	-99.00	-99.0	-99.0
06-Jul-91	23:00	4.92	157	0.01	-99.00	-99.00	-99.0	-99.00	-99.00	-99.00	-99.00	-99.0	-99.0
07-Jul-91	14:00	4.68	168	0.10	4.84	1.08	32.1	4.77	-99.00	-99.00	0.34	109.7	-0.9
08-Jul-91	15:28	5.18	158	0.05	-99.00	-99.00	-99.0	-99.00	-99.00	-99.00	-99.00	-99.0	-99.0
09-Jul-91	15:28	4.8	162	0.07	-99.00	-99.00	-99.0	-99.00	-99.00	-99.00	-99.00	-99.0	-99.0
10-Jul-91	16:23	5.45	144	0.10	3.48	0.97	25.3	4.24	-99.00	-99.00	0.45	86.4	-0.6

11-Jul-91	14:00	5.53	134	-99.00	-99.00	-99.00	-99.0	-99.00	-99.00	-99.00	-99.00	-99.0	-99.0
12-Jul-91	14:05	5.81	116	0.08	4.09	0.99	21.7	3.70	-99.00	-99.00	0.65	68.7	4.6
12-Jul-91	16:59	5.63	121	0.06	-99.00	-99.00	-99.0	-99.00	-99.00	-99.00	-99.00	-99.0	-99.0
12-Jul-91	19:36	5.6	118	0.05	-99.00	-99.00	-99.0	-99.00	-99.00	-99.00	-99.00	-99.0	-99.0
12-Jul-91	20:58	5.64	123	0.07	1.38	0.88	19.5	3.91	-99.00	-99.00	0.31	98.4	-19.7
12-Jul-91	23:29	5.96	115	0.14	-99.00	-99.00	-99.0	-99.00	-99.00	-99.00	-99.00	-99.0	-99.0
13-Jul-91	01:00	5.92	114	0.19	-99.00	-99.00	-99.0	-99.00	-99.00	-99.00	-99.00	-99.0	-99.0
13-Jul-91	03:18	6.09	109	0.25	-99.00	-99.00	-99.0	-99.00	-99.00	-99.00	-99.00	-99.0	-99.0
13-Jul-91	05:15	5.87	107	0.20	4.40	0.94	19.2	3.55	-99.00	-99.00	0.24	59.0	8.5
13-Jul-91	07:40	5.94	105	0.21	-99.00	-99.00	-99.0	-99.00	-99.00	-99.00	-99.00	-99.0	-99.0
13-Jul-91	09:28	5.98	104	0.18	-99.00	-99.00	-99.0	-99.00	-99.00	-99.00	-99.00	-99.0	-99.0
13-Jul-91	11:13	6.02	80	0.16	4.20	0.90	17.5	3.48	-99.00	-99.00	0.25	57.1	6.6
13-Jul-91	13:53	6.05	105	0.12	-99.00	-99.00	-99.0	-99.00	-99.00	-99.00	-99.00	-99.0	-99.0
14-Jul-91	14:58	5.78	78	0.11	-99.00	-99.00	-99.0	-99.00	-99.00	-99.00	-99.00	-99.0	-99.0
15-Jul-91	15:36	6	102	0.09	-99.00	-99.00	-99.0	-99.00	-99.00	-99.00	-99.00	-99.0	-99.0
16-Jul-91	15:18	5.49	123	0.05	5.83	0.83	21.9	3.60	-99.00	-99.00	0.25	67.0	8.5
17-Jul-91	15:00	6.06	116	0.00	-99.00	-99.00	-99.0	-99.00	-99.00	-99.00	-99.00	-99.0	-99.0
18-Jul-91	15:00	5.85	114	0.08	-99.00	-99.00	-99.0	-99.00	-99.00	-99.00	-99.00	-99.0	-99.0
19-Jul-91	16:43	6.08	106	0.18	-99.00	-99.00	-99.0	-99.00	-99.00	-99.00	-99.00	-99.0	-99.0
20-Jul-91	14:44	5.99	98	0.22	3.30	0.92	17.8	3.30	0.09	0.25	0.24	51.1	11.9
21-Jul-91	16:29	6.39	94	0.26	-99.00	-99.00	-99.0	-99.00	-99.00	-99.00	-99.00	-99.0	-99.0
22-Jul-91	15:00	6.18	102	0.39	-99.00	-99.00	-99.0	-99.00	-99.00	-99.00	-99.00	-99.0	-99.0
23-Jul-91	14:29	6.1	103	0.36	-99.00	-99.00	-99.0	-99.00	-99.00	-99.00	-99.00	-99.0	-99.0

24-Jul-91	16:04	6.16	122	0.76	62.70	1.41	28.5	4.90	-99.00	-99.00	78.99	83.7	7.2
25-Jul-91	15:00	6.15	146	0.44	-99.00	-99.00	-99.0	-99.00	-99.00	-99.00	-99.00	-99.0	-99.0
25-Jul-91	21:38	6.35	159	1.27	3.97	1.14	28.3	5.55	-99.00	-99.00	0.31	98.7	0.2
25-Jul-91	23:59	6.18	158	1.05	-99.00	-99.00	-99.0	-99.00	-99.00	-99.00	-99.00	-99.0	-99.0
26-Jul-91	15:28	6.05	156	0.40	-99.00	-99.00	-99.0	-99.00	-99.00	-99.00	-99.00	-99.0	-99.0
27-Jul-91	14:31	5.65	168	0.36	-99.00	-99.00	-99.0	-99.00	-99.00	-99.00	-99.00	-99.0	-99.0
28-Jul-91	17:00	6.47	171	0.38	4.05	1.15	31.3	5.72	0.04	0.27	0.71	106.9	0.5
29-Jul-91	14:47	6.03	174	0.17	-99.00	-99.00	-99.0	-99.00	-99.00	-99.00	-99.00	-99.0	-99.0
30-Jul-91	16:04	6.03	174	0.08	-99.00	-99.00	-99.0	-99.00	-99.00	-99.00	-99.00	-99.0	-99.0
31-Jul-91	15:47	6.03	190	0.08	-99.00	-99.00	-99.0	-99.00	-99.00	-99.00	-99.00	-99.0	-99.0
01-Aug-91	14:47	5.77	195	0.10	-99.00	-99.00	-99.0	-99.00	-99.00	-99.00	-99.00	-99.0	-99.0
01-Aug-91	22:00	5.09	209	0.27	1.78	1.08	36.3	5.88	0.05	0.32	0.74	130.1	-5.5
02-Aug-91	00:00	5.75	197	0.38	-99.00	-99.00	-99.0	-99.00	-99.00	-99.00	-99.00	-99.0	-99.0
02-Aug-91	02:00	5.58	193	0.45	-99.00	-99.00	-99.0	-99.00	-99.00	-99.00	-99.00	-99.0	-99.0
02-Aug-91	04:00	5.65	183	0.92	2.19	1.16	31.9	6.05	0.22	0.00	0.20	114.2	-3.4
02-Aug-91	06:00	5.53	156	1.27	-99.00	-99.00	-99.0	-99.00	-99.00	-99.00	-99.00	-99.0	-99.0
02-Aug-91	08:00	5.26	196	2.13	1.73	1.18	36.0	5.86	0.19	0.42	0.23	124.4	-3.0
02-Aug-91	10:00	5.35	193	4.02	-99.00	-99.00	-99.0	-99.00	-99.00	-99.00	-99.00	-99.0	-99.0
02-Aug-91	12:00	5.76	177	10.00	1.43	1.02	32.5	5.47	0.14	0.00	0.22	109.3	-2.5
02-Aug-91	14:00	5.25	151	-99.00	-99.00	-99.00	-99.0	-99.00	-99.00	-99.00	-99.00	-99.0	-99.0
02-Aug-91	16:00	5.54	135	-99.00	5.04	0.89	24.1	3.65	0.27	0.29	0.24	79.4	3.8
02-Aug-91	22:59	4.72	187	15.00	5.23	0.92	31.9	5.58	0.38	1.44	1.65	118.8	-0.4
03-Aug-91	22:00	4.42	265	10.17	1.79	1.01	44.0	7.08	0.14	3.39	0.24	178.1	-5.9

04-Aug-91	15:00	4.59	244	5.00	-99.00	-99.00	-99.0	-99.00	-99.00	-99.00	-99.00	-99.0	-99.0
05-Aug-91	15:00	4.41	173	15.00	1.22	0.78	28.8	5.69	0.51	1.31	0.23	112.8	-3.6
06-Aug-91	15:00	4.4	289	5.00	1.81	0.95	42.8	6.79	6.31	0.24	0.24	208.2	-15.1
07-Aug-91	17:00	4.2	334	2.02	2.50	1.06	53.9	7.42	0.28	6.36	0.44	222.6	-4.8
08-Aug-91	16:00	4.44	282	11.00	1.76	0.90	44.8	7.97	0.26	5.11	0.24	202.2	-7.8
09-Aug-91	15:11	4.12	296	1.87	-99.00	-99.00	-99.0	-99.00	-99.00	-99.00	-99.00	-99.0	-99.0
10-Aug-91	16:09	4.48	234	-99.00	1.70	1.19	42.9	5.97	0.16	2.81	0.99	160.1	-4.8
12-Aug-91	14:58	4.45	292	1.84	-99.00	-99.00	-99.0	-99.00	-99.00	-99.00	-99.00	-99.0	-99.0
13-Aug-91	14:58	4.42	298	1.12	1.98	1.16	49.3	7.92	0.25	5.29	1.13	220.9	-9.0

WIF/W

Date	Time	pH	TDS	Q l/s	Na^{+}	K^{+}	Ca^{2+}	Mg^{2+}	Fe^{2+}	Al^{3+}	Cl^{-}	SO_4^{2-}	% imbalance
31-May-91	17:44	6.06	149.0	0.001	3.43	2.37	26.3	8.34	-99	-99	7.27	84.2	6.0
01-Jun-91	22:39	5.95	161.0	0.001	1.32	2.35	25.2	8.43	-99	-99	3.28	85.9	4.7
02-Jun-91	16:59	6.06	166.0	0.001	1.56	5.79	27.1	8.79	-99	-99	3.34	87.3	9.0
03-Jun-91	09:59	6.37	64.7	-99.00	-99.00	-99.00	-99.0	-99.00	-99	-99	-99.00	-99.0	-99.0
04-Jun-91	11:45	6.67	59.3	0.34	1.15	2.58	11.1	2.57	-99	-99	1.12	34.2	8.5
04-Jun-91	15:33	6.58	40.9	2.50	-99.00	-99.00	-99.0	-99.00	-99	-99	-99.00	-99.0	-99.0
04-Jun-91	23:13	6.18	48.0	1.20	8.35	0.96	8.7	2.06	-99	-99	0.99	21.2	35.6
05-Jun-91	11:58	6.70	52.6	-99.00	-99.00	-99.00	-99.0	-99.00	-99	-99	-99.00	-99.0	-99.0
05-Jun-91	16:59	6.60	31.9	2.00	1.38	0.69	6.7	1.47	-99	-99	1.35	15.0	20.4
05-Jun-91	22:59	6.64	38.5	1.17	-99.00	-99.00	-99.0	-99.00	-99	-99	-99.00	-99.0	-99.0

06-Jun-91	10:16	6.84	54.1	0.15	1.53	1.12	10.7	2.64	-99	-99	1.28	26.8	17.7
06-Jun-91	16:09	6.08	37.3	3.00	0.59	0.66	5.9	1.34	-99	-99	0.75	13.6	18.8
06-Jun-91	22:29	6.14	27.1	3.50	0.65	0.63	4.9	1.16	-99	-99	0.66	10.9	22.2
07-Jun-91	09:48	5.95	44.9	0.78	-99.00	-99.00	-99.0	-99.00	-99	-99	-99.00	-99.0	-99.0
07-Jun-91	16:29	5.83	22.4	5.00	0.45	0.47	4.3	0.96	-99	-99	0.35	8.9	25.2
08-Jun-91	14:24	6.26	23.1	4.00	-99.00	-99.00	-99.0	-99.00	-99	-99	-99.00	-99.0	-99.0
08-Jun-91	23:44	5.78	22.4	1.80	-99.00	-99.00	-99.0	-99.00	-99	-99	-99.00	-99.0	-99.0
09-Jun-91	12:59	6.03	29.0	1.39	-99.00	-99.00	-99.0	-99.00	-99	-99	-99.00	-99.0	-99.0
09-Jun-91	17:12	5.80	21.8	2.32	-99.00	-99.00	-99.0	-99.00	-99	-99	-99.00	-99.0	-99.0
10-Jun-91	07:29	5.91	48.8	-99.00	-99.00	-99.00	-99.0	-99.00	-99	-99	-99.00	-99.0	-99.0
10-Jun-91	14:58	6.07	24.4	0.69	-99.00	-99.00	-99.0	-99.00	-99	-99	-99.00	-99.0	-99.0
11-Jun-91	12:59	6.16	32.3	0.23	-99.00	-99.00	-99.0	-99.00	-99	-99	-99.00	-99.0	-99.0
11-Jun-91	17:13	6.36	20.5	0.25	-99.00	-99.00	-99.0	-99.00	-99	-99	0.35	9.0	-99.0
12-Jun-91	15:28	5.57	18.5	0.33	0.48	0.44	3.5	0.90	-99	-99	0.34	7.9	23.9
12-Jun-91	23:49	5.97	19.8	0.20	-99.00	-99.00	-99.0	-99.00	-99	-99	-99.00	-99.0	-99.0
13-Jun-91	12:59	5.96	64.7	0.02	-99.00	-99.00	-99.0	-99.00	-99	-99	-99.00	-99.0	-99.0
13-Jun-91	16:43	6.30	29.0	0.14	4.68	0.55	5.3	1.37	-99	-99	0.37	12.3	38.4
13-Jun-91	23:29	6.06	28.4	-99.00	-99.00	-99.00	-99.0	-99.00	-99	-99	-99.00	-99.0	-99.0
14-Jun-91	14:29	6.12	44.2	0.06	-99.00	-99.00	-99.0	-99.00	-99	-99	-99.00	-99.0	-99.0
15-Jun-91	00:28	6.22	29.0	0.07	-99.00	-99.00	-99.0	-99.00	-99	-99	-99.00	-99.0	-99.0
15-Jun-91	15:14	6.33	21.8	0.17	-99.00	-99.00	-99.0	-99.00	-99	-99	-99.00	-99.0	-99.0
16-Jun-91	12:59	6.56	46.2	0.02	0.55	0.60	8.6	2.23	-99	-99	0.33	22.2	15.8
20-Jun-91	23:13	6.03	66.0	0.06	-99.00	-99.00	-99.0	-99.00	-99	-99	-99.00	-99.0	-99.0

21-Jun-91	13:29	6.43	55.4	0.11	0.72	0.78	10.6	2.58	-99	-99	0.65	26.4	16.6
21-Jun-91	16:14	6.46	35.6	0.14	1.08	0.60	6.5	1.65	-99	-99	0.66	16.4	18.6
22-Jun-91	00:14	5.85	37.0	0.17	-99.00	-99.00	-99.0	-99.00	-99	-99	-99.00	-99.0	-99.0
22-Jun-91	12:00	6.40	68.6	0.02	8.44	0.87	11.4	2.99	-99	-99	1.65	33.4	23.7
23-Jun-91	14:00	6.31	38.9	-99.00	-99.00	-99.00	-99.0	-99.00	-99	-99	-99.00	-99.0	-99.0
25-Jun-91	14:58	6.38	43.6	0.16	0.43	0.59	7.9	9.30	-99	-99	0.65	19.7	-0.2
26-Jun-91	16:30	6.17	46.9	0.11	-99.00	-99.00	-99.0	-99.00	-99	-99	-99.00	-99.0	-99.0
27-Jun-91	04:00	6.38	46.2	0.06	-99.00	-99.00	-99.0	-99.00	-99	-99	-99.00	-99.0	-99.0
27-Jun-91	15:30	6.35	35.6	0.29	-99.00	-99.00	-99.0	-99.00	-99	-99	-99.00	-99.0	-99.0
28-Jun-91	13:00	6.00	54.1	0.00	0.51	0.65	9.3	2.52	-99	-99	0.77	25.1	13.3
29-Jun-91	22:00	6.11	81.2	0.00	0.81	0.87	13.4	3.83	-99	-99	0.73	38.2	12.1
04-Jul-91	00:00	5.73	71.3	0.03	3.72	0.81	11.1	3.39	-99	-99	0.67	33.8	16.8
04-Jul-91	02:00	6.17	64.7	0.27	-99.00	-99.00	-99.0	-99.00	-99	-99	-99.00	-99.0	-99.0
04-Jul-91	04:00	5.94	60.1	0.27	-99.00	-99.00	-99.0	-99.00	-99	-99	-99.00	-99.0	-99.0
04-Jul-91	06:00	5.87	61.4	0.02	-99.00	-99.00	-99.0	-99.00	-99	-99	-99.00	-99.0	-99.0
04-Jul-91	08:00	5.99	62.7	0.01	4.02	0.78	9.9	2.99	-99	-99	0.76	28.8	20.1
04-Jul-91	10:00	5.91	60.7	0.03	-99.00	-99.00	-99.0	-99.00	-99	-99	-99.00	-99.0	-99.0
04-Jul-91	12:00	6.09	50.2	0.06	-99.00	-99.00	-99.0	-99.00	-99	-99	-99.00	-99.0	-99.0
04-Jul-91	14:00	6.16	40.9	0.13	-99.00	-99.00	-99.0	-99.00	-99	-99	-99.00	-99.0	-99.0
04-Jul-91	16:00	5.97	33.7	0.34	3.56	0.55	5.6	1.66	-99	-99	0.35	14.9	29.1
04-Jul-91	17:45	6.27	32.3	0.49	-99.00	-99.00	-99.0	-99.00	-99	-99	-99.00	-99.0	-99.0
04-Jul-91	19:00	6.04	30.4	0.57	-99.00	-99.00	-99.0	-99.00	-99	-99	-99.00	-99.0	-99.0
04-Jul-91	21:00	6.13	33.0	0.73	-99.00	-99.00	-99.0	-99.00	-99	-99	-99.00	-99.0	-99.0

04-Jul-91	23:00	6.03	34.3	0.80	-99.00	-99.00	-99.0	-99.00	-99	-99	-99.00	-99.0	-99.0
05-Jul-91	01:30	5.91	33.7	0.73	-99.00	-99.00	-99.0	-99.00	-99	-99	-99.00	-99.0	-99.0
05-Jul-91	02:30	6.28	36.3	0.60	-99.00	-99.00	-99.0	-99.00	-99	-99	-99.00	-99.0	-99.0
05-Jul-91	12:00	5.92	50.2	0.12	0.34	0.65	7.8	2.30	-99	-99	0.72	21.8	12.6 1.6*
05-Jul-91	17:00	5.16	39.6	0.48	-99.00	-99.00	-99.0	-99.00	-99	-99	-99.00	-99.0	-99.0
05-Jul-91	23:00	6.11	46.2	0.25	-99.00	-99.00	-99.0	-99.00	-99	-99	-99.00	-99.0	-99.0
06-Jul-91	01:00	6.12	48.8	0.15	-99.00	-99.00	-99.0	-99.00	-99	-99	-99.00	-99.0	-99.0
06-Jul-91	03:30	6.10	57.4	0.06	3.67	0.69	9.1	2.67	-99	-99	0.77	25.4	21.5 11.2*
06-Jul-91	23:00	6.06	62.0	0.16	-99.00	-99.00	-99.0	-99.00	-99	-99	-99.00	-99.0	-99.0
07-Jul-91	14:00	5.90	63.4	0.18	9.13	0.79	10.2	2.92	-99	-99	0.78	28.8	30.4
08-Jul-91	16:00	5.95	38.9	0.96	-99.00	-99.00	-99.0	-99.00	-99	-99	-99.00	-99.0	-99.0
09-Jul-91	15:45	5.80	48.2	0.93	-99.00	-99.00	-99.0	-99.00	-99	-99	-99.00	-99.0	-99.0
10-Jul-91	17:30	6.23	44.2	0.93	-99.00	-99.00	-99.0	-99.00	-99	-99	-99.00	-99.0	-99.0
11-Jul-91	14:00	6.05	44.2	0.64	-99.00	-99.00	-99.0	-99.00	-99	-99	-99.00	-99.0	-99.0
12-Jul-91	14:21	5.92	48.8	0.63	3.53	0.71	8.5	2.57	-99	-99	0.73	25.0	19.9
12-Jul-91	17:30	5.75	46.2	1.39	-99.00	-99.00	-99.0	-99.00	-99	-99	-99.00	-99.0	-99.0
12-Jul-91	19:36	5.85	44.9	1.84	-99.00	-99.00	-99.0	-99.00	-99	-99	-99.00	-99.0	-99.0
12-Jul-91	21:18	6.12	46.2	2.50	-99.00	-99.00	-99.0	-99.00	-99	-99	-99.00	-99.0	-99.0
12-Jul-91	23:09	6.03	46.9	2.80	-99.00	-99.00	-99.0	-99.00	-99	-99	-99.00	-99.0	-99.0
13-Jul-91	01:00	6.20	48.2	2.21	-99.00	-99.00	-99.0	-99.00	-99	-99	-99.00	-99.0	-99.0
13-Jul-91	03:18	5.95	47.5	1.81	-99.00	-99.00	-99.0	-99.00	-99	-99	-99.00	-99.0	-99.0
13-Jul-91	05:15	6.24	48.6	1.83	-99.00	-99.00	-99.0	-99.00	-99	-99	-99.00	-99.0	-99.0

13-Jul-91	07:40	6.25	49.5	1.49	-99.00	-99.00	-99.0	-99.00	-99	-99	-99.00	-99.0	-99.0
13-Jul-91	09:28	6.38	49.5	1.41	-99.00	-99.00	-99.0	-99.00	-99	-99	-99.00	-99.0	-99.0
13-Jul-91	11:00	6.20	50.2	1.17	9.96	0.69	7.9	2.43	-99	-99	0.05	22.9	37.3
13-Jul-91	13:24	6.11	49.5	1.19	-99.00	-99.00	-99.0	-99.00	-99	-99	-99.00	-99.0	-99.0
14-Jul-91	15:30	6.02	54.8	1.02	4.46	0.71	8.8	2.86	-99	-99	0.07	26.0	24.0
15-Jul-91	16:00	6.03	65.3	0.53	-99.00	-99.00	-99.0	-99.00	-99	-99	-99.00	-99.0	-99.0
16-Jul-91	15:18	6.21	78.5	4.80	3.73	0.81	12.7	3.91	-99	-99	0.70	42.0	12.1
17-Jul-91	15:00	6	79.9	0.05	-99.00	-99.00	-99.0	-99.00	-99	-99	-99.00	-99.0	-99.0
18-Jul-91	15:00	6.14	61.4	1.34	-99.00	-99.00	-99.0	-99.00	-99	-99	-99.00	-99.0	-99.0
19-Jul-91	15:00	6.3	56.8	2.20	-99.00	-99.00	-99.0	-99.00	-99	-99	-99.00	-99.0	-99.0
20-Jul-91	16:00	6.21	70.6	2.00	-99.00	-99.00	-99.0	-99.00	-99	-99	-99.00	-99.0	-99.0
21-Jul-91	14:13	5.85	80.5	1.70	-99.00	-99.00	-99.0	-99.00	-99	-99	-99.00	-99.0	-99.0
22-Jul-91	15:00	6.25	83.2	1.95	-99.00	-99.00	-99.0	-99.00	-99	-99	-99.00	-99.0	-99.0
23-Jul-91	15:44	6.28	99.0	1.80	3.25	0.90	15.3	5.22	-99	-99	0.68	52.6	9.8
24-Jul-91	17:00	6.53	107	1.74	68.44	1.27	23.5	6.22	-99	-99	76.88	71.0	12.5
25-Jul-91	15:00	6.48	130	1.10	-99.00	-99.00	-99.0	-99.00	-99	-99	-99.00	-99.0	-99.0
25-Jul-91	21:18	5.91	120	2.00	7.02	1.07	20.2	6.32	-99	-99	4.76	66.3	10.2
25-Jul-91	23:59	6.67	125	1.80	-99.00	-99.00	-99.0	-99.00	-99	-99	-99.00	-99.0	-99.0
26-Jul-91	16:37	6.45	146	0.81	3.84	1.04	23.8	7.56	-99	-99	0.84	84.5	5.8
27-Jul-91	14:31	6.35	173	0.33	3.80	1.17	28.3	9.26	-99	-99	0.91	101.0	5.3
28-Jul-91	17:00	6.17	174	-99.00	-99.00	-99.00	-99.0	-99.00	-99	-99	-99.00	-99.0	-99.0
29-Jul-91	15:00	6.48	198	0.16	-99.00	-99.00	-99.0	-99.00	-99	-99	-99.00	-99.0	-99.0
30-Jul-91	15:44	6.27	191	0.20	-99.00	-99.00	-99.0	-99.00	-99	-99	-99.00	-99.0	-99.0

31-Jul-91	16:40	6.25	205	0.26	1.19	1.25	33.0	11.27	0.03	0.42	0.76	123.2	2.3
01-Aug-91	14:47	6.28	177	0.54	-99.00	-99.00	-99.0	-99.00	-99	-99	-99.00	-99.0	-99.0
01-Aug-91	22:00	6.28	164	0.86	0.98	1.11	25.7	8.54	-99	-99	0.69	90.9	3.6
02-Aug-91	00:00	6.71	164	1.13	-99.00	-99.00	-99.0	-99.00	-99	-99	-99.00	-99.0	-99.0
02-Aug-91	02:00	6.55	157	1.09	-99.00	-99.00	-99.0	-99.00	-99	-99	-99.00	-99.0	-99.0
02-Aug-91	04:00	6.22	152	1.20	2.03	1.[illegible]	23.7	7.56	-99	-99	0.69	81.7	5.5
02-Aug-91	06:00	6.16	141	1.66	-99.00	-99.00	-99.0	-99.00	-99	-99	-99.00	-99.0	-99.0
02-Aug-91	08:00	6.56	131	3.00	1.16	1.05	21.6	7.14	-99	-99	0.75	73.2	6.0
02-Aug-91	10:00	6.22	123	3.50	-99.00	-99.00	-99.0	-99.00	-99	-99	-99.00	-99.0	-99.0
02-Aug-91	12:00	6.38	104	4.00	0.88	0.95	17.4	4.77	-99	-99	0.69	52.0	9.2
02-Aug-91	14:00	5.83	70.6	-99.00	-99.00	-99.00	-99.0	-99.00	-99	-99	-99.00	-99.0	-99.0
02-Aug-91	16:00	6.28	77.2	6.00	0.81	0.82	12.9	3.39	-99	-99	0.79	38.7	8.3
02-Aug-91	22:09	6.1	92.4	8.00	3.38	0.85	14.5	4.17	-99	-99	1.17	46.9	10.1
03-Aug-91	22:00	6.42	144	6.80	1.98	1.07	22.7	7.26	-99	-99	0.39	77.6	6.3
04-Aug-91	15:00	6.38	137	5.00	-99.00	-99.00	-99.0	-99.00	-99	-99	-99.00	-99.0	-99.0
05-Aug-91	15:00	6.52	79.2	12.00	-99.00	-99.00	-99.0	-99.00	-99	-99	-99.00	-99.0	-99.0
06-Aug-91	15:00	6.3	122	7.00	0.82	1.01	19.1	6.16	-99	-99	0.64	63.4	6.5 0.1*
07-Aug-91	17:00	6.38	149	5.00	-99.00	-99.00	-99.0	-99.00	-99	-99	-99.00	-99.0	-99.0
08-Aug-91	16:00	6.34	132	5.00	0.91	1.06	20.8	6.95	-99	-99	0.65	70.6	5.9
09-Aug-91	16:00	6.37	157	1.80	-99.00	-99.00	-99.0	-99.00	-99	-99	-99.00	-99.0	-99.0
10-Aug-91	15:00	6.41	104	4.46	-99.00	-99.00	-99.0	-99.00	-99	-99	-99.00	-99.0	-99.0
13-Aug-91	15:00	6.3	158	0.96	1.11	1.15	24.3	8.38	0.05	0.46	0.70	87.3	5.0

WIF/2

Day	Time	pH	TDS mg/l	Q l/s	Na^{+}	K^{+}	Ca^{2+}	Mg^{2+}	Fe^{2+}	Al^{3+}	Cl^{-}	SO_4^{2-}	% imbalance
05-Jun-91	11:58	6.72	92	1.06	1.33	1.46	13.5	7.38	-99	-99	1.11	56.3	6.6
05-Jun-91	16:59	6.55	103	2.00	1.76	1.27	15.0	8.17	-99	-99	1.20	72.5	-0.5
05-Jun-91	22:59	6.69	77	2.60	-99.00	-99.00	-99.0	-99.00	-99	-99	-99.00	-99.0	-99.0
06-Jun-91	10:16	6.71	86	0.69	1.17	1.51	13.2	7.04	-99	-99	1.14	53.3	7.5
06-Jun-91	16:09	6.07	114	1.02	1.89	1.38	17.0	9.58	-99	-99	1.09	76.5	3.8
06-Jun-91	22:29	6.73	89	7.02	1.53	1.28	12.8	6.53	-99	-99	1.19	51.2	7.5
07-Jun-91	09:48	6.52	103	1.30	-99.00	-99.00	-99.0	-99.00	-99	-99	-99.00	-99.0	-99.0
07-Jun-91	16:29	5.83	89	3.14	-99.00	-99.00	-99.0	-99.00	-99	-99	-99.00	-99.0	-99.0
08-Jun-91	14:24	6.76	105	3.32	1.55	1.50	15.5	7.82	-99	-99	1.09	60.8	7.9
08-Jun-91	23:44	6.33	79	2.14	1.01	1.18	12.8	5.25	-99	-99	1.92	44.0	8.3
09-Jun-91	12:59	5.05	92	0.45	-99.00	-99.00	-99.0	-99.00	-99	-99	-99.00	-99.0	-99.0
09-Jun-91	17:12	6.11	93	1.84	1.26	1.26	14.2	6.38	-99	-99	1.05	51.8	8.7
10-Jun-91	07:29	6.08	92	-99.00	-99.00	-99.00	-99.0	-99.00	-99	-99	-99.00	-99.0	-99.0
10-Jun-91	14:58	6	95	0.22	-99.00	-99.00	-99.0	-99.00	-99	-99	-99.00	-99.0	-99.0
11-Jun-91	12:59	6.27	98	0.17	-99.00	-99.00	-99.0	-99.00	-99	-99	-99.00	-99.0	-99.0
11-Jun-91	17:13	6.3	100	0.38	2.15	1.05	14.7	7.45	-99	-99	0.84	58.9	8.0
12-Jun-91	15:28	5.94	111	0.27	-99.00	-99.00	-99.0	-99.00	-99	-99	-99.00	-99.0	-99.0
12-Jun-91	23:49	5.67	114	0.04	-99.00	-99.00	-99.0	-99.00	-99	-99	-99.00	-99.0	-99.0
13-Jun-91	16:43	6.1	119	0.01	1.70	1.11	15.9	8.90	-99	-99	0.98	68.9	5.4
13-Jun-91	23:29	5.84	124	-99.00	-99.00	-99.00	-99.0	-99.00	-99	-99	-99.00	-99.0	-99.0

14-Jun-91	14:29	6.3	124	0.01	-99.00	-99.00	-99.0	-99.00	-99	-99	-99.00	-99.0	-99.0
15-Jun-91	00:28	6.32	121	0.04	-99.00	-99.00	-99.0	-99.00	-99	-99	-99.00	-99.0	-99.0
15-Jun-91	15:14	6.4	124	0.02	-99.00	-99.00	-99.0	-99.00	-99	-99	-99.00	-99.0	-99.0
16-Jun-91	12:59	6.43	129	0.02	1.65	1.07	17.4	9.99	-99	-99	0.83	76.1	5.3
20-Jun-91	23:13	6.19	129	0.05	2.39	1.01	17.8	9.76	-99	-99	1.43	77.1	5.1
21-Jun-91	13:29	6.28	137	0.03	-99.00	-99.00	-99.0	-99.00	-99	-99	-99.00	-99.0	-99.0
21-Jun-91	16:14	6.42	137	0.00	3.23	1.19	18.5	10.31	-99	-99	0.77	81.8	5.9
22-Jun-91	12:00	6.39	141	-99.00	-99.00	-99.00	-99.0	-99.00	-99	-99	-99.00	-99.0	-99.0
23-Jun-91	14:00	6.2	125	-99.00	-99.00	-99.00	-99.0	-99.00	-99	-99	-99.00	-99.0	-99.0
25-Jun-91	14:58	6.18	133	-99.00	-99.00	-99.00	-99.0	-99.00	-99	-99	-99.00	-99.0	-99.0
26-Jun-91	16:30	6.2	100	0.00	1.17	1.00	14.6	5.52	-99	-99	0.13	49.8	9.6 0.8*
10-Jul-91	17:30	5.9	97	0.00	-99.00	-99.00	-99.0	-99.00	-99	-99	-99.00	-99.0	-99.0
21-Jul-91	14:13	6.43	105	0.20	-99.00	-99.00	-99.0	-99.00	-99	-99	-99.00	-99.0	-99.0
22-Jul-91	15:00	6.29	103	0.40	-99.00	-99.00	-99.0	-99.00	-99	-99	-99.00	-99.0	-99.0
23-Jul-91	15:44	6.48	111	-99.00	-99.00	-99.00	-99.0	-99.00	-99	-99	-99.00	-99.0	-99.0
24-Jul-91	17:00	6.62	107	0.40	-99.00	-99.00	-99.0	-99.00	-99	-99	-99.00	-99.0	-99.0
25-Jul-91	15:00	6.16	119	-99.00	-99.00	-99.00	-99.0	-99.00	-99	-99	-99.00	-99.0	-99.0
25-Jul-91	21:18	6.41	113	0.70	3.94	1.03	15.2	7.42	-99	-99	0.04	60.5	10.7
26-Jul-91	16:37	6.54	124	0.80	-99.00	-99.00	-99.0	-99.00	-99	-99	-99.00	-99.0	-99.0
28-Jul-91	17:00	6.25	214	0.15	5.78	1.32	27.5	17.3	0.02	0.47	1.14	135.7	4.6 1.2*
29-Jul-91	15:00	6.5	222	0.03	-99.00	-99.00	-99.0	-99.0	-99	-99	-99.00	-99.0	-99.0
01-Aug-91	22:00	6.36	437	0.49	9.09	1.79	48.5	41.5	-99	-99	0.68	300.5	0.0

02-Aug-91	00:00	6.55	381	0.75	-99.00	-99.00	-99.0	-99.0	-99	-99	-99.00	-99.0	-99.0
02-Aug-91	02:00	6.29	351	1.20	-99.00	-99.00	-99.0	-99.0	-99	-99	-99.00	-99.0	-99.0
02-Aug-91	04:00	6.23	336	1.40	4.80	1.49	38.7	31.8	-99	-99	0.05	221.4	1.9
02-Aug-91	06:00	6.29	302	1.60	-99.00	-99.00	-99.0	-99.0	-99	-99	-99.00	-99.0	-99.0
02-Aug-91	08:00	6.23	270	2.00	3.79	1.33	31.8	24.2	-99	-99	0.65	174.8	1.6
02-Aug-91	10:00	6.24	254	2.60	-99.00	-99.00	-99.0	-99.0	-99	-99	-99.00	-99.0	-99.0
02-Aug-91	12:00	6.4	226	3.50	2.99	1.14	26.0	89.4	-99	-99	0.23	141.3	-33.8
02-Aug-91	14:00	6.12	153	-99.00	-99.00	-99.00	-99.0	-99.0	-99	-99	-99.00	-99.0	-99.0
02-Aug-91	16:00	6.13	98	-99.00	1.29	0.82	13.6	5.89	-99	-99	0.03	52.3	6.4
02-Aug-91	22:09	6.33	74	12.00	-99.00	-99.00	-99.0	-99.00	-99	-99	0.72	38.8	-99.0
03-Aug-91	22:00	6.5	204	4.00	2.66	1.21	24.0	15.7	-99	-99	0.32	122.7	1.5
04-Aug-91	15:00	6.42	218	5.00	-99.00	-99.00	-99.0	-99.0	-99	-99	-99.00	-99.0	-99.0
05-Aug-91	15:00	6.25	138	18.00	2.35	1.12	17.9	11.8	-99	-99	0.66	89.3	3.0
06-Aug-91	15:00	6.31	180	-99.00	-99.00	-99.00	-99.0	-99.0	-99	-99	-99.00	-99.0	-99.0
07-Aug-91	17:00	6.38	240	3.00	1.00	1.09	23.0	7.21	-99	-99	0.36	79.0	4.5
08-Aug-91	16:00	6.4	210	4.50	2.87	1.33	24.6	15.4	-99	-99	0.66	122.1	1.8
09-Aug-91	16:00	6.39	250	2.00	-99.00	-99.00	-99.0	-99.00	-99	-99	-99.00	-99.0	-99.0
10-Aug-91	15:00	6.35	137	-99.00	1.64	1.11	18.7	9.09	-99	-99	0.28	80.4	2.8
13-Aug-91	15:00	6.38	296	-99.00	4.67	1.66	33.7	27.1	0.01	0.36	0.47	100.0	33.4

EIF SOIL MINI-PIEZOMETER

Date	pH	TDS	Na^+	K^+	Ca^{2+}	Mg^{2+}	Fe^{2+}	AL^{3+}	Cl^-	SO_4^{2-}	% imb.
EIF/A											
01-Jul-91	4.16	180									
04-Jul-91	4.26	210									
04-Jul-91	3.98	227									
06-Jul-91	4.3	192	4.78	1.01	30.0	5.14	0.33	3.42	0.74	132	-4.2
06-Jul-91	4.12	186									
08-Jul-91	4.19	195									
09-Jul-91	4.15	197									
09-Jul-91	4.28	192									
12-Jul-91	4.28	183	8.82	1.08	30.7	4.04			1.09	120	-5.32
15-Jul-91	4.12	185									
20-Jul-91	4.05	232	4.21	1.02	43.3	4.69			0.73	167	-11.8
26-Jul-91	4.27	343	4.86	0.91	58.9	5.11	0.17	8.47	0.70	269	-10.6
31-Jul-91	4.15	394	2.75	1.08	64.1	5.50	0.12	10.74	0.54	274	-6.82
02-Aug-91	4.15	346	5.70	0.89	50.1	4.93	0.14	11.08	0.90	253	-9.08
09-Aug-91	4.02	502									
13-Aug-91	4.11	482	2.83	0.86	74.2	6.15	0.15	15.3	0.64	397	-15.4
EIF/E											
20-Jul-91	3.18	566	6.91	1.26	58.3	5.88	3.12	15.8	0.93	389	-17.9
26-Jul-91	3.3	612	14.97	0.67	54.2	7.76	3.48	22.9	5.53	488	-21.0
31-Jul-91	3.26	697	5.16	0.57	60.5	8.25	3.27	24.1	1.07	523	-23.3
02-Aug-91	3.06	939	12.37	0.85	71.9	10.4	15.30	37.1	7.15	731	-21.5
09-Aug-91	2.94	1192									
13-Aug-91	3.02	1140	7.03	0.54	90.1	11.7	22.3	72.7	1.33	700	1.57
EIF/B											
20-Jul-91	4.34	244	4.45	1.30	44.9	4.8			0.95	164	-9.2
26-Jul-91	4.3	337									
31-Jul-91	4.2	355	2.71	1.03	61.9	5.58			0.54	268	-20.6
02-Aug-91	4.2	314	6.50	1.08	47.1	5.09					
09-Aug-91	4.06	504									
13-Aug-91	4.11	479									

WIF SOIl MIMI-PIEZOMETER

Date	pH	TDS	Na^+	K^+	Ca^{2+}	Mg^{2+}	Cl^-	SO_4^{2-}	% imb.
WIF/H									
06-Jul-91	5.5	85.8							
08-Jul-91	5.83	83.8	4.22	1.13	13.4	4.24	0.05	47.2	10.9
12-Jul-91	6.08	79.9							
21-Jul-91	6.16	70.6	7.02	1.28	10.7	3.47	0.88	37.7	17.6
26-Jul-91	6.17	75.9							
31-Jul-91	6.02	85.8	1.68	1.33	13.2	4.23	0.86	44.9	7.4
02-Aug-91	6.24	52.8	3.48	0.91	6.2	2.67	1.18	26.9	8.3
09-Aug-91	5.83	86.5							
13-Aug-91	5.98	90.4							
WIF/G									
01-Jul-91	6.07	139							
02-Jul-91	6.22	135	1.40	1.21	20.0	8.60	0.71	82.1	1.9
04-Jul-91	5.83	141							
04-Jul-91	6.19	142							
04-Jul-91	5.79	143							
06-Jul-91	6.16	142							
08-Jul-91	5.95	144							
12-Jul-91	6.23	136							
15-Jul-91	6.02	135							
20-Jul-91	6.46	137							
26-Jul-91	6.12	130							
31-Jul-91	6.08	139							
02-Aug-91	6.24	143	5.68	1.14	19.3	9.18	0.73	80.7	7.9
09-Aug-91	6.14	119							
13-Aug-91	6.07	127							

LAKE MINI-PIEZOMETER

Loc.	Date	pH	TDS	Na^+	K^+	Ca^{2+}	Mg^{2+}	Fe^{2+}	Al^{3+}	Cl^-	SO_4^{2-}	% imb.
MP4/B	04-Jul-91	5.62	515	12.1	6.8	86.6	31.2			0.83	400	-4.7
MP4/B	09-Jul-91	5.64	579	13.0	7.24	95.3	35.4			0.94	452	-5.7
MP4/B	21-Jul-91	5.68	624	16.4	8.80	108	39.2	0.46	0.62	1.08	486	-2.5
MP4/B	11-Aug-91	5.71	560	11.1	7.94	90.5	32.6			0.96	419	-5.2
MP4/A	12-Aug-91	5.85	649	15.1	3.90	109	37.5					
MP2	28-Jun-91	5.7	385									
MP2	30-Jun-91	5.47	375									
MP2	1-Jul-91	5.08	380									
MP2	28-Jul-91	6.43	232	6.51	1.91	40.7	12.1			1.19	154	1.7
MP2	10-Aug-91	6.19	164	1.34	1.48	27.2	7.8	0.10	0.09	0.71	100	0.45
MP6	28-Jul-91	3.48	849	9.51	2.60	141	21.8	1.19	23.4	5.23	716	-11.4
MP6	11-Aug-91	3.47	1300	6.56	2.12	327	17.8	1.72	43.1	5.21	1334	-9.6
MP8	13-Aug-91	2.65	2237	5.57	0.25	479	18.0	179	25.6	5.81	2101	-7.1
ECP4	12-Aug-91	5.5	772	14.4	16.1	133	36.3			5.44	664	-13.5
ECP2	11-Aug-91	4.74	743							5.23	599	
MP5	13-Aug-91	5.63	1203							8.56		

SEEPS AND MISCELLENIOUS STREAM CHEMISTRY

Loc.	Date	TDS	pH	Na^+	K^+	Ca^{2+}	Mg^{2+}	Cl^-	SO_4^{2-}	% imb.
Stream B	04-Jun-91	154	6.42	6.43	0.61	35.2	0.56	0.05	103	-1.0
No Name creek	04-Jun-91	205	5.84	0.75	0.79	29.3	15.45	1.21	142	-3.5
No Name creek	05-Jun-91	176	6.2							
No Name creek	06-Jun-91	162	5.57							
No Name creek	06-Jun-91	162	5.57							
No Name creek	02-Aug-91	232	5.87							
No Name creek	02-Aug-91	266	5.67							
No Name creek	08-Aug-91	303	5.89							
No Name creek	09-Aug-91	315	5.43							
No Name creek	12-Aug-91	321	5.86							
SW Seep	30-Jun-91	149	5.66							
SW Seep	02-Jul-91	143	5.97							
SW Seep	14-Jul-91	129	5.85							
SW Seep	22-Jul-91	114	5.95							
SW Seep	24-Jul-91	124	6.3							
SW Seep	25-Jul-91	158	6.48	3.41	1.18	25.3	7.84	0.68	94	2.5
SW Seep	02-Aug-91	100	5.94							
NW Seep	25-Jul-91	702	6.83	29.81	2.91	85.0	81.66	0.08	584	0.7
NW Seep	02-Aug-91	489	6.61							
NW Seep	02-Aug-91	337	6.53							
Gordon Cr.	08-Aug-91	1412	2.98							